GLAXOSMITHKLINE

UNIVERSITY OF STRATHCLYDE

DEPARTMENT OF PURE AND APPLIED CHEMISTRY

New Treatments for Inflammatory Diseases: Optimisation and Understanding of Key Processes

Suzanne H. Davies

MPhil

2012

Declaration of Authenticity and Author's Rights

This thesis is the result of the author's original research. It has been composed by the author and has not been previously submitted for examination which has led to the award of a degree.

Signed: Date:

Contents

Acknowledgements

My thanks go to Andy H, Andy K and Billy for supervision and assistance throughout the programme. I also thank Matt, Stuart, Neil and Chris on the Syk project, and the many past and present members of the darapladib team in former Chemical Development. In particular, I am grateful to John, Nic, Noel, Pat and Paul for carrying out GC analyses; Simon, Alec, Ian and Tony for spectroscopy assistance; Dan and Ivana for experimental design support, and Mark for kinetics expertise and guidance through DynoChem®.

Abbreviations List

4-FBnCl	4-Fluorobenzyl chloride
A	Pre-exponential factor (Arrhenius parameter)
Ac	Acetyl
API	Active pharmaceutical ingredient
ATP	Adenosine triphosphate
BINAP	2,2'-Bis(diphenylphosphino)-1,1'-binaphthalene
Bn	Benzyl
Boc	*tert*-Butyloxycarbonyl
br	broad
Bu	Butyl
Cbz	Benzyloxycarbonyl
CDI	Carbonyldiimidazole
CHD	Coronary heart disease
d	doublet
DCE	1,2-Dichloroethane
DCM	Dichloromethane
de	diastereomeric excess
DIPEA	*N*,*N*-Diisopropylethylamine
DMAP	*N*,*N*-Dimethylpyridin-4-amine
DMF	*N*,*N*-Dimethylformamide
DMS	Dimethylsulfide
DMSO	Dimethylsulfoxide
E_a	Activation energy
EDC	1-Ethyl-3-(3-dimethylaminopropyl)carbodiimide
ee	enantiomeric excess
ES^+	Positive electrospray ionisation

equiv.	Molar equivalents
Et	Ethyl
GC	Gas chromatography
GSK	GlaxoSmithKline
h	hour(s)
HMDS	1,1,1,3,3,3-Hexamethyldisilazane
HMG-CoA	3-Hydroxy-3-methylglutaryl-coenzyme A
HOBT	1-Hydroxybenzotriazole
HPLC	High pressure liquid chromatography
HRMS	High resolution mass spectrometry
i	*iso*
IG	Intermediate grade
IMS	Industrial methylated spirits
IPA	*iso*-Propanol
IR	Infra red
k	Rate constant
K	Equilibrium constant
LCMS	Liquid chromatography mass spectrometry
LDL	Low density lipoprotein
Lp-PLA_2	Lipoprotein-associated phospholipase A_2
m	multiplet
Me	Methyl
MIBK	Methyl *iso*-butyl ketone
min	minute(s)
MS	Mass spectrometry
N/A	Not applicable
NMP	*N*-Methyl-2-pyrrolidone
NMR	Nuclear magnetic resonance

p-	*para*-
Ph	Phenyl
ppm	parts per million
Pr	Propyl
q	quartet
r	Response relative to internal standard
R	Ideal gas constant (8.3145 $JK^{-1}mol^{-1}$)
s	singlet
Syk	Spleen tyrosine kinase
t	*tertiary*
t	triplet
t	time
T	Temperature
$t_{½}$	Half life
TBME	*tert*-Butylmethylether
TEEDA	*N*,*N*,*N*',*N*'-Tetraethylethylenediamine
Tf	Trifluoromethylsulfonyl
TFA	Trifluoroacetic acid
THF	Tetrahydrofuran
TIC	Total ion count
TMS	Tetramethylsilane
TMSCl	Trimethylsilyl chloride
UV	Ultra violet
VOC	Volatile organic compound
vol	Volumes = L / kg of limiting reagent
wt	Weight relative to limiting reagent

1 Abstract

This thesis is split into two main parts, both concerned with new treatments for inflammatory diseases. Section 3 details the investigation and optimisation of an azide reduction to prepare a key amine intermediate, which was required in the synthetic route to a desired spleen tyrosine kinase (Syk) inhibitor. This targeted compound was required for toxicological studies prior to commencing phase I clinical trials for the treatment of inflammatory diseases such as rheumatoid arthritis and urticaria. The chemistry was optimised to allow preparation of 552 g of the requisite amine in quantitative yield with excellent control over a number of process impurities.

Section 4 discusses darapladib, an inhibitor of lipoprotein-associated phospholipase A_2, which is in phase III clinical trials for the treatment of atherosclerosis. The preparation of a key carboxylic acid intermediate was investigated, incorporating experimental design methods to determine the effect of varying work-up parameters on impurities and yield. The main impurity of interest was 4-fluorobenzyl chloride. In order to demonstrate control over this impurity, its fate and effects in the downstream chemistry were determined. The development and verification of a predictive kinetic model for the reaction of 4-fluorobenzyl chloride during the final amidation transformation are discussed.

The thesis also provides an overview of the variable work programmes typically experienced by process chemists. In particular, the contrast between the level of detail and understanding required for late phase projects, and the need for rapid material delivery in early phase projects, is exemplified.

2 Introduction to Process Chemistry

The manufacture of pharmaceutical products at large scale is not a trivial matter. It takes many years of development to ensure that intermediates and active pharmaceutical ingredients (APIs) can be manufactured in the most cost effective and efficient manner, whilst maintaining quality and presenting no risk to patient safety. The primary responsibility of a process chemist is to decide on the final route of manufacture, whilst developing the chemistry into robust and efficient processes.[1] The focus for process development work varies depending on the project requirements.

2.1 Early Process Development

It is the responsibility of medicinal chemists to identify target molecules. Once a promising molecule has been identified larger quantities are usually required and, at this stage, scale-up and development of the chemistry is tasked to the process chemists. Initially, a project will only need to deliver up to 1 kg of an API in a relatively short period of time. In this case, it is often appropriate to use the route employed in the original medicinal chemistry studies. This strategy allows for focus on removal of undesirable reagents or operations, whilst meeting a demanding schedule for material delivery.

There are certain operations routinely carried out in research laboratories which are impractical to carry out at large scale. Chromatography is one such procedure and, although possible, it is removed from processes as a priority. Column chromatography is typically expensive, requiring vast quantities of both solvent mobile phase and stationary phase relative to the amount of API or intermediate. The cost rises considerably if a chiral stationary phase is required to separate enantiomeric compounds. An additional consideration related to the use of chromatography is disposal of the associated waste. A second example is the use of rotary evaporators to remove solvent. Rotary evaporation is impractical on large scale, but batches may be concentrated by distillation. However, the concentration of a batch to low volumes can require application of high temperatures. This heating may result in exposure of organic substances to conditions that could cause their

decomposition, and generate more heat. Ultimately, explosions might occur. Accordingly, process chemists must devise alternative methods for compound purification and isolation.

The most straightforward way to obtain desired materials is by crystallisation, and this is the main avenue for isolation of intermediates. Developing an effective crystallisation will not only allow the isolation of the required substance, but can also purify the compound, leaving unwanted impurities in solution. When dealing with liquid products, or intermediates with handling difficulties (*e.g.* due to toxicity or lack of a stable crystalline form) it is not uncommon for a process to be continued into the next chemical step without isolation of the intermediate. This is known as "telescoping" and can be advantageous since reducing the number of isolation steps may lower operating costs. However, one of the main disadvantages of this approach is that without an isolation step the material undergoes little purification and impurities may be present through many stages of chemistry.

Scheme 1 shows an example of a published process chemistry route to β-aminoester **5** which was run using 35 kg input of compound **1**.[2] The first three steps to form salt **4** were telescoped together, avoiding isolation of intermediates **2** and **3**. The final stage to prepare compound **5** uses a Curtius rearrangement,[3,4] which is fairly unusual to see run at scale due to safety concerns of the highly reactive intermediates. The Curtius chemistry was run on 55 kg scale of compound **4**, and extreme care and extra safety precautions were employed when using the unstable and highly toxic diphenylphosphorylazide. The example therefore also shows that it is possible to run highly reactive and potentially dangerous chemistry at scale provided the risks are well assessed and the hazards are understood.

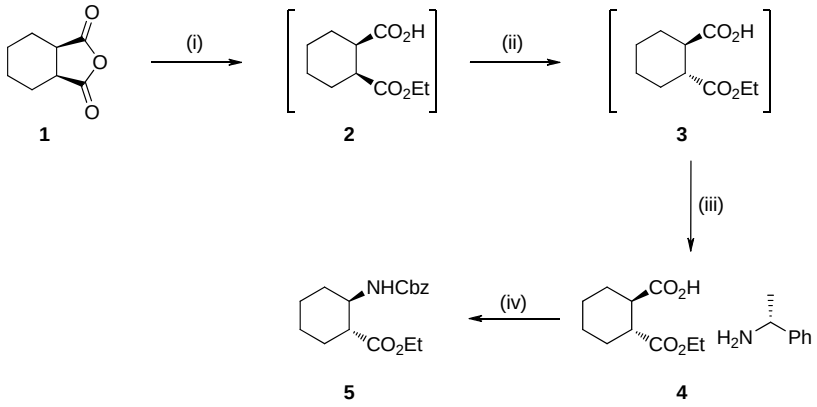

Reagents & conditions: (i) EtOH, (+)-quinidine, toluene, -15 °C; (ii) Potassium *t*-amylate, toluene, -15 °C; (iii) (*R*)-(+)-α-methylbenzylamine, TBME, 40 °C, 65% (3 steps); (iv) (a) HCl, water, toluene; (b) Diphenylphosphorylazide, Et_3N, toluene, 85 °C; (c) BnOH, 110 °C, 87%.

Scheme 1: Published telescoped process.

2.2 Continuing Process Development

For projects at later stages of development, the quantities of API required extend to the region of tens to hundreds of kilograms for use in clinical trials. The existing route, which may still be the medicinal chemistry route, generally requires significant redevelopment. Investigations into alternative routes, optimisation of existing chemistry, and detailed studies of mechanisms and impurity formation become the main requirements. It is not unusual for chemists to concentrate on single transformations for months or years at a time, supporting the running of such reactions at larger scale, and developing a detailed understanding of the chemistry.

At this stage of development it is appropriate to examine the reagents and solvents used in greater detail. The use of more environmentally-friendly solvents is important for the development of sustainable processes,[5] and solvent selection guides have been produced.[6] Early synthetic routes to prepare compounds often use undesirable solvents, characterised by safety, environmental, or health issues. For example, dichloromethane (DCM) is frequently used for both reactions and extractive work-ups. However, it has adverse effects on human health, and emissions are carefully regulated due to environmental effects. In the USA it is classified as a hazardous airborne pollutant. A number of alternative solvents to DCM are

recommended, including 2-methyltetrahydrofuran and ethyl acetate.[6,7] Accordingly, and in a more general sense, process chemists will attempt to replace solvents of concern.

Equally, reagents come under similar scrutiny, and some efforts have been made to categorise reagent classes in terms of greenness, scalability, and broadness of scope.[6] Expensive or toxic reagents are frequently used in research laboratories, but these attributes often rule out their use at large scale. For example, even the widely employed base triethylamine is not necessarily the best choice of reagent: its high volatility leads to environmental problems and risks to human health, particularly by inhalation. Alternative inorganic bases, or less volatile amines, may be a better choice if a process can tolerate the change.

A review of reactions used in the preparation of drug molecules indicated that acylation reactions accounted for 12% of those surveyed.[8] This placed acylations in the top three transformations behind heteroatom alkylation or arylation, and deprotections. Of these acylations, 66% were *N*-acylations to form amides. Reagents to effect amide bond formation are many and varied,[9] but none are considered ideal from a green chemistry perspective.[6] In relation to this, a variety of coupling reagents have been developed based on carbodiimides and benzotriazoles.[10] The reagent carbonyldiimidazole (CDI) is widely used as it is relatively inexpensive, and the by-products (imidazole and carbon dioxide) generally cause few problems.[11] When choosing a reagent to effect amide bond formation, consideration must be given to environmental, health, and safety aspects, as well as determining which reagents provide the best yield and selectivity.

2.3 Experimental Design

Once the route, reagents, and solvents are determined for a process it is necessary to ensure that it produces the best possible results. Processes are optimised to give the highest yield and purest product by investigating the process parameters, such as time, temperature, and reagent charges. Traditionally, the optimisation may be carried out by examining the effects of varying a single parameter at a time (Figure 1).

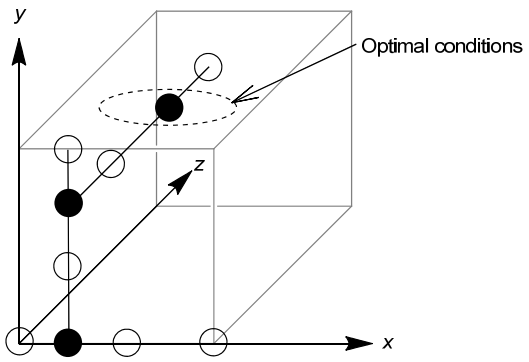

Figure 1: Illustration of experimental space explored when varying one factor at a time.

Figure 1 shows three parameters, *x*, *y*, and *z*, represented in three dimensions as a cube. Initially, factor *x* is varied whilst all other parameters are kept constant (shown as white circles), and an optimum value is chosen (depicted as a black circle). The best conditions are then taken forward, and parameters *y* and *z* are explored in a similar manner. The optimal conditions identified in this example are circled. If the cube is considered to depict the entire process space, the single parameter method covers only a small proportion of the possible volume. However, the exploration of a process in this way can lead to much improved knowledge and understanding of the effects of individual parameters.

An alternative way to consider process optimisation is to use experimental design methods.[12] These use statistical techniques to design experiments and analyse the results, and are widely used, not only to optimise chemical processes,[13,14] but also in the wider scientific community.[15] Two-level factorial designs are of most use for initial process chemistry investigations (Figure 2).

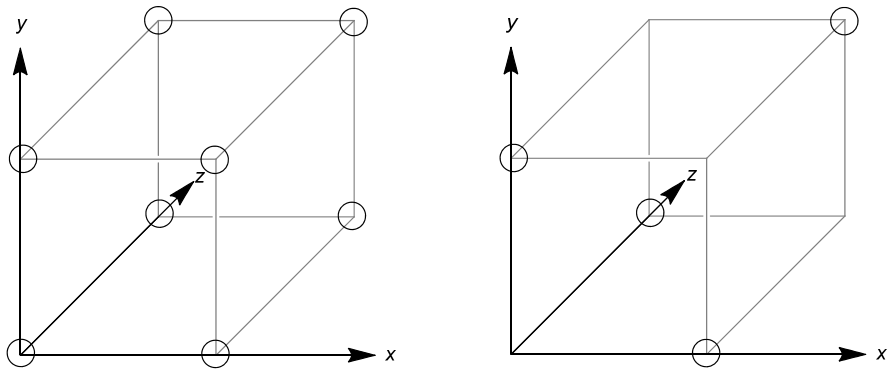

Figure 2: Three-factor full factorial (left) and half factorial (right) designs.

Factorial designs investigate each parameter at two extremes, including all possible combinations of these parameters (Figure 2, left, three parameters give eight experiments, denoted by circles at the corners of the cube). The entire process space is explored. Statistical analysis of a response of interest (*e.g.* yield) is completed to identify which parameters have the greatest effect on the response. In addition, the analysis of the data provides information about interactions between parameters. This is one of the main benefits from completing factorial studies, as varying a single factor cannot identify interactions. An *N*-variable factorial design allows determination of individual factor effects, two-factor interactions, right up to *N*-factor interactions. In reality, effects above two-factor interactions are rare and there is no need to investigate these higher interactions. Additionally, the number of experiments required for a full factorial study rapidly becomes impractical as the number of factors is increased. For example, investigating eight parameters in a full factorial design would need 256 (2^8) experiments to complete all possible combinations. For these reasons, it is often considered appropriate to use a fractional factorial design. Figure 2 (right) shows a half factorial design for three parameters, which results in four experiments; half the number of experiments are completed compared to the full design.

The caveat of using a fractional factorial design is that effects can no longer be estimated independently, and are, instead, aliased with one another. This means, for example, it may be impossible to tell whether the main effect on a response is due to a single factor or an interaction of two other factors. The more fractioned the design, the more effects are aliased with one another. Nevertheless, careful choice of design,

prior knowledge of the reaction or process, and chemical intuition can be used together to confidently determine the factors of greatest importance.

For some designs it may be necessary to identify areas that may introduce errors to the study. This could include using multiple batches of a reagent, using different pieces of equipment, or having two people completing the experiments. Each of these changes during the experimental work could give different results. The design can be split into blocks to allow estimation of any effects derived from making such a change within a study. However, the block effect is typically aliased with some of the model terms, and it becomes very difficult to identify whether an effect is due to the block or the aliased model term. If the aliased term is not identified as being significant it can be said that no major block effect exists, and the design can be analysed as a single block.

When completing an experimental design it is routine to include at least two (ideally more) centre point runs. These are completed at the mid-point of the range for all parameters simultaneously, and are used to estimate the experimental error. They also determine whether curvature is present in a chosen model (Figure 3).

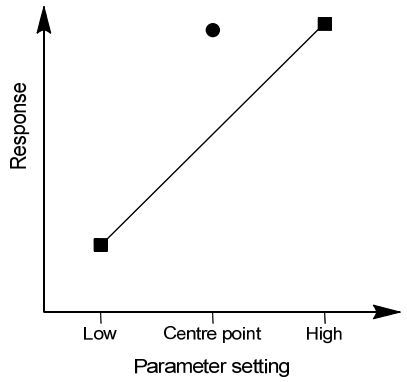

Figure 3: Illustration of curvature within a model.

Figure 3 shows that when the parameter (*e.g.* temperature) is increased the response (*e.g.* yield) increases. The centre point run performs much better than would be anticipated from the linear model shown, and this indicates that a non-linear model would be more appropriate. Further experimentation would then typically be recommended.

Fractional factorial designs are used to screen a reaction or process to identify the most important parameters and interactions. In order to fully optimise the reaction or process, and to accurately model curvature, further experiments are required. Response surface methods are typically used for this purpose, and these produce more accurate models, which can be depicted pictorially as surface representations of processes.[16] Response surfaces are particularly useful in identifying which parameter ranges result in consistent results, or whether tight control over parameter settings may be required to avoid process failure.

Design and analysis of factorial studies are usually carried out in commercially available software packages such as Design-Expert®. The statistical methods used in such programmes is beyond the scope of the present introduction.[12] Each response is analysed to generate a half-normal plot (Figure 4, left).

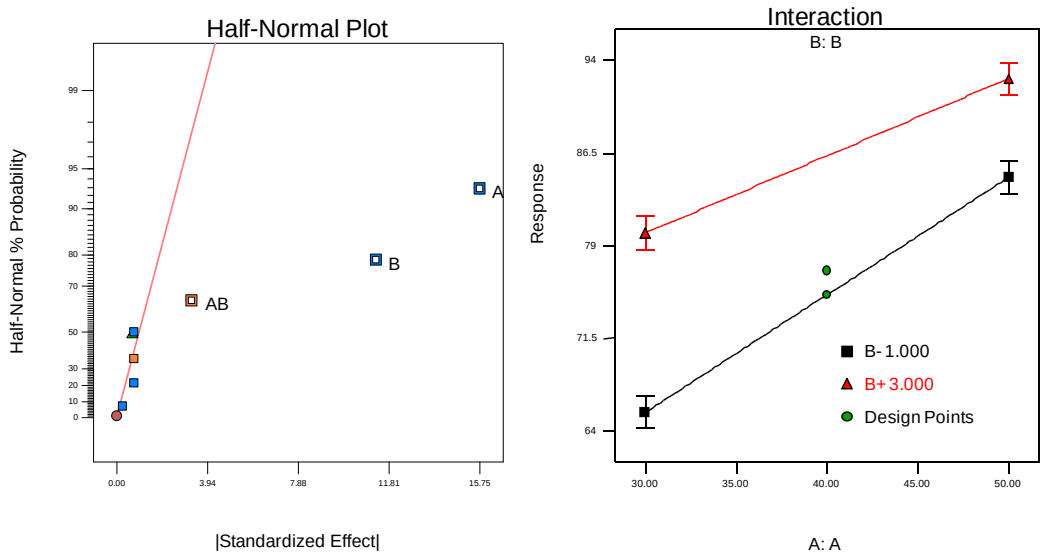

Figure 4: Example half-normal (left) and interaction (right) plots.

In the half-normal plot the factors and interactions showing the most significant effect on the response are furthest to the right. The most important terms are selected to build the most statistically significant model. The effect of each parameter on the response can then be viewed. Interactions are visualised as interaction plots (Figure 4, right). The example in Figure 4 shows factors A and B, plus the interaction of these terms (AB), are significant for the response under investigation. The interaction

plot shows that the response can be maximised when both A and B are at the highest settings.

Experimental design methods are incredibly valuable when optimising a process for scale-up, particularly for identifying parameter interactions. Additionally, accurate predictive mathematical models of a process space can be prepared. These can be used to prove that a process is robust to small changes in parameter settings, or identify areas of the process space where improved results could be obtained.

2.4 Quality

When development is complete the processes used to prepare a new API are usually well understood. Importantly in this regard, the detailed examination of the effects of process parameters ensures excellent knowledge of the conditions that could cause the process to fail. Failure generally means that isolated material is uncharacteristic, perhaps being the wrong colour, containing a new impurity, or containing an impurity at higher than acceptable levels. All of these factors could have an adverse effect on patient safety and therefore must be avoided. Quality guidance for new drugs is provided by The International Conference on Harmonisation of Technical Requirements for Registration of Pharmaceuticals for Human Use (ICH).[17]

Process chemistry is a diverse field and no two processes are the same. Significant development is required to ensure the correct product is reproducibly manufactured. Whilst cost and environmental effects are important factors, maintaining patient safety is essential both during development and once the product is marketed.

3 Spleen Tyrosine Kinase (Syk) Inhibitors for Inflammatory Diseases

3.1 Introduction

3.1.1 Role of Syk in Inflammatory Diseases

Inflammatory diseases encompass a wide range of conditions from asthma to rheumatoid arthritis, incorporating diverse biological pathways involving multiple enzymes. There are therefore many possible targets against which a pharmaceutical agent may be operable when considering therapies for inflammatory diseases. One such target under current investigation is the enzyme spleen tyrosine kinase (Syk).[18] Syk was discovered in 1991 and was found to have a crucial role in signalling within many types of inflammatory cell, such as B-cells and macrophages, which are essential parts of the immune system.[19]

Whilst immune responses are generally protective, fighting off unwanted agents and pathogens, over-activity of the immune system may lead to auto-immune diseases where the body attacks itself. Rheumatoid arthritis is one such auto-immune disease. It is anticipated that inhibition of Syk could have positive effects in the treatment of this debilitating condition by affecting the immune system response through the inflammatory cell pathways.[20] Syk is thought to play important roles in all main stages of the progression of arthritis and may, therefore, have very broad activity.

Another inflammatory condition that could be treated by inhibition of Syk is urticaria. This condition is characterised by severe skin rashes or hives. Urticaria is often (but not always) a result of an allergic reaction; hence the main current treatment is typically antihistamines. Inhibition of Syk may also be applicable to the treatment of asthma, multiple sclerosis, and allergies (*e.g*. seasonal allergic rhinitis) *via* inflammatory mechanisms.

Despite affecting parts of the immune system itself, inhibition of Syk is not anticipated to lead to immunosuppression, as there are multiple mechanisms within the body responsible for regulating the immune system response.[18] This is in direct contrast to glucocorticoids, which are broad acting agents traditionally prescribed to

treat auto-immune or inflammatory diseases, and may result in severe suppression of the immune system following long-term use.[21]

Within our laboratories, and the wider scientific community, there is interest in developing small molecule Syk inhibitors for the treatment of inflammatory, allergic and auto-immune diseases. Additionally, as an alternative treatment approach, there are efforts underway to identify oligonucleotide therapies to prevent expression of the Syk enzyme.[22,23]

3.1.2 Small Molecule Inhibitors of Syk

As a tyrosine kinase, Syk is responsible for transferring phosphate groups from adenosine triphosphate (ATP) to proteins within cells. This phosphorylation mechanism is important for signalling within cells. It is therefore recognised that small molecules need to interact selectively with the ATP binding site of Syk, preferentially over other kinases, to cause an inhibitory response. A number of small molecule Syk inhibitors are documented in the literature. For example, Rigel Pharmaceuticals are investigating a number of structurally related compounds based around a pyrimidine core (Figure 5).

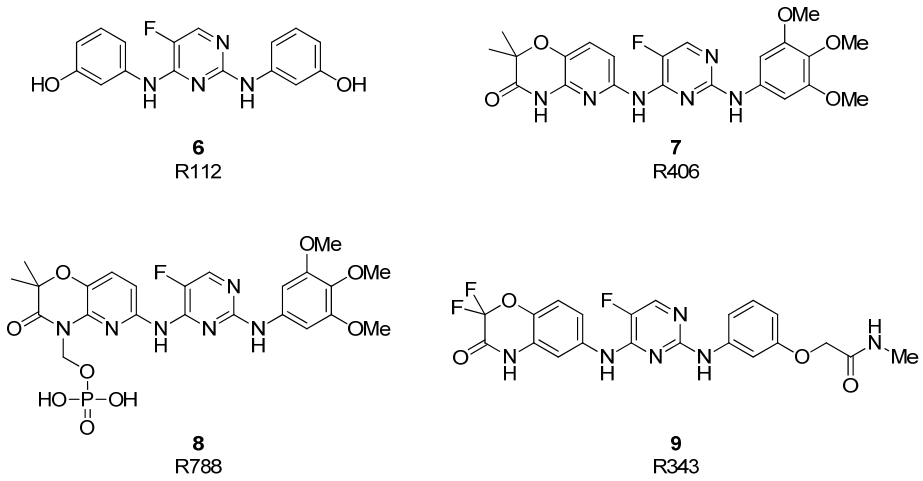

Figure 5: Selected Rigel Pharmaceuticals Syk inhibitors.

Compound **6** (R112)[24] has completed phase II trials for allergic rhinitis, but showed poor results due to a very short duration of action, and has been superseded by other candidates.[25] Fostamatinib **8** (R788),[26] the prodrug of **7** (R406)[27] was licensed by AstraZeneca and is in phase III clinical trials as a therapy for rheumatoid arthritis.

Rigel also developed **9** (R343)[28] as a candidate for treatment of allergic asthma. R343 has completed phase I trials and is expected to begin phase II trials during 2012.

Other molecules with different heterocyclic cores have been developed as small molecule Syk inhibitors (Figure 6). An oxindole series exemplified by **10** was reported by Aventis in 2003,[29] whilst Boehringer Ingelheim have documented a 1,6-naphthyridine series including **11**.[30] There are many other molecules based on a pyrimidine core, such as the triazolopyrimidines (*e.g.* **12**) described by scientists at Kissei.[31]

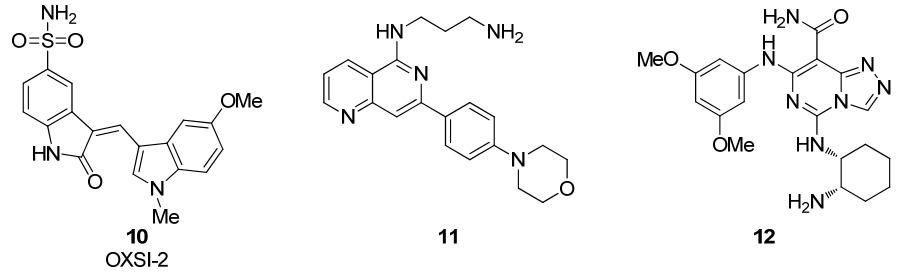

Figure 6: Small molecule Syk inhibitors in development.

Despite significant research and development into selective Syk inhibitors, none are currently on the market for the treatment of inflammatory and auto-immune conditions. Early indications from clinical trials suggest that such pharmaceutical entities may be applicable for a broad range of inflammatory conditions, and are therefore of significant interest within our laboratories.

3.1.3 GSK's Approach to Syk Inhibitors

At GSK a number of compounds have been documented as Syk inhibitors. Many of the compounds within the associated patent literature are centred on a pyrimidine core connected to an indazine moiety *via* an amine linker, and these are exemplified by the structures in Figure 7.[32-35]

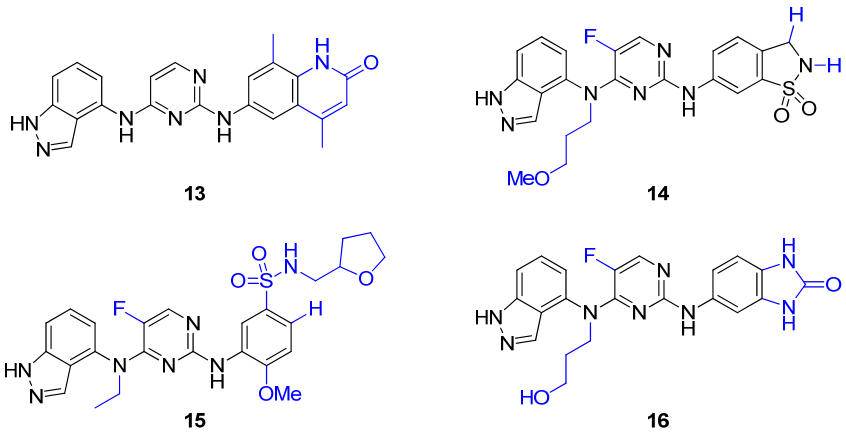

Structure parts in blue illustrate documented sites of variation.

Figure 7: Pyrimidine series.

Further examples of Syk inhibitors are focused on a pyrrolopyrimidine core as exemplified by **17** in Figure 8.[36,37] A more recent patent discloses chiral pyrimidine compound **18** (Figure 8).[38]

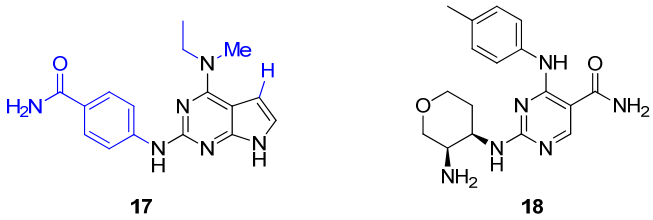

Structure parts in blue illustrate documented sites of variation.

Figure 8: Pyrrolopyrimidine and pyrimidine carboxamide examples.

Current investigations within our laboratories have now led to the discovery of chiral naphthyridine **19** as an inhibitor of Syk (Figure 9). Specifically, naphthyridine **19** was identified as a potential therapy for inflammatory conditions including urticaria, rheumatoid arthritis, auto-immune conditions, asthma, and allergic rhinitis.[39]

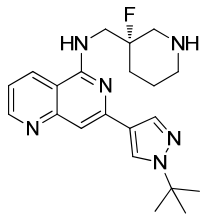

19

Figure 9: Syk inhibitor for development.

For initial toxicity studies and investigations into dose determination, approximately 200 g of compound **19** was required, which was to be prepared in our Scale-Up Laboratory.* As with all early phase projects the main requirement was rapid delivery of the required material of appropriate quality. As a result, the amount of time available for comprehensive process development was severely limited and instead concentrated on eliminating particularly disadvantageous steps from the synthetic route (*vide infra*, section 3.1.4).

3.1.4 Medicinal Chemistry Route to 19

The route initially used within our laboratories to prepare naphthyridine **19** is shown in Scheme 2.[39] This route was used to prepare small quantities of the target molecule for initial biological studies; therefore minimal consideration was given to its applicability on a large scale. Furthermore, the route was used to prepare multiple potential Syk inhibitors and was therefore not tailored specifically to the preparation of **19**.

* At the GSK site in Stevenage we have laboratory facilities up to 20 L scale which are used for small scale preparations of APIs as required for early clinical trials and toxicity testing. For larger scale preparations our appropriate pilot plant facilities are used.

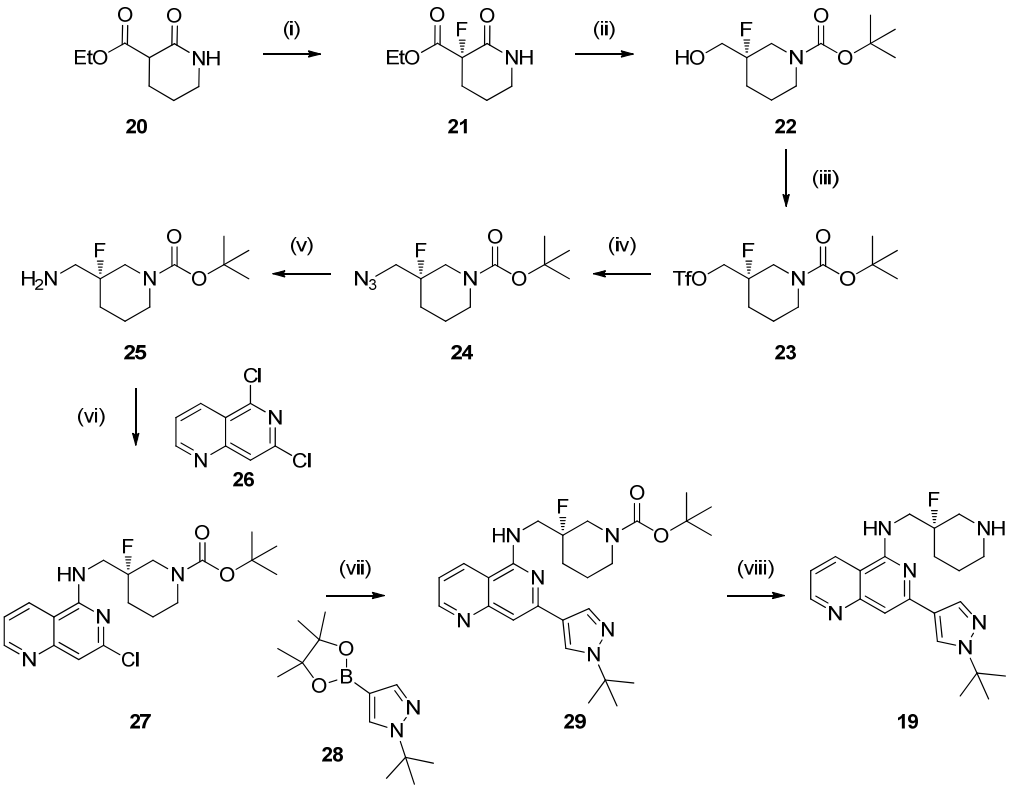

Reagents & conditions: (i) (a) 2,6-Lutidine, [Pd-(*S*)-BINAP(H_2O)$_2$](OTf)$_2$, ($PhSO_2$)$_2$NF, ethanol, 0 °C to room temperature; (b) Chiral preparative chromatography, 50% (2 steps); (ii) (a) BH_3·THF, THF, reflux; (b) Et_3N, Boc_2O, DCM, room temperature, 86% (2 steps); (iii) Tf_2O, Et_3N, DCM, -10 to 0 °C, quantitative; (iv) NaN_3, DMF, 80 °C, quantitative; (v) Pd/C, H_2, ethanol, room temperature, quantitative; (vi) DIPEA, NMP, 100 °C, 84%; (vii) $Pd(PPh_3)_4$, Cs_2CO_3, 1,4-dioxane/water (5:1), 130 °C, microwave, quantitative; (viii) TFA, DCM, room temperature, 57%.

*Scheme 2: Medicinal chemistry route to **19**.*

The route began with commercially available lactam **20**, which was fluorinated using *N*-fluorobenzenesulfonimide in the presence of a chiral palladium catalyst derived from (*S*)-BINAP.[40] Despite the use of a chiral catalyst, the stereoselectivity observed in the reaction was poor, resulting in only 44% ee. The enantiomeric excess of the desired (*R*)-isomer was improved to >99% ee by chiral preparative chromatography, which is not amenable to scale-up. With the stereogenic centre set, fluorinated lactam **21** was reduced using BH_3·THF at reflux in THF, then protected as the *t*-butoxycarbonyl (Boc) derivative *in situ* to furnish **22**. Whilst the reduction and protection were high yielding, the reaction conditions presented us with immediate

processing issues. General safety limitations regarding the use of BH_3·THF preclude its use at >40 °C due to decomposition of the complex to the highly unstable and explosive diborane (B_2H_6) at temperatures above 50 °C.[41]

Alcohol **22** was converted into amine **25** *via* a three step sequence. Thus, triflate **23** was prepared by reaction with triflic anhydride, and was then converted directly into azide **24**. Hydrogenation of the azide gave access to amine **25** of acceptable quality for direct use in the next stage. Although preparation of a potentially highly reactive intermediate azide species is not generally desirable, this route was deemed acceptable for early scale-up activities. However, it was noted that sodium azide is incompatible with dichloromethane due to the formation of highly explosive diazidomethane.[42] The use of DCM in the preparation of triflate **23**, with subsequent concentration *in vacuo*, risked leaving residual DCM which would be present during the formation of azide **24**. This potential safety hazard meant that alternative reaction conditions were required for the preparation of triflate **23**.

The reaction of amine **25** with naphthyridine **26** was achieved by heating in NMP in the presence of a suitable base. A Suzuki-Miyaura reaction was then carried out to install the pyrazole moiety.[43,44] This latter reaction used $Pd(PPh_3)_4$ as the catalyst. Whilst this catalyst can be employed, alternatives are generally sought due to its tendency to degrade. Moreover, when $Pd(PPh_3)_4$ is purchased, significant batch to batch variation can be observed; therefore it is usually prepared *in situ*.

The final stage of the synthesis was the removal of the Boc group under classical conditions to furnish the desired naphthyridine **19**. Handling of TFA at scale can be an issue and, as discussed, DCM is an undesired process solvent from an environmental perspective (*vide supra*, section 2.2).

Based on the observations above there were a number of areas for immediate investigation within the existing route to **19**. In addition, steps (i) and (vi) to (viii) required chromatography to isolate the product. For the remaining steps the products were isolated by evaporation and, as a consequence, improved isolation procedures for all stages were required. It was accepted that for the initial 200 g preparation of **19**, concentration to dryness and chromatography were viable options, which could

be implemented in a straight forward manner if suitable alternatives were not forthcoming. Nevertheless, any improvements to the processes would be advantageous for future preparations of Syk inhibitor **19** at larger scale within our pilot plant.

3.1.5 Revised Route to 19

With the timelines short for delivery of the requisite 200 g of Syk inhibitor **19** it was decided to continue with the existing route rather than develop a new pathway. This strategy ensured that, rather than generating completely unknown potential issues, priority could be given to the existing processes with the greatest synthetic challenges.

The first area for investigation was the stereoselective fluorination reaction. The existing transformation showed poor enantioselectivity, despite using a chiral catalyst, and required chiral preparative chromatography to improve the ee to an acceptable level. It was speculated that using a bulky ester rather than ethyl ester **20** could improve the enantioselectivity. Furthermore, a bulky chiral ester, in combination with the matched chiral catalyst, might allow for a highly diastereoselective fluorination reaction. Additionally, if necessary, the required diastereomer of the product could then be further purified by crystallisation. This strategy envisaged the preparation of menthol derivative **30**, using inexpensive and readily available (+)- or (–)-menthol (Scheme 3).

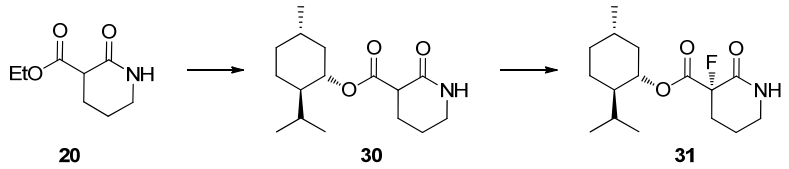

20 **30** **31**

Scheme 3: Proposed strategy for diastereoselective fluorination using ((+)- menthol derivative shown).

Accordingly, transesterification was carried out to prepare menthyl ester **30**.* Diastereoselective fluorination of the (+)-menthol derivative, in combination with the catalyst derived from (*S*)-BINAP, resulted in preparation of lactam **31** in 94% de after optimisation (Scheme 4).[39,45] The diastereomeric excess was improved to >99.9% de following recrystallisation from ethanol. The improved fluorination process was successfully carried out at 1 kg scale to provide fluorinated lactam **31** in 70% yield. Whilst the redeveloped route now consisted of one extra step, the yield was improved, and excellent diastereoselectivity was obtained without chromatography.

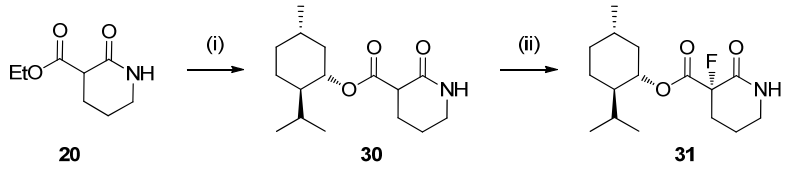

20 **30** **31**

Reagents & conditions: (i) (+)-Menthol, DMAP, toluene, reflux; (ii) 2,6-Lutidine, [Pd-(*S*)-BINAP(MeCN)$_2$](OTf)$_2$, (PhSO$_2$)$_2$NF, ethanol, 0 – 20 °C, 70% (2 steps).

Scheme 4: Formation of menthyl ester and subsequent diastereoselective fluorination.

The next challenge was achieving global reduction of fluorinated lactam **31** without using BH_3·THF at reflux due to the noted safety limitations. It was rapidly demonstrated that reaction at 40 °C was unacceptably slow, therefore, alternative reducing agents were investigated.[46] The dimethylsulfide complex of borane (BH_3·DMS) was identified as a suitable reagent for the transformation, with the main benefit being its increased thermal stability.[41] As a result, it is possible to utilise BH_3·DMS at reflux in THF, and this strategy was successfully used to effect the reduction of menthyl ester **31** to form alcohol **32** (Scheme 5).[47] Following *in situ* Boc protection of the amine group, alcohol **22** was isolated in 74% yield at 1 kg scale.

* Both (+)- and (–)-menthol compounds were prepared for assessment with the (*S*)- and (*R*)-BINAP catalysts.[45]

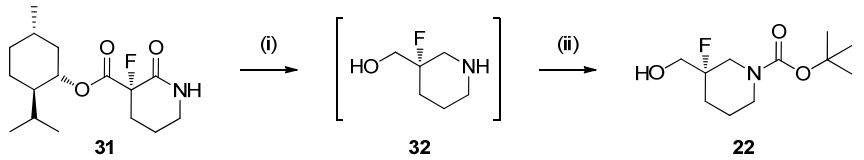

Reagents & conditions: (i) BH_3·DMS, THF, reflux; (ii) Boc_2O, DCM, NaOH (aq), room temperature, 74% (2 steps).

Scheme 5: Reduction and Boc protection process.

Redevelopment of the triflation was next required to substitute DCM for an alternative solvent on safety grounds. It should be noted that the use of DCM in the Boc protection process was not a particular issue since alcohol **22** was isolated as a solid from heptane, washed with further heptane, and dried *in vacuo.* This sequence of events ensured the DCM content of **22** was negligible and would not be carried through the synthesis.* The far greater safety risk was the use of DCM during formation of triflate **23**, since the product was isolated by concentration *in vacuo* and, as a result, such chlorinated solvent residues could remain within the crude product. Complete removal of solvent by rotary evaporation becomes more difficult as the scale is increased. Pyridine was identified as a suitable solvent and base for the preparation of triflate **23**, and this method was implemented on 635 g scale in 92% yield (Scheme 6).[45] The preparation of azide **24** was carried out without major modification from the original route. At 955 g scale azide **24** was isolated in 93% yield.[45]

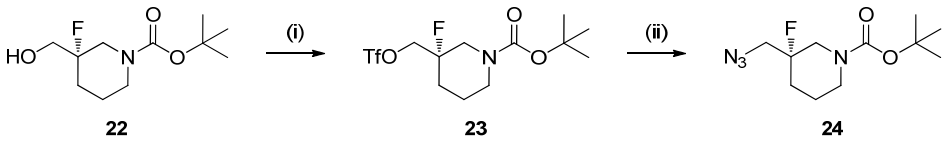

Reagents and conditions: (i) Tf_2O, pyridine, -10 °C, 92%; (ii) NaN_3, DMF, 30 °C, 93%.

*Scheme 6: Modified preparation of azide **24**.*

* Although DCM is generally removed from processes on environmental grounds, the use of DCM was continued in the preparation of alcohol **22** as a viable alternative was not forthcoming during the limited investigational time available prior to scale-up.

The next stage requiring scale-up was the azide hydrogenation to form amine **25** and this provides the main topic for discussion within this section of the present thesis. The modifications made to the subsequent stages in the synthesis of naphthyridine **19** will not be discussed in detail, and are summarised in section 3.5.

3.2 Project Objectives

With the preparation of Syk inhibitor **19** well underway in our scale-up facilities, the next stage requiring attention was that to form amine **25** from azide **24**, with the ultimate aim of preparing approximately 500 g of this key intermediate (Scheme 7). A number of strategies for azide reduction are documented within the literature,[4] with the main approaches being hydrogenation with a variety of catalysts,[48] reaction with lithium aluminium hydride[49] or reduction under Staudinger conditions using triphenylphosphine.[50]

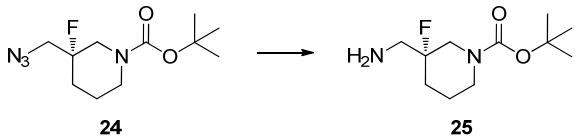

Reagents & conditions: Pd/C, H_2, ethanol, room temperature.

*Scheme 7: Reduction of azide **24**.*

The Staudinger conditions are mild and accomplish the selective reduction of azides in the presence of other sensitive functional groups. However, the main drawback is the use of stoichiometric PPh_3, which is converted to triphenylphosphine oxide during the course of the reaction. The result is a difficult to remove by-product, and large quantities of waste for disposal. Nevertheless, Merck used PPh_3 in a published synthesis of MK-0364 (taranabant **35**), which is in development for the treatment of obesity (Scheme 8).[51] Hydrogenation conditions were examined but it was noted that a number of impurities formed, and poor reproducibility was observed on scaling up the process. The Staudinger conditions were carried out at 2.6 kg scale of azide **33** in excellent overall yield.

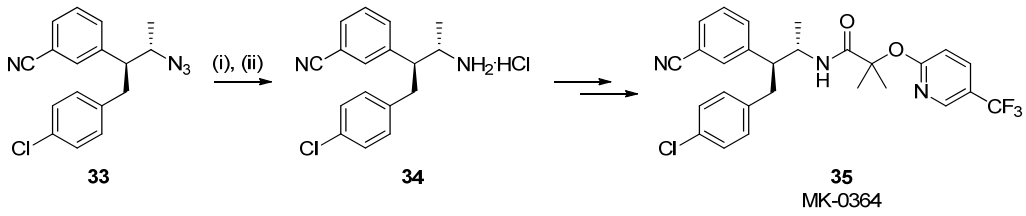

Reagents & conditions: (i) PPh_3, toluene, water, 70 °C; (ii) HCl/IPA, 81% (2 steps).

Scheme 8: Large scale Staudinger reaction.

As an alternative to hydrogenation, transfer hydrogenation, using ammonium formate as a hydrogen donor, has also been used to accomplish reductions of azides.[52] This strategy may be favourable since it is safer than using highly explosive hydrogen gas.

The existing procedure for preparation of amine **25** shown in Scheme 7 used hydrogenation conditions to bring about the reduction of azide **24**. The process was considered to be appropriate for development, not only for the required 200 g preparation of **19**, but also for longer term manufacture, since hydrogenations are atom economical and generally perform well at scale. Accordingly, other methods to achieve the desired reduction of azide **24** were not investigated.

3.3 Results & Discussion

3.3.1 Preparation of Amine 25

3.3.1.1 Initial Screening Experiments

The first experiments during our development work on the preparation of amine **25** concentrated on screening a number of catalysts for the transformation to determine whether the currently used palladium on carbon catalyst appeared optimal (Table 1).

Entry	Catalyst	Conversion 15.5 h / %[a]	Conversion 19.5 h / %[a]	Conversion - extra catalyst & 15 h / %[a]
1	PtO_2[b]	31	30	49
2	Pt/C F1[c]	13	16	16
3	Pd/C E1[c]	36	38	72
4	Pd/C 395M[d]	39	42	100
5	Pd/C 434[d]	41	46	92
6	$Pd(OH)_2$	41	46	97

Conditions: 0.0055 equiv. metal (corrected for assay), ethanol, 5 psi hydrogen, 19.5 h, remove catalyst and recharge, then 15 h under 5 psi hydrogen, ambient temperature, 800 rpm.

[a] Conversion (from LCMS, MS ES^+:TIC trace) = % area **25** x 100 / (% area **24** + % area **25**).

[b] 0.018 equiv. PtO_2 was used.

[c] Catalyst types from Evonik.

[d] Catalyst types from Johnson Matthey.

Table 1: Results of initial catalyst screening.

All reactions carried out were observed to stall after leaving overnight. In fact, the same result had been observed by our medicinal chemistry colleagues, who had demonstrated that filtering and recharging fresh catalyst was sufficient to restart the reaction.[53] The same strategy was applied here, and successfully showed that complete conversion of the starting material could be achieved. It thus appeared that possible catalyst poisoning could be occurring within the system and, although this problem could be easily overcome by a filtration and a second catalyst charge, the extra costs, waste, and increased process steps were not desired.

After the catalyst recharge, complete reaction was observed for a Pd/C catalyst (entry 4), whilst the $Pd(OH)_2$ reaction was almost finished (entry 6). The Pt catalysts had significant levels of starting material remaining (entries 1 & 2). The results suggested that use of a palladium catalyst rather than a platinum species would be preferred for the hydrogenation of azide **24**.

3.3.1.2 Identification of Secondary Amine Impurity 36

Continuing with catalyst screening, a number of other palladium on carbon catalysts were examined since palladium appeared superior from the initial experiments (Table 2).

Entry	Catalyst	Product 25 / %	Impurity 36 / %
1	Pd/C 395M[a]	70.6	29.4
2	Pd/C 39[a]	73.1	26.9
3	Pd/C E101 NO/W[b]	74.7	25.3

Conditions: 0.0055 equiv. metal (corrected for assay), ethanol, 5 psi hydrogen, 2 h, ambient temperature, 800 rpm.

Ratio of **25** to **36** is quoted from mass extraction in LCMS MS ES^+: TIC trace.

[a] Catalyst types from Johnson Matthey.

[b] Catalyst type from Evonik.

Table 2: Evaluation of Pd/C catalysts.

On this occasion, the reactions showed no stalling and were found to be complete within two hours. The only change which had been made was the input batch of azide **24**. The experiments in Table 1 used a batch of azide **24** derived from steps (iii) and (iv) in Scheme 2 (page 16), whilst the experiments in Table 2 used azide **24** from the newly developed processes shown in Scheme 6 (page 20). From these results it appeared that the old process azide may have contained some species responsible for deactivating the catalyst. Since all future available batches of azide **24** were to be prepared by the revised processes, the problem of the hydrogenation reaction stalling now seemed to be solved.

Having stated all of this, the experiments recorded in Table 2 introduced a new problem to the synthesis of amine **25**. An additional major peak was observed in the

LCMS trace, with the impurity level being fairly consistent between batches. In order to investigate whether this impurity could be an intermediate in the hydrogenation reaction, the reactions in Table 2 (entries 1 and 3) were continued for a further 3 h under the same conditions. There was no observable change on reanalysis suggesting that intermediates were not being formed.

Although the LCMS data were not quantitative, the impurity appeared to be present at a significant level. Mass spectrometry data allowed us to postulate that the unknown impurity may be a dimeric secondary amine **36** (Figure 10).

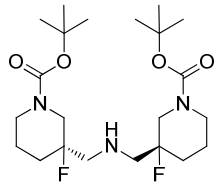

36

*Figure 10: Proposed secondary amine dimer impurity on hydrogenation of azide **24**.*

A search of the literature revealed that secondary amine dimers are a known by-product in azide hydrogenations although, to our knowledge, the phenomenon has not been widely reported.[54] There are, however, reports of the formation of secondary amine dimers during the closely related reduction of nitriles.[55] A potential mechanism for formation of secondary amines *via* reductive dimerisation during azide hydrogenations has been reported (Scheme 9).[56] It is suggested that the terminal azide nitrogen extracts the α-proton, which may be facilitated by complexed palladium. Subsequent loss of nitrogen then occurs to form the imine **38**. The primary amine product **25** from hydrogenation of the imine may react with imine **38** to form aminal **39**, which loses ammonia to form the *N*-substituted imine **40**. Hydrogenation then forms the secondary amine dimer **36**. Alternatively, hydrogenolysis of **39** could provide the secondary amine directly.

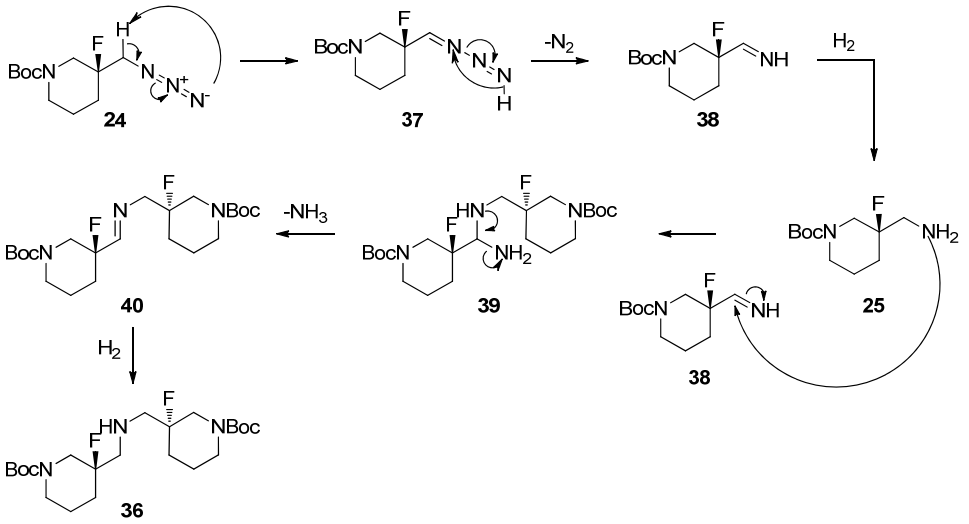

Scheme 9: Reported possible mechanism for formation of secondary amines via reductive dimerisation.

The group of Ahn support the mechanism given in Scheme 9, but they also suggest that a nitrile may be observed in the mechanism, since they cite evidence for the presence of nitriles within such reaction mixtures.[54] They propose that the nitrile may form by a dehydrogenation reaction, and the amine may add to this in a similar fashion to the addition of amine **25** to imine **38** in the above scheme.

The reaction mixture in entry 2 (Table 2) was worked up to isolate the crude product as a mixture of amine **25** and dimer **36**. The isolated material was subjected to preparative HPLC to obtain samples of each for characterisation. Spectroscopic data supported the postulated secondary amine structure **36**, but the exact ratio of the two amines was not determined.

3.3.1.3 Identification of N-Alkyl Impurities

The secondary amine formation was considered a risk to the process as it was occurring in unquantified amounts and had the potential to react further as part of the subsequent downstream chemistry. Reaction conditions to disfavour its formation were then investigated. The literature suggested that one way of reducing the amount of secondary amine formed would be to use alternative solvents; therefore a solvent screen was carried out (Table 3).[54]

Entry	Solvent	Product 25 / %	Secondary amine 36 / %
1	Ethanol	72.6	27.4
2	IPA	67.2	32.8
3	THF	71.4	28.6
4	Ethyl acetate	78.4	21.6
5	9:1 v/v ethanol:acetic acid	56.4	43.6

Conditions: 5% Pd/C 395M (10% w/w), 5 psi hydrogen, ambient temperature, 800 rpm. Ratio of **25** to **36** is quoted from mass extraction in LCMS MS ES^+: TIC trace.

Table 3: Solvent screen for azide hydrogenation.

The reactions in all solvents were run until no residual starting material was detected. Use of ethanol (entry 1) produced similar results to those observed previously (Table 2), whereas use of an alternative alcohol solvent, IPA, gave even higher amounts of secondary amine **36**. THF also showed no improvement (entry 3). It was noted that ethyl acetate showed some beneficial effect; however, the level of dimer **36** was still high (entry 4).

At this stage, it was postulated that addition of an acid could protonate the amine product **25**, and minimise the likelihood of this species reacting with the intermediate imine **38** (Scheme 9), thus limiting the formation of secondary amine **36**. This strategy has been successfully used to minimise secondary amine formation in the hydrogenation of nitriles.[55,57] However, use of acetic acid in the presence of ethanol was unsuccessful and resulted in a large number of impurities (Table 3, entry 5).

Further inspection of the data generated from the experiments in Table 3 revealed the presence of additional species in each case. Based on mass spectrometric data a number of *N*-alkyl impurities were proposed, which were postulated to form from reaction with the solvent (Figure 11). These proposed species have not been isolated or characterised. Thus the *N*-isopropyl impurity **41** could form from reaction with IPA (entry 2), **42** could form by ring opening of THF (entry 3) and the *N*-ethyl species **43** could derive from reaction with ethanol (entry 1).

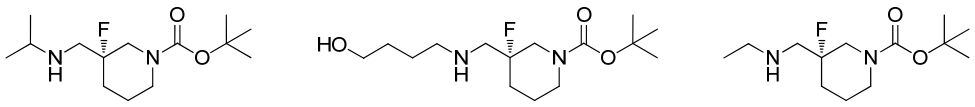

41 42 43

Figure 11: Proposed N-alkyl impurities observed in azide hydrogenations.

The data in Table 3 were reanalysed to include data on the *N*-alkyl impurities (Table 4). Thus it was observed that *N*-alkylation with the alcohol solvents was occurring in similar amounts for both ethyl and *iso*-propyl alcohols (entries 1 & 2).

Entry	Solvent	Product 25 / %	Secondary amine 36 / %	*N*-alkyl impurity / %
1	Ethanol	63.1	23.9	13.0 (**43**)
2	Propan-2-ol	57.7	28.2	14.1 (**41**)
3	THF	64.1	25.7	10.2 (**42**)
4	Ethyl acetate	78.4	21.6	- [a]
5	9:1 v/v ethanol:acetic acid	49.8	38.4	11.8 (**43**)

Conditions: 5% Pd/C 395M (10% w/w), 5 psi hydrogen, ambient temperature, 800 rpm. Ratio of **25** to **36** to *N*-alkyl impurity is quoted from mass extraction in LCMS MS ES^+: TIC trace.

[a] Proposed *N*-alkyl impurity masses were not extracted for this sample. Evidence for *N*-acylation was observed but not further investigated.

Table 4: Reanalysis of solvent screening data.

Mono- and bis-ethylation of amines has been reported during the hydrogenation of nitriles in ethanol, and it has been speculated that such impurities were being formed by reductive ethylation of an imine intermediate, but no proposed mechanistic details were provided.[58] Additionally, alkylation of amino acids during hydrogenation to remove protecting groups has also been reported.[59] In 1939, Schwoegler and Adkins reported a possible mechanism for the observed formation of secondary amines from the reaction between primary amines and alcohols under hydrogenation conditions.[60] They proposed that *in situ* dehydrogenation of the alcohol resulted in the formation of the corresponding aldehyde or ketone. The dehydrogenation of alcohols to aldehydes and ketones in the presence of palladium is generally carried out in the

presence of oxygen gas or hydrogen acceptors to ensure the active sites on the metal are reoxidised.[61] The process can, therefore, be catalytic in metal.

Applying this mechanism, ethanol could undergo dehydrogenation in the presence of the metal catalyst to result in the formation of acetaldehyde (Scheme 10). Reaction of amine **25** with acetaldehyde, and reduction of the resulting imine **44**, could furnish *N*-ethyl product **43**.

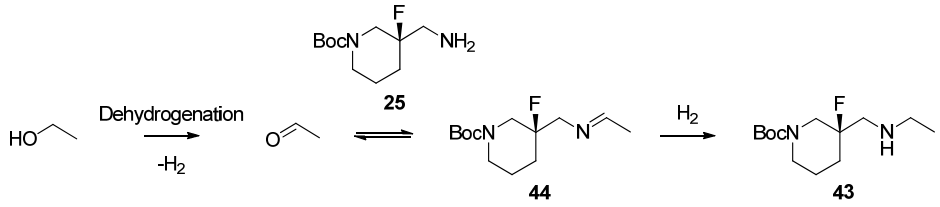

Scheme 10: Postulated mechanism for the formation of N-ethylated products.[60]

A similar mechanism could be proposed for the formation of the suggested *N*-alkyl impurity from reaction with THF (Scheme 11). Potentially, dehydrogenation forms oxonium species **45**, which undergoes imine formation and ring opening with amine **25**. Hydrogenation could then result in the impurity **42**.

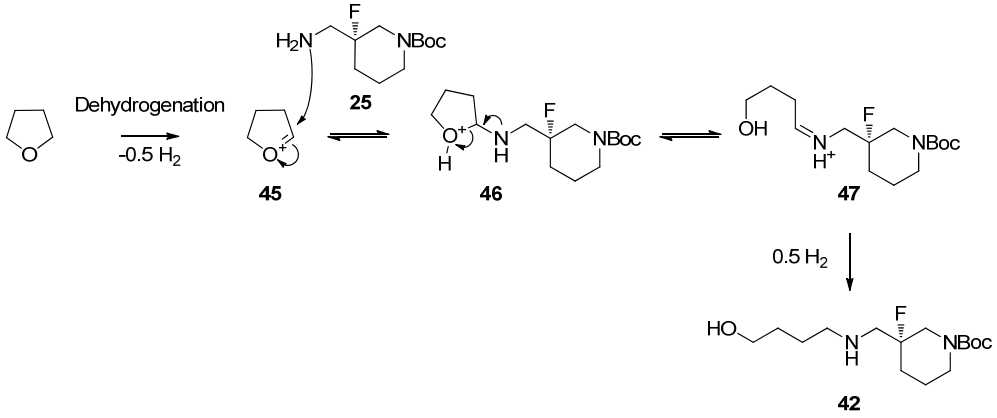

Scheme 11: Proposed impurity formation with THF.

3.3.1.4 Catalyst Identification

With the reduction of azide **24** now complicated by the identification of further impurities, it was decided to revisit the catalyst screen. Use of a different catalyst could affect the impurity levels observed during the reaction, and could offer significant benefits to the final product purity.

A second catalyst screen was carried out in ethanol, investigating both palladium and platinum metals (Table 5). All reactions were run until no starting material was detected and showed that, while palladium catalysts gave a faster reaction, the platinum catalysts gave lower amounts of secondary amine impurity **36**. In contrast, the platinum catalysts produced more *N*-ethyl impurity **43**. However, since this impurity is solvent dependent it was considered that this problem could be circumvented. Consequently, platinum appeared to be emerging as the better catalyst for the hydrogenation of azide **24**.

Entry	Catalyst	Reaction Time / h	Product 25 / %	Secondary amine 36 / %	*N*-Ethyl 43 / %
1	Pd/C 395M[a]	1	57.6	31.8	10.6
2	Pt/C F1[b]	2.5	66.5	3.3	30.3
3	$Pd(OH)_2$	1	64.9	23.6	11.5
4	PtO_2	2.5	74.2	5.5	20.3

Conditions: 0.0055 equiv. metal (corrected for assay), ethanol, 5 psi hydrogen, ambient temperature, 800 rpm.

Ratio of **25** to **36** to *N*-ethyl impurity **43** is quoted from mass extraction in LCMS MS ES^+: TIC trace.

[a] Catalyst type from Johnson Matthey.

[b] Catalyst types from Evonik.

Table 5: Second catalyst screen.

The reaction mixtures in entries 2 and 4 were worked up to isolate the crude material. ^{1}H NMR analysis showed the presence of extra quartet and triplet signals (not consistent with ethanol) lending further weight to the proposed *N*-ethyl structure **43**.

With promising results now being obtained it was decided to use a Pt/C catalyst for the hydrogenation since it produced the lowest amount of secondary amine **36**. Modification of the solvent should ensure that *N*-alkyl impurities could be avoided.

3.3.1.5 Solvent Identification

With the chosen catalyst identified as Pt/C, alternative solvents and conditions were next investigated to determine the effects on impurity levels (Table 6). The type of

Pt/C catalyst was changed from this point onwards to use a batch which was available within our pilot plant. The new catalyst was tested, and was shown to perform more effectively than the Pt/C catalyst previously used in terms of the impurity levels (compare Table 6, entry 1 with Table 5, entry 2, 78.4% *vs*. 66.5% **25**). The catalyst loading in ethanol was investigated briefly but this resulted in a slower reaction and more of the secondary amine impurity **36** (entries 1 & 2), and therefore offered no benefit. Ethyl acetate gave poor results with a high level of secondary amine **36**, and was not investigated further (entry 4).

Entry	Catalyst amount / % w/w	Solvent	Time / h	Product 25 / %	Secondary amine 36 / %	*N*-Alkyl / %
1	8.5	Ethanol	2.5	78.4	1.3	20.3 (**43**)
2	4.1	Ethanol	18.5[a]	65.8	10.2	24.0 (**43**)
3	8.5	Ethanol + 2.5 equiv. NH_3[b]	2.5	84.3	1.4	14.3 (**43**)
4	7.9	Ethyl acetate	18.5[a]	86.0	11.1	3.0[c] (**43**)
5	8.3	Ethanol/NH_3[b] 9:1 v/v	2.5	94.3	0.5	5.2 (**43**)
6	8.0	Toluene	4.5	98.6	1.4	-
7	8.1	TBME	4.5	97.9	2.1	-
8	8.2	THF	2.5	91.8	1.3	6.9 (**42**)

Conditions: 10% Pt/C (type 128, Johnson Matthey), 5 psi hydrogen, ambient temperature, 800 rpm.

Ratio of **25** to **36** to *N*-alkyl impurity is quoted from mass extraction in LCMS MS ES^+: TIC trace.

[a] Experiment left on overnight, although is expected to have been complete in less than 18.5 h.

[b] Concentrated aqueous ammonia solution (33% w/w in water).

[c] *N*-ethyl impurity could form from use of ethyl acetate, equally *N*-acylation could be postulated to occur, although this was not investigated in detail.

Table 6: Investigation of conditions with Pt/C catalyst.

For the reduction of nitriles it has been observed that addition of ammonia can reduce the amount of secondary amine impurities formed (Scheme 12).[60] It is proposed that ammonia reacts with intermediate imine **49** and the resulting *gem*-diamine **53** undergoes hydrogenolysis to give the primary amine **50**. A kinetic effect could be proposed such that the reaction of imine **49** with ammonia is faster than the competing reaction of imine **49** with the amine product **50** ($k_B > k_A$). In this way the amount of aminal **51** will be minimised, resulting in less of the secondary amine

dimer. Alternatively, a thermodynamic effect could be suggested: an excess of ammonia will favour the reaction of imine **49** with ammonia rather than amine **50**, sending the equilibrium to the side of **53**.

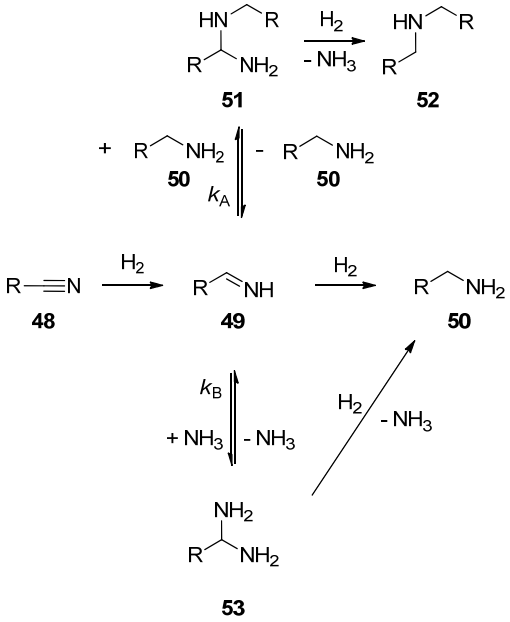

Scheme 12: Proposed effect of ammonia in hydrogenation of nitriles.

An experiment using aqueous ammonia and ethanol was performed (Table 6, entry 3). The addition of ammonia had no noticeable effect on the amount of secondary amine **36** formed in the reduction of azide **24** (compare entries 1 & 3). However, it did appear to have decreased the amount of the *N*-ethyl impurity **43**. The decrease in the amount of **43** may be a result of ammonia reacting with any acetaldehyde present to form the corresponding imine **54** (Scheme 13). Again, both kinetic and thermodynamic effects can be proposed. If reaction of ammonia with acetaldehyde is faster than the reaction of acetaldehyde with amine **25**, then the amount of ethylated product **43** would be minimised ($k_B > k_A$). On the other hand, the excess of ammonia may send the equilibrium position towards imine **54**. It was postulated that an increase in the amount of ammonia may result in lower levels of the *N*-ethyl impurity **43**, and may also have an effect on the amount of secondary amine **36**.

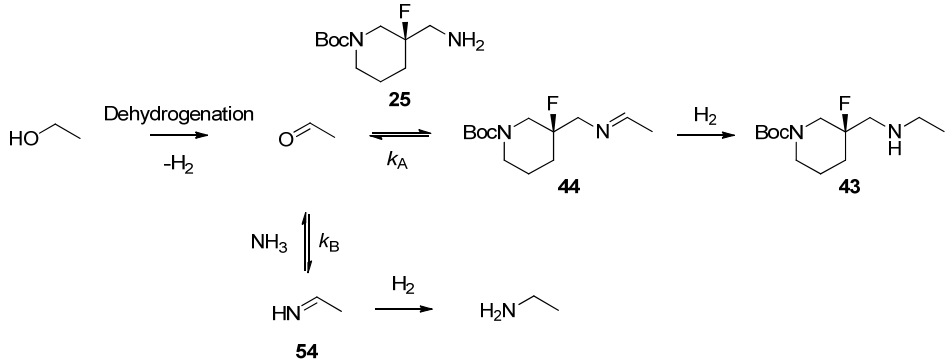

Scheme 13: Postulated mechanism for the effect of ammonia in the formation of N-ethylated products.

The use of ammonia was investigated in more detail. Gratifyingly, when the amount of ammonia was increased the level of both dimer **36** and *N*-ethyl impurity **43** were considerably lower (Table 6, entry 5).

Despite the advantages observed when using ammonia as an additive, two solvents expected to be inert to the formation of *N*-alkyl impurities were investigated (entries 6 & 7). Both toluene and TBME gave excellent results, with a low level of the dimer impurity **36**, but the reactions were slower. It is suggested that the increase in reaction time is a consequence of using water wet catalysts in water immiscible solvents.

Finally, THF was investigated (entry 8) and showed an acceptably low level of secondary amine dimer **36**. In addition, the amount of *N*-alkyl impurity **43** was also relatively low, especially when compared to the ethanol system (*e.g.* entry 1). It was speculated that addition of ammonia solution to THF could have a beneficial effect on the reaction impurities.

Returning to TBME, the use of this solvent was particularly attractive for a number of reasons. Firstly, the initial results appeared promising (Table 6) and, secondly, there was the potential to telescope the hydrogenation with the previous stage. In relation to this latter point, it should be noted that the process to prepare azide **24** was carried out in DMF, but worked up from TBME (Scheme 6). On a small scale azide **24** was isolated by concentration *in vacuo*. This method of isolation cannot be used at large scale; therefore using the azide/TBME solution directly for the hydrogenation

could provide a way of telescoping these two transformations. Experiments carried out to investigate the use of TBME are shown in Table 7.

Entry	Solvent	Pressure / psi	Agitation rate / rpm	Time / h	Product 25 / %	Secondary amine 36 / %
1	TBME	5	800	4.66	99.1	0.9
2	TBME/NH_3[a] 9:1 v/v	5	800	6.66[b]	99.7	0.3
3	TBME	42	800	4.5	97.5	2.5
4	TBME	5	150	6.5	98.2	1.8

Conditions: 10% Pt/C (8.3% w/w), room temperature.

Table shows final sample taken for each experiment.

Ratio of **25** to **36** is quoted from mass extraction in LCMS MS ES^+: TIC trace.

[a] Concentrated aqueous ammonia solution (33% w/w in water).

[b] Reaction not complete as residual starting material remained, ratio of **25** : **36** : **24** = 99.1 : 0.3 : 0.6.

Table 7: Investigations of hydrogenation in TBME.

The standard TBME repeat reaction was marginally better than the previous run with less secondary amine present (compare Table 7, entry 1 with Table 6, entry 7). Addition of ammonia to the TBME resulted in the fewest impurities overall, however, the reaction was considerably slower and not complete after 6 h 40 min (Table 7, entry 2). In this case the catalyst was observed to have become attached to the sides of the glass tube, presumably due to TBME and aqueous ammonia being immiscible. Increasing the pressure was not beneficial and resulted in considerable amounts of the secondary amine compared to the other runs (entry 3). The experiment with low agitation rate was expected to be slower due to poor mass transfer, and these conditions also resulted in more of the secondary amine (entry 4). This observation seems logical if it is assumed that poor agitation results in a build-up of imine intermediate **38** as the rate of its reduction decreases. The reaction of imine **38** with primary amine product **25** could then be more favourable (Scheme 14). Nevertheless, there is some promise for the use of TBME for the azide

hydrogenation. However, despite these results, the use of TBME was not pursued further as other conditions appeared to more effectively control the levels of secondary amine dimer impurity **36** (*vide infra*, Table 8).

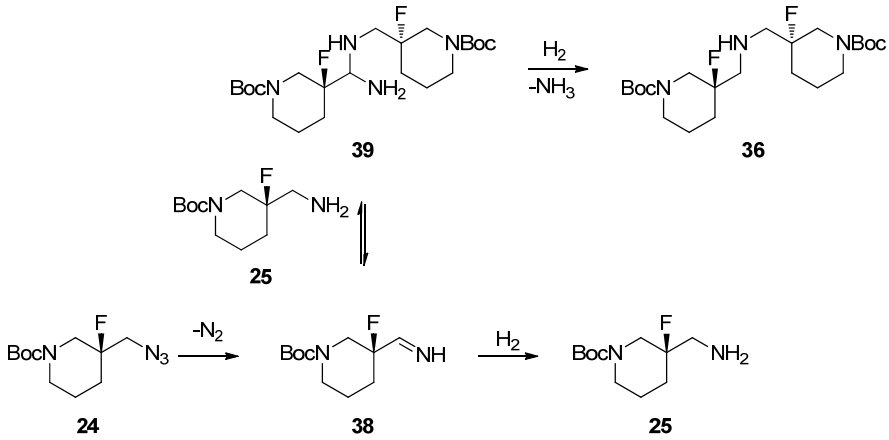

Scheme 14: Azide hydrogenation reaction pathways.

Returning to ammonia-containing solvent systems, it was of interest to further investigate the effect of ammonia on impurity levels in the azide hydrogenations (Table 8). Use of aqueous ethanol showed that ammonia (rather than water) is required to ensure the *N*-ethyl impurity level remains low (entry 1). Di-isopropyl ethyl amine (DIPEA) was investigated as an alternative base, but this resulted in both *N*-ethyl and *N*-isopropyl impurities being observed by LCMS (entry 2). Presumably the *N*-isopropyl impurity must have formed from reaction with the DIPEA, as there was no other source of an isopropyl group in the reaction mixture.

Entry	Solvent	Time / h	Product 25 / %	Secondary amine 36 / %	*N*-alkyl impurity / %
1	EtOH/water 9:1 v/v	2.5	79.8	2.3	17.9 (**43**)
2	Ethanol/DIPEA[a]	6	63.2	3.0	12.9 (**43**) 20.8 (**41**)
3	THF/NH_3[b] 9:1 v/v	6	99.5	0.1	0.4 (**42**)
4	THF/water 9:1 v/v	2.5	94.8	1.0	4.2 (**42**)

Conditions: 10% Pt/C (8.3% w/w), hydrogen (5 psi), room temperature, 800 rpm.
Ratio of **25** to **36** to *N*-alkyl impurity is quoted from mass extraction in LCMS MS ES^+: TIC trace.

[a] DIPEA amount 8.9 equiv. to be consistent with the ammonia amount.

[b] Concentrated aqueous ammonia solution (33% w/w in water).

Table 8: Investigations into the effect of ammonia.

The use of THF/ammonia resulted in low levels of both the secondary amine and *N*-alkyl impurities (entry 3). However, when using aqueous THF, with no ammonia, the secondary amine and *N*-alkyl impurity levels were higher, again emphasising the unique effect of aqueous ammonia in preventing impurity formation (entry 4). Having stated this, the use of aqueous THF compared to THF alone has improved the selectivity of the reaction towards the product and decreased the amount of impurities formed (compare Table 8, entry 4 with Table 6, entry 8).

With the THF/ammonia system showing such good results when compared to ethanol/ammonia in terms of minimising impurity levels, it was decided to concentrate further efforts on developing the THF/ammonia system for scale-up.

3.3.1.6 Process Scale-up

The experiments carried out at larger scale are recorded in Table 9.

Entry	Azide 24 mass / g	THF / vol	Time / h	Product 25 / %	Secondary amine 36 / %	*N*-alkyl 42 / %
1	2.7	20	22.5	99.1	0.9	0
2	0.15	13	18	99.7	0.1	0.2
3	4	13	35.25	99.7	0.1	0.2
4	616	13	39	99.6[a] (99.4)	0.2[a] (0.3)	0.2[a] (0.3)

Conditions: 10% Pt/C (8.3% w/w), NH_3 (33% w/w aqueous solution, 8.9 equiv.), hydrogen (5 psi), room temperature; for stirrer rate for each entry see experimental section.
Ratio of **25** to **36** to *N*-alkyl impurity **42** is quoted from mass extraction in LCMS MS ES^+: TIC trace. Values in parentheses are for the isolated product.
[a] LCMS data at 38.5 h.

Table 9: Larger scale experiments.

For the initial scale-up (entry 1) a slight modification was made to the process due to a limited amount of azide **24** available for use. Thus, in order to cover the agitator in the vessel, an increase in the solvent volume was required: the amount of THF was increased from 18 to 20 volumes, and the amount of ammonia was kept at 8.9 equivalents as in previous experiments. The ratio of THF to aqueous ammonia was therefore 10:1 v/v and the solvent phase was observed to be biphasic.

After 4 hours hydrogenation under 5 psi hydrogen significant starting material remained (67% conversion), and it was noticed that a large proportion of the catalyst was attached to the vessel walls. After 22.5 hours the catalyst was observed to be better dispersed, and there was no starting material present with low impurity levels. At this stage of development the long reaction time was not perceived to be a particular problem, although in the long-term, ideally, this should be optimised. It appears that the biphasic solvent, with the noted issues of catalyst adhering to the

vessel walls may be causing the reaction to proceed more slowly than in the smaller scale runs.

After filtration to remove the catalyst, the resulting solution, which was now a single phase, was concentrated *in vacuo* to obtain crude amine **25**. The material was successfully used in the next stage of chemistry, without further purification, to give the chloronaphthyridine product **27** in 87% yield.[47]

With conditions determined for scale-up it was again necessary to modify the process slightly. In this case, a lower volume of solvent was required in order to ensure an appropriate fill volume in our 20 L equipment. In view of this, an experiment was carried out in 13 volumes of THF with 8.9 equiv. aqueous ammonia (6.5:1 v/v) for 18 hours (entry 2). The reaction was considerably slower than reactions carried out previously at lower concentration at this scale. As a result, it was anticipated that on further scale-up to the 20 L vessel at least 18 hours reaction time would likely be required. With the exception of the longer reaction time, the solvent volume appeared not to have had a significant effect on impurities in the reaction mixture.

The conditions for scale-up were repeated at larger scale to ensure the batches of azide **24** and catalyst for use in the scale-up laboratory would perform adequately (entry 3). Again the reaction was observed to be slow and took over 35 hours until no starting material was detected (Figure 12). The impurity levels were identical to the smaller scale run. It was decided that the hydrogenation reaction would be run until azide **24** was no longer detected to ensure that it would not be present in the next stage where the high temperature reaction could pose safety hazards.

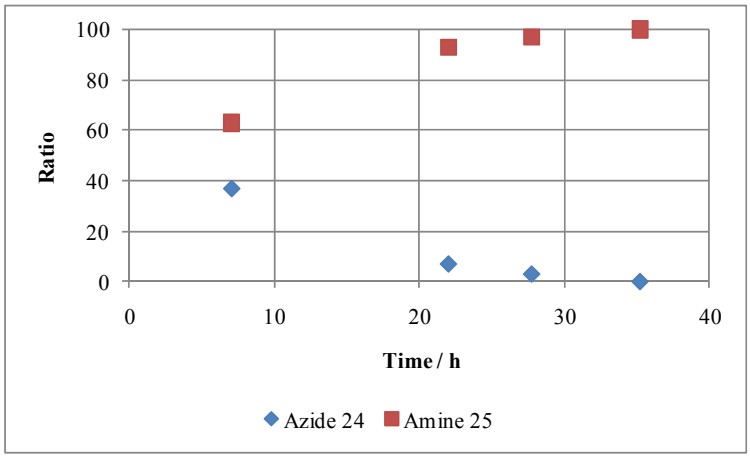

Figure 12: Reaction progress over time in THF (13 vol) & concentrated aqueous ammonia (2 vol).

Based on the accumulated developments to this stage, the hydrogenation of azide **24** was carried out in our scale up laboratory at 616 g scale (Table 9, entry 4). After 23 hours hydrogenation there was 88% conversion, and the reaction was complete within 38.5 hours. Crucially, the level of the impurities was observed to be low. Removal of the catalyst and concentration of the filtrate resulted in 552 g of material with no THF detected by ^{1}H NMR spectroscopy; however, the batch may still have contained some water which was not quantified.

3.4 Conclusions & Future Work

Following investigations into the hydrogenation of azide **24**, a process capable of delivering more than 500 g of amine **25** was devised. Process development identified two key secondary amine impurities: dimer **36**, and *N*-alkyl impurities, such as **42**. Control of these impurities was achieved by tuning both the catalyst and solvent system to minimise their formation. Of particular note was the addition of concentrated aqueous ammonia to the solvent, which was able to suppress the formation of the two impurities. Literature-based mechanistic proposals have been invoked to explain the effect of the ammonia additive.

The developed process to prepare amine **25** is not amenable to further scale up. The principal reason for this is that the isolation is a concentration *in vacuo*. The most straightforward way to progress the amine through the next stage would be to change the solvent after completing the hydrogenation. Addition of NMP and distillation to remove the THF could achieve this aim. The starting material azide **24** is also currently isolated by a concentration *in vacuo* from TBME. As it has been shown that the hydrogenation of azide **24** in TBME is viable, it is suggested that this should be one of the main areas to investigate prior to further scale-up.

One facet of scale-up to consider is the batch size and throughput. The azide hydrogenation reaction documented here was carried out in a total of 15 volumes of solvent (13 vol THF and 2 vol concentrated aqueous ammonia), which is relatively dilute (in process development terms) and will limit throughput. Additionally, the reaction was slow. These factors need to be carefully considered in order to develop a process suitable for use at pilot plant scale.

The emphasis of this project was on rapid development with short timelines to deliver amine **25** of appropriate quality. In this respect, the developed process represents a typical “fit for purpose” approach to process chemistry for early phase projects. Sufficient information was gathered to allow the material to be prepared. However, it is highly likely that the process, and even the route to Syk inhibitor **19**, will be changed significantly as a result of future research. This does, of course, depend on the project progressing successfully.

3.5 Project Status

The remaining synthetic stages towards Syk inhibitor **19** were completed in our scale-up laboratory (Scheme 15).

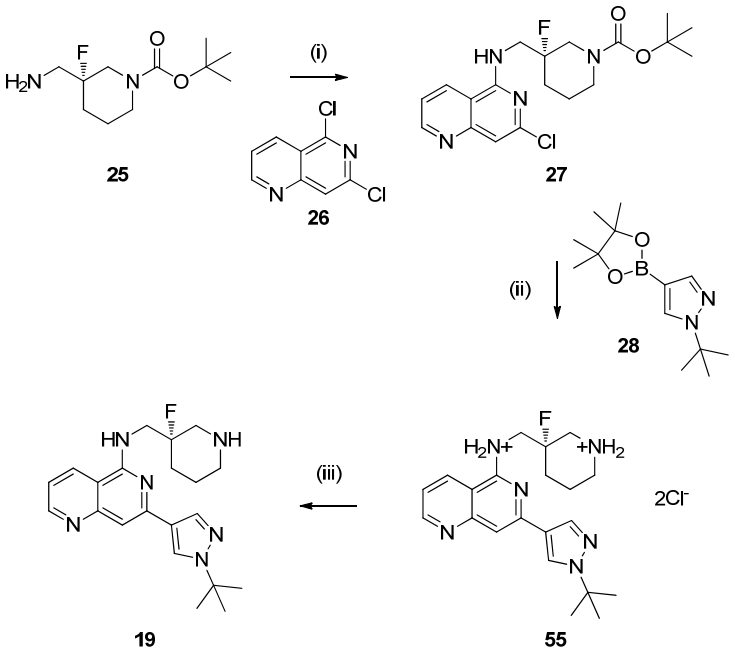

Reagents & conditions: (i) DIPEA, NMP, 110 °C, 92%; (ii) (a) $NaHCO_3$, 1,1'-bis(di-*t*-butylphosphino)ferrocene palladium dichloride, 1,4-dioxane/water (4:1), reflux; (b) 4 M HCl in 1,4-dioxane, toluene, 60 °C, 94% (2 steps); (iii) Aqueous NaOH, ethyl acetate, then *n*-BuOAc, TBME, 57%.

*Scheme 15: Final stages to Syk inhibitor **19**.*

Chloronaphthyridine **27** was prepared using a process very similar to the medicinal chemistry procedure. Chromatography was avoided by crystallisation of the product with water. The process was carried out at 400 g scale to prepare **27** in 92% yield.[62] The Suzuki-Miyaura chemistry was modified to use 1,1'-bis(di-*tert*-butylphosphino)ferrocene palladium dichloride as the catalyst (0.5 mol %). Furthermore, the Boc deprotection was carried out directly without isolation of the Suzuki-Miyaura product. This process was completed in 94% yield at 630 g scale to isolate the di-hydrochloride salt **55**.[63] In the final step the di-hydrochloride salt was

converted to the free base at 700 g scale in 57% yield,* thus preparing over 330 g of Syk inhibitor **19** for testing and development.[62]

A second campaign to prepare approximately 8 kg of the API has also since been completed.[64]

* The relatively poor yield for this apparently simple transformation was a result of difficulties in crystallising free base **19**. This remains an area for further optimisation.

4 Darapladib

4.1 Introduction

4.1.1 Atherosclerosis and Treatment

Coronary heart disease (CHD) is one of the most common causes of death in the developed world. Published statistics indicate that CHD caused 1 in 6 deaths in the USA in 2008.[65] One of the main causes of CHD is atherosclerosis, which is a build-up of plaques inside the arteries. These plaques may consist of fats, cholesterol, and calcium, and lead to two main issues. First, the presence of atherosclerotic plaques within arteries leads to narrowing of the artery and restriction of blood flow. Restriction of blood flow to the heart muscle can result in angina and heart attack. Secondly, the plaques are prone to rupture, leading to immediate formation of blood clots and major clinical events such as myocardial infarction, strokes, and cardiovascular death.[66]

There is currently no direct treatment for atherosclerosis. In the absence of targeted medicines the primary therapies to control the progression of the disease are incorporation of lifestyle changes (*e.g.* diet and exercise), cessation of smoking, and treatment of other contributing diseases, such as diabetes and hypertension. These are so-called risk factors relating to atherosclerosis.[67] The alternative is to use existing drugs to treat atherosclerosis, by an indirect biological mode of action.

Since one of the main components of atherosclerotic plaques is cholesterol, statins are prescribed to treat patients at high risk of coronary events (Figure 13).[68] Statins reduce cholesterol production in the liver by inhibiting the enzyme 3-hydroxy-3-methylglutaryl-coenzyme A (HMG-CoA) reductase. This leads to decreased levels of low density lipoprotein (LDL) cholesterol, and hence results in fewer arterial plaques. Clinical evidence from a number of studies suggests that use of statins can halt the formation of plaques.[68] A reduction in the size of atherosclerotic plaques has been reported when dosing patients with high intensity Crestor (rosuvastatin), **57**, therapy.[69]

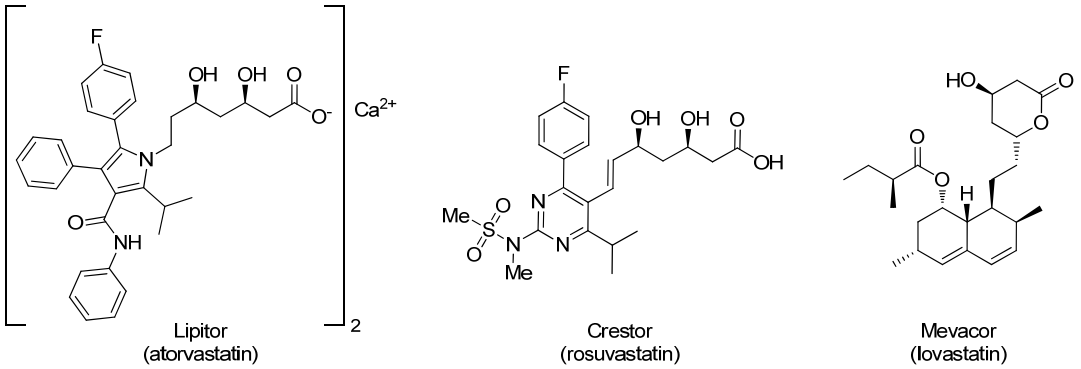

Figure 13: Examples of marketed statins.

Statins are amongst the biggest selling prescribed drugs in the world. Lipitor (atorvastatin) **56** is a worldwide best-selling drug.[70] The global sales figures for 2010 were over $10 billion. Nevertheless, there remains an unmet medical need in the direct treatment of atherosclerosis by novel treatments that target alternative biological modes of action involved in the formation of arterial plaques.

4.1.2 Lp-PLA$_2$ – A New Target for Atherosclerotic Therapy

In 1995 scientists at GSK reported isolation, sequencing, and cloning of the enzyme lipoprotein-associated phospholipase A_2 (Lp-PLA$_2$).[71,72] This serine lipase is produced by inflammatory cells and circulates in the bloodstream with LDL cholesterol. LDL collects in arteries around arterial plaques and is oxidised *in situ*. The oxidation produces a phospholipid component, which is hydrolysed by Lp-PLA$_2$ to form two lipid products. These lipids become a part of the atherosclerotic plaques and exacerbate the condition. Plaques grow as more circulating cells and components are incorporated into the structure, and this causes arteries to narrow, eventually resulting in plaque rupture and clinical events.[66,73] Lp-PLA$_2$ is also thought to be expressed by the inflammatory cells within the plaque itself. Measurement of the level of Lp-PLA$_2$ in blood plasma appears to be an excellent indicator of the risk of future cardiac events.[74] With Lp-PLA$_2$ playing a key role in the development of plaques, it is believed that inhibitors of this enzyme could have therapeutic uses in the treatment of atherosclerosis, potentially by stabilising those plaques at risk of rupture, preventing plaque growth, and reducing plaque size.

4.1.3 GSK's Approach to Small Molecule Lp-PLA$_2$ Inhibitors

The identification of potent small molecule Lp-PLA$_2$ inhibitors within our laboratories has been an area of focus since the isolation of the enzyme. The structure of these inhibitors has developed over time to reach an optimum target with the required levels of inhibition and physicochemical properties.

Early small molecule inhibitors of Lp-PLA$_2$ investigated by GSK were based on structures with a β-lactam core, for example **59** (both enantiomers and the racemate) and **60**,[75,76] including derivatives of clavulanic acid **61** (Figure 14).[77]

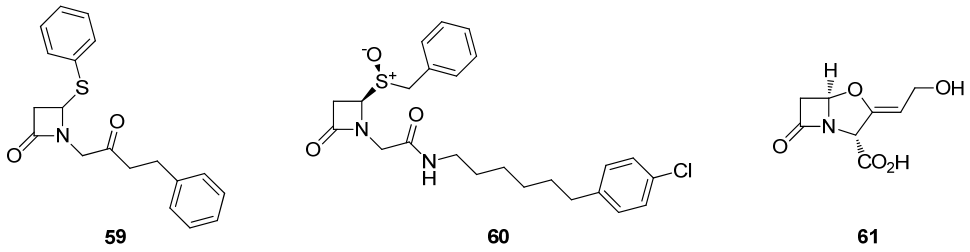

Figure 14: β-Lactam derivatives as Lp-PLA$_2$ inhibitors.

These molecules underwent covalent interactions with the serine residue within the enzyme active site, *via* hydrolysis of the lactam, and were relatively modest inhibitors (Scheme 16).[75] Hence, alternative reversible Lp-PLA$_2$ inhibitors were required with improved activity, to be able to identify and progress a suitable drug candidate.

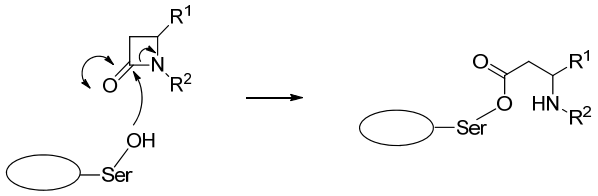

Scheme 16: Proposed covalent interactions of β-lactams with Lp-PLA$_2$.

Whilst searching for small molecule Lp-PLA$_2$ inhibitors, some investigations were carried out to examine natural products as inhibitors. SB-253514, **62**, isolated from the bacterium *Pseudomonas fluorescens*, was shown to demonstrate high levels of inhibition of Lp-PLA$_2$ (Figure 15).[78] Thus, a series of compounds was prepared using **62** as a basis. The sugar moiety was shown not to play a role in inhibitory activity;

consequently, derivatives of the bicyclic proline-derived enol-carbamate structure **63** were prepared. Limited examples are documented within the cited publication, with the R group being restricted to various alkyl chains. It was noted that longer alkyl chains resulted in increased inhibition of Lp-PLA_2.

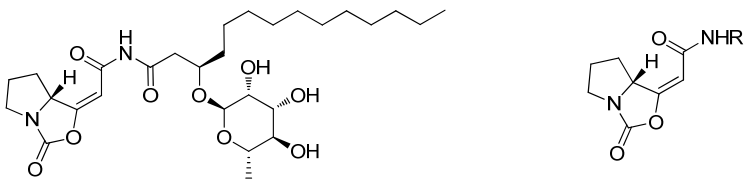

62
SB-253514

63

*Figure 15: SB-253514 (**62**) as a template for a natural product based Lp-PLA_2 inhibitor.*

Presumably a similar covalent mechanism to that shown in Scheme 16 operates with the bicyclic proline derivatives **63**, *via* opening of the carbamate by a serine residue. Therefore, these species were non-ideal and the search turned towards reversible Lp-PLA_2 inhibitors. High throughput screening within our laboratories showed that structures containing a pyrimidone moiety **64** were weak, reversible inhibitors of Lp-PLA_2 (Figure 16).[79] Exploration of the 2- and 5-pyrimidone substituents led to the preparation of structures exemplified by **65**.[80] However, compounds of this type exhibited little activity *in vivo*.

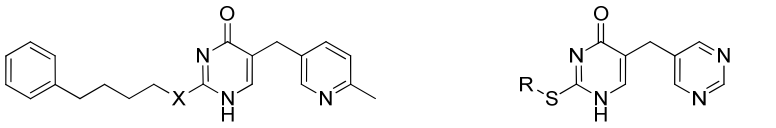

X = O, S

64

R = $(CH_2)_7COC_6H_4$(4-Cl), CH_2Ph

65

Figure 16: Pyrimidone structures as Lp-PLA_2 inhibitors.

Investigations into substituents at the pyrimidone N^1- and N^3-positions showed that inhibition of Lp-PLA_2 was improved in the presence of an N^1 substituent; therefore, further structures of this type were explored.[80,81] Amide N^1 substituents proved to be effective and modification of the *S*-benzyl group to include a 4-fluoro group increased potency (**66**, Figure 17). However, these structures were poorly water soluble and were not suitable for further progression. In an effort to improve the

solubility of the compounds, molecules such as **67** were prepared.[82,83] These species were very active when dosed intravenously. However, there was still a desire to prepare orally active Lp-PLA_2 inhibitors.

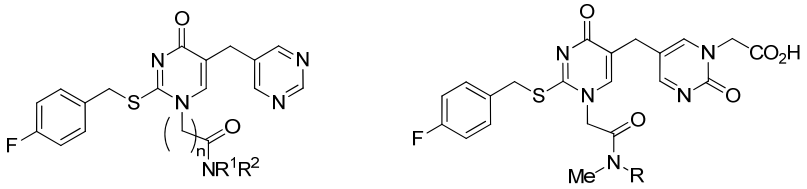

66 **67**

Figure 17: N^1-substituted pyrimidones.

Whilst working to identify orally active compounds, piperazine amides such as **68** were prepared (Figure 18).[84,85] Although the oral availability was improved it was speculated that further enhancements would be possible if a biaryl group was introduced. This led to the preparation of structures illustrated by **69**.[86,87] Once again issues were encountered, this time with difficulties formulating the compounds for *in vivo* studies. Therefore, alternative molecular targets were required.

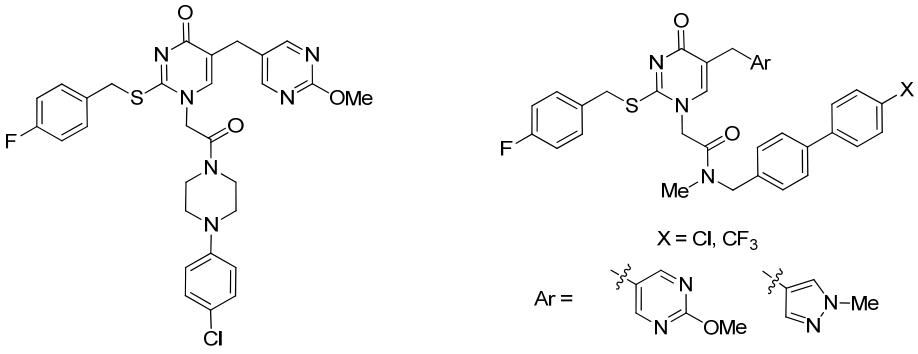

68 **69**

Figure 18: Development of orally active Lp-PLA_2 inhibitors.

More polarity was added to the amide substituent by introducing alcohol and amine groups.[87,88] SB-435495, **70**, showed excellent results and was identified as a potential candidate for evaluation in humans (Figure 19). In an effort to identify equally potent compounds of lower molecular weight, the molecule was further simplified by

modification of the pyrimidone 5-substituent.[89] Introduction of a cyclopentyl group fused at the 5-/6-position of the pyrimidone produced darapladib **71** (SB-480848)[90] which was successfully progressed into clinical trials in humans.

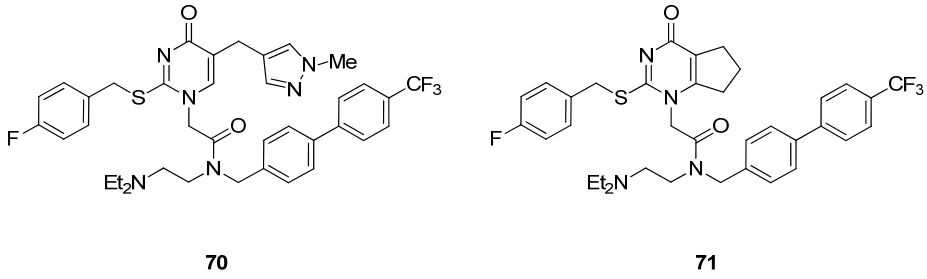

Figure 19: SB-435495 ***70*** *and darapladib (SB-480848)* ***71*** *- inhibitors of Lp-PLA$_2$.*

Darapladib is currently in phase III clinical trials for treatment of atherosclerosis by inhibition of the enzyme Lp-PLA$_2$.

4.1.4 Early Routes to Darapladib

The first published route to darapladib **71** is shown in Scheme 17.[89,90] The route was used for multiple similar compounds therefore no optimisation was carried out. Keto-ester **72** was condensed with thiourea to form a thiouracil,[91] which was alkylated with 4-fluorobenzyl chloride **78** (4-FBnCl) to form **73**. A second alkylation with *t*-butyl iodoacetate was carried out followed by deprotection of the *t*-butyl ester to yield carboxylic acid **74**. Amine **77** was prepared starting from a Suzuki-Miyaura cross-coupling reaction between 4-bromobenzaldehyde **75** and 4-trifluoromethylbenzene boronic acid. The biaryl aldehyde product **76** underwent imine formation with *N*,*N*-diethylethylenediamine, followed by reduction with sodium borohydride to form amine **77**. Amide bond formation between carboxylic acid **74** and amine **77** used the coupling reagent 1-ethyl-3-(3-dimethylaminopropyl)carbodiimide (EDC) to furnish darapladib **71**.

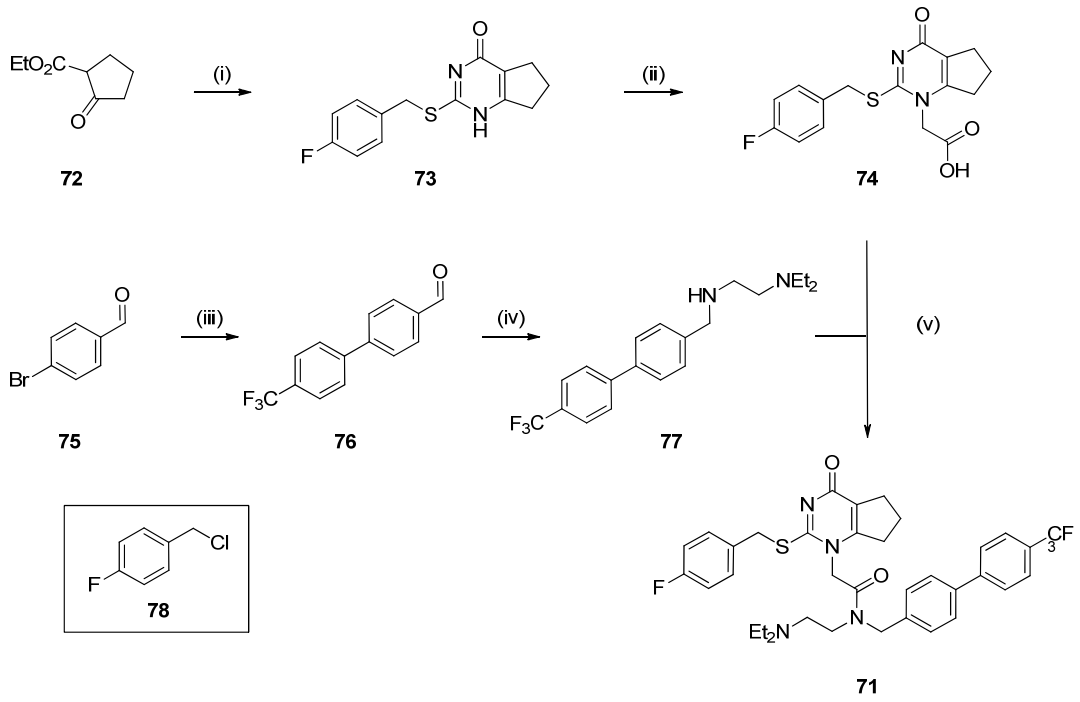

Reagents & conditions: (i) (a) Thiourea, NaOEt, EtOH, reflux; (b) 4-FBnCl **78**, K_2CO_3, DMF, 90 °C; (ii) (a) *t*BuO_2CCH_2I, *i*Pr_2NEt, CH_2Cl_2, room temperature; (b) TFA, CH_2Cl_2, room temperature; (iii) 4-trifluoromethylbenzene boronic acid, $Pd(PPh_3)_4$, Na_2CO_3, dimethoxyethane, reflux; (iv) (a) *N*,*N*-diethylethylenediamine, CH_2Cl_2, room temperature; (b) $NaBH_4$, EtOH, 0-50 °C; (v) EDC, HOBT, DMF, room temperature, 64%.[*]

Scheme 17: Reported medicinal chemistry route to darapladib.

This medicinal chemistry route was deemed acceptable as a starting point for further development work, thus the intermediates *en route* to darapladib remained the same as in Scheme 17. However, one area in need of development was the reaction to alkylate thiouracil **73** on N^1 to form ester **79** (Scheme 18). Effectively no regioselectivity was observed during this process, with alkylation on both N^3 and *O* also occurring. Chromatography was necessary to separate the three regioisomers that formed and, as a result, the desired product was typically isolated in poor yield (up to only 38% of **79**).[92]

[*] The patent documenting this route only quotes the yield for the final transformation.[90]

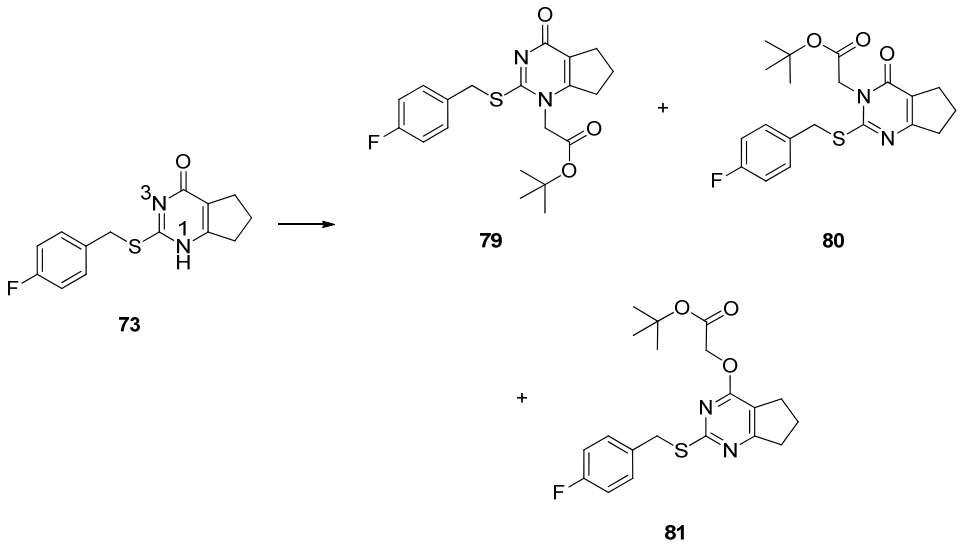

Reagents & conditions: tBuO$_2$CCH$_2$I, iPr$_2$NEt, CH$_2$Cl$_2$, room temperature. Ratio of isomers not recorded.

Scheme 18: Alkylation of thiouracil ***73****.*

In order to address the regioselectivity issues, a new process using silylation to block the unwanted formation of the N^3- and *O*-regioisomers was developed.[93] On treatment of **73** with 1,1,1,3,3,3-hexamethyldisilazane (HMDS), in the presence of catalytic saccharin,[94] intermediate **82** was formed, which was alkylated with triflate **83** to provide **84** as the major product (Scheme 19). The methyl ester was hydrolysed directly to form carboxylic acid **74** in 69% yield. The use of deactivated pyrimidone intermediate **82** required the use of the more reactive triflate electrophile rather than the iodide used previously.

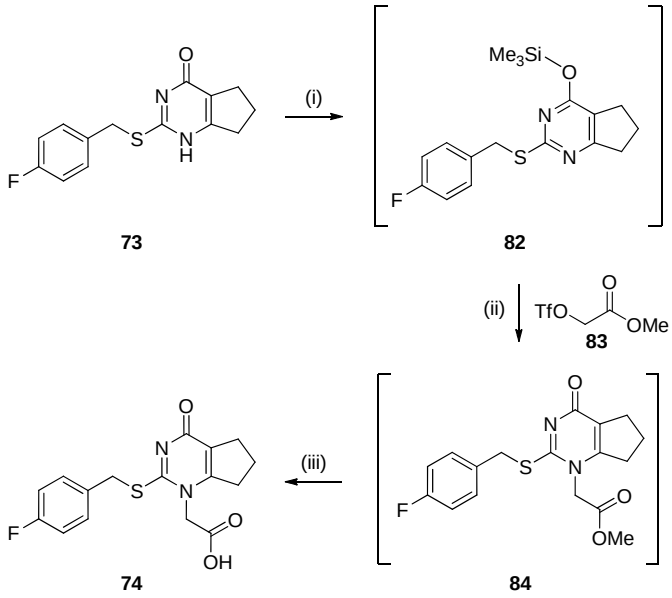

73 **82** **83** **74** **84**

Reagents & conditions: (i) Saccharin (1.5 mol%), HMDS, CH_2Cl_2, reflux; (ii) Reflux; (iii) Aqueous NaOH, IPA, 69%.

*Scheme 19: Regioselective alkylation to form carboxylic acid **74**.*

Whilst this silylation-alkylation method was adequate for early development, and used to produce over 30 kg of darapladib,[95] it was not considered acceptable for long term use. The triflate was prepared from reaction of the corresponding alcohol with triflic anhydride. The cost and safe handling of triflic anhydride were of some concern, as was the potential for supply limitations. Additionally, after running the chemistry shown in Scheme 19 at 20 kg scale it was noted that stringent control of the reaction parameters was required throughout the process.[96]

Alternative methods for performing the key regioselective alkylation step were investigated, and it was postulated that a standard haloester could be used in the presence of another reagent, such as a Lewis acid, without silylation. The Lewis acid could co-ordinate with the oxygen and act in similar fashion to the silyl group, without the formation of a (stronger) covalent bond. After considerable experimentation and optimisation work, zinc bromide was identified as being a suitable reagent, and the alkylation was carried out with *t*-butyl bromoacetate to furnish *t*-butyl ester **79** in typically 65-69% isolated yield.[97]

The most recently used reagents and conditions to form darapladib by this route are shown in Schemes 20 to 22. Over 5000 kg of darapladib have been prepared by this route to provide material for clinical trials. As in the medicinal chemistry route, keto ester **72** is condensed with thiourea then *S*-alkylated with 4-FBnCl to form **73** (Scheme 20). The regioselective *N*-alkylation using zinc bromide forms ester **79**, which is deprotected using concentrated sulfuric acid in acetic acid.

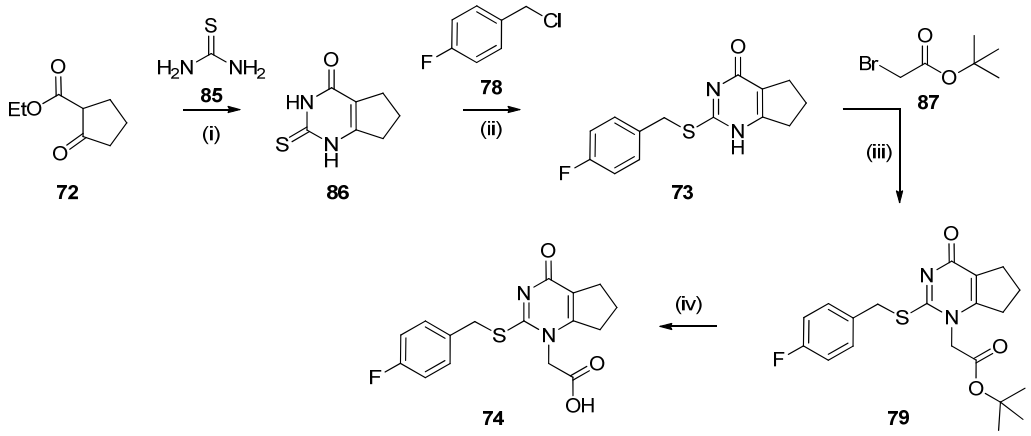

Reagents and conditions:* (i) Piperidine, toluene, reflux, 80-90%; (ii) KOH, aqueous IPA, 50 °C, 91-97%; (iii) $ZnBr_2$, *i*$PrNEt_2$, NMP, MeCN, 60 °C, 65-69%; (iv) Conc. H_2SO_4, AcOH, 45 °C, 89-95%.

*Scheme 20: Preparation of carboxylic acid **74**.*

The amine coupling partner **77** is prepared from aryl bromide **75** and boronic acid **88** *via* a Suzuki-Miyaura reaction with palladium on carbon catalyst (Scheme 21).[98] A reductive amination strategy is then used to form amine **77**, employing a palladium catalysed hydrogenation.

* Yield ranges are quoted for all stages. This is typical practice when scaling up since variation is observed during development work and in plant batches.

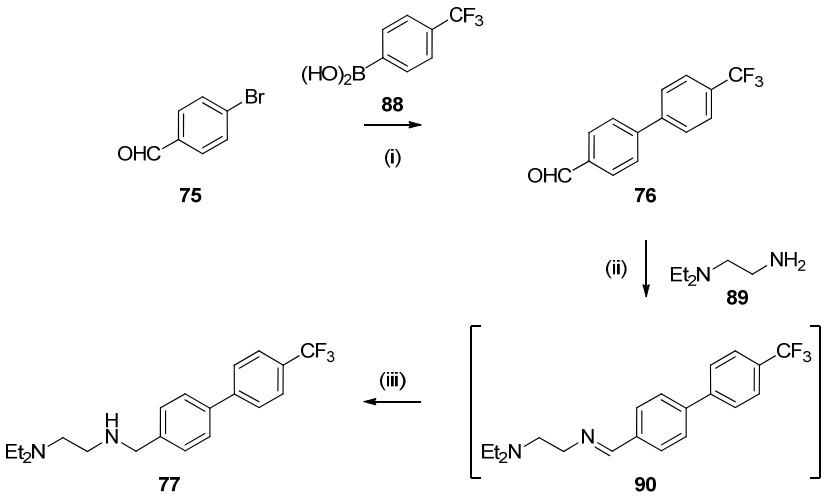

Reagents and conditions: (i) Pd/C, Na_2CO_3, IMS, reflux, 86-95%; (ii) Pd/C, toluene, 20 °C; (iii) 50 psi H_2, 20 °C, quantitative (2 steps).

*Scheme 21: Preparation of amine **77**.*

Reaction of carboxylic acid **74** with amine **77** using carbonyldiimidazole (CDI) allows preparation of darapladib intermediate grade (IG) (Scheme 22). The API is then prepared by recrystallisation from *iso*-propyl acetate, which also produces the most thermodynamically stable solid state form.[93]

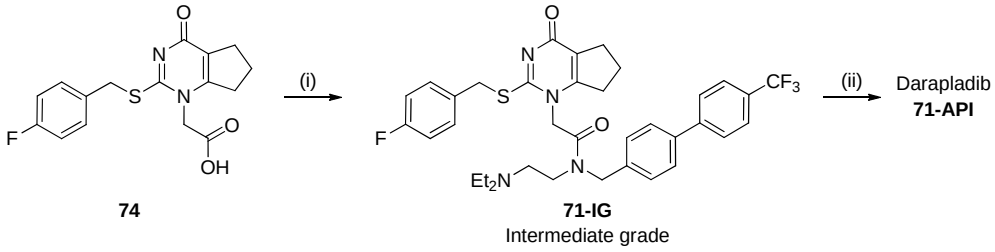

Reagents and conditions: (i) (a) CDI, MIBK, 70 °C; (b) **77**, 92 °C; 75-90%; (ii) *i*PrOAc, 89-92%.

Scheme 22: Preparation of darapladib.

Despite the development work involved in identifying the route and conditions shown, a number of problems remained which rendered the route unattractive for use in long-term manufacture. Again, the key alkylation stage to form ester **79** was identified as being problematic. The chemistry was low yielding when compared to the other stages, and the stoichiometric use of zinc bromide resulted in a large aqueous zinc-containing waste stream during the process work-up. At manufacturing

scale this must be transported for treatment and incineration. Whilst the waste disposal cost is relatively low (estimated at £11/kg of API) the environmental impact from the transportation and incineration reduces the process sustainability in the long-term. Efforts to find improved process conditions, for example using different solvents and investigating alternative Lewis acids, were ultimately unproductive, and offered few benefits over the existing route.[99]

4.1.5 New Route Identification

After considerable work within our laboratories[100] a new route to carboxylic acid **74** was identified (Scheme 23).[101]

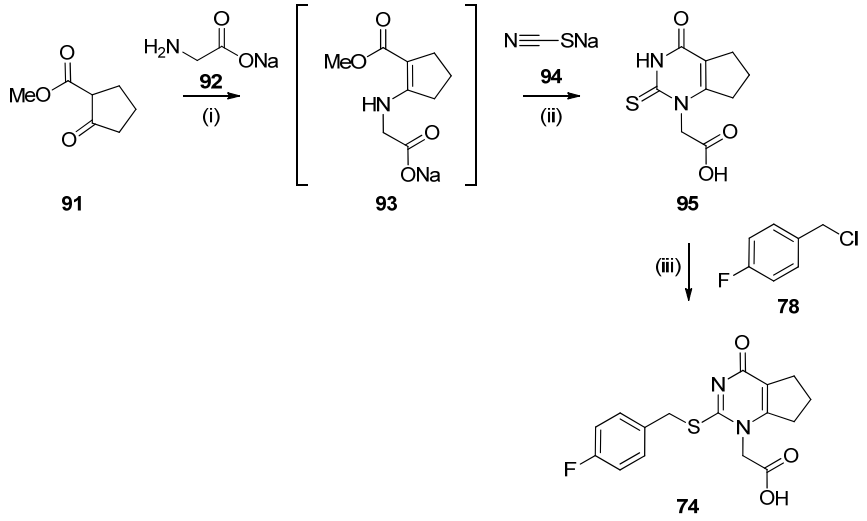

Reagents and conditions: (i) NMP, 60 °C; (ii) TMSCl, reflux, 64-79% (2 steps); (iii) NaOH, Na_2CO_3, IPA, water, 40 °C, 90-95%.

*Scheme 23: New route to carboxylic acid **74**.*

The route begins with methyl ester **91** rather than ethyl ester **72**.* Enamine **93** is formed from condensation of **91** with sodium glycinate **92**. The product enamine is not isolated, but telescoped into the next stage of the process, where reaction with sodium thiocyanate **94** forms thiouracil **95**. This process was developed based upon a similar literature approach.[102] Significant development work identified sodium

* Either the methyl or ethyl ester can be used; it was decided to use the methyl ester following a thorough assessment of contributing factors such as cost and availability.

thiocyanate as an alternative reagent to trimethylsilylisothiocyanate, which was used in the literature example. Advantageously, sodium thiocyanate is cheaper and more readily available than trimethylsilylisothiocyanate. The use of trimethylsilyl chloride (TMSCl) was introduced to facilitate the reaction and reduce the amount of thiocyanate reagent needed.[103] Further experimental work within our laboratories showed that using anhydrous acid was also beneficial for the reaction.[103,104] This has led us to speculate that activation of the ester is required for a successful and high yielding reaction. Activation may occur by silylation with trimethylsilylisothiocyanate or TMSCl (**A**, Scheme 24); alternatively, activation by acid may take place (**C**). It is also possible that TMSCl may react with the water by-product from the enamine formation (**91** to **93**) to form HCl *in situ*.

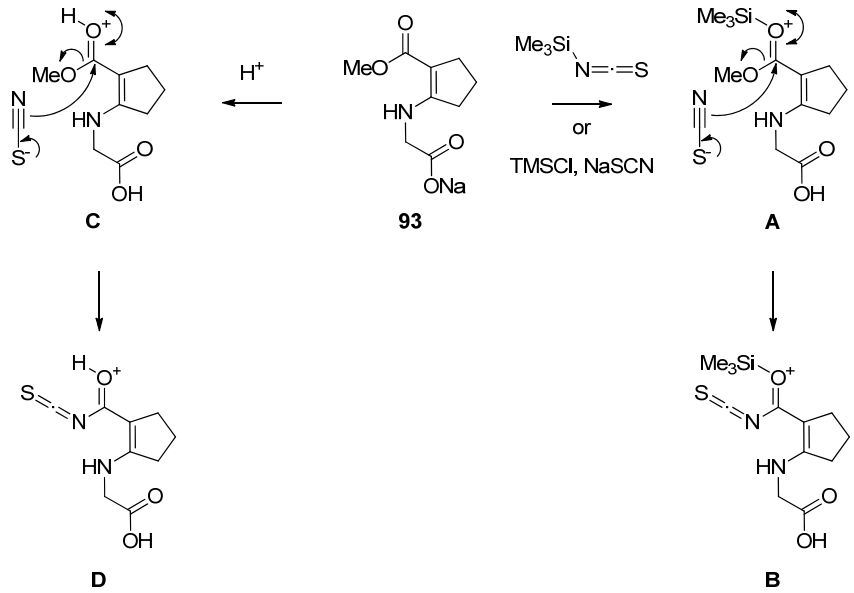

Scheme 24: Proposed effect of silylating reagents or acid to activate thiouracil ***93****.*

Synthesis of carboxylic acid **74** was completed by alkylation of thiouracil **95** on sulfur with 4-FBnCl **78** (Scheme 23). The synthetic route to acid **74** is now only three steps from commercially available starting materials (and two if one counts only isolated compounds) compared to four in the previous route. The route to amine **77** and the final steps to darapladib API remain unchanged (Schemes 21 & 22, page 55).

The new route was successfully operated at scale to deliver over 430 kg of carboxylic acid **74** in our pilot plant.[105] The redeveloped route offers a number of improvements over the previous sequence. The overall yield is improved from 37.0% to 50.3%* based on ketoesters **72** and **91** respectively; the number of stages is decreased from seven to five (counting isolated intermediates only); and the requirement for stoichiometric zinc is circumvented.

The new route also needs to be able to provide high quality material, and demonstrate control over impurities. In particular, understanding the origin and fate of organic impurities is important to ensure quality targets can be routinely met. One species of interest in the new route is 4-FBnCl as it is now used at a (relatively) later stage in the synthesis than it was previously. There are a number of areas which need to be investigated for this impurity: (i) control of 4-FBnCl during the reaction to form carboxylic acid **74**; (ii) understanding the mechanisms leading to reaction of 4-FBnCl when forming **74**; (iii) understanding the fate of 4-FBnCl in the subsequent amidation step to form darapladib IG; and (iv) determining the purging capability of 4-FBnCl during the amidation reaction.

* Calculated using average of yield ranges provided.

4.2 Project Objectives

The project as a whole aims to perform a series of investigations relating to the process development of the route to darapladib. The areas of focus identified for study are detailed herein.

4.2.1 Fate and Effects of 4-FBnCl

As discussed in the introductory section there is a large knowledge gap regarding the use and fate of 4-FBnCl (*vide supra,* section 4.1.5). Experiments to prepare darapladib IG will be carried out in the presence of a variety of levels of 4-FBnCl and the amount of 4-FBnCl in the isolated darapladib IG will be determined. Following this, it is also essential to understand the fate of any 4-FBnCl present during the amide bond formation to prepare darapladib IG. In theory, 4-FBnCl could react with any nucleophile present in the reaction mixture. However, if this does not occur, or occurs at a very low rate, then there is likely to be residual 4-FBnCl remaining in the reaction mixture. The principal methods for removing the 4-FBnCl become the filtration and cake washing, and removal could be complicated if any 4-FBnCl becomes entrained within the particles of darapladib during crystallisation. Additionally, it is possible that poor cake washes could result in elevated levels of 4-FBnCl in darapladib IG.

4.2.2 Existing Strategies for 4-FBnCl Control

Since 4-FBnCl is the reagent used to prepare carboxylic acid **74** it is logical to suggest that control over the amount of 4-FBnCl going into the amidation reaction should derive from this alkylation process (Scheme 25). In order to achieve control a number of different strategies have been employed.* When the process was first run at large scale the charge of 4-FBnCl was substoichiometric, which allowed complete reaction with thiouracil **95** to occur (Cork Campaign 1).[105] Secondly, the reaction mixture was monitored by HPLC to ensure 4-FBnCl was not detected. Additionally, further testing using GC was employed to measure the 4-FBnCl level at even lower concentrations, since the HPLC method was insufficiently sensitive. Using this

* See Appendix 1 for process details.

strategy the 4-FBnCl level was controlled at the alkylation stage to <20 ppm in isolated carboxylic acid **74**.* The product was isolated in 90.7% average yield across four batches using 32 kg input of thiouracil **95** per batch.

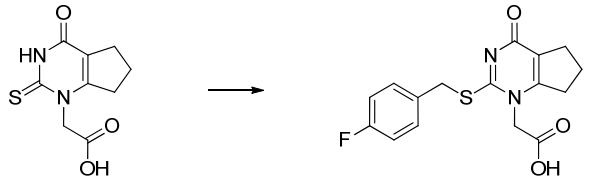

Reagents & conditions: MOH, M_2CO_3, 4-FBnCl, water, IPA, 40 °C, 91-96%.
(M = K or Na)

*Scheme 25: Process to form carboxylic acid **74**.*

For our second campaign a few modifications were made. The potassium bases were changed to sodium bases (after proving equivalence at laboratory scale[106]) due to the bulk availability of NaOH at our proposed manufacturing site. Furthermore, following experimental design investigations,[107] the Na_2CO_3 charge was increased to 0.25 equivalents to allow better control over organic impurities. Additionally, the 4-FBnCl charge was increased to 0.98 equivalents to increase the yield, whilst still maintaining control over the level of 4-FBnCl in isolated **74**. The remainder of the process was essentially unchanged. The process delivered material in 91.7% yield (average from 4 batches, 52.5 kg input of **95** per batch, Cork Campaign 2a, Appendix 1).[105] The 4-FBnCl level was controlled at <15 ppm in isolated carboxylic acid **74** by virtue of using this substoichiometric charge approach.

In order to deliberately produce material with higher 4-FBnCl levels two further batches were prepared (Cork Campaign 2b, Appendix 1). This strategy was to allow evaluation of the effect of residual 4-FBnCl at scale in the subsequent transformation. The 4-FBnCl charge was increased to 1.05 equivalents whilst the base charges were also modified. The aim was to reproduce laboratory scale experiments in which material containing approximately 400-600 ppm 4-FBnCl was

* The first batch isolated contained 209 ppm 4-FBnCl due to an error in plant set-up.

prepared.[106] Consequently, the process was run using 1.99 equivalents of NaOH and 0.16 equivalents of Na_2CO_3. The product was isolated in 95.8% average yield (two batches, 52.5 kg input of **95** per batch) with 4-FBnCl levels being 226 and 290 ppm.[105] The material prepared in these batches was later successfully processed through to darapladib IG. We were pleased to observe that complete purging of 4-FBnCl occurred producing **71**-IG containing <1 ppm 4-FBnCl.[108] These results provide a basis on which to begin further studies to investigate the tolerance of the amidation process to 4-FBnCl and, equally, the fate of 4-FBnCl under the reaction conditions.

4.2.3 Process Understanding and Control of 4-FBnCl During Alkylation

The alkylation of thiouracil **95** to prepare acid **74** is complicated by the presence of side reactions that also involve 4-FBnCl (Scheme 26).

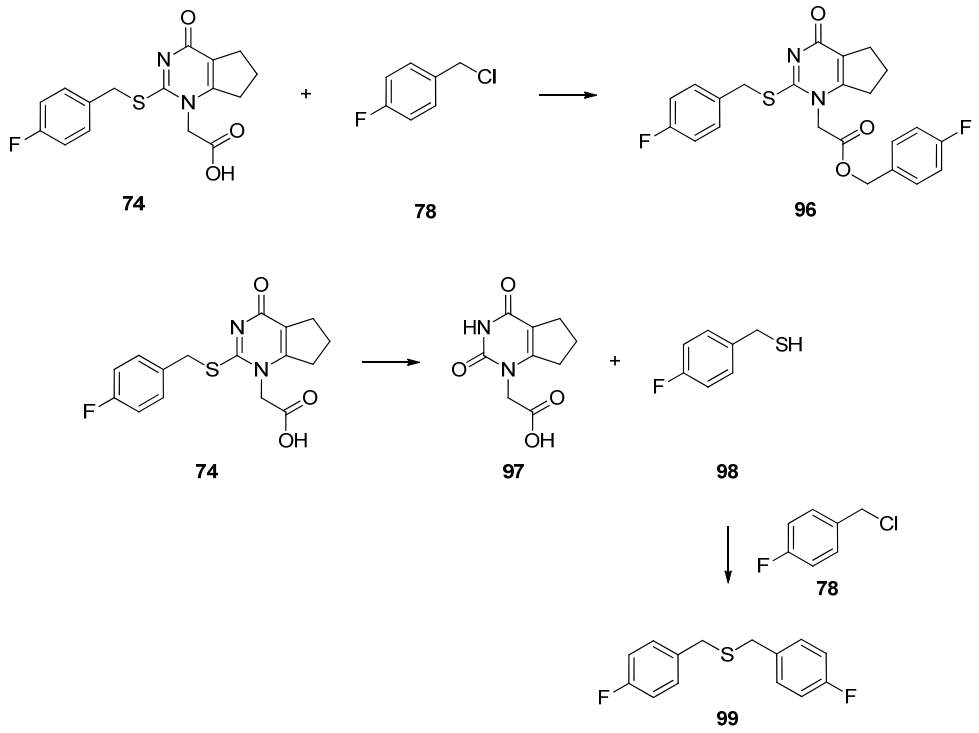

*Scheme 26: Side reactions of 4-FBnCl during the formation of **74**.*

Over-alkylation of **74** can occur to form benzyl ester **96**. This mechanism occurs to a greater extent when the charge of 4-FBnCl is higher.[107] In order to control the amount of the benzyl ester impurity (and in the absence of further information as to

its fate downstream) a higher base charge results in less of this impurity, perhaps by increasing its rate of hydrolysis.[107]

The second important pathway involving 4-FBnCl is the reaction with 4-fluorobenzyl mercaptan **98**. This thiol forms from degradation of carboxylic acid **74** by a hydrolytic mechanism. The hydrolysis to uracil **97** and thiol **98** is more rapid at extremes of pH, particularly under pH 4.[106] It is also observed when more than two molar equivalents of hydroxide are used during the alkylation reaction.[109] After the addition of formic acid for crystallisation, the decomposition mechanism becomes more prevalent as the pH drops, leading to production of **97** and **98**. Any 4-FBnCl present may therefore react with the thiol to form dibenzyl sulfide **99**. This reaction pathway may actually be beneficial in two ways: (i) the 4-FBnCl level is decreased; and (ii) the amount of thiol is also reduced. This latter point is worthy of note since the waste streams from the alkylation process can be highly odorous, which is of concern for long-term manufacture and, in particular, for waste disposal.

Reconsidering the data obtained during scale-up activities, use of more than one equivalent of 4-FBnCl is viewed as beneficial since higher yields can be achieved. Moreover, favourable purging of up to 290 ppm 4-FBnCl downstream has also been observed, which further supports the proposed process change. Understanding the effect of varying the alkylation process parameters on the amount of 4-FBnCl in acid **74** is thus a crucial area for study. The alkylation process needs to be robust, that is, operable over a wide range of parameter values, in order to allow for inevitable variation during routine manufacturing. Noting the side reactions above, it suddenly becomes much more difficult to ensure complete control and, potentially, prediction of the 4-FBnCl level in acid **74**.

The alkylation process has also been identified as a control point for another attribute of darapladib API: the inorganic content (also termed “ash”). The specification for the inorganic content of the API is set at 0.3% w/w. The alkylation process is the last point at which inorganic reagents are introduced into the synthesis. Due to the

absence of aqueous washes later in the synthetic route, the process also provides the last point for removal of inorganic compounds during the cake washes.[*] It is therefore crucial to control the inorganic content at this stage.

The project aims to define the process for the preparation of carboxylic acid **74** and, in particular, those parameters associated with the work-up. Understanding how these parameters affect impurities in acid **74** is crucial. Above all, the process must control the amount of two key impurities; namely 4-FBnCl and inorganic content.

[*] The final recrystallisation of darapladib IG to API in *i*PrOAc includes filtration of a solution of the API as a requirement, thus inorganic compounds have the potential to be removed at a later point. However, if high levels of inorganic materials remain it is possible that the filter may block resulting in severe processing issues and delays to production.

4.3 Results & Discussion

4.3.1 Preparation of Carboxylic Acid 74

With considerable focus on the key alkylation process for preparation of carboxylic acid **74** being required, initial efforts were concentrated on the reaction work-up. The work-up consists of addition of formic acid to crystallise the product, followed by filtration.* A number of parameters were thought to be important to define: the charge of formic acid, its rate of addition, the temperature for the crystallisation, and the final stir time and temperature. In particular, further understanding of the effect of these parameters on the level of 4-FBnCl and inorganic residues in acid **74** was required.

4.3.1.1 Formic Acid Charge

The first series of experiments concentrated on investigating the amount of formic acid. We were interested to understand the effect on product yield, and also to probe whether altering the charge affected the level of inorganic species and 4-FBnCl in the product. Three experiments were carried out with various formic acid charges (Table 10).

* Crystallisation is achieved by addition of an acid to decrease the pH of the reaction mixture. A number of acids had previously been screened during our route identification work, and we were satisfied that formic acid was an appropriate reagent to employ.[100]

Entry	Formic acid / equiv.	Yield of 74 / %	Purity / % area[a]	4-FBnCl / ppm[b]	Inorganic content / % w/w[c]
1	1.5	89	99.26	1158	<0.1
2	2.3	95	99.38	1820	<0.1
3	3.0	96	99.36	1958	<0.1

Conditions: Acid **95** (1.0 equiv.), NaOH (1.90 equiv.), Na_2CO_3 (0.25 equiv.), 4-FBnCl (1.05 equiv.), 40 °C, 2.5 to 3 h, cool to room temperature then formic acid as specified.

[a] HPLC Method D.

[b] Determined by GC.

[c] Determined by sulfated ash analysis.

Table 10: Investigations into formic acid charge.

The amount of formic acid added directly determined the product yield. The existing charge of 2.3 equivalents seemed to be appropriate, and increasing the charge had only a marginal positive effect on yield. The inorganic content of the products was consistently below the reportable limit; therefore varying the formic acid amount does not affect this attribute of acid **74**.

There appeared to be a trend between the 4-FBnCl levels and the formic acid charge. However, on closer inspection of the data, it was noticed that the amount of 4-FBnCl going into the crystallisation was different in each case, and also directly correlated with the 4-FBnCl amount in the product (Table 11).

Entry	Formic acid / equiv.	4-FBnCl before crystallisation / % area[a]	4-FBnCl / ppm[b]
1	1.5	0.69	1158
2	2.3	0.91	1820
3	3.0	1.01	1958

[a] HPLC Method C.

[b] Determined by GC.

*Table 11: 4-FBnCl data in acid **74** when varying formic acid charge.*

The low level of 4-FBnCl before crystallisation in entry 1 is a result of leaving the batch overnight at room temperature prior to carrying out the crystallisation. It is

therefore difficult to draw conclusions about how the formic acid charge affects the 4-FBnCl level from these data.

To further investigate the effect of formic acid charge on 4-FBnCl, a series of experiments were carried out using a single input batch split into portions for crystallisation with differing amounts of formic acid (Table 12).

Entry	Formic acid / equiv.	Yield of 74 / %	Purity / % area[a]	4-FBnCl / ppm[b]
1	1.5	87	99.27	1545
2	2.3	93	99.30	1596
3	3.0	93	99.31	1682

Conditions: Acid **95** (1.0 equiv.), NaOH (1.90 equiv.), Na_2CO_3 (0.25 equiv.), 4-FBnCl (1.05 equiv.), 40 °C, 2.5 to 3 h. Batch split into portions for parallel crystallisations with formic acid as specified.

[a] HPLC Method D.

[b] Determined by GC.

Table 12: Results from crystallisations with consistent input material.

The data in Table 12 show that whilst there is an increase in the amount of 4-FBnCl in the isolated product **74** as the formic acid charge is increased, the rise is marginal. The main effect from altering the formic acid charge is thus on the yield of the product rather than on the two attributes of interest. It is proposed to proceed with a formic acid charge of around 2.5 equiv., although the acceptability of this charge will need to be confirmed experimentally.

4.3.1.2 Addition Time of Formic Acid

The second parameter to investigate was the addition time of the formic acid. Experiments within our laboratory had previously investigated two extremes of formic acid addition: (1) all at once, and (2) 23 h addition.[110] The results suggested that the amount of 4-FBnCl in the solid product **74** was lower when the addition time was longer. A second point of interest was that the amount of 4-FBnCl in carboxylic acid **74** was not observed to alter significantly during the cake washes.[111] These observations led us to conclude that the 4-FBnCl becomes entrained within the solid

product, but the amount entrained depends on the conditions used during the crystallisation. We set about to investigate the addition time and its effect on the 4-FBnCl level in more detail. Three experiments were carried out with formic acid added over various times (Table 13).

Entry	Addition time / min	Yield 74 / %	Purity / % area[a]	4-FBnCl before crystallisation / % area[b]	4-FBnCl / ppm[c]	Inorganic content / % w/w[d]
1	5	97	99.24	1.00	2104	<0.1
2	90	97	99.07	0.97	1606	<0.1
3	292	97	99.28	0.51	570	<0.1

Conditions: Acid **95** (1.0 equiv.), NaOH (1.90 equiv.), Na_2CO_3 (0.25 equiv.), 4-FBnCl (1.05 equiv.), 40 °C, 2.5 to 3 h, cool to room temperature, formic acid (2.3 equiv.) over time specified.

[a] HPLC Method D.

[b] HPLC Method C.

[c] Determined by GC.

[d] Determined by sulfated ash analysis.

Table 13: Investigation into varying formic acid addition time.

In line with previous observations,[110] increasing the addition time resulted in reduced amounts of 4-FBnCl in the isolated solid. However, once again the amount of 4-FBnCl present in the reaction mixture prior to crystallisation should be considered. Entry 3 was crystallised after leaving the reaction mixture overnight, hence the amount of 4-FBnCl going into the crystallisation was significantly lower. It is therefore unclear whether it is the 4-FBnCl level pre-crystallisation, or the addition rate of formic acid, which is having the greater influence over the amount of 4-FBnCl in isolated acid **74**. The yield was not affected by varying the addition time of the formic acid. There was also no detectable effect on the inorganic content of the product from varying the addition time.

The limitation with the above study (Table 13) was the use of different input batches with variable 4-FBnCl content following the reactive chemistry. A further four

experiments were carried out in parallel with a single input batch split into portions for crystallisation (Table 14).

Entry	Addition time / min	Yield 74 / %	Purity / % area[a]	4-FBnCl before crystallisation / % area[b]	4-FBnCl / ppm[c]
1	5	94	99.17	0.93	1408
2	90	95	99.12	0.93	964
3	300	93	99.14	0.93	672
4	5[d]	94	99.22	0.88	1108

Conditions: Acid **95** (1.0 equiv.), NaOH (1.90 equiv.), Na_2CO_3 (0.25 equiv.), 4-FBnCl (1.05 equiv.), 40 °C, 2.5 h. Batch split into portions for parallel crystallisations using formic acid (2.3 equiv.).

[a] HPLC Method D.

[b] HPLC Method C.

[c] Determined by GC.

[d] Stirred at room temperature for 300 min prior to crystallisation.

Table 14: Constant input batch with variable formic acid addition time.

The trend between addition time and 4-FBnCl in the product was now clearly confirmed (entries 1 to 3). Comparing entries 1 and 4 showed that stirring the reaction mixture at room temperature prior to crystallisation caused the 4-FBnCl level in solution to decrease. However, the effect of this stir was not as great as that observed from increasing the addition time.

At the current time, we are anticipating setting a specification for 4-FBnCl in carboxylic acid **74** at around 0.2% w/w (2000 ppm)[*] based on our knowledge of downstream purging (see section 4.3.2). Since the batches of acid **74** discussed above are within this proposed specification, it is anticipated that the addition time parameter will be defined based on manufacturability criteria rather than effect on 4-FBnCl. For instance, the time required for operations, the filtration characteristics of

[*] This is a conservative estimate of the specification for 4-FBnCl level in carboxylic acid **74**. The finalised specification may be at a higher value.

the solid and process safety (particularly gas evolution) will all need to be considered. However, it is still of great importance to have a thorough understanding of the parameters contributing to the variation of 4-FBnCl levels. This knowledge will ensure carboxylic acid **74** does not fail specification at any time.

4.3.1.3 Temperature Parameters

The temperature at which the crystallisation of acid **74** is carried out was next examined. In our current process formic acid is added at 20 ± 3 °C, yet the reaction is carried out at 40 °C. It was of interest to us to investigate the effect on the product of crystallising at 40 °C (Table 15). The data from Table 13, entry 2 are shown for direct comparison.

Entry	Crystallisation temperature / °C	Yield 74 / %	Purity / % area[a]	4-FBnCl / ppm[b]	Uracil 97 in liquors / % area[c]	Thiol 98 in liquors / % area[c]
1 (Table 13, entry 2)	20	97	99.07	1606	1.31	ND
2	40	95	99.12	965	15.95	3.71

Conditions: Acid **95** (1.0 equiv.), NaOH (1.90 equiv.), Na_2CO_3 (0.25 equiv.), 4-FBnCl (1.05 equiv.), 40 °C, 2.5 to 3 h, adjust temperature (if required), then formic acid (2.3 equiv.) over 90 min.

[a] HPLC Method D.

[b] Determined by GC.

[c] HPLC Method A.

ND Not detected

Table 15: Comparison of batches crystallised at different temperatures.

The yield of product **74** when crystallising at 40 °C was a little low which indicated the possibility of decomposition to uracil **97** and thiol **98** having occurred. This was confirmed by analysing the reaction liquors, which showed significantly higher levels of both impurities compared to crystallisation at room temperature. The product purity was not affected, and the 4-FBnCl level was shown to be lower. However, the decomposition and the lower yield were of some concern and could be even more pronounced on scaling up. It was therefore decided to continue with the crystallisation at 20 °C.

The isolation temperature was investigated in more detail (Table 16). It was thought that filtering acid **74** at lower temperature could improve the yield further, and this was indeed shown to be the case (entry 1). The product was isolated in almost quantitative yield, with negligible inorganic impurities present.

Entry	Addition time / min	Isolation temperature / °C	Yield 74 / %	Purity / % area[a]	4-FBnCl / ppm[b]	Inorganic content / % w/w[c]
1	0	2	99	99.06	1689	<0.1
2	0	20	96	99.20	1527	<0.1
3	0	2	48	99.55	999	0.18
4	5	2	97	99.17	1526	-
5	90	2	95	99.16	1087	-

Conditions: Acid **95** (1.0 equiv.), NaOH (1.90 equiv.), Na_2CO_3 (0.25 equiv.), 4-FBnCl (1.05 equiv.), 40 °C, 2.5 h, cool to room temperature then formic acid (2.3 equiv.) over time specified. Entries 2 and 3 were from the same input batch split into two portions. Entries 4 and 5 were from the same input batch split into two portions.

[a] HPLC Method D.

[b] Determined by GC.

[c] Determined by sulfated ash analysis.

Table 16: Crystallisations under various conditions.

Next it was decided to directly compare isolation at room temperature and 2 °C by completing parallel crystallisations (entries 2 and 3). Some abnormal behaviour was observed during these experiments as solid was observed to adhere to the vessel walls during crystallisation. For entry 2 the solid quickly became a free flowing slurry; however, for entry 3, solid remained stuck to the flask throughout. The result of this uncharacteristic crystallisation was a low yield, with the rest of the material remaining within the vessel. Analysis of this residual material showed significantly decreased purity.

The unusual crystallisation was something of a concern for us, since this could render our process non-robust, and a repetition at plant scale could result in low yields, failure to deliver the required quantities of material, or failure of quality

specifications. It was speculated that the rapid addition of the formic acid, combined with a quick cool to 2 °C may have been the root cause of this problem. A further two experiments were carried out (entries 4 and 5) with variable addition rates of formic acid. Both these experiments proceeded in a normal fashion with no atypical crystallisation observed. The 4-FBnCl results were consistent with those obtained previously with different addition times and the isolation temperature appears to have had no noticeable effect on the levels.

The experiments completed suggest that reducing the isolation temperature can be beneficial for the product yield; however, it is thought that the crystallisation should be well established prior to cooling to ensure material is not lost through adhesion to the vessel. It may, therefore, be prudent to charge the formic acid over a slightly longer time to mitigate any possible risk of unusual crystallisation occurring. In addition, the effect of temperature on the 4-FBnCl content appears to be negligible; thus isolation at approximately 2 °C should be appropriate.

4.3.1.4 Stir Time

The final parameter for investigation was the stir time post crystallisation prior to isolating the batch. Clearly, if insufficient time is allowed then not all the product will have crystallised and the yield will suffer as a consequence. Our existing alkylation process specifies at least 1 hour for this parameter. Information was gathered over time to further investigate (Figure 20).

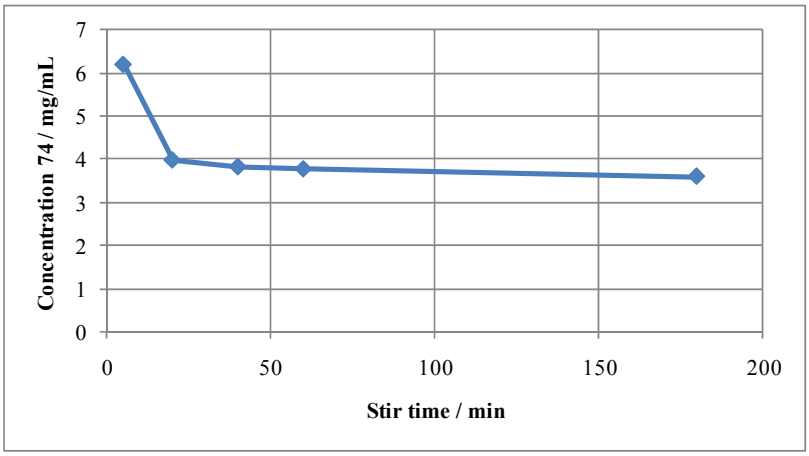

*Figure 20: Concentration of carboxylic acid **74** in liquors post crystallisation at room temperature.*[*]

Since the concentration of acid **74** in the liquors reached a plateau within approximately 20 minutes, the current 1 hour specified for the hold time appears to be appropriate. Also of interest was how the 4-FBnCl content and the purity of the solid were affected during an extended stir (Table 17).

Entry	Stir time / h	Purity / % area[a]	4-FBnCl / ppm[b] (% decrease)
1	1	99.32	1229 (0)
2	24	99.35	1108 (-9.8)
3	96	99.35	1048 (-14.7)
4	168	99.37	820 (-33.3)

Conditions: Acid **95** (1.0 equiv.), NaOH (1.90 equiv.), Na_2CO_3 (0.25 equiv.), 4-FBnCl (1.05 equiv.), 40 °C, 2.5 h, cool to room temperature then formic acid (2.3 equiv.).

[a] HPLC Method D.

[b] Determined by GC.

*Table 17: Effect of stir time on purity and 4-FBnCl content of **74**.*

The experiment revealed that the level of 4-FBnCl decreased during the prolonged stir. We were also pleased to observe that the purity of acid **74** was not affected by

[*] Note: this experiment was completed prior to deciding to reduce the isolation temperature to 2°C.

increasing the stir time; therefore this suggested that a maximum stir time of at least a week could be specified without affecting the quality of the product.

Supplementary experimental work also investigated the effect on purity and 4-FBnCl in more detail (Table 18).

Entry	Formic acid / equiv.	Main batch purity[a] / % area[b]	Purity after 1 week / % area[b]	Main batch 4-FBnCl[a] / ppm[c]	4-FBnCl level after 1 week / ppm[c] (% decrease)
1	1.5	99.26	99.20	1158	1018 (-12)
2	2.3	99.38	99.39	1820	1653 (-9)
3	3.0	99.36	99.39	1958	1864 (-5)

Aliquot of reaction slurries (2 mL) from Table 10 left unstirred for one week.

[a] Taken from Table 10.

[b] HPLC Method D.

[c] Determined by GC.

*Table 18: Further stability data for carboxylic acid **74**.*

These results gave us further confidence that the purity of acid **74** would not be significantly affected by stirring the crystallised batch for an extended time. Also of interest was the observation that the reduction in 4-FBnCl level was smaller for these unstirred batches than in the stirred system (compare Table 18 entry 2, with Table 17). Additionally, the relative decrease in 4-FBnCl content was greater when the formic acid charge was lower.

The reduction in 4-FBnCl level was interesting to observe, yet unlikely to be useful practically since the fall was relatively minor. However, we were interested in the fate of the 4-FBnCl so analysis of the liquors was completed (Table 19).

Time / h	Carboxylic acid 74 / % area	Uracil 97 / % area	4-Fluorobenzyl alcohol / % area	Thiol 98 / % area	4-FBnCl / % area
0	81.09	1.36	3.88	0	9.07
168	64.31	12.44	9.45	3.96	0

HPLC Method A.

Experiment conditions as in Table 10, entry 2.

Table 19: Analysis of reaction liquors over time.

The analysis revealed decomposition to have taken place, with the presence of both uracil **97** and thiol **98** being observed. The other main species present in the liquors was confirmed to be 4-fluorobenzyl alcohol, presumably derived from direct hydrolysis of the 4-FBnCl. Since thiol **98** was also present, it therefore appeared that reaction between 4-FBnCl and this thiol to form dibenzyl sulfide **99** had not occurred and, indeed, no peak with the correct retention time for this compound was evident. It is known that dibenzyl sulfide **99** can form under the alkylation reaction conditions when the pH is high. The mechanism to form **99** may, therefore, only operate under basic conditions when a proportion of thiol **98** would be deprotonated and act as a more reactive nucleophile. These investigations have thus given some insight into the fate of 4-FBnCl during the alkylation process.

4.3.1.5 Application of Experimental Design

As documented above, a large number of experiments on the crystallisation were completed in univariate fashion, by varying a single factor and examining the effects. These data provided much information about how individual factors affect key attributes of the product, acid **74**. However, two process parameters could interact together to result in a greater or lesser effect on the 4-FBnCl level, or the amount of inorganic impurities in acid **74**. Consequently, it was decided to complete an experimental design work package in order to determine whether interaction effects were present. Any information on interactions would also be of use in potential future experimental design work packages to be carried out on this specific process.

Factors for Investigation

Based on the work already completed, four factors were chosen to be further investigated using experimental design methods (Table 20).

Factor	Proposed range for design	
	Low	High
Amount of formic acid	2 equiv.	3 equiv.
Formic acid addition temperature	20 °C	30 °C
Addition time of formic acid	5 min	175 min
Isolation temperature	0 °C	20 °C

Table 20: Factors chosen for investigation.

In addition, we were also interested to further investigate the effect of the stir time prior to isolating the product. This was not included as a parameter within the design; instead, samples were to be taken at two different time points for analysis (1 and 24 h). The approach permitted us to design a four factor, half factorial design, to be completed in eight experiments (plus two centre points). The chosen design gives independent estimation of single factor effects, and aliasing of two-factor interactions with each other. In contrast, a five factor design of eight experiments would be a quarter factorial design, and result in aliasing of two-factor interactions with single factor effects. This would significantly complicate the analysis. The chosen four factor design should give maximum information at minimal experimental cost.

In order to ensure a consistent input reaction mixture composition, a single reaction mixture was split into ten portions for use. However, to ensure minimal variation between design runs it was necessary to run all ten experiments simultaneously. Since it was impractical for a single chemist to complete these experiments, it was decided that two chemists would complete the crystallisations, each using identical equipment.[*] For the design to be able to account for any potential variation between chemist, or equipment, or both, a block was introduced (Table 21). The design was generated and analysed in Design-Expert® version 7.1.1 software (DX7).

[*] Block 1 was carried out by the author; block 2 was carried out by Andrew Kennedy. Both blocks were completed in equivalent Systag Flexylab equipment, and were run simultaneously.

Standard	Run	Block	Type	A:Formic acid amount / equiv.	B:Formic acid addition temp / °C	C:Formic acid addition time / min	D:Isolation temp / °C
6	1	1	Factor	3	20	175	0
2	2	1	Factor	3	20	5	20
9	3	1	Centre	2.5	25	90	10
7	4	1	Factor	2	30	175	0
3	5	1	Factor	2	30	5	20
1	6	2	Factor	2	20	5	0
4	7	2	Factor	3	30	5	0
5	8	2	Factor	2	20	175	20
10	9	2	Centre	2.5	25	90	10
8	10	2	Factor	3	30	175	20

*Table 21: Design used in study investigating crystallisation of acid **74**.*

The aliasing structure means that the block effect is aliased with the interactions AB and CD.* The design was carefully planned to ensure that those factors not anticipated to interact were assigned to factors A and B, and C and D.

Preliminary Experiments

It was the intention to analyse the design as a single block, despite having set up the design as two blocks as a precaution. A prior equivalence study was completed to gain confidence that there would be minimal differences between chemists and equipment (Table 22). If equivalence was not demonstrated, the design would have to be reassessed.

* See experimental for details.

Entry*	Total yield 74 / %	Purity 1 h / % area[a]	4-FBnCl 1 h / ppm[b]	Purity 4 h / % area[a]	4-FBnCl 4 h / ppm[b]
1	94	99.39	857	99.39	856
2	94	99.38	652	99.29	648

Conditions: Acid **95** (1.0 equiv.), NaOH (1.90 equiv.), Na_2CO_3 (0.25 equiv.), 4-FBnCl (1.05 equiv.), 40 °C, 2.5 h, then cooled and split into two portions. Formic acid (2.5 equiv.) added over 90 min at 25 °C, then cooled to 10 °C. Slurry sampled at 1 h and batch isolated after 4 h.†

[a] HPLC Method D.

[b] Determined by GC.

Table 22: Equivalence experiments prior to main crystallisation design.

The data obtained showed minimal differences between experiments. The yields were identical, and the HPLC data at both time points were comparable. Although there were some differences between the 4-FBnCl data, it was anticipated that there would be a much greater range observed in the full study.

With these results in hand, we were confident that minimal variations were being observed between chemist and equipment, and that there was unlikely to be a statistically significant block effect observed during the study.

Design Results and Discussion

The full experimental design work package was carried out as in Table 21, and the results were analysed in DX7. The isolated yield of acid **74** could not be modelled, which indicates the yield was very robust to the changing reaction conditions. Indeed, the observed range of yields was 93 to 95%. As an alternative, the mother liquor assays produced adequate models and have been used as an indication of

* Entry 1 was carried out by the author in one Systag Flexylab; entry 2 was carried out by Andrew Kennedy in the second Systag Flexylab.

† The products from the equivalence experiments were isolated after 4 h, rather than 24 h as in the full study, due to time constraints.

yield. No model could be generated for sulfated ash results since all batches were reported as < 0.1% w/w.

The mother liquors HPLC data was used as a measure of the decomposition of acid **74** to uracil **97**. It was found that using the liquors % area data was not informative since the concentration varied significantly. Peak area data for uracil **97** were used for modelling purposes.

Data were obtained at both 1 h and 24 h. The responses and results used for modelling at 1 h are shown in Table 23. The models generated from these data are summarised in Table 24.

Run	1 h 4-FBnCl / ppm[a]	1 h mother liquors assay / mg/mL[b]	1 h liquors uracil 97 / peak area[b]	1 h acid 74 / % area[c]	1 h benzyl ester 96 / % area[c]
1	719	1.0	7.573	99.17	0.42
2	1375	2.2	5.775	99.22	0.34
3	**549**	**1.9**	**9.060**	**99.19**	**0.40**
4	339	2.1	18.796	99.19	0.46
5	994	4.2	10.754	99.27	0.35
6	1276	1.1	6.576	99.24	0.35
7	1155	0.9	12.404	99.27	0.34
8	694	3.7	7.818	99.16	0.43
9	**611**	**1.3**	**7.983**	**99.19**	**0.42**
10	432	2.0	17.022	99.21	0.43

Centre points highlighted in bold (runs 3 & 9).

[a] Determined by GC.

[b] HPLC Method A, with assay of acid **74**.

[c] HPLC Method D.

Table 23: Data for modelling at 1 h.

Attribute	4-FBnCl / ppm	Mother liquors assay / mg/mL	Liquors uracil 97 / area	Acid 74 / % area	Benzyl ester 96 / % area
Response Range	339 – 1375	0.9 – 4.2	5.775 – 18.796	99.16 – 99.27	0.34 – 0.46
Target	Minimise	Minimise	Minimise	Maximise	Minimise
A:Formic acid amount / equiv.	↓ (3)	↑ (2)			
B:Formic acid addition temp / °C	↑ (2)		↓ (1)	↑ (2)	
C:Formic acid addition time / min	↑ (1)		↓ (2)	↓ (1)	↓ (1)
D:Isolation temp / °C		↓ (1)			
Interactions	None	None	BC (3)	None	None

Arrows indicate high (↑) or low (↓) setting of the parameter is required to achieve the target for each response.

Numbers in parentheses indicate the order of importance of the parameters, with 1 being the most important.

Table 24: Summary of 1 h models for each response.

The analysis of the 4-FBnCl data reveals factor C (formic acid addition time) to be the most important followed by B (addition temperature) and A (formic acid charge). The half-normal plot for 1 h 4-FBnCl data is displayed in Figure 21, and clearly shows the three most dominant effects as being the ones furthest to the right of the plot.

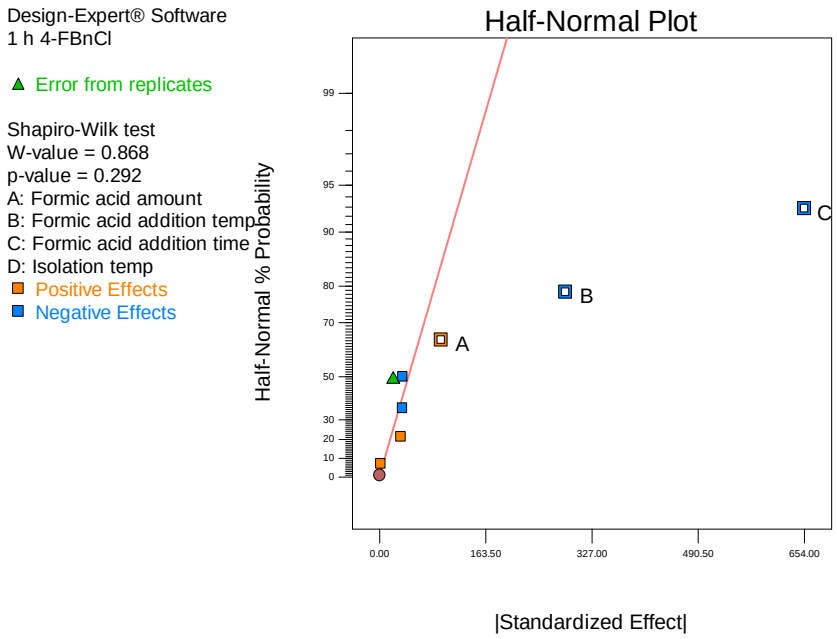

Figure 21: Half-normal plot for 1 h 4-FBnCl data.

These significant parameter effects are in excellent agreement with the data observed during the earlier crystallisation experiments. The addition time for formic acid has again been shown to be the main parameter affecting the level of 4-FBnCl in the product. The analysis also reveals no interactions between any of the investigated parameters. The effect of three factors can be visualised using a cube plot (Figure 22).

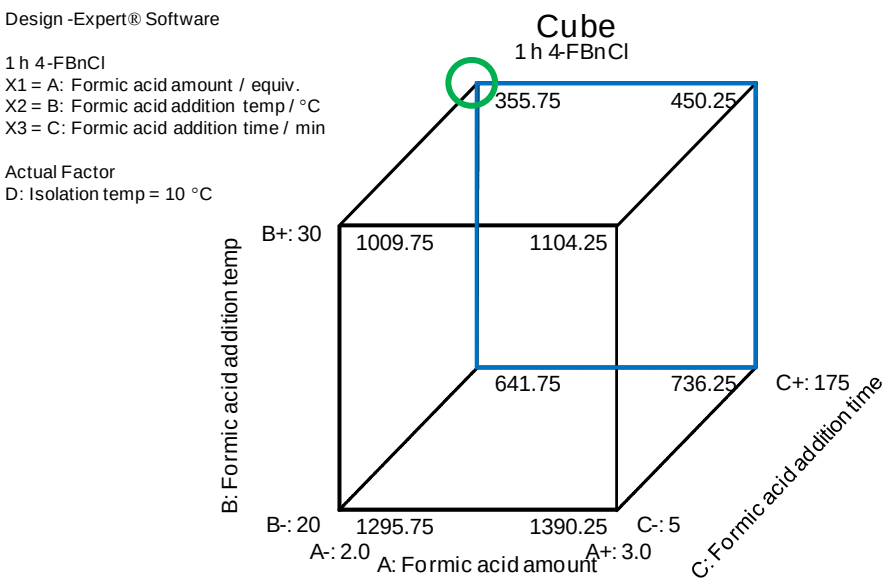

Figure 22: Cube plot for model for 1 h 4-FBnCl data.

The cube plot indicates that in order to minimise 4-FBnCl, the best settings are when C is high (shown in blue), combined with high B and low A to provide the best overall result (green circle). It should be noted that all of the batches in this experimental design study passed our provisional specification of ≤ 2000 ppm 4-FBnCl in acid **74**.

The assay data for the mother liquors indicated that the isolation temperature (D) and the amount of formic acid (A) were the most important factors. The model suggests that for maximum yield a higher charge of formic acid and lower isolation temperature will be beneficial. Small improvements could be possible by using more formic acid, and decreasing the isolation temperature.

The level of uracil **97** in the liquors gives an indication of the amount of degradation that has occurred during the process. The modelling showed that the addition temperature of the formic acid (B) and the addition time (C) were the most important parameters at 1 h. In order to minimise degradation it is important to keep these parameters at the lower settings, since higher temperature for a longer time during the crystallisation results in increased decomposition. Note that the yield was not

affected throughout the study; therefore, the level of degradation observed has had only minimal negative effect.

Factors C (formic acid addition time) and B (addition temperature) were identified as being significant for the HPLC purity data for acid **74**. However, this model is of limited use as a very small variation was observed between the maximum and minimum results for this response (99.16 to 99.27% area). The main impurity is benzyl ester **96**. The only parameter which shows an effect on this species is the addition time (C), which should be low to minimise the amount of ester impurity. The level of ester **96** and, hence, purity of acid **74**, is determined by the reactive chemistry, and relatively little control over this attribute appears possible during the crystallisation.

Having completed modelling of the 1 h data the 24 h results were analysed similarly. The responses and results used for modelling are shown in Table 25. The models generated from these data are summarised in Table 26.

Run	24 h 4-FBnCl / ppm[a]	24 h mother liquors assay / mg/mL[b]	24 h liquors uracil 97 / peak area[b]	24 h acid 74 / % area[c]	24 h benzyl ester 96 / % area[c]
1	668	0.66	7.843	99.17	0.42
2	1198	2.27	16.525	99.24	0.34
3	**512**	**1.59**	**10.507**	**99.20**	**0.40**
4	330	1.36	18.790	99.20	0.46
5	914	4.10	19.656	99.26	0.35
6	1153	1.00	6.774	99.19	0.35
7	1126	0.64	12.676	99.24	0.34
8	661	3.52	12.969	99.16	0.43
9	**558**	**1.23**	**8.677**	**99.18**	**0.42**
10	402	1.99	23.080	99.20	0.43

Centre points highlighted in bold (runs 3 & 9).

[a] Determined by GC.

[b] HPLC Method A, with assay of acid **74**.

[c] HPLC Method D.

Table 25: Data for modelling at 24 h.

Attribute	4-FBnCl / ppm	Mother liquors assay / mg/mL	Liquors uracil 97 / area	Acid 74 / % area	Benzyl ester 96 / % area
Response Range	330 – 1198	0.64 – 4.1	6.774 – 23.08	99.16 – 99.26	0.34 – 0.46
Target	Minimise	Minimise	Minimise	Maximise	Minimise
A:Formic acid amount / equiv.		↑ (2)			
B:Formic acid addition temp / °C	↑ (2)		↓ (1)	↑ (2)	
C:Formic acid addition time / min	↑ (1)			↓ (1)	↓ (1)
D:Isolation temp / °C		↓ (1)	↓ (2)		
Interactions	None	AD (3)	None	None	None

Arrows indicate high (↑) or low (↓) setting of the parameter is required to achieve the target for each response.

Numbers in parentheses indicate the order of importance of the parameters, with 1 being the most important.

Table 26: Summary of 24 h models for each response.

The effects identified at 24 h were much the same as those identified at 1 h. The analysis of the 4-FBnCl data reveals the same main effects, but now the amount of formic acid (A) is not significant. The mother liquors assay response also shows the interaction term AD to be significant (Figure 23). The interaction plot shows that a higher amount of formic acid will produce lower losses to liquors, and that this can be further enhanced by isolating at low temperature. At the lower temperature the effect of the formic acid charge is less pronounced.

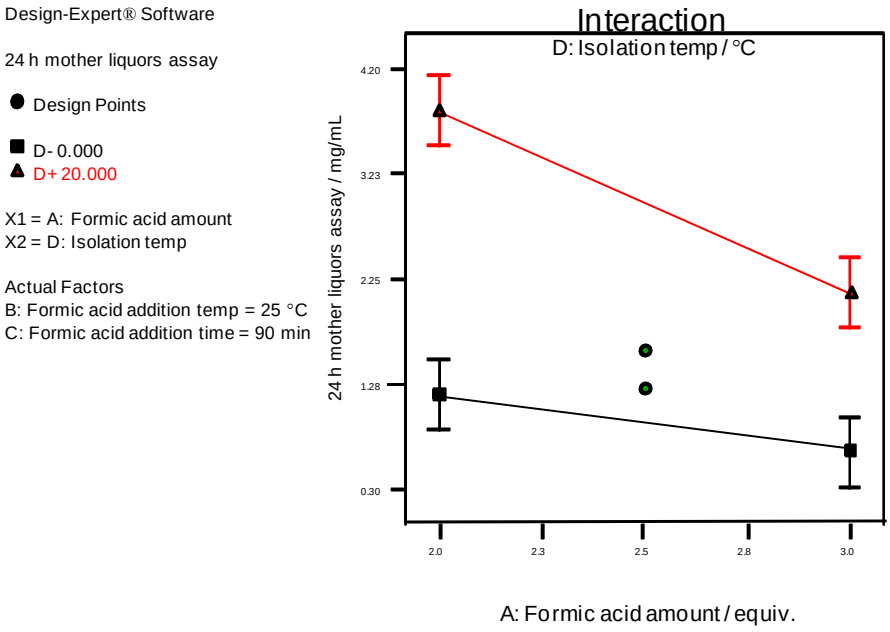

Figure 23: Interaction plot for mother liquors assay at 24 h.

The model for uracil **97** no longer includes the term for formic acid addition time (C). Instead, the isolation temperature (D) was shown to be significant. Both temperature parameters B and D should be kept at a low setting to minimise the amount of possible degradation. This is crucial because degradation leads to the production of thiol **98**, which is malodorous. The HPLC data analysis gave C as the main effect, as for the 1 h data.

In all the models, very few interaction effects were identified, and those that were showed low significance compared to the single factors. In addition, none of the interaction terms were aliased with the block. The fact that the centre point runs were consistent between blocks, and the absence of any terms which could be aliased with the block, are strong indications that no block effect was present in this study. This conclusion suggests that analysis of the data as a single block was appropriate.*

* The data were also analysed as two blocks with the same general overall conclusions. The models from this analysis did not include any two-factor interactions which could be aliased with the block effect.

The data at two time points can also be used to show how the responses change over time. Of all the responses investigated, three demonstrate consistent trends across all the runs: 4-FBnCl (Figure 24), mother liquors assay (Figure 25) and uracil **97** in the liquors (Figure 26). Case profile plots were generated for the purpose of visualisation.* The data are coloured by run order. The centre points (runs 3 and 9) are coloured green and are in general agreement in all cases.

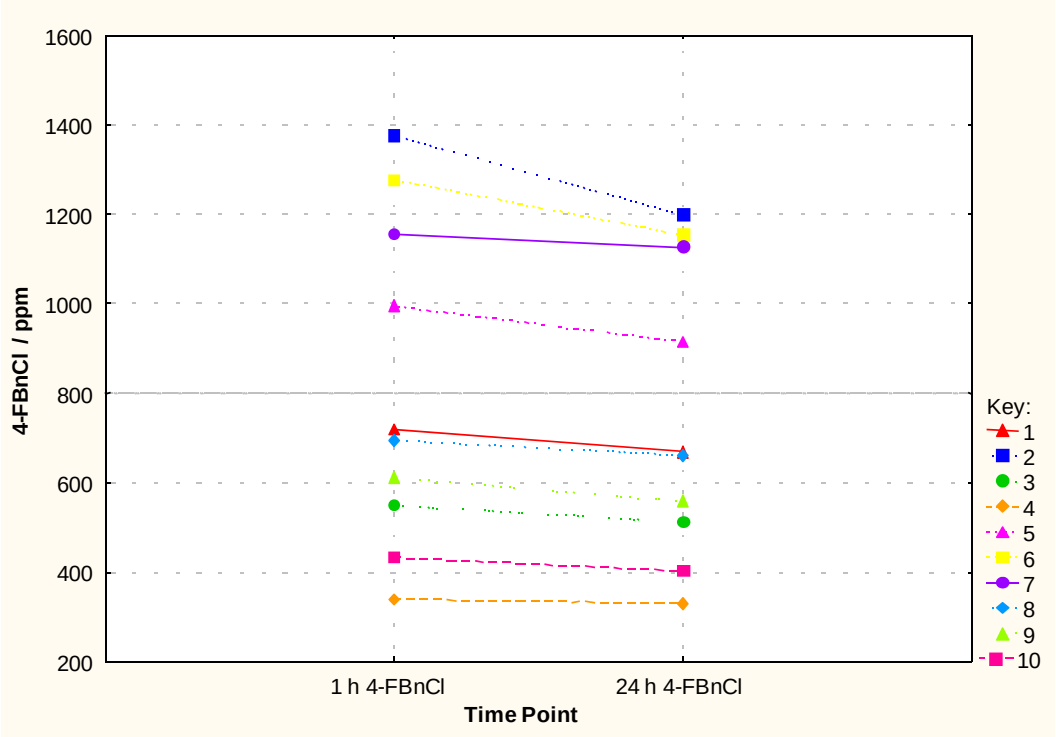

Figure 24: Case profile plot for 4-FBnCl (coloured by run order).

Consistent with earlier reported data, 4-FBnCl is shown to decrease over time (Figure 24). This is thought to be due to the hydrolysis of 4-FBnCl to 4-fluorobenzyl alcohol (see Table 19, page 74). There is no evidence for contamination of product acid **74** by 4-fluorobenzyl alcohol.

* Case profile plots were generated in Statistica by I. Damjanov, GSK, Stevenage.

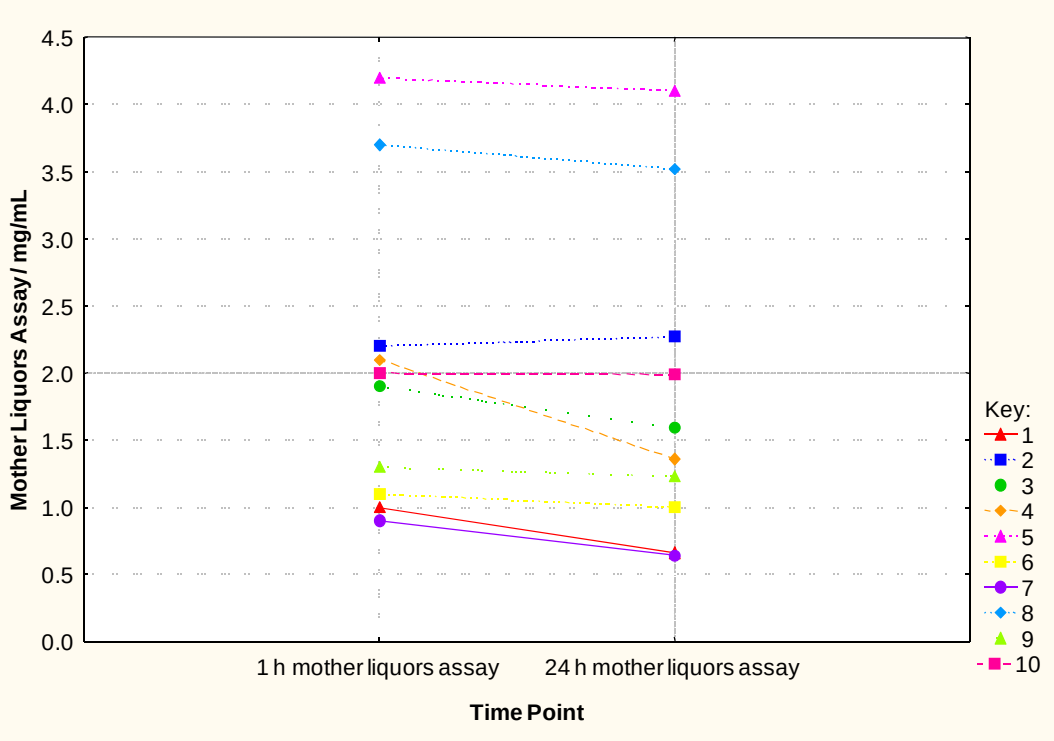

Figure 25: Case profile plot for mother liquors assay (coloured by run order).

The mother liquor assays are observed to decrease over time, with the exception of run 2, which shows a minor increase (Figure 25). The decrease in assay may, in part, be due to more material coming out of solution over time, but might also be a result of degradation of the acid **74** to uracil **97**, which reduces its concentration (see Table 19, page 74).

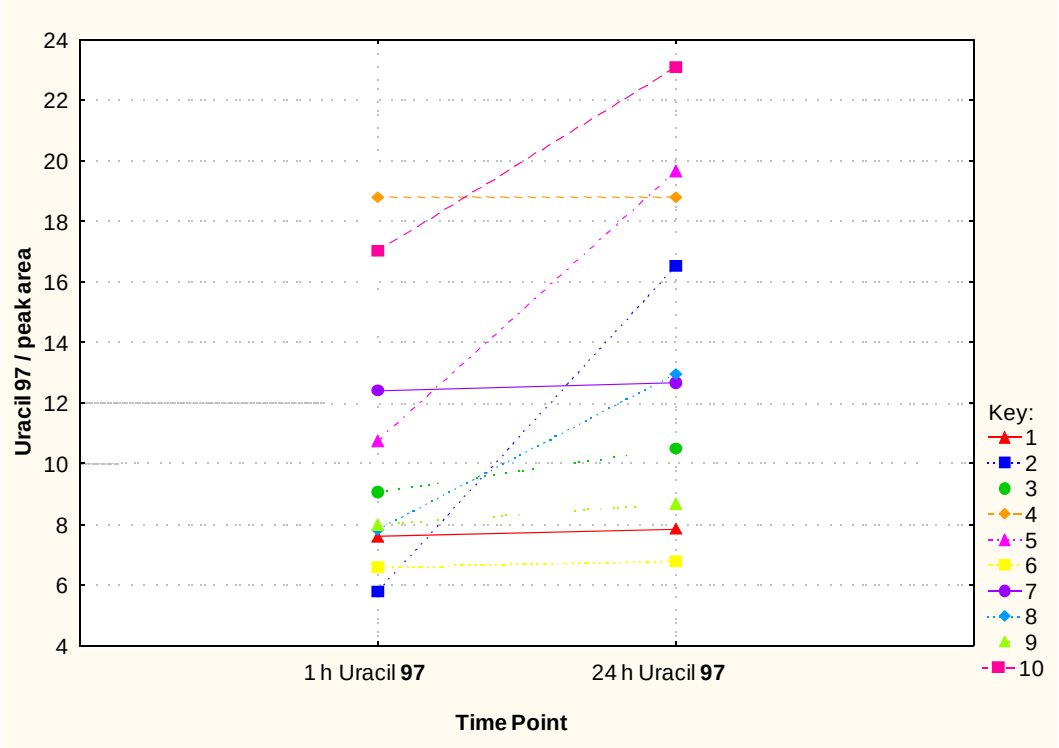

Figure 26: Case profile plot for uracil ***97*** *in liquors (coloured by run order).*

The amount of uracil **97** is shown to increase over time for all runs (Figure 26). This is a result of degradation of acid **74**. The greatest increases in uracil **97** over time are from runs 2, 5, 8 and 10, which were all stirred at 20 °C for 24 h, thus demonstrating the effect of temperature on degradation over an extended time. Ideally, degradation should be minimised to avoid yield loss and generation of odour from thiol **98**, which is also produced. The fact that the yield variations observed were very small (93 to 95%) suggests that the decomposition mechanism was actually a minor pathway. The yields were all slightly lower than would be typically observed; this can be attributed to mechanical losses from splitting a large batch into portions.

In summary, the experimental design work has identified that each of the four parameters investigated could be used at any setting within the range examined to provide adequate quality and yield of acid **74**. This indicates that the crystallisation appears to be quite robust to variations in these parameters. However, set points for each of these parameters must be defined for the process based on experimental findings. The following settings are proposed for the crystallisation of acid **74**:

- The formic acid charge should be high to ensure the yield is maximised;
- The addition temperature for formic acid should be low to minimise degradation to the thiol **98**. However, a higher temperature may give higher quality product, and an intermediate setting may be an appropriate compromise;
- The formic acid addition time should be at an intermediate setting to minimise the potential for decomposition, minimise the amount of 4-FBnCl, and ensure the evolution of gas (CO_2) can be safety controlled;
- The isolation temperature should be low to maximise yield;
- The final hold time should be at least one hour to maximise yield, but no detrimental effects were observed when this hold was increased.

In practice, the settings for each of the parameters investigated will be finalised based on manufacturing criteria, including cost, cycle time, filtration rate, and safety. In addition, it will also be necessary to define acceptable ranges for each of the parameters.

Of great importance to us was our increased understanding of the effect of the crystallisation parameters on the level of 4-FBnCl in acid **74**. The experimental work completed suggested that 4-FBnCl levels could be readily controlled at ≤ 2000 ppm in acid **74**. The next step was to determine the effect of the downstream chemistry on this impurity, discover whether it is reactive or inert under the amidation conditions, and to investigate the level which could be acceptably tolerated.

4.3.2 Investigations Into 4-FBnCl

4.3.2.1 Purging of 4-FBnCl During Preparation of Darapladib IG

The formation of darapladib from carboxylic acid **74** and amine **77** is carried out using the coupling reagent carbonyldiimidazole (CDI) **100** (Scheme 27). Reaction of the carboxylic acid with CDI initially forms the mixed anhydride **101**, into which imidazole adds to form the imidazolide **102**. The carboxylic acid is now suitably activated to react with amine **77** to form darapladib **71**.[9]

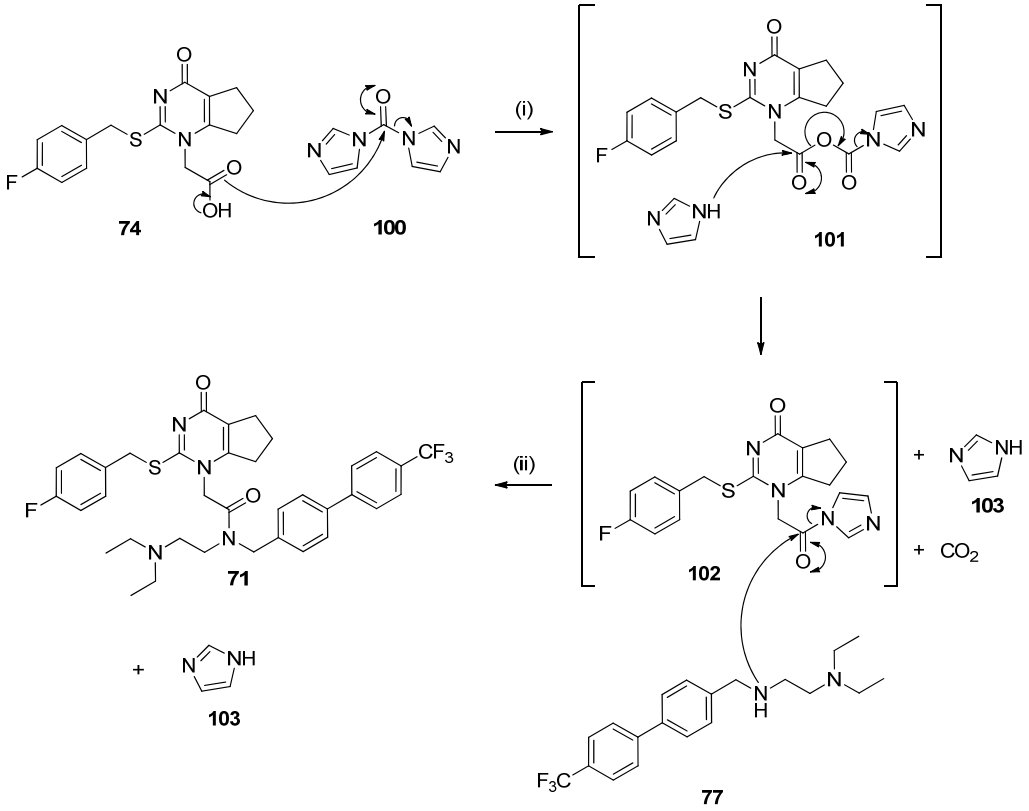

Reagents & conditions: (i) **74** (1.0 equiv.), CDI (1.2 equiv.), MIBK (6 vol), 70 °C, 0.5 h; (ii) **77** (1.1 equiv.), 92 °C, 2 h.

Scheme 27: Formation of darapladib IG.

Initially, a number of experiments to form darapladib IG were carried out to ascertain the level of 4-FBnCl purging observed during the reaction (Table 27). It was already known from results at scale during development campaigns that up to approximately 300 ppm was successfully purged (*vide supra*, section 4.2.2),[108] but further information with batches of **74** containing higher levels of 4-FBnCl was needed.

From experimentation during the alkylation stage to prepare carboxylic acid **74** a number of batches containing >300 ppm 4-FBnCl were available for use (Table 27). Thus batches containing approximately 1000 and 1300 ppm 4-FBnCl were carried through the standard amidation process. Both experiments resulted in <1 ppm 4-FBnCl in the isolated darapladib, demonstrating that at least approximately 1300 ppm 4-FBnCl was tolerated. In both experiments the yield of the product was at the lower end of the quoted range. It was speculated that this could be an effect of the presence of 4-FBnCl in the reaction mixture affecting the solubility of darapladib during the crystallisation.

Entry	4-FBnCl content of 74 / ppm[a]	4-FBnCl in darapladib IG / ppm[a]	Yield 71 / %
1	968	<1	77
2	1276	<1	75

Conditions: (i) **74** (1.0 equiv.), CDI (1.2 equiv.), MIBK (6 vol), 70 °C, 80 – 90 min; (ii) **77** (1.1 equiv.), 92 °C, 125-150 min.

[a] Analysis by GC.

Table 27: Purging of 4-FBnCl in formation of darapladib IG.

Although the data obtained were very encouraging, we were still concerned that much higher 4-FBnCl levels could occur in carboxylic acid **74** due to possible variations in the process parameters. Further experiments were completed to extend our knowledge beyond the limits of the initial data. In order to do this, extra 4-FBnCl was added to the reaction mixture at the beginning of the process. Initially, a spike of 0.5% w/w (5000 ppm) relative to carboxylic acid **74** was used, followed by a much larger spike of 7% w/w (70000 ppm) (Table 28). The 7% w/w value was chosen as this was calculated as the potential absolute worst case scenario for 4-FBnCl carrying

through from the previous stage,* although this was considered to be a gross overestimation of what was truly likely.

Entry	4-FBnCl spike / ppm (% w/w)	4-FBnCl in darapladib IG / ppm[a]	Yield 71 / %
1	5000 (0.5)	<1	82
2	70000 (7.0)	<1	79
3	70000 (7.0)	<1	78

Conditions: (a) **74** (1.0 equiv.), CDI (1.2 equiv.), MIBK, 70 °C then 4-FBnCl (amount as above), 60 – 140 min; (b) **77** (1.1 equiv.), 92 °C, 120 – 150 min.

[a] Analysis by GC.

Table 28: Spiking experiments in amide bond formation.

Once again, despite the large amount of 4-FBnCl added, the quantity of 4-FBnCl in the isolated material was reduced to <1 ppm at both levels tested. A repeat run with 7% w/w spike confirmed the results (entry 3). The isolated product yields were also slightly improved in this case, with 82% (entry 1) being a more typical result. The root cause of the yield variation may be an effect of the presence of 4-FBnCl although this has not been proven. Nevertheless, all yields were within the typical range. In these experiments the quality of the product, in particular the 4-FBnCl content, was the most important attribute.

4.3.2.2 Identification of Species Formed From 4-FBnCl

The purging ability of 4-FBnCl during the amidation process was clearly evident. The next challenge was to determine the fate of the 4-FBnCl under the reaction conditions used. Two options were possible: (i) removal of 4-FBnCl in the liquors and by cake washing; and (ii) reaction of 4-FBnCl with species present in the reaction mixture. Analysis of the filtrate and the washes from a spike experiment

* Calculations were based on an assumed overcharge of 4-FBnCl of 5%, combined with an undercharge of thiouracil **95** by 5% in the alkylation chemistry. All unreacted 4-FBnCl was then assumed to not be removed elsewhere in the process. Realistically, much would remain in the liquors and be removed by filtration.

(Table 28, entry 2) by GC* and LCMS suggested that 4-FBnCl was not present at any appreciable level. Therefore, this species must be reacting under the conditions of the process.

By considering the potential nucleophiles present in the reaction mixture during formation of darapladib IG, a number of species were proposed as being capable of reacting with 4-FBnCl (Figure 27). 4-FBnCl could react with imidazole to form **104** (a), or with carboxylic acid **74** to form ester **96** (b). Reaction with the amine **77** could form **105** or **106** from monoalkylation (c), and potentially **107** or **108** from bis-alkylation (d & e). 4-FBnCl could react with methanol, which is the crystallisation solvent, to give **109** (f). In addition, 4-FBnCl could react with darapladib itself to form a quaternary ammonium species such as **110** (g). No further species were considered at this stage.

* Unpublished method.

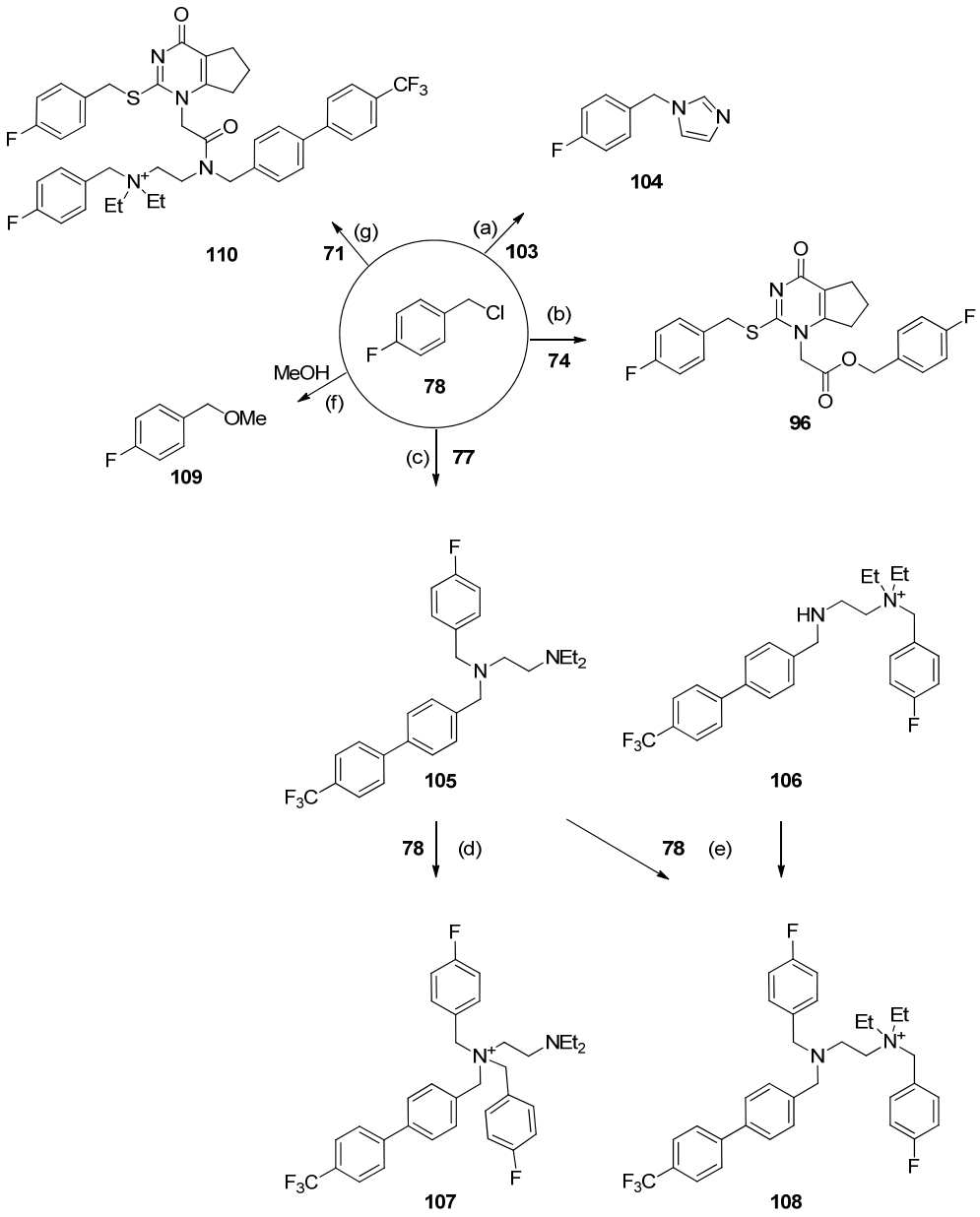

Note: The counterion for all cations is assumed to be chloride.

Figure 27: Postulated reactions for 4-FBnCl during formation of darapladib IG.

LCMS analysis (Table 28, entry 2) showed that alkylated imidazole derivative **104** was forming during the preparation of imidazolide **102**. It was also speculated that further alkylation of **104** could occur to form bis-alkylated species **111**, however, this species was not specifically sought at this stage (Figure 28).

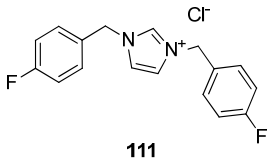

111

*Figure 28: Bis-alkylated imidazole impurity **111**.*

Additionally, after addition of amine **77** to the reaction mixture there was also evidence for formation of diamine **105** or **106**. At this point in time, distinguishing between diamines **105** and **106** was not possible, although both could conceivably be formed. Of the remaining postulated species in Figure 27, none were identified by LCMS analysis.

4.3.2.3 Preparation of 4-FBnCl Derived Impurities

Samples of both imidazole derived impurities **104** and **111** were prepared following a literature method (Scheme 28).[112] The benzyl chloride was used instead of the benzyl bromide specified in the literature. Following work-up **104** was isolated in 64% yield, and spectral data matched that reported.[113] Isolation of **111** was less trivial and sufficient material was obtained for use as a retention marker, and for NMR spectroscopic analysis. The sample was contaminated with imidazole, estimated at 33% w/w by quantification using ^{1}H NMR spectroscopy, but was otherwise consistent with literature data.[114*]

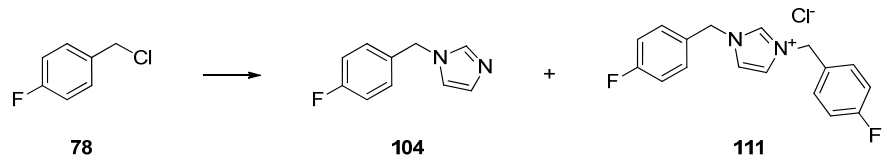

78 **104** **111**

Reagents and conditions: Imidazole (2.0 equiv.), K_2CO_3 (0.5 equiv.), THF, reflux, 24 h, **104**: 64%, **111**: 2%.

*Scheme 28: Preparation of imidazole impurities **104** & **111**.*

The alkylation of amine **77** with 4-FBnCl was carried out (Scheme 29). Analysis showed that two products had formed, one preferred over the other (20:1 ratio of

[*] Data are cited for bromide salt in d_6-DMSO.

products by HPLC). Following work-up and chromatography of a portion of the crude mixture the major product was isolated and found to be **105** by NMR spectroscopic analysis. LCMS analysis suggested that the minor product was the quaternary ammonium species **106**, although to date this has eluded isolation and characterisation.

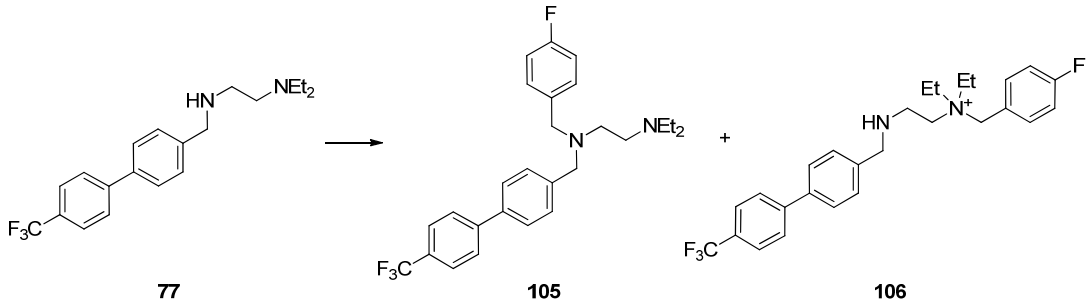

Reagents and conditions: **77** (1.1 equiv.), 4-FBnCl (1.0 equiv.), toluene, 90 °C, 25 h, **105**: 12%.

*Scheme 29: Alkylation of amine **77**.*

Analysis of darapladib IG from the 7% w/w 4-FBnCl spiking experiments (Table 28, entries 2 & 3) showed that a single new impurity was present, although below the reportable limit of 0.05% area. By completing HPLC spiking studies the impurity identity was confirmed as being diamine **105**. At this low level the impurity poses no concern.

4.3.2.4 Reaction Monitoring

The formation of impurities was investigated in more detail, with the ultimate aim of quantifying the amount of each impurity, and accounting for all of the 4-FBnCl present. The level of 4-FBnCl was monitored during the formation of intermediate imidazolide **102**. Within this part of the process it was assumed that 4-FBnCl would react with imidazole **103**. Data were gathered at two temperatures since two temperatures are used during the process to form darapladib (Figure 29).

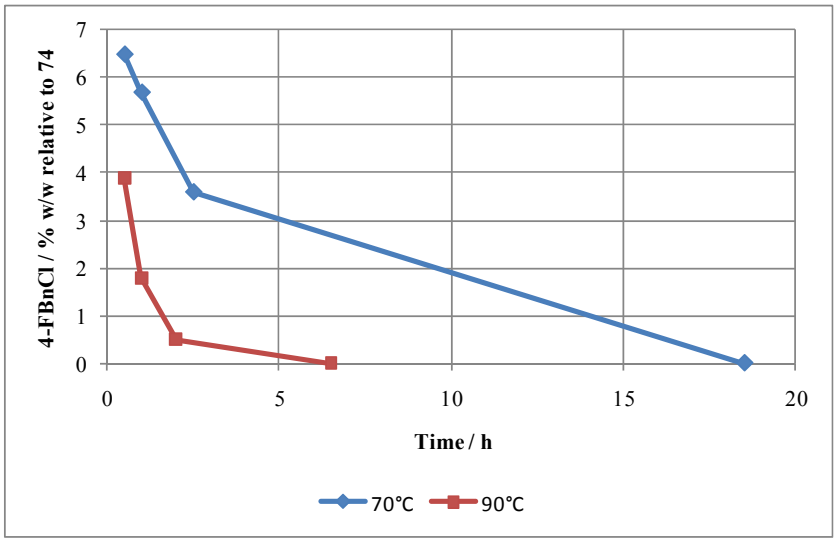

Reagents and conditions: **74** (1.0 equiv.), CDI (1.2 equiv.), 4-FBnCl (0.16 equiv., 7% w/w relative to **74**), MIBK, 70 °C or 90 °C.

*Figure 29: Reaction of 4-FBnCl during formation of imidazolide **102**.*[*]

The data show that under the conditions used to form imidazolide **102** (70 °C for 30 min) the reaction of 4-FBnCl with imidazole did not proceed very far. However, after overnight reaction, 4-FBnCl was not detected. At the higher temperature the reaction was considerably faster. Since amine **77** was not present in these experiments, the results show that reaction with imidazole could be a major pathway for reaction of 4-FBnCl. Imidazole is present in large excess over 4-FBnCl when forming darapladib, since one equivalent is released from the initial reaction to form imidazolide **102** and a second is released when amine **77** reacts with **102** (*vide supra*, Scheme 27, page 90). Furthermore, under the conditions used for the experiments in Figure 29, LCMS evidence was obtained to support the formation of the proposed bis-alkylated species **111**.

[*] ^{19}F NMR spectroscopy was used to quantify the level of 4-FBnCl relative to **74** (4-FBnCl peak at -113.55 ppm and carboxylic acid **74** peak at -114.83 ppm).

Having obtained information for the reaction of 4-FBnCl during the formation of imidazolide **102**, subsequent reaction monitoring was completed to investigate the remainder of the process. Thus, imidazolide **102** was prepared *via* the standard process, in the presence of 4-FBnCl. Following addition of amine **77** the formation of 4-FBnCl derived impurities **104** and **105** was monitored (Figure 30).

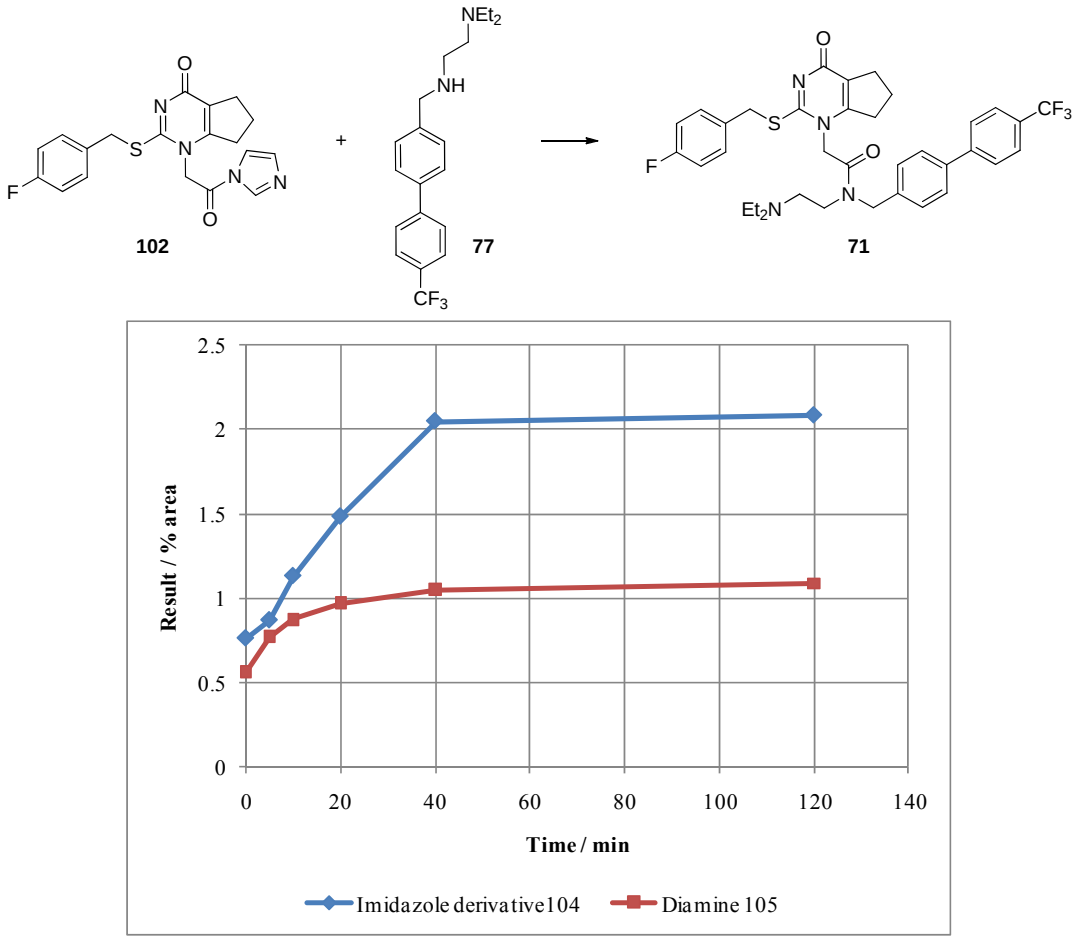

Conditions: (a) **74** (1.0 equiv.), CDI (1.2 equiv.), MIBK, 70 °C then 4-FBnCl (0.16 equiv.), 1 h; (b) **77** (1.1 equiv.), 92 °C, 2 h.

*Figure 30: Reaction monitoring of alkylated imidazole **104** and diamine **105** during the preparation of darapladib.*[*]

[*] Data are not quantitative. Analysis was carried out on two different HPLC methods (Methods A & B) at different wavelengths.

The data suggest that for both species the majority of the reaction is complete within 40 minutes. This implies that the 4-FBnCl has reacted completely within this timeframe. However, the data give no indication of reaction rate (*i.e*. kinetic data) or quantitative information. Quantification was viewed as important at this point, because any discrepancy in the mass balance would suggest that some previously unidentified species are also forming from reaction of 4-FBnCl under the reaction conditions.

4.3.2.5 Quantification of Impurities

In order to accurately quantify the species forming on reaction with 4-FBnCl, an internal standard needed to be identified. Using this strategy an unreactive material can be added to a reaction mixture, and then detected using an appropriate analytical method (*e.g*. HPLC). Provided a response factor, termed an "*r*" value, has been calculated for any analyte requiring quantification relative to the internal standard, accurate data on the mass of species present can be obtained at various time points.

The two species in question, imidazole derivative **104** and diamine **105**, have maximum UV spectrum responses at different wavelengths. This meant that using the same internal standard for both was impractical. Additionally, due to the presence of other impurities in the reaction mixture, two HPLC methods were required to ensure sufficient resolution of the peaks in question to allow identification and quantification. Values for *r* were identified for **104** and **105** relative to two internal standards as shown in Table 29.

Entry	Analyte	HPLC Method	Approx. λ_{max} / nm	Internal standard	*r* value[a]
1	**104**	Method A	205	Methyl *p*-tolyl sulfone	3.204
2	**105**	Method B	260	Biphenyl	1.844

[a] See experimental for calculation details.

Table 29: r values for 4-FBnCl-derived impurities.

As a first test of the newly calculated *r* values, the reaction liquors and cake washes from the two experiments, which used 7% w/w 4-FBnCl, were investigated (Table 28, entries 2 & 3, page 92). An aliquot of each liquor or wash sample was taken, the

internal standard was added, and samples were run on the appropriate HPLC method (Table 30).

Entry	Sample	Yield 104 / %[a]	Yield 105 / %[b]	Total yield / %
1 (Table 28, entry 2)	Liquors	69.5	10.4	79.9
	Wash 1	16.6	2.1	18.7
	Wash 2	0.7	0.1	0.8
	Total	*86.7*	*12.6*	***99.3***
2 (Table 28, entry 3)	Liquors	74.2	9.0	83.2
	Wash 1	15.4	1.9	17.3
	Wash 2	1.5	0.2	1.7
	Total	*91.1*	*11.1*	***102.2***

[a] HPLC Method A.

[b] HPLC Method B.

Table 30: Analysis of liquors and washes from experiments containing 7% w/w 4-FBnCl.

Pleasingly, the data showed excellent mass balance over both sets of samples, suggesting that imidazole derivative **104** and diamine **105** were the main species forming. With these data in hand, further experiments to investigate the formation of both impurities over time during the reaction were carried out. The two impurities were investigated separately due to the requirement for different internal standards. After the reaction the second internal standard was added to quantify the other compound.

Investigation into the quantitative formation of diamine **105** was carried out under standard reaction conditions in the presence of 7% w/w 4-FBnCl (Figure 31). As the diamine only forms after addition of amine **77**, only this part of the reaction was monitored. Formation of imidazolide **102** typically results in a thick slurry which persists for a time after charging amine **77** and heating to 92 °C. Representative sampling of a slurry is usually difficult; therefore, samples were only taken after obtaining a solution.

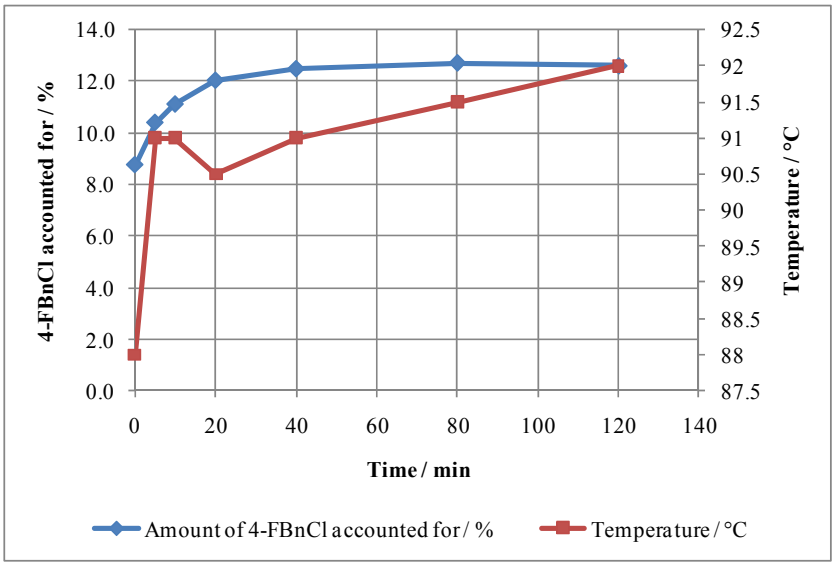

Reaction conditions: (i) **74** (1.0 equiv.), CDI (1.2 equiv.), 4-FBnCl (0.16 equiv., 7% w/w relative to **74**), MIBK (6 vol), 70 °C, 50 min; (ii) **77** (1.1 equiv.), heat to 92 ± 3 °C, stir 2 h.

*Figure 31: Formation of diamine **105** during preparation of darapladib IG.*

It can be seen that over 8% of the 4-FBnCl was already accounted for when the first sample was taken. Quantification showed that 12.6% of the charged 4-FBnCl was accounted for by reaction to form diamine **105**. Calculation of the amount of imidazole derivative **104** after the reaction showed 87.6% of the 4-FBnCl was accounted for, giving an overall mass balance of 100.2%.

A second experiment was carried out in similar fashion, this time quantifying imidazole derivative **104** throughout the entirety of the darapladib-forming reaction (Figure 32). Despite the presence of a slurry during formation of imidazolide **102**, seemingly robust data were obtained throughout the experiment.

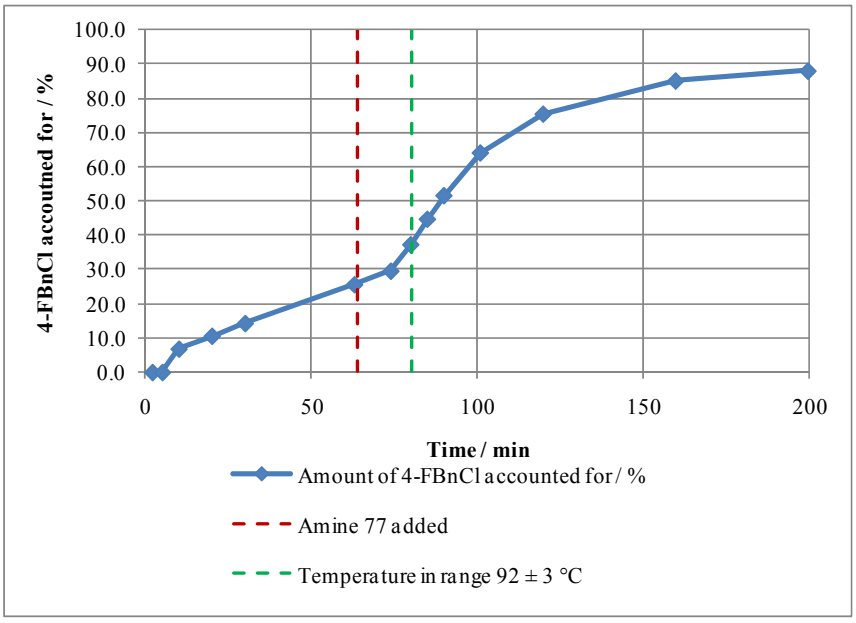

Reaction conditions: (i) **74** (1.0 equiv.), CDI (1.2 equiv.), 4-FBnCl (0.16 equiv., 7% w/w relative to **74**), MIBK (6 vol), 70 °C, 64 min; (ii) **77** (1.1 equiv.), heat to 92 ± 3°C, 2 h.

*Figure 32: Formation of imidazole derivative **104** during preparation of darapladib IG.*[*]

During the formation of imidazolide **102** (over 1 h) 25.6% of the 4-FBnCl was accounted for. After the preparation of darapladib 88.0% of the 4-FBnCl had been reacted to form imidazole derivative **104**. Quantification of diamine **105** was carried out after the reaction and showed 11.8% of 4-FBnCl had reacted *via* this pathway. The mass balance for 4-FBnCl forming **104** and **105** was therefore 99.8%, showing excellent agreement with the previous results.

The investigations into the quantification of the impurities deriving from 4-FBnCl have shown that two main species form. Given that the mass balance for these impurities is excellent across four experiments it is likely that any other reactions of 4-FBnCl, which occur during the reaction to form darapladib IG are at a low level and are insignificant under standard reaction conditions.

[*] Temperature data were not recorded at every time point during this experiment.

Whilst the data obtained were excellent and encouraging, a predictive mathematical model would be of great value. This would allow the effect of any proposed variation in reaction conditions on the 4-FBnCl level to be assessed. Fundamental reaction kinetics would achieve this aim and, potentially, provide further useful information such as the half life of 4-FBnCl under the reaction conditions employed.

4.3.2.6 Kinetics Investigations

The kinetics of the reaction of 4-FBnCl in the reaction mixture to form darapladib IG were considered to be complicated, with competing reactions of 4-FBnCl with imidazole and amine **77**. It was decided to simplify the system by considering the imidazole reaction pathway first, as this had been shown to be responsible for the reaction of the majority of the 4-FBnCl.

Quantification of 4-FBnCl was achieved on HPLC Method A relative to methyl *p*-tolyl sulfone (r = 1.484).* Quantification of imidazole was not possible by HPLC as it was not observable by the methods available.

Experiments to investigate the kinetics of the reaction between 4-FBnCl and imidazole were carried out as shown in Table 31.

* See experimental for full details.

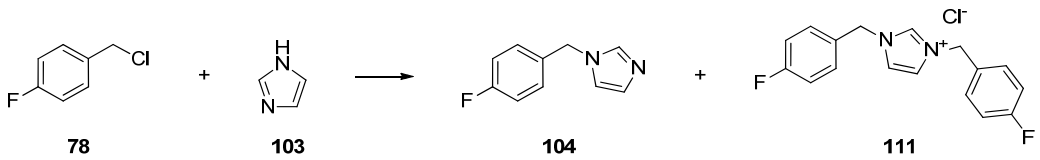

78 103 104 111

Entry	4-FBnCl 78 / equiv.	Imidazole 103 / equiv.	Temperature / °C	MIBK / vol	Concentration 4-FBnCl / g/mL
1	1	1.5	70	6	0.167
2	1	1.5	90	50	0.02
3	1	15	90	100	0.01
4	1	7.5	90	100	0.01
5	1	1.5	90	100	0.01
6	1	15	80	100	0.01

Table 31: Experiment conditions to investigate the kinetics during reaction of 4-FBnCl with imidazole.

The initial experiment (entry 1) with 1.5 equivalents of imidazole suffered from formation of solids. Isolation and ^{1}H NMR spectroscopic analysis of a sample of the solid suggested it was composed predominantly of imidazole hydrochloride salt and bis-alkylated product **111**. There did not appear to be any 4-FBnCl within the solid, suggesting that the solution data for 4-FBnCl could be of use for kinetics modelling. In an effort to ensure no solid crystallisation occurred, the reaction volumes and the temperature were increased (entry 2). Again, solids were observed prompting a move to even more dilute conditions with a vast excess of imidazole (entry 3). This strategy was successful in preventing solid formation. Additional experiments were then carried out to vary the concentration of imidazole and the temperature (entries 4 to 6); of these, only entry 6 remained a solution throughout.

The solution yield data were plotted to provide immediate pictorial comparisons of the various conditions. The settings used in entry 1 do not directly compare with any of the other data sets (Figure 33). Imidazole derivative **104** was observed to rise initially, and then diminish as it is further alkylated to form dialkylated impurity **111**. The formation of **111** was evident from the HPLC data, but was not quantifiable due to lack of a suitable HPLC *r* value and a pure sample with which to determine it.

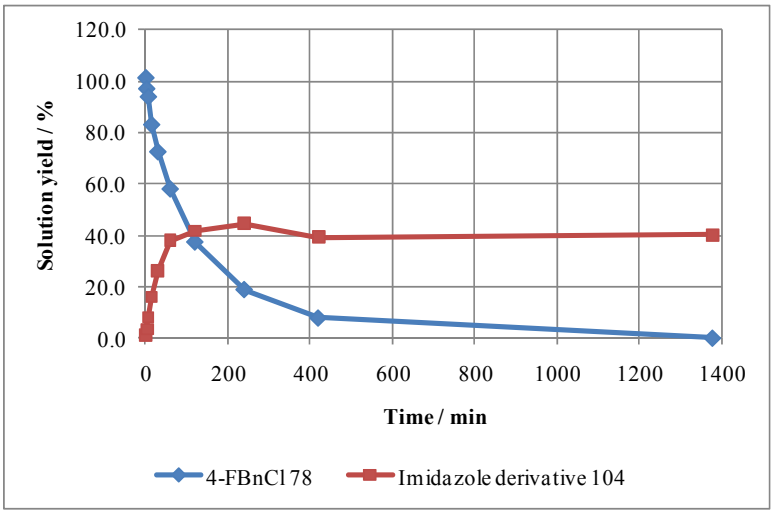

Figure 33: Initial experiment (Table 31, entry 1).

Entries 3 and 6 can be compared to show the effect of temperature (Figure 34). The rate of reaction of 4-FBnCl is significantly faster at the higher temperature.

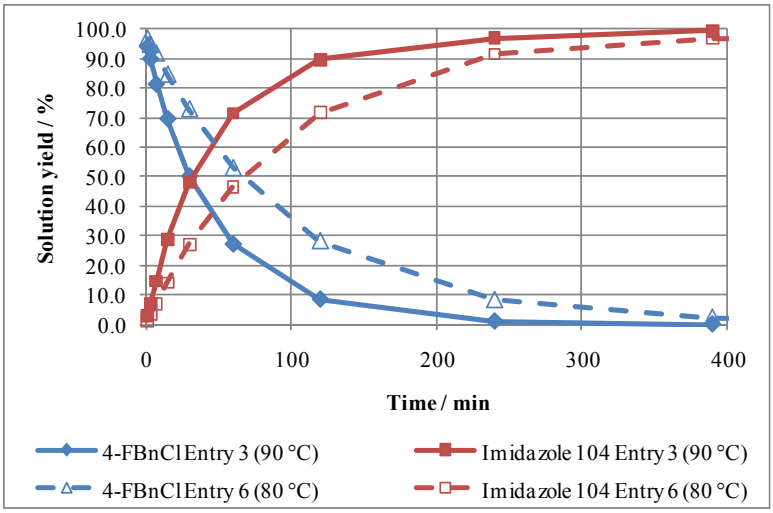

Figure 34: Effect of temperature (Table 31, entries 3 and 6).

The effect of varying imidazole concentration on the rate of reaction is evident from comparing the data from entries 3 to 5 (Figure 35). The reaction of 4-FBnCl is considerably faster in the presence of a vast excess of imidazole.

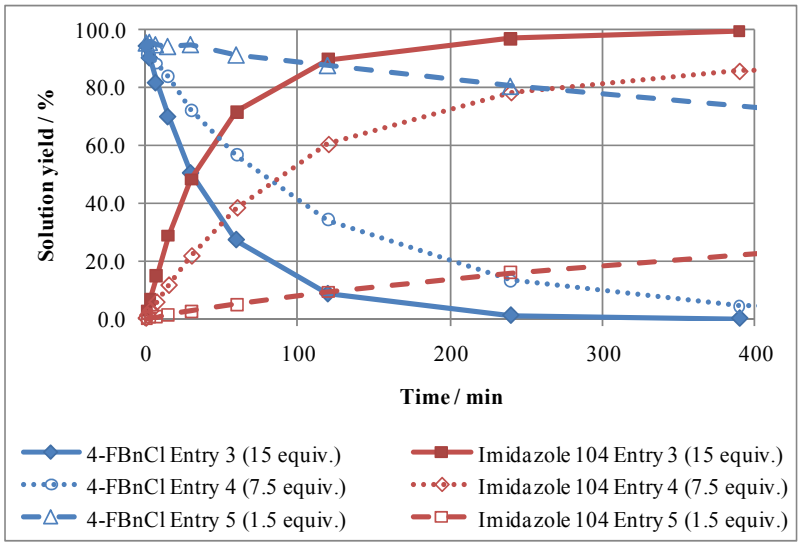

Figure 35: Effect of variation of imidazole concentration (Table 31, entries 3 to 5).

Finally, comparison of entries 2 and 5 show the effect of varying the reaction mixture concentration (Figure 36). Under more dilute conditions the reaction is slower.

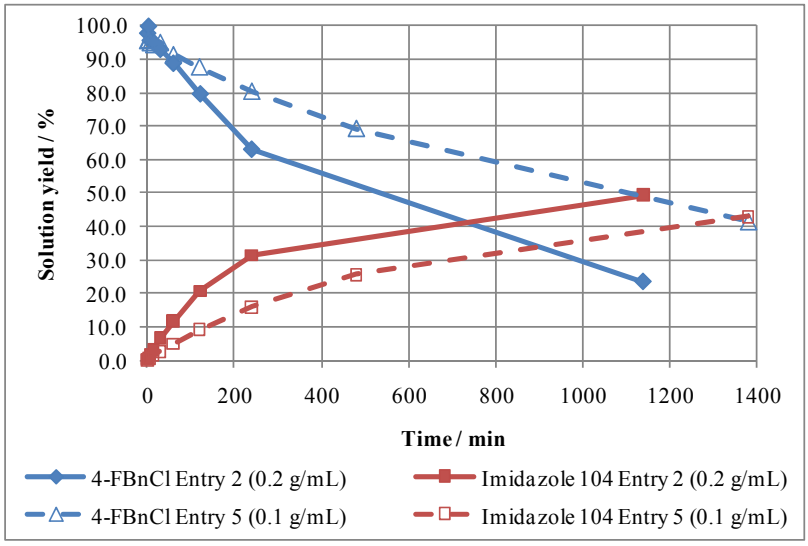

Figure 36: Effect of varying solvent concentration (Table 31, entries 2 and 4).

For first order kinetics it can be shown that for a reactant A:[115]

$$\ln[A] = \ln[A]_0 - kt$$

Where: $[A]$ = Concentration of reactant A at any time t

$[A]_0$ = Concentration of A at time t = 0

k = Rate constant

t = Time

Thus, a plot of ln[A] *versus* time will give a straight line if the reaction is first order in reactant A. The data for 4-FBnCl were plotted in this way, and showed that the reaction was first order in 4-FBnCl at high dilution, or high imidazole concentration, or both (Table 31, entries 3 to 6, Figure 37). When the amount of imidazole is high its concentration can be considered to be constant. Hence, rather than the standard second order rate equation, a first order rate equation with the rate constant *k*' can be used as an approximation:

$$\text{Rate} = k\,[\text{4-FBnCl}][\text{imidazole}]$$

$$\text{Rate} \approx k'\,[\text{4-FBnCl}]$$

Where : k' = $k\,[\text{imidazole}]$

The reaction is termed pseudo first order by use of this approximation. The gradient of each of the plotted lines is equal to the rate constant *k*' for each set of conditions. The first order approximation could not be applied for those experiments at low dilution with low imidazole content (entries 1 & 2).

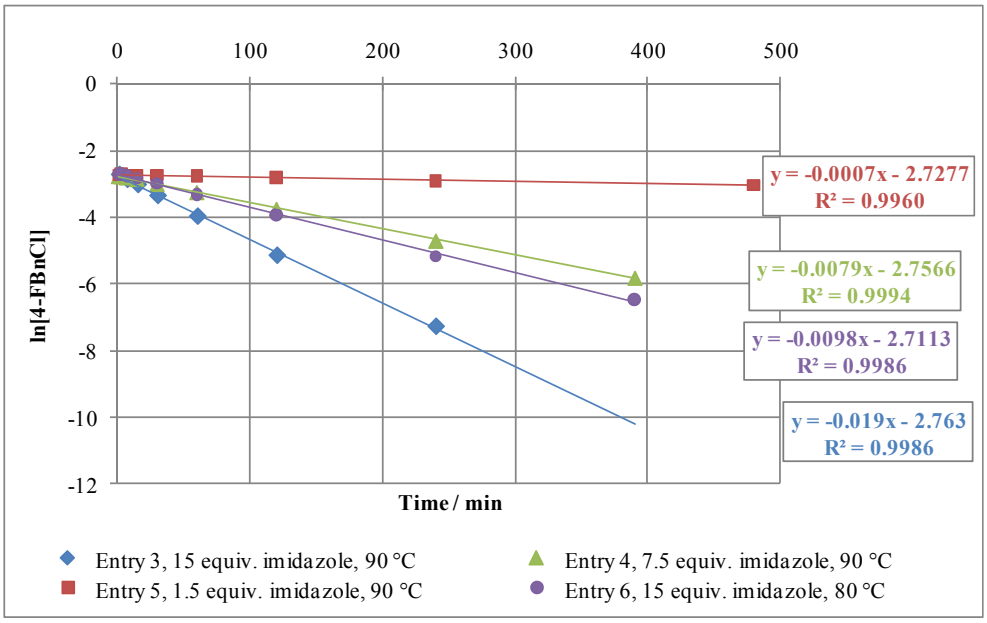

Figure 37: Log plots showing pseudo first order kinetics of 4-FBnCl (Table 31, entries 3 to 6).

The data generated need to be considered with reference to the original system under investigation, *i.e.* the reaction conditions to form darapladib IG in the presence of a 4-FBnCl spike. In this situation imidazole is present in vast excess, and the reaction mixture is very dilute relative to 4-FBnCl. In this respect, the conditions used in entries 3 & 6 in Table 31 are very applicable to the real system. Hence, it should be possible to use these data as a good estimation of the real situation.

The log plots shown in Figure 37 can allow determination of the pseudo first order rate constant *k*'for the reaction of 4-FBnCl with imidazole (Table 32).

Entry	Temperature / °C	Pseudo first order rate constant *k*' / min^{-1}	$t_{½}$ / min
1 (Table 31, entry 3)	90	0.019	36.5
2 (Table 31, entry 6)	80	0.0098	70.7

Conditions: Imidazole **103** (15 equiv.), 4-FBnCl (1.0 equiv.), MIBK (100 vol).

Table 32: Kinetic data for 4-FBnCl reaction with excess imidazole at high dilution.

Once the rate constant is known, the half life, $t_{½}$, for a reactant (here 4-FBnCl) can be calculated. The half life is the time taken for the concentration of a reactant to be reduced by half. For a first order reaction it can be shown that:[115]

$$t_{½} = \frac{\ln 2}{k}$$

The half life of 4-FBnCl can be calculated at the two temperatures investigated (Table 32). The typical time of the amide bond formation to prepare darapladib at approximately 90 °C is 2 hours and this represents about four half lives of 4-FBnCl. Therefore, the amount of 4-FBnCl should be reduced by 2^4, or 16 times. However, this does not agree with the experimental observations that a spike of 7% w/w 4-FBnCl can be reduced to effectively zero, and suggests there are limitations to these very basic calculations and the simplifications imposed.

With data at different temperatures available, the activation energy, E_a, can also be estimated by using the Arrhenius equation:[115]

$$\ln k = \ln A - \frac{E_a}{RT}$$

Where:

	A	=	Pre-exponential factor (same units as *k*, min^{-1})
	E_a	=	Activation energy ($Jmol^{-1}$ or $kJmol^{-1}$)
	R	=	Ideal gas constant (8.3145 $JK^{-1}mol^{-1}$)
	T	=	Temperature (K)

A plot of ln*k* versus 1/T is a straight line, and E_a can be calculated from the gradient of the line, with A being determined from the *y*-intercept. Consequently, E_a for the reaction of 4-FBnCl under dilute conditions with excess imidazole is estimated as 70.5 $kJmol^{-1}$, and A, the pre-exponential factor, is estimated as 2.68 x 10^8 min^{-1}.* Use of the Arrhenius equation can then allow calculation of the rate constant *k* at any temperature T.

* The Arrhenius parameters are estimated as data at only two temperatures was obtained. More conclusive figures could be obtained by repeating the experiments at a third temperature.

As mentioned above, the data analysed represent a very simplistic view. In reality the situation is more complicated. As identified, there are a number of other competing reactions in which 4-FBnCl plays a role, and these have not been taken into account. For example, the formation of diamine **105** has been shown to account for approximately 10% of the 4-FBnCl charged. In addition, the real darapladib system has two different sets of reaction conditions in the process. So initially 4-FBnCl can undergo reaction with imidazole during the formation of imidazolide **102** at 70 °C. As demonstrated, this can account for approximately 25% of the 4-FBnCl charged after approximately 1 hour reaction time (*vide supra*, Figure 32, page 102). Therefore, of the 70,000 ppm of 4-FBnCl which was charged, only approximately 52,500 ppm remains when amine **77** is added. Even so, this is still a large figure, and the estimated four half lives available for its reaction does not appear to adequately account for the observed result of <1 ppm in the isolated material.

The data from the experiments illustrated by Figures 31 and 32 can be used together to obtain an estimation of the observed half life of 4-FBnCl in the real system, where both impurities **104** and **105** were observed to form. Unfortunately, due to limitations in the analytical methods used, 4-FBnCl cannot be directly measured by reanalysing the data sets from these reactions. Within HPLC Method A, 4-FBnCl and darapladib co-elute, whilst with HPLC Method B, 4-FBnCl has a very low response at the set wavelength of 260 nm.

A number of assumptions need to be applied since the two experiments were carried out separately to quantify a single impurity in each case. However, the same conditions were used for both. If it is assumed that the distribution of the products is the same in each experiment, an estimate of the solution concentration of 4-FBnCl can be obtained based on the amounts of products formed. Using the same calculations discussed above, a log plot can be generated for the reaction of 4-FBnCl under the reaction conditions of the coupling (Figure 38).

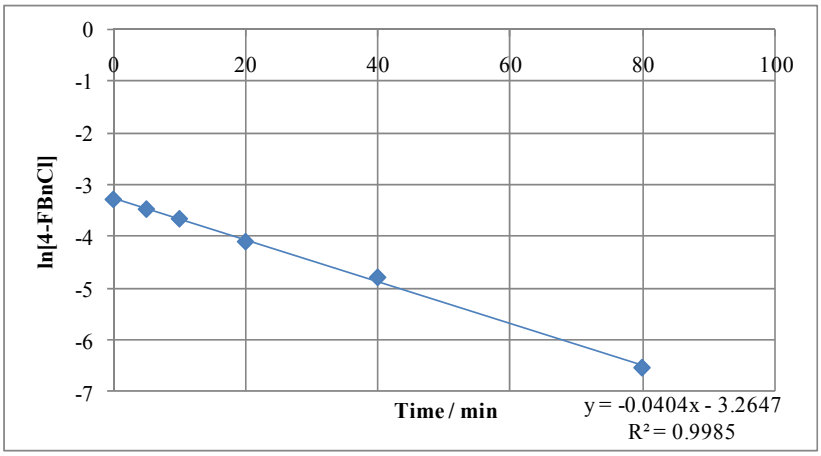

Figure 38: Log plot for estimated 4-FBnCl concentration under amidation conditions.

The linear log plot agrees with pseudo first order kinetics as anticipated. The half life is calculated as 17.2 min. For the specified 2 h for the coupling reaction, this is approximately seven half lives, or a 128-fold reduction of 4-FBnCl. Thus for an initial charge of 70,000 ppm, with approximately 25% being reacted during the imidazolide formation, followed by a 128-fold reduction of the remainder, the result is a figure of around 400 ppm 4-FBnCl remaining in the reaction mixture prior to crystallisation and isolation. It is highly plausible that this level of 4-FBnCl will remain in solution and be easily removed from the isolated solid by the cake washes. As a result, the observed experimental figures of <1 ppm in isolated darapladib IG seem rational based on these estimations for the half life. Therefore, any model for the real system needs to be able to predict a half life of around 17 minutes in order to be realistic.

Based on all of the above, the experiments carried out thus far were underestimating the reaction rate by about 50%. These observations prompted us to consider whether some alternative mechanism may be occurring to accelerate the reaction of 4-FBnCl with imidazole. It was postulated that any base present in the system (*e.g.* amine **77** or darapladib itself) could be deprotonating imidazole, resulting in an equilibrium between imidazole and its anion (Figure 39). The anionic species **112** could then react with 4-FBnCl more quickly than imidazole itself.

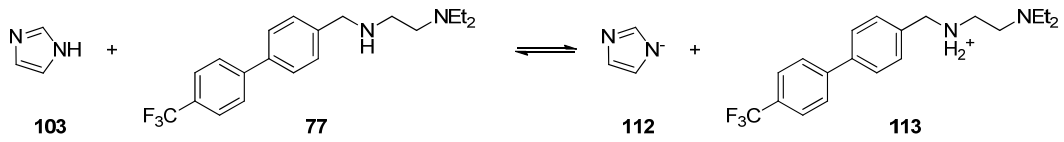

Figure 39: Possible acceleratory effect of bases on imidazole under reaction conditions to form darapladib.

Consideration of the pK_as of relevant amines suggests that it is unlikely that deprotonation of imidazole could be achievable (Table 33). The pK_a for amine **77** is not available, but it seems reasonable to suggest that the first pK_a would be similar to TEEDA (*ca* 6.2) and the second would be similar to *N*-ethylbenzylamine (*ca* 9.8).

Acid	Conjugate base	pK_{aH} (in H_2O)[116-119]
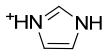		7.13
		12.7
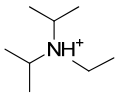	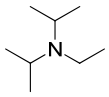	11.45
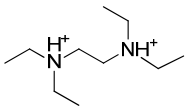	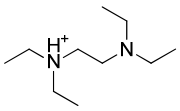	6.18
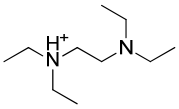	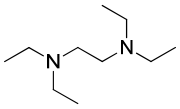	9.55
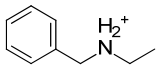	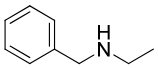	9.83

Table 33: pK_a values for amines.

However, a number of experiments were carried out to investigate the effect of various amines on the reaction rate of 4-FBnCl (Table 34).

Entry	4-FBnCl 78 / equiv.	Imidazole 103 / equiv.	Temperature / °C	MIBK / vol	Additive (equiv.)
1	1	15	90	100	Amine **77** (6.8)
2	1	15	90	100	DIPEA (6.8)
3	1	15	90	100	TEEDA (6.8)

Table 34: Experiments to investigate possible acceleratory effect of amines.

Entry 1 used amine **77** as an additive. It was observed that the distribution of products was significantly different to that seen in the real case when darapladib is prepared, with imidazole derivative **104** being observed in approximately 60% yield rather than >85% (Figure 40). Presumably, these differences are a result of there being no competing reaction for amine **77**.

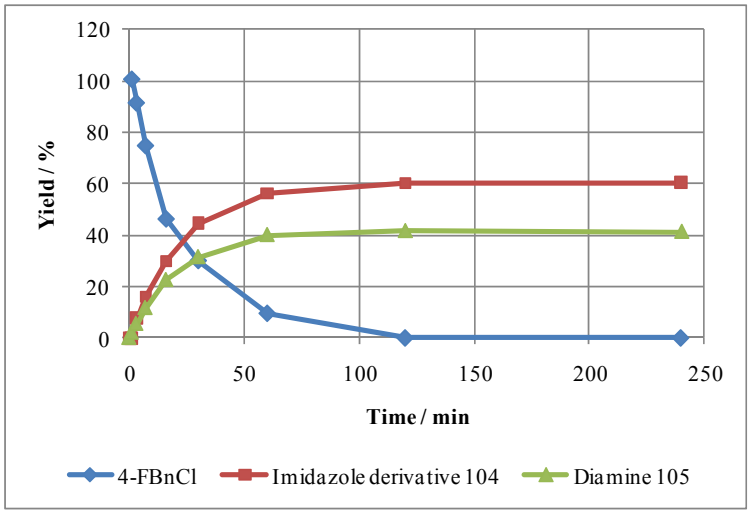

*Figure 40: Reaction mixture data in the presence of amine **77**.*

Comparison of solution yield profiles for this experiment with entry 3 in Table 31 suggested some rate acceleration (Figure 41).

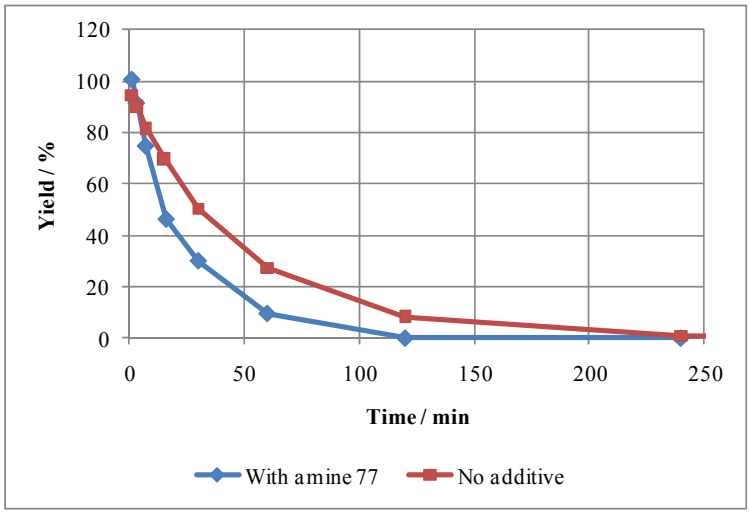

Figure 41: Comparison of 4-FBnCl data from Table 34, entry 1 and Table 31, entry 3.

DIPEA was next investigated as an additive (Table 34, entry 2) in an effort to obtain data without a competing alkylation reaction occurring with the additive. Comparing the yield data with the additive-free experiment (Table 31, entry 3) suggested minimal rate difference. The use of tetraethylethylenediamine (TEEDA) was investigated since it is similar to amine **77** but less likely to undergo reaction itself (Table 34, entry 3). The data also showed only a minor rate increase, but a poor mass balance was observed in this case, and an unidentified peak in the HPLC trace suggested that the TEEDA was actually being alkylated under the reaction conditions. The formation of this alkylated by-product was not quantified or investigated further.

To allow better comparison, log plots for the three experiments were prepared (Figure 42). This treatment revealed some differences which were not so obvious from the solution yield data, and suggested that the presence of the additives did indeed result in a faster rate of reaction and a smaller half life under the pseudo first order kinetics assumption.

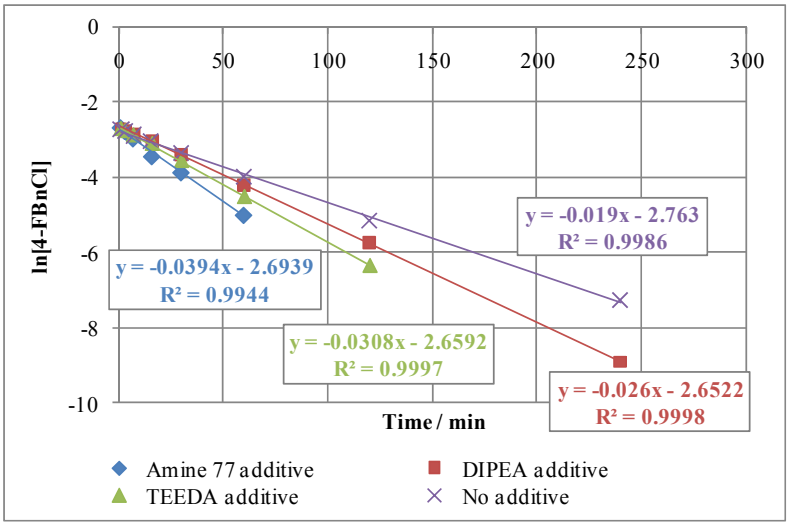

Figure 42: Log plots from experiments including additives (Table 34) compared with no additive (Table 31, entry 3).

The half lives for 4-FBnCl calculated for each of the above log plots are shown in Table 35. The figure of 17.6 min in the presence of amine **77** is approaching that required to match the real case.

Entry	Additive	Pseudo first order rate constant *k*' / min^{-1}	$t_{1/2}$ / min
Table 31, entry 3	None	0.019	36.5
Table 34, entry 1	Amine **77**	0.0394	17.6
Table 34, entry 2	DIPEA	0.026	26.7
Table 34, entry 3	TEEDA	0.0308	22.5

Table 35: Calculated rate constants and half lives for reaction with additives.

On balance, and with consideration of the pK_a data, it was decided that any rate acceleration due to the deprotonation of imidazole by amines would be negligible, and the increased reaction rates observed were a result of there being multiple mechanisms by which 4-FBnCl could react simultaneously. In order to simplify the kinetics model the deprotonation pathway was not considered further.

4.3.2.7 DynoChem® Modelling

At this stage it seemed appropriate to carry out full kinetics analysis using DynoChem® software from Performance Fluid Dynamics. Only the final kinetics model generated is discussed here. The case under investigation is thus: the reaction between amine **77** and acid **74** to prepare darapladib is carried out. Depending on the conditions used to prepare acid **74** it will contain varying quantities of 4-FBnCl. The 4-FBnCl has been shown to react to form imidazole derivative **104** and alkylated amine **105** under the conditions of the coupling reaction. All these reactions must be defined within the kinetic model in order to be able to accurately model the whole system in question (Figure 43).*

The main reaction of 4-FBnCl is the formation of imidazole derivative **104** ([1]). Proton transfer steps are also required by DynoChem® to ensure balanced equations are present within the model ([2], [4] and [5]). These proton transfers are generally assumed to be very fast. The secondary reaction for 4-FBnCl is the formation of amine **105** ([3]).

* The model discussed concentrates on the second part of the coupling reaction, and does not extend to consider the reactions of 4-FBnCl occurring during the formation of imidazolide **102**.

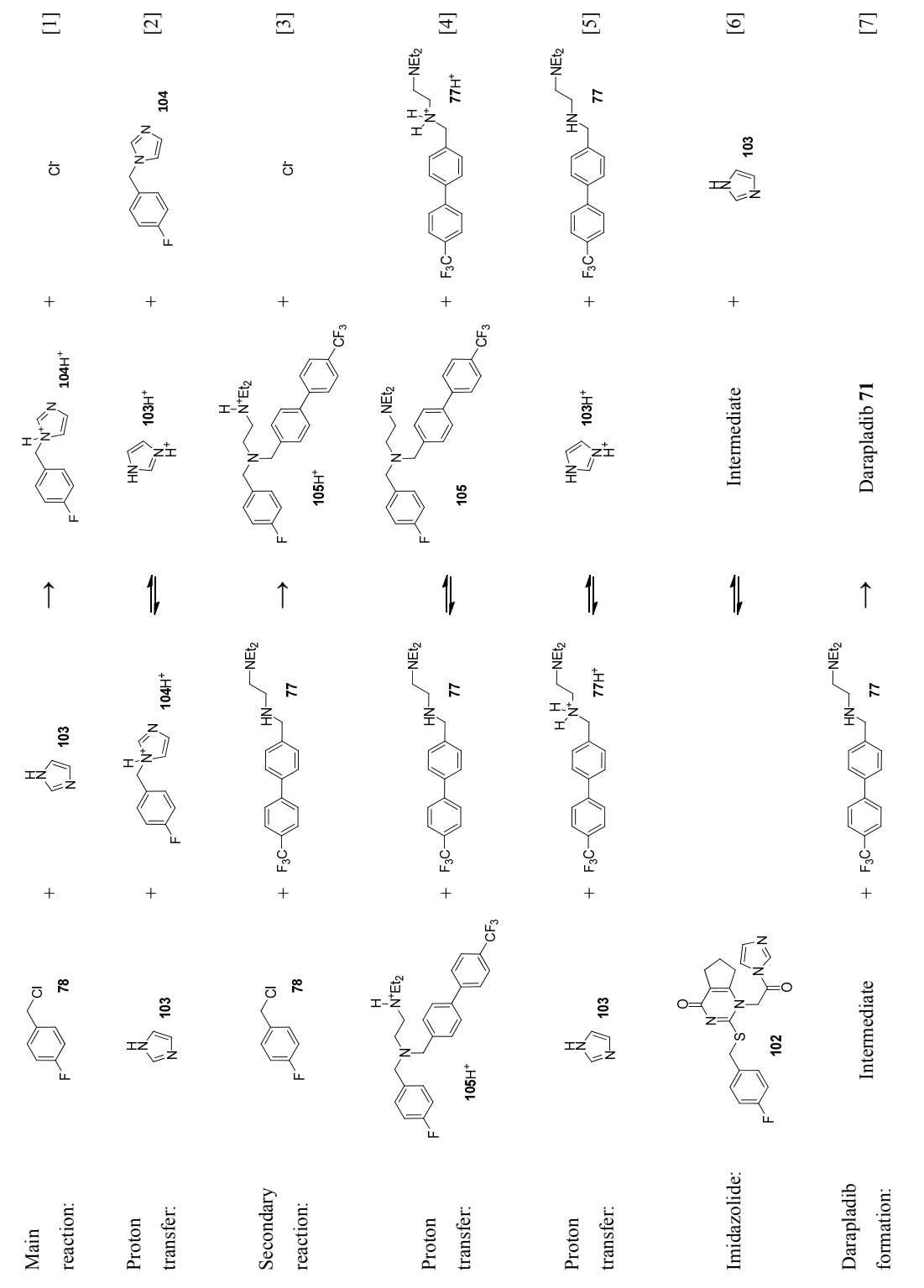

Figure 43: Reactions as defined in DynoChem®.

The kinetics for the amide formation to darapladib have previously been determined within our laboratories ([6] & [7]).[120] This reaction must also be included in the current model to fully account for the reactions of amine **77**. For this part of the model an intermediate species formed from imidazolide **102** was required, which would react with amine **77** to form darapladib. In the absence of confirmatory data it is speculated that this intermediate could be a ketene. These reactive species can be prepared from acid chlorides by utilising organic bases such as triethylamine[121] and, as such, may be intermediates during amidation reactions of acid chlorides.[9] Indeed, loss of optical purity in amidations with chiral acid chlorides has been attributed to the formation of intermediate planar ketenes.[122] The similar behaviour of imidazolides in the generation of ketenes has not been found within the literature. However, ketene formation may be possible in analogous fashion to acyl chlorides (Scheme 30).

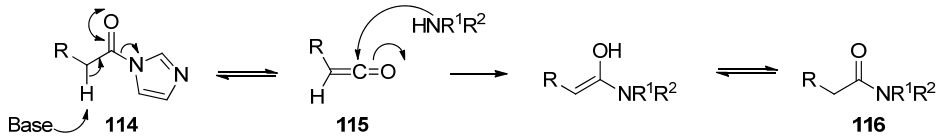

Scheme 30: Formation of a ketene as a potential intermediate.

A base, presumably imidazole or amine **77**, could remove the proton alpha to the carbonyl, and result in ketene intermediate **115** upon loss of imidazole. This ketene could then react with the amine to form the amide **116**.

Through the fitting of data within DynoChem®, and from existing values for the rate constants (at the temperature given), equilibrium constants and activation energies were defined for the above reactions:

k_1 = 3.70 x 10^{-4} $Lmol^{-1}s^{-1}$ at 90 °C (fitted)

E_{a1} = 78.5 $kJmol^{-1}$ (fitted)

k_2 = 1 $m^3mol^{-1}s^{-1}$ at 90 °C (assumed)

K_2 = 1.00 (assumed)

k_3 = 6.54 x 10^{-4} $Lmol^{-1}s^{-1}$ at 90 °C (fitted)

E_{a3} = 49.6 $kJmol^{-1}$ (fitted)

k_4 = 1 $m^3mol^{-1}s^{-1}$ at 90 °C (assumed)

K_4 = 1.00 (assumed)

k_5 = 1 $m^3mol^{-1}s^{-1}$ at 90 °C (assumed)

K_5 = 1 x 10^{-3} (estimated based on pK_a values)

k_6 = 0.0047 s^{-1} at 92 °C (from previous data)

K_6 = 1.25 x 10^{-5} $molL^{-1}$ (from previous data)

E_{a6} = 40.1 $kJmol^{-1}$ (from previous data)

k_7 = 3.89 x 10^{-2} $Lmol^{-1}s^{-1}$ at 92 °C (from previous data)

E_{a7} = 0 $kJmol^{-1}$ (from previous data)

The data used to generate Figure 38 were used to test the above model (Figure 44).

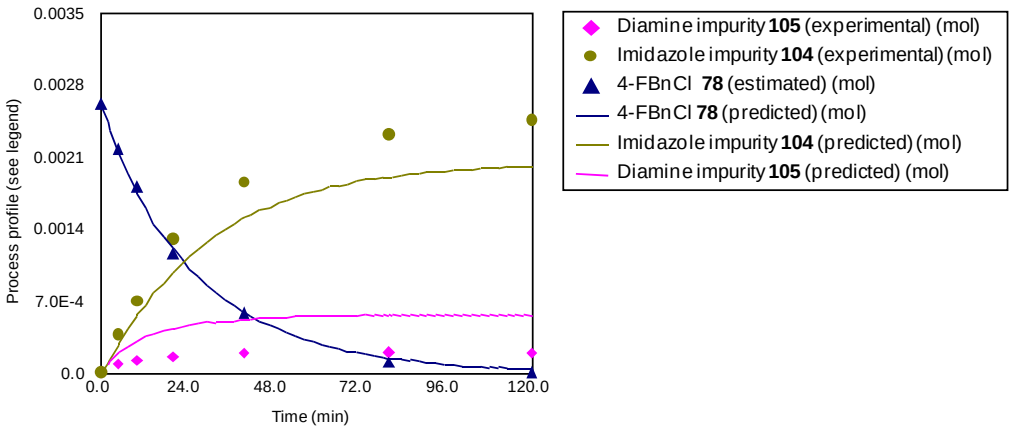

Note: the 4-FBnCl data were estimated (*in lieu* of having actual data) based on the amounts of diamine **105** and imidazole derivative **104**.

Figure 44: Modelled data using DynoChem® model.

The estimated data for 4-FBnCl showed a good fit for the model; however the predictions for the products were somewhat less accurate. Nevertheless, since the reaction of 4-FBnCl is the main area of interest the model above appears to be adequate for predictive purposes. Verification of this model was next attempted by obtaining real data for 4-FBnCl throughout the reaction.

4.3.2.8 Model Verification

Quantification of 4-FBnCl using HPLC methods was unfeasible due to co-elution of 4-FBnCl with darapladib or other unidentified impurities. As a result, GC analysis was used for quantification. The verification experiments quantified 4-FBnCl levels only, and not the formation of imidazole derivative **104** or amine **105**.

Verification of the prepared model was completed by carrying out the amidation reaction in the presence of a spike of 4-FBnCl (0.16 equiv. or 70,000 ppm). Comparison of the data obtained with the predictions from the model show excellent agreement, particularly for the later time points (Figure 45). Some slight discrepancies are observed for some of the initial time points, which could indicate limitations in the predictive power of the model. A possible explanation for the discrepancies is the heterogeneous reaction mixture, which could have resulted in unrepresentative sampling. Alternatively, it could be an indication of the model not adequately compensating for the temperature changes in the system during the first 15 minutes when the reaction mixture was heated from 70 to 92 °C.

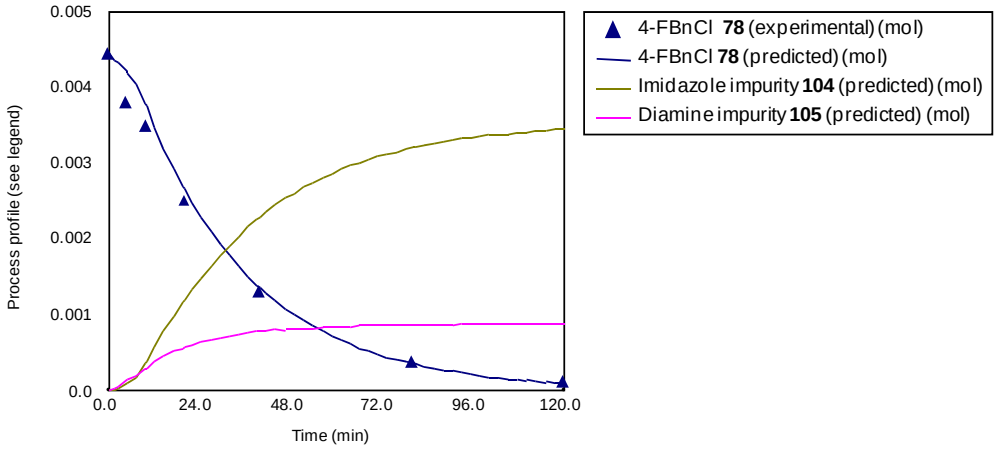

Figure 45: Verification of model for 4-FBnCl in coupling reaction.

The ability of the model to predict the level of 4-FBnCl appeared to be excellent and suitable for use. For confirmation, a second verification experiment was completed in the presence of 4-FBnCl at a more typical level (2104 ppm, as measured in acid **74**). The coupling data showed excellent agreement with the model, particularly towards the end of the reaction (Figure 46). As observed in the first verification experiment the first few data points show a faster reaction than the model is predicting (*vide supra*, Figure 45).

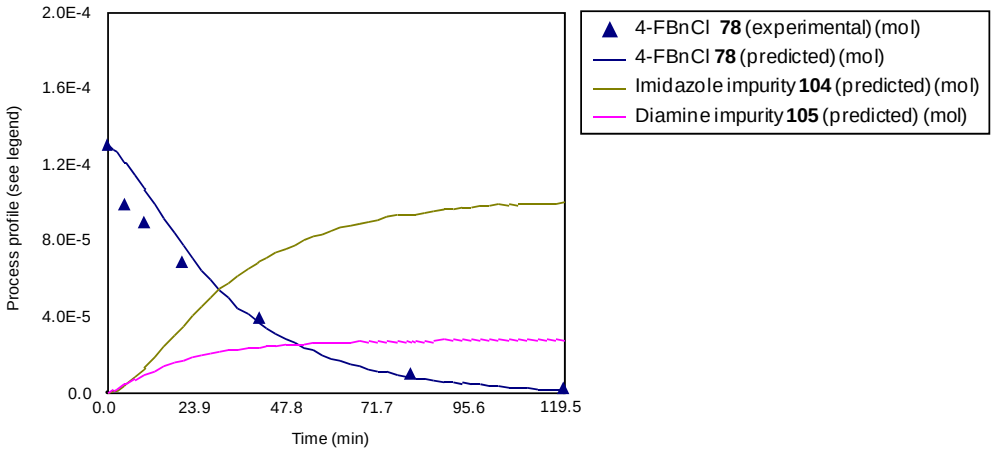

Figure 46: Verification of model for coupling reaction at typical 4-FBnCl level.

Pseudo first order kinetics can be applied to the above data sets to provide an estimation of the half life of 4-FBnCl under the reaction conditions (Figure 47).

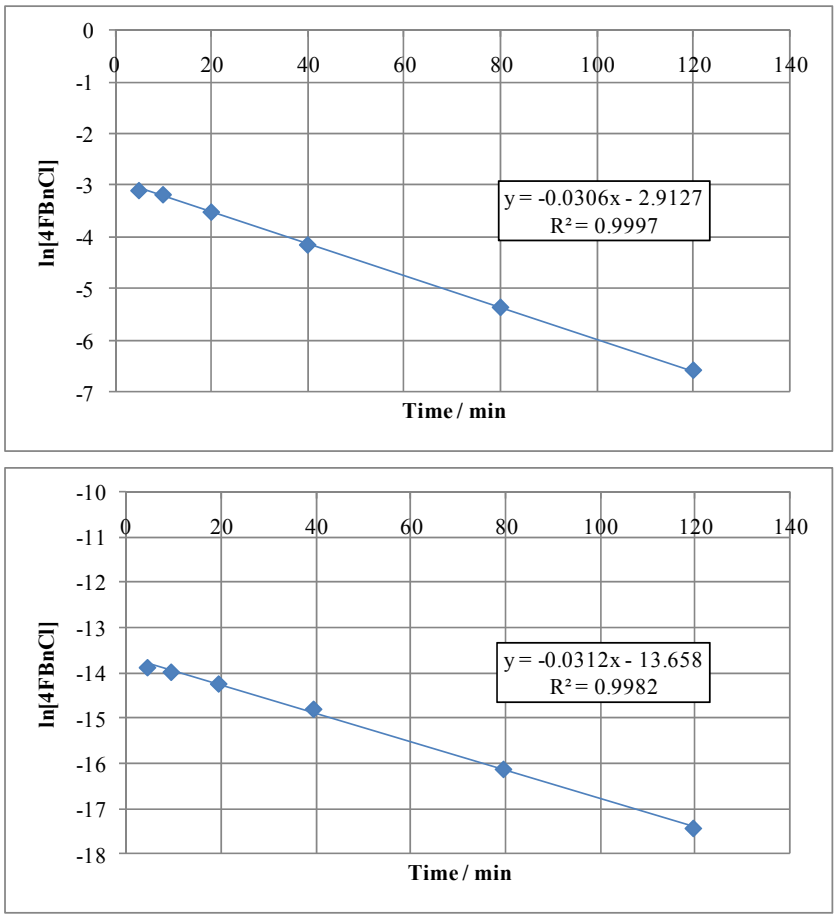

Figure 47: Log plots for coupling reaction during verification runs at 0.16 equiv. (70,000 ppm, top) and 2104 ppm (bottom).

The calculated half lives from these plots are shown in Table 36. The half life is shown to be slightly higher than estimated previously (Figure 38, page 111), however, both data sets are in agreement at ~22 min.

Entry	Amount 4-FBnCl	Pseudo 1st order rate constant *k*' at 92 °C / min^{-1}	$t_{½}$ / min
1	Spike of 0.16 equiv. (70,000 ppm)	0.0306	22.7
2	2104 ppm	0.0312	22.2

Table 36: Calculated half lives for 4-FBnCl during verification experiments at 92 °C.

Thus, during the course of the coupling reaction (2-3 hours) there are likely to be five to eight half lives, resulting in a significant reduction in the level of 4-FBnCl. Considering that the typical level of 4-FBnCl present will be ≤ 2000 ppm, the amount of 4-FBnCl in the coupling reaction will rapidly be reduced to very low levels.* In addition, this analysis does not include the imidazolide **102** reaction, which can also account for approximately 25% reduction in the 4-FBnCl level.

Analysis of the isolated products from these verification runs showed <1 ppm 4-FBnCl in both cases. This demonstrates that whilst low levels of 4-FBnCl remained in solution at the end of the reaction, it was completely purged during the crystallisation and isolation of darapladib IG.

* Five half lives would result in a 32-fold reduction, *i.e.* 2000 ppm would be decreased to 62.5 ppm in solution. Eight half lives is equivalent to a 256-fold decrease, giving 8 ppm 4-FBnCl from an initial charge of 2000 ppm.

4.4 Conclusions & Future Work

A series of experiments investigating the optimisation of the process to prepare carboxylic acid **74** have been completed, specifically focusing on the crystallisation parameters. Improved knowledge regarding the effects of such parameters on the level of two key impurities (4-FBnCl and inorganic residues) has been acquired. Additionally, experimental design methods have been applied in order to determine the main parameters and interactions affecting the process. Overall, the results from the study indicate that the crystallisation of acid **74** is very robust, particularly in terms of yield and HPLC purity. As such, set points for each of the parameters could be defined anywhere within the ranges investigated. However, manufacturing criteria, such as filtration rate and cycle time also need to be considered, and may, ultimately, define the actual parameter set points. The study identified few interactions, none of which were of high significance in the models generated. The design did not investigate agitation rate, and it is possible that different agitation rates could alter the behaviour of the crystallisation. The effect of agitation rate, particularly on product quality, should be the focus of future investigation. A high agitation rate could cause particle attrition, which may result in slow filtration rates, and could lead to poor washing of the filter cake. A low agitation speed could give poor mixing and uncontrolled crystallisation, which might affect purity.

Remaining work on the process to acid **74** will focus on finalising the process conditions, and then completing experiments to investigate the robustness of the entire process by further use of experimental design methods. These studies are intended to allow us to specify operable ranges for the process parameters to ensure control over the quality of acid **74**.

The purging of 4-FBnCl in the formation of darapladib has been shown to be excellent. A spike of 70,000 ppm (7% w/w) relative to carboxylic acid **74** was reduced to less than 1 ppm in darapladib IG material at laboratory scale. This degree of purging should provide sufficient confidence that the process can tolerate 4-FBnCl to well beyond the typical level.

Investigations into the fate of 4-FBnCl during the amidation reaction have shown that two main pathways operate: reaction with the imidazole by-product and reaction

with amine **77**. The proposed impurities have been isolated and structures confirmed by spectroscopic analysis. Further quantitative analyses have shown that imidazole derivative **104** is the main species obtained from 4-FBnCl under the reaction conditions. The formation of diamine **105** is a secondary reaction pathway. The results are logical when considering that imidazole is present in vast excess (>2 equivalents) whereas amine **77** is only present in a small excess (0.1 equivalents). Furthermore, the 4-FBnCl charged has been completely accounted for by these mechanisms with excellent mass balance data being obtained (within the realms of experimental error, and without moving to more sensitive analytical techniques).

Investigations into the kinetics of the reactions involving 4-FBnCl during the formation of darapladib have been completed. A predictive kinetic model has been prepared and verified at two levels of 4-FBnCl charge. It is the intention that this model will be of use in demonstrating control over this impurity.

5 Summary

The work documented in this thesis has demonstrated the diversity of process chemistry projects. The Syk project is an example of an early phase programme and illustrates that rapid scale-up of chemical processes can be readily achieved. In this case, the focus centred on delivering amine **25** of high quality, and this was achieved by understanding the reaction mechanisms and conditions leading to the formation of undesired impurities. The focus on product quality, and the short time for investigations, meant that the work-up was not studied in any detail. This aspect remained for further development. Nevertheless, much useful information was gathered, which was used to good effect when the chemistry was scaled up further in our pilot plant.[64]

In direct contrast to the Syk project, the work on darapladib exemplified the depth of knowledge required as a project approaches the culmination of clinical trials, and submission to regulatory authorities. In this latter project, the processes were much better understood and conditions were in place that reliably produced the required materials. This, in itself, was only a starting point for further experimental work. As discussed, exploration of parameter ranges was shown to be an important facet of process chemistry. The work completed on the development of the process to carboxylic acid **74** will contribute to the definition of acceptable process parameter ranges for the long-term manufacture of this compound at production scale.

Aside from being able to produce pharmaceutical compounds at large scale, ensuring high quality of the final API is the principal aim. This aspect of process development was typified by the detailed studies into the fate and effects of 4-FBnCl in the downstream chemistry. In addition to spiking studies, the application of kinetics methods complemented the initial investigations and added further weight to the strong scientific evidence that this impurity could be readily controlled. The knowledge obtained will contribute to preparation of a comprehensive risk mitigation strategy for 4-FBnCl, to ensure that the specification for this impurity can be met.

In summary, the development of new therapies for a wide range of inflammatory diseases continues to be a key area of focus in the pharmaceutical industry. As

projects progress, increasingly detailed information and ever more robust processes are required. This approach enables complex organic molecules to be produced at large scale to supply patients with new medicines for currently unmet medical needs. The work described here has contributed specific and detailed information to meet the requirements of active process chemistry research projects within our laboratories.

6 Experimental

6.1 General

All solvents and reagents used were standard laboratory grade unless stated, and were employed without further purification.

All experiments were carried out under an atmosphere of nitrogen gas unless otherwise stated.

Atoms on compounds prepared are numbered within the experimental section to assist in assigning spectral data.

NMR data were obtained on a Bruker DPX 400 or Bruker AV 400 spectrometer, operating at 400.2 MHz for ^{1}H spectra, 100.63 MHz for ^{13}C spectra, and 376.56 MHz for ^{19}F spectra. Chemical shifts in ^{1}H and ^{13}C spectra are reported on the δ scale relative to tetramethylsilane (TMS). ^{13}C spectra were proton decoupled. ^{19}F spectra were proton decoupled and data are reported on the δ scale relative to $CFCl_3$. All NMR data were obtained at 299 K in d_6-DMSO or $CDCl_3$ unless otherwise stated.

HPLC data were obtained on a number of different methods as detailed below:

Method A

Column details	Phenomenex Luna C18(2), 50 x 2.0 mm, 3 µm		
Column Temperature	40 °C		
Mobile Phase A	0.05% v/v Trifluoroacetic acid in water		
Mobile Phase B	0.05% v/v Trifluoroacetic acid in acetonitrile		
Flow rate	1 mL/min		
Gradient Profile	Time / min	% A	% B
	0	100	0
	8	5	95
	8.01	100	0
	11	100	0
Detector Wavelength	UV at 220 nm (unless otherwise stated)		
Injection volume	1 µL		
Sample diluent	Acetonitrile/water mixtures		

This method is also set up for determining the concentration of species in samples by assay relative to a benzophenone standard.

Method B

Column details	Zorbax Bonus RP rapid resolution, 150 x 4.6 mm, 3.5 µm		
Column Temperature	50 °C		
Mobile Phase A	0.05 M pH 3.0 ammonium formate		
Mobile Phase B	Acetonitrile		
Flow rate	1.5 mL/min		
Gradient Profile	Time / min	% A	% B
	0	75	25
	33	42	58
	33.1	75	25
	45	75	25
Detector Wavelength	UV at 260 nm		
Injection volume	5 µL		
Sample diluent	45:55 Acetonitrile : 0.05 M pH 6.8 aqueous sodium hydrogen phosphate buffer solution. Sample concentration 0.32 mg/mL		

Method C

Column details	Agilent Zorbax SB-C18, 50 x 3.0 mm, 1.8 µm		
Column Temperature	60 °C		
Mobile Phase A	0.05% v/v Trifluoroacetic acid in water		
Mobile Phase B	0.05% v/v Trifluoroacetic acid in acetonitrile		
Flow rate	1.5 mL/min		
Gradient Profile	Time / min	% A	% B
	0	100	0
	2.5	5	95
	2.7	5	95
	2.71	100	0
	3.3	100	0
Detector Wavelength	UV at 220 nm (unless otherwise stated)		
Injection volume	1 µL		
Sample diluent	Acetonitrile/water mixtures		

Method D

Column details	Waters Sunfire C18, 150 x 4.6 mm, 3.5 µm		
Column Temperature	40 °C		
Mobile Phase A	0.05% v/v Trifluoroacetic acid in water		
Mobile Phase B	0.05% v/v Trifluoroacetic acid in acetonitrile		
Flow rate	1 mL/min		
Gradient Profile	Time / min	% A	% B
	0	90	10
	50	15	85
	50.1	90	10
	60	90	10
Detector Wavelength	UV at 250 nm		
Injection volume	5 µL		
Sample diluent	1:1 Acetonitrile : 0.05 M pH 5.0 aqueous ammonium acetate buffer solution. Sample concentration 0.4 mg/mL.		

Preparative HPLC was carried out using the method detailed below:

Column details	Waters Xbridge C18, 100 x 19 mm, 5 µm		
Column Temperature	Room temperature		
Mobile Phase A	10 mM pH 10 aqueous ammonium bicarbonate		
Mobile Phase B	Acetonitrile + 0.1% concentrated aqueous NH_3		
Flow rate	20 mL/min		
Gradient Profile	Time / min	% A	% B
	0	50	50
	1	50	50
	20	1	99
	24	1	99
Detector Wavelength	UV at 210 nm		
Sample diluent	Sample (10-100 mg) dissolved in 1 mL DMSO		

LCMS data were obtained using HPLC Method A coupled to a mass spectrometer, which used positive electrospray ionisation with a quandrupole detector.

High resolution mass spectrometry data were obtained using HPLC Method A coupled to a Thermo-Finnigan Orbitrap Fourier-transform mass spectrometer running in positive electrospray ionisation mode.

Melting points were obtained using a Stuart SMP40 melting point apparatus.

4-FBnCl content in samples of carboxylic acid **74** and darapladib IG **71** was determined by a gas chromatography (GC) method: 50% phenyl – 50% dimethylpolysiloxane column (15 m x 0.32 mm, with 0.5 μm film thickness), oven temperature 70 to 290 °C ramped at 20 °C/min, injector temperature 200 °C, detector temperature 300 °C, injection volume 1 μL. A splitless injector with appropriate liner was used with an electron capture detector, with helium as carrier gas. 4-FBnCl approximate retention time: 3.2 min. Standards of various concentrations were prepared and a calibration line was produced using the measured responses (peak area). The concentration in the sample was calculated from this calibration line. 4-FBnCl standards were prepared by dissolving the requisite amount of 4-FBnCl in heptane and extracting with an equal amount of 1% v/v triethylamine in acetonitrile. The heptane layer was then sampled for analysis. For sample preparation the analyte was dissolved in 1% v/v triethylamine in acetonitrile at an approximate concentration of 15 mg/mL, extracted with an equal volume of heptane, and the upper layer removed for GC analysis.

Infra red (IR) spectra were obtained on a Perkin Elmer Spectrum One instrument with a diamond attenuated total reflection accessory. Only data for main functional groups and strong peaks are reported.

Sulfated ash analyses for determination of inorganic content were carried out using a suitable microwave ashing system in which the sample was heated in the presence of concentrated sulfuric acid.

Screening hydrogenations were carried out in glass tubes in a multi-well steel autoclave with magnetic stirring, with hydrogen from a hydrogen generator. Larger scale hydrogenations were carried out in a glass miniclave vessel with a turbine mechanical stirrer, and hydrogen from a hydrogen generator. The scale-up laboratory equipment was a glass controlled laboratory reactor with hydrogen from cylinders.

Chromatography was carried out using a Biotage SP4 instrument, with pre-packed silica columns. Details of solvent system, column size, silica type, flow rate and column loading are provided for individual examples.

6.2 Experimental for Chapter 3

Preparation of (*R*)-*tert*-butyl 3-(aminomethyl)-3-fluoropiperidine-1-carboxylate (25)

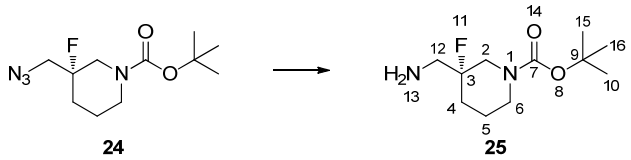

General Procedure 1: Small Scale Hydrogenation Screening

Azide **24** (A) was dissolved in the appropriate solvent (B) then transferred to a tube containing the catalyst (C). The azide was washed in with further solvent (D) then the additive (E) was added (if appropriate). The tube was purged three times with nitrogen to 3 bar (with stirring at 400 rpm), then three times with hydrogen to 50 psi (no stirring). The hydrogen generator was then set to the required pressure (F), and the system purged and vented until the pressure in hydrogen generator had reached the required pressure, then purged once with hydrogen at the required pressure with stirring at 400 rpm, and left under hydrogen at the required pressure at ambient temperature with stirring at the desired rate (G) for the required time (H). The extent of reaction completion was monitored by LCMS (I). Where conversions are recorded the calculation was:

Conversion = % area **25** x 100 / (% area **24** + % area **25**).

Quoted ratios for species of interest were calculated by using the peak area of the relevant compound mass ion in the MS ES^+: TIC trace and is not quantitative. Amounts of other unidentified impurities are not reported.

Work-up Procedure 1: Small Scale Hydrogenation Screening

The reaction mixture post-hydrogenation was filtered through a Whatman 0.2 μm syringe filter and washed through with the appropriate solvent (J), then concentrated *in vacuo* to yield the crude product as a colourless to pale yellow oil (K).

Experimental for Sections 3.3.1.1 to 3.3.1.5: Screening Experiments

The experiments documented in Tables 1 to 8 were carried out using General Procedure 1. Details for each entry are provided below. When the crude product was

isolated, Work-up Procedure 1 was followed. For isolated products only ^{1}H NMR spectroscopic data were obtained, and these matched that given below with the exception of residual solvents and minor impurities.

Table 1

Entry 1: A: 101.5 mg, 0.393 mmol; B: ethanol (1 mL); C: PtO_2 (2.0 mg, 7.1 μmol, Johnson Matthey, metal assay 81.04%); D: ethanol (1 mL); E: N/A; F: 5 psi; G: 800 rpm; H: 19.5 h; I: 31% conversion at 15.5 h, 30% conversion at 19.5 h; J: N/A; K: N/A.
Following filtration, catalyst was recharged (0.8 mg, 2.9 μmol) and reacted under the same conditions for 15 h giving 49% conversion.

Entry 2: A: 101.9 mg, 0.395 mmol; B: ethanol (1 mL); C: 5% Pt/C F1 (18.5 mg, 2.1 μmol, Evonik, metal assay 5%, 55.2% water); D: ethanol (1 mL); E: N/A; F: 5 psi; G: 800 rpm; H: 19.5 h; I: 13% conversion at 15.5 h, 16% conversion at 19.5 h; J: N/A; K: N/A.
Following filtration, catalyst was recharged (19.0 mg, 2.2 μmol) and reacted under the same conditions for 15 h giving 16% conversion.

Entry 3: A: 102.8 mg, 0.398 mmol; B: ethanol (1 mL); C: 5% Pd/C E1 (14.3 mg, 2.2 μmol, Evonik, metal assay 5%, 67.8% water); D: ethanol (1 mL); E: N/A; F: 5 psi; G: 800 rpm; H: 19.5 h; I: 36% conversion at 15.5 h, 38% conversion at 19.5 h; J: N/A; K: N/A.
Following filtration, catalyst was recharged (14.1 mg, 2.1 μmol) and reacted under the same conditions for 15 h giving 72% conversion.

Entry 4: A: 99.6 mg, 0.386 mmol; B: ethanol (1 mL); C: 5% Pd/C 395M (10.6 mg, 2.3 μmol, Johnson Matthey, metal assay 4.86%, 53.4% water); D: ethanol (1 mL); E: N/A; F: 5 psi; G: 800 rpm; H: 19.5 h; I: 39% conversion at 15.5 h, 42% conversion at 19.5 h; J: N/A; K: N/A.
Following filtration, catalyst was recharged (10.0 mg, 2.1 μmol) and reacted under the same conditions for 15 h giving 100% conversion.

Entry 5: A: 101.5 mg, 0.393 mmol; B: ethanol (1 mL); C: 5% Pd/C 434 (10.1 mg, 2.1 μmol, Johnson Matthey, metal assay 4.74%, 53.3% water); D: ethanol (1 mL); E:

N/A; F: 5 psi; G: 800 rpm; H: 19.5 h; I: 41% conversion at 15.5 h, 46% conversion at 19.5 h; J: N/A; K: N/A.
Following filtration, catalyst was recharged (10.3 mg, 2.1 μmol) and reacted under the same conditions for 15 h giving 92% conversion.

Entry 6: A: 102.9 mg, 0.398 mmol; B: ethanol (1 mL); C: $Pd(OH)_2$ (2.9 mg, 2.1 μmol, Aldrich, metal assay 20%, 50% water); D: ethanol (1 mL); E: N/A; F: 5 psi; G: 800 rpm; H: 19.5 h; I: 41% conversion at 15.5 h, 46% conversion at 19.5 h; J: N/A; K: N/A.
Following filtration, catalyst was recharged (3.3 mg, 2.3 μmol) and reacted under the same conditions for 15 h giving 97% conversion.

Table 2

Entry 1: A: 99.8 mg, 0.386 mmol; B: ethanol (1 mL); C: 5% Pd/C 395M (10.3 mg, 2.2 μmol, Johnson Matthey, metal assay 4.86%, 53.4% water); D: ethanol (1 mL); E: N/A; F: 5 psi; G: 800 rpm; H: 2 h; I: 100% conversion, ratio **25**:**36** = 70.6:29.4; J: N/A; K: N/A. The batch was reanalysed after a total of 5 h hydrogenation. No difference in profile was observed; ratio calculations were not completed.

Entry 2: A: 103.1 mg, 0.399 mmol; B: ethanol (1 mL); C: 5% Pd/C 39 (11.5 mg, 2.2 μmol, Johnson Matthey, metal assay 4.86%, 58.3% water); D: ethanol (1 mL); E: N/A; F: 5 psi; G: 800 rpm; H: 2 h; I: 100% conversion, ratio **25**:**36** = 73.1:26.9; J: ethanol (2 x 0.5 mL); K: 90.7 mg as a mixture of **25** and **36**. The crude product was subjected to preparative HPLC to isolate **36** (see page 139).

Entry 3: A: 100.5 mg, 0.389 mmol; B: ethanol (1 mL); C: 5% Pd/C E101 N/OW (12.0 mg, 2.1 μmol, Evonik, metal assay 5%, 62.4% water); D: ethanol (1 mL); E: N/A; F: 5 psi; G: 800 rpm; H: 2 h; I: 100% conversion, ratio **25**:**36** = 74.7:25.3; J: N/A; K: N/A. The batch was reanalysed after a total of 5 h hydrogenation. No difference in profile was observed; ratio calculations were not completed.

Tables 3 & 4

Note: Variable reaction times were recorded due to some reactions being run overnight.

Entry 1: A: 99.0 mg, 0.383 mmol; B: ethanol (1 mL); C: 5% Pd/C 395M (10.1 mg, 2.1 µmol, Johnson Matthey, metal assay 4.86%, 53.4% water); D: ethanol (1 mL); E: N/A; F: 5 psi; G: 800 rpm; H: 1 h; I: 100% conversion, ratio **25**:**36** = 72.6:27.4 (Table 3), ratio **25**:**36**:**43** = 63.1:23.9:13.0 (Table 4); J: N/A; K: N/A.

Entry 2: A: 99.6 mg, 0.386 mmol; B: IPA (1 mL); C: 5% Pd/C 395M (9.9 mg, 2.1 µmol, Johnson Matthey, metal assay 4.86%, 53.4% water); D: IPA (1 mL); E: N/A; F: 5 psi; G: 800 rpm; H: 16 h; I: 100% conversion, ratio **25**:**36** = 67.2:32.8 (Table 3), ratio **25**:**36**:**41** = 57.7:28.2:14.1 (Table 4); J: N/A; K: N/A.

Entry 3: A: 100.2 mg, 0.388 mmol; B: THF (1 mL); C: 5% Pd/C 395M (10.3 mg, 2.2 µmol, Johnson Matthey, metal assay 4.86%, 53.4% water); D: THF (1 mL); E: N/A; F: 5 psi; G: 800 rpm; H: 16 h I: 100% conversion, ratio **25**:**36** = 71.4:28.6 (Table 3), ratio **25**:**36**:**42** = 64.1:25.7:10.2 (Table 4); J: N/A; K: N/A.

Entry 4: A: 99.6 mg, 0.386 mmol; B: ethyl acetate (1 mL); C: 5% Pd/C 395M (9.8 mg, 2.1 µmol, Johnson Matthey, metal assay 4.86%, 53.4% water); D: ethyl acetate (1 mL); E: N/A; F: 5 psi; G: 800 rpm; H: 16 h; I: 100% conversion, ratio **25**:**36** = 78.4:21.6 (Table 3); J: N/A; K: N/A.

Entry 5: A: 99.4 mg, 0.385 mmol; B: ethanol/acetic acid (9:1 v/v, 1 mL); C: 5% Pd/C 395M (10.1 mg, 2.1 µmol, Johnson Matthey, metal assay 4.86%, 53.4% water); D: ethanol/acetic acid (9:1 v/v, 1 mL); E: N/A; F: 5 psi; G: 800 rpm; H: 1 h; I: 100% conversion, ratio **25**:**36** = 56.4:43.6 (Table 3), ratio **25**:**36**:**43** = 49.8:38.4:11.8 (Table 4); J: N/A; K: N/A.

Table 5

Entry 1: A: 100.3 mg, 0.388 mmol; B: ethanol (1 mL); C: 5% Pd/C 395M (10.0 mg, 2.1 µmol, Johnson Matthey, metal assay 4.86%, 53.4% water); D: ethanol (1 mL); E: N/A; F: 5 psi; G: 800 rpm; H: 1 h; I: 100% conversion, ratio **25**:**36**:**43** = 57.6:31.8:10.6; J: N/A; K: N/A.

Entry 2: A: 100.9 mg, 0.391 mmol; B: ethanol (1 mL); C: 5% Pt/C F1 (18.4 mg, 2.1 µmol, Evonik, metal assay 5%, 55.2% water); D: ethanol (1 mL); E: N/A; F: 5 psi; G: 800 rpm; H: 2.5 h; I: 100% conversion, ratio **25**:**36**:**43** = 66.5:3.3:30.3; J:

ethanol (0.5 mL); K: 88.4 mg as a mixture of **25**, **36** & **43**. The ^{1}H NMR spectrum (400 MHz, $CDCl_3$) showed the presence of an extra ethyl group: δ 1.11 (t, *J* = 7.1 Hz), 2.68 (q, *J* = 7.1 Hz), providing evidence for the proposed *N*-ethyl impurity **43**.

Entry 3: A: 100.4 mg, 0.389 mmol; B: ethanol (1 mL); C: $Pd(OH)_2$ (3.4 mg, 2.4 μmol, Aldrich, metal assay 20%, 50% water); D: ethanol (1 mL); E: N/A; F: 5 psi; G: 800 rpm; H: 1 h; I: 100% conversion, ratio **25**:**36**:**43** = 64.9:23.6:11.5; J: N/A; K: N/A.

Entry 4: A: 101.1 mg, 0.391 mmol; B: ethanol (1 mL); C: PtO_2 (1.9 mg, 6.8 μmol, Johnson Matthey, metal assay 81.04%); D: ethanol (1 mL); E: N/A; F: 5 psi; G: 800 rpm; H: 2.5 h; I: 100% conversion, ratio **25**:**36**:**43** = 74.2:5.5:20.3; J: ethanol (0.5 mL); K: 88.2 mg as a mixture of **25**, **36** & **43**. The ^{1}H NMR spectrum (400 MHz, $CDCl_3$) showed the presence of an extra ethyl group: δ 1.11 (t, *J* = 7.1 Hz), 2.68 (q, *J* = 7.1 Hz), providing evidence for the proposed *N*-ethyl impurity **43**.

Table 6

Entry 1: A: 99.6 mg, 0.386 mmol; B: ethanol (1 mL); C: 10% Pt/C 128 (8.5 mg, 2.2 μmol, Johnson Matthey, metal assay 10%, 50% water); D: ethanol (1 mL); E: N/A; F: 5 psi; G: 800 rpm; H: 2.5 h; I: 100% conversion, ratio **25**:**36**:**43** = 78.4:1.3:20.3; J: ethanol (0.5 mL); K: 90.0 mg as a mixture of **25**, **36** and **43**.

Entry 2: A: 100.8 mg, 0.390 mmol; B: ethanol (1 mL); C: 10% Pt/C 128 (4.1 mg, 1.1 μmol, Johnson Matthey, metal assay 10%, 50% water); D: ethanol (1 mL); E: N/A; F: 5 psi; G: 800 rpm; H: 18.5 h; I: 100% conversion, ratio **25**:**36**:**43** = 65.8:10.2:24.0; J: N/A; K: N/A.

Entry 3: A: 99.7 mg, 0.386 mmol; B: ethanol (1 mL); C: 10% Pt/C 128 (8.5 mg, 2.2 μmol, Johnson Matthey, metal assay 10%, 50% water); D: ethanol (1 mL); E: ammonia (56 μL, 0.968 mmol, 33% w/w solution in water); F: 5 psi; G: 800 rpm; H: 2.5 h; I: 100% conversion, ratio **25**:**36**:**43** = 84.3:1.4:14.3; J: N/A; K: N/A.

Entry 4: A: 101.2 mg, 0.392 mmol; B: ethyl acetate (1 mL); C: 10% Pt/C 128 (8.0 mg, 2.1 µmol, Johnson Matthey, metal assay 10%, 50% water); D: ethyl acetate (1 mL); E: N/A; F: 5 psi; G: 800 rpm; H: 18.5 h; I: 100% conversion, ratio **25**:**36**:**43** = 86.0:11.1:3.0; J: ethyl acetate (0.5 mL); K: 91.5 mg as a mixture of **25**, **36** & **43**.

Entry 5: A: 100.1 mg, 0.388 mmol; B: ethanol (0.8 mL); C: 10% Pt/C 128 (8.3 mg, 2.1 µmol, Johnson Matthey, metal assay 10%, 50% water); D: ethanol (1 mL); E: ammonia (0.2 mL, 3.45 mmol, 33% w/w solution in water); F: 5 psi; G: 800 rpm; H: 2.5 h; I: 100% conversion, ratio **25**:**36**:**43** = 94.3:0.5:5.2; J: ethanol (0.5 mL); K: 87.7 mg as a mixture of **25**, **36** & **43**.

Entry 6: A: 99.9 mg, 0.387 mmol; B: toluene (1 mL); C: 10% Pt/C 128 (8.0 mg, 2.1 µmol, Johnson Matthey, metal assay 10%, 50% water); D: toluene (1 mL); E: N/A; F: 5 psi; G: 800 rpm; H: 4.5 h; I: 100% conversion, ratio **25**:**36** = 98.6:1.4; J: toluene (0.5 mL); K: 87.5 mg as a mixture of **25** and **36**.

Entry 7: A: 99.2 mg, 0.384 mmol; B: TBME (1 mL); C: 10% Pt/C 128 (8.0 mg, 2.1 µmol, Johnson Matthey, metal assay 10%, 50% water); D: TBME (1 mL); E: N/A; F: 5 psi; G: 800 rpm; H: 4.5 h; I: 100% conversion, ratio **25**:**36** = 97.9:2.1; J: TBME (0.5 mL); K: 82.8 mg as a mixture of **25** and **36**.

Entry 8: A: 100.1 mg, 0.388 mmol; B: THF (1 mL); C: 10% Pt/C 128 (8.2 mg, 2.1 µmol, Johnson Matthey, metal assay 10%, 50% water); D: THF (1 mL); E: N/A; F: 5 psi; G: 800 rpm; H: 2.5 h; I: 100% conversion, ratio **25**:**36**:**42** = 91.8:1.3:6.9; J: THF (0.5 mL); J: 91.0 mg as a mixture of **25**, **36** and **42**.

Table 7

Entry 1: A: 101.5 mg, 0.393 mmol; B: TBME (1 mL); C: 10% Pt/C 128 (8.4 mg, 2.2 µmol, Johnson Matthey, metal assay 10%, 50% water); D: TBME (1 mL); E: N/A; F: 5 psi; G: 800 rpm; H: 4.66 h; I: 100% conversion, ratio **25**:**36** = 99.1:0.9; J: TBME (0.5 mL); K: 88.1 mg as a mixture of **25** and **36**.

Entry 2: A: 100.3 mg, 0.388 mmol; B: TBME (0.9 mL); C: 10% Pt/C 128 (8.1 mg, 2.1 µmol, Johnson Matthey, metal assay 10%, 50% water); D: TBME (0.9 mL); E:

ammonia (0.2 mL, 3.45 mmol, 33% w/w solution in water); F: 5 psi; G: 800 rpm; H: 6.66 h; I: 96% conversion, ratio **25**:**36** = 99.7:0.3; J: N/A; K: N/A.

Entry 3: A: 100.9 mg, 0.391 mmol; B: TBME (1 mL); C: 10% Pt/C 128 (8.6 mg, 2.2 µmol, Johnson Matthey, metal assay 10%, 50% water); D: TBME (1 mL); E: N/A; F: 42 psi; G: 800 rpm; H: 4.5 h; I: 100% conversion, ratio **25**:**36** = 97.5:2.5; J: N/A; K: N/A.

Entry 4: A: 100.2 mg, 0.388 mmol; B: TBME (1 mL); C: 10% Pt/C 128 (8.1 mg, 2.1 µmol, Johnson Matthey, metal assay 10%, 50% water); D: TBME (1 mL); E: N/A; F: 5 psi; G: 150 rpm; H: 6.5 h; I: 100% conversion, ratio **25**:**36** = 98.2:1.8; J: N/A; K: N/A.

Table 8

Entry 1: A: 100.3 mg, 0.388 mmol; B: ethanol/water (9:1 v/v, 1 mL); C: 10% Pt/C 128 (8.0 mg, 2.1 µmol, Johnson Matthey, metal assay 10%, 50% water); D: ethanol/water (9:1 v/v, 1 mL); E: N/A; F: 5 psi; G: 800 rpm; H: 2.5 h; I: 100% conversion, ratio **25**:**36**:**43** = 79.8:2.3:17.9; J: N/A; K: N/A.

Entry 2: A: 100.0 mg, 0.387 mmol; B: ethanol (1 mL); C: 10% Pt/C 128 (8.4 mg, 2.2 µmol, Johnson Matthey, metal assay 10%, 50% water); D: ethanol (1 mL); E: DIPEA (0.602 mL, 3.45 mmol); F: 5 psi; G: 800 rpm; H: 6 h; I: 100% conversion, ratio **25**:**36**:**43**:**41** = 63.2:3.0:12.9:20.8; J: N/A; K: N/A.

Entry 3: A: 99.2 mg, 0.384 mmol; B: THF (0.9 mL); C: 10% Pt/C 128 (8.4 mg, 2.2 µmol, Johnson Matthey, metal assay 10%, 50% water); D: THF (0.9 mL); E: ammonia (0.2 mL, 3.45 mmol, 33% w/w solution in water); F: 5 psi; G: 800 rpm; H: 6 h; I: 100% conversion, ratio **25**:**36**:**42** = 99.5:0.1:0.4; J: THF (0.5 mL); K: 85.0 mg as a mixture of **25**, **36** and **42**.

Entry 4: A: 100.9 mg, 0.391 mmol; B: THF/water (9:1 v/v, 1 mL); C: 10% Pt/C 128 (8.4 mg, 2.2 µmol, Johnson Matthey, metal assay 10%, 50% water); D: THF/water (9:1 v/v, 1 mL); E: N/A; F: 5 psi; G: 800 rpm; H: 2.5 h; I: 100% conversion, ratio **25**:**36**:**42** = 94.8:1.0:4.2; J: THF (0.5 mL); K: 88.9 mg as a mixture of **25**, **36** and **42**.

Experimental for Section 3.3.1.6: Process Scale-up

Table 9

Entry 1: Azide **24** (2.73 g, 10.6 mmol) was dissolved in THF (27 mL), then transferred to the hydrogenation vessel, and washed in with THF (27 mL). Ammonia (5.44 mL, 93.9 mmol, 33% w/w solution in water) was added followed by 10% Pt/C (50% wet paste, 0.224 g, 57.0 µmol). The reactor was purged three times to 3 bar with nitrogen (stirring at 200 rpm), then three times with hydrogen to 50 psi (no stirring). The pressure in the hydrogen generator was set to 5 psi and the system purged and vented until the pressure in the generator reached 5 psi. A final purge to 5 psi with hydrogen (stirring at 300 rpm) was completed, and then the reaction mixture was stirred under 5 psi hydrogen at 700 rpm. The conversion was determined at various time points: 4 h (67%), 7.66 h (85%) and 22.5 h (100%). After 22.5 h the ratio of **25**:**36**:**42** was 99.1:0.9:0. The reaction mixture was filtered through a glass microfibre filter, and washed through with THF (5.4 mL). The filtrate was concentrated *in vacuo* to yield the crude product as a yellow oil (2.37 g as a mixture of **25** and **36**). ^{1}H NMR spectroscopic data matched that given below. No other data were obtained.

Entry 2: (Carried out using General Procedure 1) A: 150.9 mg, 0.584 mmol; B: THF (1 mL); C: 10% Pt/C 128 (12.3 mg, 3.2 µmol, Johnson Matthey, metal assay 10%, 50% water); D: THF (0.95 mL); E: ammonia (0.3 mL, 5.17 mmol, 33% w/w solution in water); F: 5 psi; G: 800 rpm; H: 18 h; I: 58% conversion after 3 h, 100% conversion after 18 h, ratio **25**:**36**:**42** = 99.7:0.1:0.2; J: N/A; K: N/A.

Entry 3: Azide **24** (4 g, 15.5 mmol) was dissolved in THF (52 mL), then transferred to the hydrogenation vessel. Ammonia (8 mL, 138 mmol, 33% w/w solution in water) was added followed by 10% Pt/C (50% wet paste, 0.332 g, 85.2 µmol). The reactor was purged three times to 3 bar with nitrogen (stirring at 300 rpm), then three times with hydrogen to 50 psi (no stirring). The pressure in the hydrogen generator was set to 5 psi and the system purged and vented until the pressure in the generator reached 5 psi. A final purge to 5 psi with hydrogen (stirring at 300 rpm) was completed, and then the reaction mixture was stirred under 5 psi hydrogen at 700 rpm for 35.25 h. The conversion was determined at various time points: 7 h (63%),

22 h (93%), 27.25 h (97%), 35.25 h (100%). After 35.25 h the ratio of **25**:**36**:**42** was 99.7:0.1:0.2. The reaction mixture was filtered through a glass microfibre filter, and washed through with THF (12 mL). The filtrate was concentrated *in vacuo* to yield the crude product as a yellow oil (3.58 g as a mixture of **25**, **36** and **42**). ^{1}H NMR spectroscopic data matched that given below. No other data were obtained.

Entry 4:

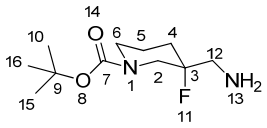

25

Azide **24** (616 g, 2.38 mol) was dissolved in THF (6.8 L), transferred to a 20 L vessel and washed in with THF (1.23 L). 10% Pt/C (50% wet paste, 8.3% w/w, 51.13 g) was added followed by ammonia (1.23 L, 21.21 mol, 33% w/w solution in water). The vessel was evacuated and purged with nitrogen to 1 bar three times, then evacuated and purged with hydrogen to 1 bar three times and stirred under 1 bar hydrogen for a total of 39 hours at 280 rpm. The conversion was determined at various time points: 23 h (88%) and 38.5 h (100%). After 38.5 h the ratio of **25**:**36**:**42** was 99.6:0.2:0.2. The reaction mixture was filtered, washed through with THF (1.85 L) and concentrated *in vacuo* to isolate the unpurified product as a yellow oil (552 g as a mixture of **25**, **36** & **42** in the ratio 99.4:0.3:0.3 as determined by LCMS). FTIR ν /cm^{-1} 3388 (N-H, weak), 1685 (C=O), 1156 (C-F); ^{1}H NMR (400 MHz, $CDCl_3$)* δ 1.37 (2H, br s, H13), 1.46 (9H, s, H10, H15, H16), 1.48-1.57 (1H, m, H5), 1.58-1.71 (1H, m, H4), 1.72-1.83 (1H, m, H5'), 1.84-1.96 (1H, m, H4'), 2.74-2.88 (2H, m, H12), 3.19 (1H, br t, J = 10.3 Hz, $H6_{ax}$), 3.31 (1H, dd, J = 22.5, 13.9 Hz, $H2_{ax}$), 3.59 (1H, br s, $H6_{eq}$), 3.68 (1H, dd, J = 13.7, 8.6 Hz, $H2_{eq}$); ^{13}C NMR

* Despite detection by LCMS, peaks for dimer **36** and *N*-alkyl impurity **42** were not visible in the NMR spectra suggesting they were only present at very low level. No sample of **42** was prepared or isolated. Peaks for butylated hydroxyl toluene were observed in the NMR spectra as it was present as a stabiliser in the THF.

(100 MHz, $CDCl_3$)* δ 21.6 (CH_2, br, C5), 28.4 (CH_3, C10, C15, C16), 31.7 (CH_2, d, $^2J_{C\text{-}F}$ = 22 Hz, C4), 43.4 and 44.4 (CH_2, br , C6), 47.5 (CH_2, d, $^2J_{C\text{-}F}$ = 23 Hz, C12), 48.2 and 49.3 (CH_2, br , C2), 79.9 (C, C9), 93.3 (C, d, $^1J_{C\text{-}F}$ = 175 Hz, C3), 154.9 (C, C7); HRMS *m/z* calculated for $C_{11}H_{22}FN_2O_2^+$ $[M+H]^+$ 233.1660, found 233.1659.

Preparation of (3*R*,3'*R*)-di-*tert*-butyl 3,3'-(azanediylbis(methylene))bis(3-fluoropiperidine-1-carboxylate) (36)

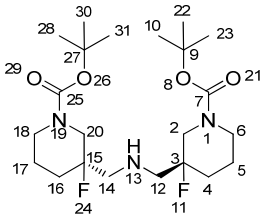

36

The isolated product from Table 2, entry 2 was dissolved in DMSO (1 mL) and subjected to preparative HPLC. The appropriate fractions were combined and ethyl acetate (30 mL) was added. The layers were extracted, and the aqueous layer was extracted with ethyl acetate (30 mL). The combined organic layers were concentrated *in vacuo* to yield the title compound **36** as an oil (10.0 mg, 22.3 μmol, 11% yield). FTIR ν /cm^{-1} 1689 (C=O), 1155 (C-F); ^{1}H NMR (400 MHz, $CDCl_3$)† δ 1.46 (18H, s, H10, H22, H23, H28, H30, H31), 1.47-1.97 (8H, 4 x br m, H4, H5, H16, H17), 2.69-2.86 (4H, m, H12, H14), 2.98-3.20 and 3.70-4.05 (8H, 4 x br m, H2, H6, H18, H20); ^{13}C NMR (100 MHz, $CDCl_3$)‡ δ 21.2 (CH_2, br, C5, C17), 28.4 and 28.5 (CH_3, C10, C22, C23, C28, C30, C31), 31.9 (CH_2, d, $^2J_{C\text{-}F}$ = 22 Hz, C4, C16), 43.3, 44.3, 49.1 and 50.2 (2 x CH_2, br, C2, C6, C18, C20), 55.3 (CH_2, br s, C12, C14), 79.3 and 79.7 (C, C9, C27), 93.7 (C, $^1J_{C\text{-}F}$ = 175 Hz, C3, C15), 155.0 and 155.1 (C, C7, C25); HRMS *m/z* calculated for $C_{22}H_{40}F_2N_3O_4^+$ $[M+H]^+$ 448.2981, found 448.2960.

---

* A number of the signals in the ^{13}C NMR spectrum are observed to exist as broad signals, or two signals, which is due to the rotameric effect of the *N*-Boc group.

† NMR spectral quality was poor due to very broad signals being observed. Lack of sample precluded further analysis being carried out.

‡ The ^{13}C NMR spectrum contained a number of signals which had two peaks of very close chemical shift (*e.g.* C7 and C25), suggesting that the carbons were not quite equivalent.

6.3 Experimental for Chapter 4

6.3.1 Experimental for Section 4.3.1

Preparation of 2-(2-((4-fluorobenzyl)thio)-4-oxo-4,5,6,7-tetrahydro-1*H*-cyclopenta[d]pyrimidin-1-yl)acetic acid (74)

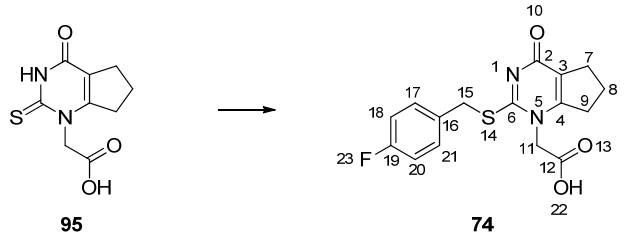

General Procedure 2: Preparation of Carboxylic Acid 74

Thiouracil **95** (A) was slurried in a mixture of water (B) and IPA (C). Concentrated aqueous sodium hydroxide solution (D, corrected for purity) was charged, washed in with water (E), and then followed by sodium carbonate (F). The resulting solution was heated to 40 ± 3 °C and 4-FBnCl (G) was charged, and washed in with IPA (H). The reaction mixture was stirred for 2.5 to 3 h, and reaction completion was checked by HPLC (Method C, [I]). After cooling to room temperature formic acid (J) was charged over the required time (K). The temperature of the resulting slurry was adjusted to the required temperature (L), and stirred for at least 1 h at this temperature. Following filtration to isolate the product the solid was washed twice with a mixture of 4:1 water and IPA (M), and then with IPA (N). The solid was dried overnight *in vacuo* at 50 °C, 50 – 100 mbar, to yield the title compound as a white solid (O).

Experimental for Section 4.3.1.1: Formic Acid Charge

All preparations of carboxylic acid **74** were carried out according to General Procedure 2. Minor differences in processing are recorded for each entry where applicable. An addition time of 0 min implies that the formic acid was added as quickly as reasonably possible. Full characterisation was carried out for a single batch; the remainder were analysed by HPLC (Method D), ^{1}H NMR and GC. Some batches were also analysed to determine inorganic content by sulfated ash.

Table 10

Entry 1: A: 20.0 g, 88.4 mmol; B: 112 mL; C: 20 mL; D: 13.2 g, 168 mmol (50.9% w/w aqueous solution); E: 10 mL; F: 2.35 g, 22.2 mmol; G: 13.41 g, 92.7 mmol; H: 12 mL; I: 0.69% area 4-FBnCl; J: 5.1 mL, 133 mmol; K: 0 min; L: 20 °C; M: 40 mL; N: 40 mL; O: 26.3 g, 78.7 mmol, 89%. HPLC (Method D) 14.8 min, 99.26% area; 4-FBnCl 1158 ppm by GC; inorganic content <0.1% w/w. ^{1}H NMR data matched that recorded below.
Note: Following the reaction the batch was left overnight at room temperature rather than continuing directly into the crystallisation. The HPLC data (I) were recorded just before effecting crystallisation.

Entry 2: A: 20.0 g, 88.4 mmol; B: 112 mL; C: 20 mL; D: 13.2 g, 168 mmol (50.9% w/w aqueous solution); E: 10 mL; F: 2.34 g, 22.1 mmol; G: 13.33 g, 92.2 mmol; H: 12 mL; I: 0.91% area 4-FBnCl; J: 7.8 mL, 203 mmol; K: 0 min; L: 20 °C; M: 40 mL; N: 40 mL; O: 28.2 g, 84.3 mmol, 95%. Mp 182.8 – 183.7 °C (decomposed); FTIR ν / cm^{-1} 2466 (O-H, weak, br), 1718 ($C=O_{acid}$), 1631 ($C=O_{pyrimidone}$), 1509 (aromatic C=C), 1221 (C-F); ^{1}H NMR (400 MHz, d_6-DMSO) δ 1.93-2.02 (2H, m, H8), 2.60 (2H, t, J = 7.3 Hz, H7), 2.84 (2H, t, J = 7.5 Hz, H9), 4.44 (2H, s, H15), 4.69 (2H, s, H11), 7.14 (2H, t, J = 8.8 Hz, H18, H20), 7.48 (2H, dd, J = 8.8, 5.6 Hz, H17, H21); ^{13}C NMR (100 MHz, d_6-DMSO) δ 20.1 (CH_2, C8), 27.9 (CH_2, C7), 31.2 (CH_2, C15), 34.4 (CH_2, C9), 49.9 (CH_2, C11), 115.2 (CH, d, $^{2}J_{C\text{-}F}$ = 21 Hz, C18, C20), 119.6 (C, C3), 131.1 (CH, d, $^{3}J_{C\text{-}F}$ = 8 Hz, C17, C21), 133.0 (C, $^{4}J_{C\text{-}F}$ = 3 Hz, C16), 156.4 (C, C4), 160.4 (C, C6), 161.1 (C, d, $^{1}J_{C\text{-}F}$ = 243 Hz, C19), 165.3 (C, C2), 168.2 (C, C12); HRMS *m/z* calculated for $C_{16}H_{16}FN_2O_3S^+$ $[M+H]^+$ 335.0860, found 335.0862; HPLC (Method D) 14.8 min, 99.38% area; 4-FBnCl 1820 ppm by GC; inorganic content <0.1% w/w.

Entry 3: A: 20.0 g, 88.4 mmol; B: 112 mL; C: 20 mL; D: 13.2 g, 168 mmol (50.9% w/w aqueous solution); E: 10 mL; F: 2.36 g, 22.3 mmol; G: 13.33 g, 92.2 mmol; H: 12 mL; I: 1.01% area 4-FBnCl; J: 10.2 mL, 265 mmol; K: 0 min; L: 20 °C; M: 40 mL; N: 40 mL; O: 28.4 g, 84.9 mmol, 96%. HPLC (Method D) 14.8 min, 99.36% area; 4-FBnCl 1958 ppm by GC; inorganic content <0.1% w/w. ^{1}H NMR data matched that recorded above.

An aliquot (2 mL) was taken from each of the above experiments directly prior to filtration to fund the studies recorded in Table 18 (see page 146).

Table 12

A: 32.0 g, 141 mmol; B: 179 mL; C: 32 mL; D: 21.1 g, 269 mmol (50.9% w/w aqueous solution); E: 16 mL; F: 3.8 g, 35.9 mmol; G: 21.5 g, 149 mmol; H: 19 mL; I: 1.24% area 4-FBnCl. The batch was then split into four portions each with an assumed input of 8 g (35.4 mmol) thiouracil **95**. Three of the portions were crystallised in parallel to generate the data in Table 12.

Entry 1: J: 2.03 mL, 52.9 mmol; K: 0 min; L: 20 °C; M: 16 mL; N: 16 mL; O: 10.3 g, 30.8 mmol, 87%. HPLC (Method D) 14.8 min, 99.27% area; 4-FBnCl 1545 ppm by GC. ^{1}H NMR data matched that recorded below.

Entry 2: J: 3.12 mL, 81.3 mmol; K: 0 min; L: 20 °C; M: 16 mL; N: 16 mL; O: 11.0 g, 32.9 mmol, 93%. HPLC (Method D) 14.8 min, 99.30% area; 4-FBnCl 1596 ppm by GC. ^{1}H NMR data matched that recorded below.

Entry 3: J: 4.07 mL, 106 mmol; K: 0 min; L: 20 °C; M: 16 mL; N: 16 mL; O: 11.0 g, 32.9 mmol, 93%. HPLC (Method D) 14.8 min, 99.31% area; 4-FBnCl 1682 ppm by GC. ^{1}H NMR data matched that recorded below.

The fourth portion was used to generate the data shown in Table 17, see page 147 for experimental details.

Experimental for Section 4.3.1.2: Addition Time of Formic Acid

All preparations of carboxylic acid **74** were carried out according to General Procedure 2. Minor differences in processing are recorded for each entry where applicable. The isolated products were analysed by HPLC (Method D), ^{1}H NMR and GC. Some batches were also analysed to determine inorganic content by sulfated ash.

Table 13

Entry 1: A: 20.0 g, 88.4 mmol; B: 112 mL; C: 20 mL; D: 13.2 g, 168 mmol (50.9% w/w aqueous solution); E: 10 mL; F: 2.32 g, 21.9 mmol; G: 13.36 g, 92.4 mmol; H: 12 mL; I: 1.00% area 4-FBnCl; J: 7.8 mL, 203 mmol; K: 5 min (93.6 mL/h); L: 20 °C; M: 40 mL; N: 40 mL; O: 28.6 g, 85.5 mmol, 97%. HPLC

(Method D) 14.8 min, 99.24% area; 4-FBnCl 2104 ppm by GC; inorganic content <0.1% w/w. ^{1}H NMR data matched that recorded above.

Entry 2: A: 20.0 g, 88.4 mmol; B: 112 mL; C: 20 mL; D: 13.2 g, 168 mmol (50.9% w/w aqueous solution); E: 10 mL; F: 2.34 g, 22.1 mmol; G: 13.46 g, 93.1 mmol; H: 12 mL; I: 0.97% area 4-FBnCl; J: 7.8 mL, 203 mmol; K: 90 min (5.2 mL/h); L: 20 °C; M: 40 mL; N: 40 mL; O: 28.7 g, 85.8 mmol, 97%. HPLC (Method D) 14.8 min, 99.07% area; 4-FBnCl 1606 ppm by GC; inorganic content <0.1% w/w; liquors analysis (Method A): uracil **97** 1.31% area, thiol **98** not detected. ^{1}H NMR data matched that recorded above. Data generated in this experiment are also shown in Table 15.

Entry 3: A: 20.0 g, 88.4 mmol; B: 112 mL; C: 20 mL; D: 13.2 g, 168 mmol (50.9% w/w aqueous solution); E: 10 mL; F: 2.34 g, 22.1 mmol; G: 13.34 g, 92.3 mmol; H: 12 mL; I: 0.51% area 4-FBnCl; J: 7.8 mL, 203 mmol; K: 292 min (1.6 mL/h); L: 20 °C; M: 40 mL; N: 40 mL; O: 28.8 g, 86.1 mmol, 97%. HPLC (Method D) 14.8 min, 99.28% area; 4-FBnCl 570 ppm by GC; inorganic content <0.1% w/w. ^{1}H NMR data matched that recorded above.
Note: Following the reaction the batch was left overnight at room temperature rather than continuing directly into the crystallisation. The HPLC sample (I) was taken just prior to crystallisation.

Table 14

A: 32.0 g, 141 mmol; B: 179 mL; C: 32 mL; D: 21.12 g, 269 mmol (50.9% w/w aqueous solution); E: 16 mL; F: 3.7 g, 34.9 mmol; G: 21.5 g, 149 mmol; H: 19 mL; I: 0.93% area 4-FBnCl. The reaction mixture was cooled to room temperature and left overnight prior to starting the crystallisation studies. The HPLC result (I) was from just before commencing crystallisations. The batch was then split into four portions each with an assumed input of 8 g (35.4 mmol) thiouracil **95**. The portions were crystallised in parallel to generate the data in Table 14.

Entry 1: J: 3.12 mL, 81.3 mmol; K: 5 min (37.4 mL/h); L: 20 °C; M: 16 mL; N: 16 mL; O: 11.1 g, 33.2 mmol, 94%. HPLC (Method D) 14.8 min, 99.17% area; 4-FBnCl 1408 ppm by GC. ^{1}H NMR data matched that recorded above.

Entry 2: J: 3.12 mL, 81.3 mmol; K: 90 min (2.08 mL/h); L: 20 °C; M: 16 mL; N: 16 mL; O: 11.2 g, 33.5 mmol, 95%. HPLC (Method D) 14.8 min, 99.12% area; 4-FBnCl 964 ppm by GC. ^{1}H NMR data matched that recorded above.

Entry 3: J: 3.12 mL, 81.3 mmol; K: 300 min (0.62 mL/h); L: 20 °C; M: 16 mL; N: 16 mL; O: 11.0 g, 32.9 mmol, 93%. HPLC (Method D) 14.8 min, 99.14% area; 4-FBnCl 672 ppm by GC. ^{1}H NMR data matched that recorded above.

Entry 4: The batch was stirred at room temperature for 5 h prior to commencing the crystallisation and resampled for HPLC (Method C). I: 0.88% area 4-FBnCl; J: 3.12 mL, 81.3 mmol; K: 5 min (37.4 mL/h); L: 20 °C; M: 16 mL; N: 16 mL; O: 11.1 g, 33.2 mmol, 94%. HPLC (Method D) 14.8 min, 99.22% area; 4-FBnCl 1108 ppm by GC. ^{1}H NMR data matched that recorded above.

Experimental for Section 4.3.1.3: Temperature Parameters

The isolated products were analysed by HPLC (Method D), ^{1}H NMR and GC. Some batches were also analysed to determine inorganic content by sulfated ash.

Table 15

Entry 1: See Table 13, entry 2 for experimental details.

Entry 2: Thiouracil **95** (20.0 g, 88.4 mmol) was slurried in a mixture of water (112 mL) and IPA (20 mL). Concentrated aqueous sodium hydroxide solution (13.2 g, 168 mmol, 50.9% w/w aqueous solution) was charged, washed in with water (10 mL), and then followed by sodium carbonate (2.34 g, 22.1 mmol). The resulting solution was heated to 40 ± 3 °C and 4-FBnCl (13.44 g, 93.0 mmol) was charged, and washed in with IPA (12 mL). The reaction mixture was stirred for 3 h (HPLC [Method C] 1.15% area 4-FBnCl). Formic acid (7.8 mL, 203 mmol) was charged over 90 min (5.2 mL/h), then the resulting slurry was cooled to 20 °C at 1 °C/min. The slurry was stirred at 20 °C for 65 min, and then filtered to isolate the solid, which was washed with a mixture of 4:1 water and IPA (2 x 40 mL), and then with IPA (40 mL). The solid was dried overnight *in vacuo* at 50 °C, 50 – 100 mbar, to yield the title compound as a white solid (28.18 g, 84.3 mmol, 95%). HPLC (Method D) 14.8 min, 99.12% area; 4-FBnCl 965 ppm by GC; inorganic content <0.1% w/w;

liquors analysis (Method A): uracil **97** 15.95% area, thiol **98** 3.71% area. ^{1}H NMR data matched that recorded above.

The identity of 4-fluorobenzyl mercaptan **98** was confirmed by comparison of HPLC retention time with a purchased sample (HPLC Method A retention time 4.8 min). Uracil **97** was prepared by the procedure detailed below.

Preparation of 2-(2,4-dioxo-2,3,4,5,6,7-hexahydro-1*H*-cyclopenta[d]pyrimidin-1-yl)acetic acid (97)

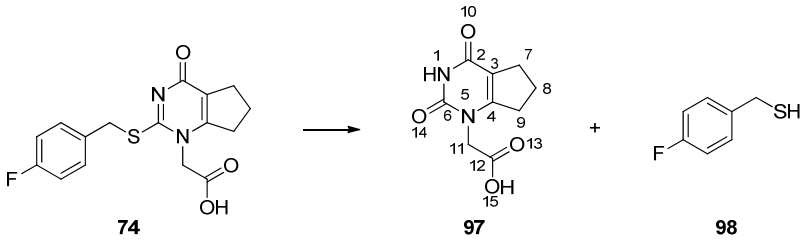

Acid **74** (10 g, 29.9 mmol) and water (100 mL) were heated at 90 °C for 24 h. Stirring was stopped, and the layers were allowed to separate. The lower layer was removed (HPLC Method A showed this to be predominantly thiol **98**, 4.8 min, 94.9% area). The upper layer was cooled to 26 °C and the resulting slurry was filtered to isolate the solid. The solid was washed with water (2 x 20 mL) and dried overnight *in vacuo* at 50 °C, 50 – 100 mbar, to yield uracil **97** as a white crystalline solid (5.81 g, 27.6 mmol, 92% yield). ^{1}H NMR (400 MHz, d_6-DMSO) δ 1.86-2.08 (2H, m, H8), 2.53-2.62 (2H, m, H7), 2.77 (2H, t, J = 7.21 Hz, H9), 4.42 (2H, s, H11), 11.19 (1H, s, H15); HPLC (Method A) 1.8 min, 98.2% area; LCMS 1.24 min, $[M+H]^+$ *m/z* 211.01.

Table 16

All preparations of carboxylic acid **74** were carried out according to General Procedure 2. Minor differences in processing are recorded for each entry where applicable.

Entry 1: A: 20.0 g, 88.4 mmol; B: 112 mL; C: 20 mL; D: 13.2 g, 168 mmol (50.9% w/w aqueous solution); E: 10 mL; F: 2.35 g, 22.2 mmol; G: 13.4 g, 92.7 mmol; H: 12 mL; I: 0.89% area 4-FBnCl; J: 7.8 mL, 203 mmol; K: 0 min; L: 2 °C; M: 40 mL; N: 40 mL; O: 29.2 g, 87.3 mmol, 99%. HPLC (Method D)

14.8 min, 99.06% area; 4-FBnCl 1689 ppm by GC; inorganic content <0.1% w/w. ^{1}H NMR data matched that recorded above. The batch was stirred at room temperature for about 5 minutes to allow the crystallisation to establish prior to cooling to 2 °C with an ice bath.

Entries 2 & 3: A: 20.0 g, 88.4 mmol; B: 112 mL; C: 20 mL; D: 13.2 g, 168 mmol (50.9% w/w aqueous solution); E: 10 mL; F: 2.35 g, 22.2 mmol; G: 13.5 g, 93.4 mmol; H: 12 mL; I: 1.39% area 4-FBnCl. The batch was then split into two portions which were crystallised in parallel with an assumed input of 10 g (44.2 mmol) thiouracil **95**.

Entry 2: J: 3.90 mL, 102 mmol; K: 0 min; L: 20 °C; M: 20 mL; N: 20 mL; O: 14.2 g, 42.5 mmol, 96%. HPLC (Method D) 14.8 min, 99.20% area; 4-FBnCl 1527 ppm by GC; inorganic content <0.1% w/w. ^{1}H NMR data matched that recorded above.

Entry 3: J: 3.90 mL, 102 mmol; K: 0 min; L: 2 °C; M: 20 mL; N: 20 mL; O: 7.1 g, 21.2 mmol, 48%. HPLC (Method D) 14.8 min, 99.55% area; 4-FBnCl 999 ppm by GC; inorganic content 0.18% w/w. ^{1}H NMR data matched that recorded above. This batch crystallised abnormally and there remained a considerable amount of solid on the vessel walls (not quantified). Analysis of a sample of this material was carried out: HPLC (Method D) 14.8 min, 98.50% area; inorganic content 6.1% w/w. ^{1}H NMR data matched that recorded above with minor differences in chemical shift observed, particularly H11 (δ 4.69 ppm, 2H, s). Formic acid was also present (δ 8.18 ppm, s) at 2.9% w/w as quantified from the ^{1}H NMR spectrum.

Entries 4 & 5: A: 20.0 g, 88.4 mmol; B: 112 mL; C: 20 mL; D: 13.2 g, 168 mmol (50.9% w/w aqueous solution); E: 10 mL; F: 2.34 g, 22.1 mmol; G: 13.4 g, 92.7 mmol; H: 12 mL; I: 1.14% area 4-FBnCl. The batch was then split into two portions which were crystallised in parallel with an assumed input of 10 g (44.2 mmol) thiouracil **95**.

Entry 4: J: 3.90 mL, 102 mmol; K: 5 min (46.8 mL/h); L: 2 °C; M: 20 mL; N: 20 mL; O: 14.3 g, 42.8 mmol, 97%. HPLC (Method D) 14.8 min, 99.17% area; 4-FBnCl 1526 ppm by GC. ^{1}H NMR data matched that recorded above.

Entry 5: J: 3.90 mL, 102 mmol; K: 90 min (2.6 mL/h); L: 2 °C; M: 20 mL; N: 20 mL; O: 14.1 g, 42.2 mmol, 95%. HPLC (Method D) 14.8 min, 99.16% area; 4-FBnCl 1087 ppm by GC. ^{1}H NMR data matched that recorded above.

Experimental for Section 4.3.1.4: Stir Time

All preparations of carboxylic acid **74** were carried out according to General Procedure 2. Minor differences in processing are recorded for each entry where applicable. The isolated products were analysed by HPLC (Method D), ^{1}H NMR and GC.

Figure 20 & Table 17

The fourth portion from the large batch prepared for use in earlier crystallisation studies (Table 12) was used for these investigations according to General Procedure 2. See earlier entry for experimental details for this preparation (page 142).

I: 0.85% area 4-FBnCl; J: 3.12 mL, 81.3 mmol; K: 0 min; L: 20 °C; M: 16 mL; N: 16 mL; O: 10.9 g, 32.6 mmol, 92%. HPLC (Method D) 14.8 min, 99.37% area; 4-FBnCl 820 ppm by GC. ^{1}H NMR data matched that recorded above. The final stir was carried out for a total of 1 week. Various samples of the liquors (filtered to ensure no solid was present) were taken for HPLC assay (Method A, 250 nm) during the stir and used to generate Figure 20 (Table 37). Samples of the slurry (1 mL) were taken at 1, 24, and 96 h, which were filtered and washed with 4:1 water/IPA (1 mL) and IPA (1 mL) and dried overnight *in vacuo* at 50-100 mbar at 50 °C. HPLC (Method D) 14.8 min: 99.32% area (1 h), 99.35% area (24 h), 99.35% area (96 h); 4-FBnCl by GC: 1229 ppm (1 h), 1108 ppm (24 h), 1048 ppm (96 h).

Stir time / min	Concentration 74 / mg/mL
5	6.203
20	3.971
40	3.812
60	3.762
180	3.591

*Table 37: Assay data for carboxylic acid **74** during final stir.*

Table 18

An aliquot (2 mL) was taken from each of the experiments in Table 10 immediately prior to filtration. All were stored unstirred at room temperature. After one week the slurries were filtered and the solids were washed with 4:1 water/IPA (2 x 1 mL) followed by IPA (1 mL) and dried overnight *in vacuo* at 50 – 100 mbar at 50 °C. ^{1}H NMR data matched that recorded above.

Entry 1: HPLC (Method D) 14.8 min: 99.20% area; 4-FBnCl 1018 ppm by GC.

Entry 2: HPLC (Method D) 14.8 min: 99.39% area; 4-FBnCl 1653 ppm by GC. Sampling of the liquors from this experiment generated the data shown in Table 19 (see below).

Entry 3: HPLC (Method D) 14.8 min: 99.39% area; 4-FBnCl 1864 ppm by GC.

Table 19

Samples of the liquors (from Table 18, entry 2) were analysed by HPLC (Method A) on commencing the study (0 h) and after 168 h (50 µL in 1 mL of Method D diluent). Start (0 h): acid **74** 81.09% area, uracil **97** 1.36% area, 4-fluorobenzyl alcohol 3.88% area, thiol **98** 0% area, 4-FBnCl 9.07% area; end (168 h): acid **74** 64.31% area, uracil **97** 12.44% area, 4-fluorobenzyl alcohol 9.45% area, thiol **98** 3.96% area, 4-FBnCl 0% area. The presence of 4-fluorobenzyl alcohol was confirmed by comparison of retention times with a genuine sample on HPLC (Method A, 2.7 min), and by LCMS ($[2M+H]^+$ *m/z* 253.07, 2.5 min).

Experimental for Section 4.3.1.5: Application of Experimental Design

Table 22

Thiouracil **95** (40.0 g, 177 mmol) was slurried in a mixture of water (224 mL) and IPA (40 mL). Concentrated aqueous sodium hydroxide solution (25.6 g, 336 mmol, 50.7 %w/w aqueous solution) was charged, washed in with water (20 mL), and then followed by sodium carbonate (4.7 g, 44.3 mmol). The resulting solution was heated to 40 ± 3 °C and 4-FBnCl (26.8 g, 186 mmol) was charged, and washed in with IPA (24 mL). The reaction mixture was stirred for 2.5 h then cooled to room temperature and split into two equal portions (180 mL) with an assumed input of 20 g of thiouracil **95**. The portions were stored overnight at 6 °C prior to crystallisation.

Crystallisations were carried out in Systag Flexylab equipment simultaneously. The portions were charged to the vessels at 20 °C and the temperature was adjusted to 25 °C with stirring at 250 rpm. Formic acid (10.17 g, 221 mmol) was charged over 90 min to crystallise the product, and then the batch was stirred at 25 °C for 15 min. The temperature was adjusted to 10 °C over 30 min (0.5 °C/min) and the slurry was stirred for 1 h. An aliquot of the slurry (5 mL) was taken, which was filtered and washed with 4:1 water/IPA (2 x 5 mL) and then with IPA (5 mL). All washes were completed with room temperature solvent. After a further 3 h the main batch was isolated by filtration and washed with 4:1 water/IPA (2 x 40 mL) and then with IPA (40 mL). Both solids were dried overnight *in vacuo* at 50 °C, 50 – 100 mbar, to yield acid **74**.

There were a number of small differences observed during experimentation that could account for the variation in the 4-FBnCl results. An overshoot in temperature for entry 2 prior to reaching 25 °C for crystallisation was observed. To prevent this in the full design a ramp (15 min) was included when adjusting to the initial temperature, followed by a hold (15 min) to allow the temperature to stabilise. The batches were observed to crystallise at different points during the formic acid addition which may also have contributed to the differing levels of 4-FBnCl in the isolated solids.

Entry 1:
Batch crystallised after addition of 5.5 g of formic acid.
1 h sample: acid **74** (0.7 g, 2.09 mmol, 2%). HPLC (Method D) 15.1 min, 99.39% area; 4-FBnCl 857 ppm by GC. ^{1}H NMR data matched that recorded previously.
4 h sample: acid **74** (27.1 g, 81.0 mmol, 92%; total yield: 27.8 g, 83.1 mmol, 94%). HPLC (Method D) 15.1 min, 99.39% area; 4-FBnCl 856 ppm by GC. ^{1}H NMR data matched that recorded previously.

Entry 2: (Carried out by Andrew Kennedy.)
Batch crystallised after addition of 3.2 g of formic acid.
1 h sample: acid **74** (0.73 g, 2.18 mmol, 2%). HPLC (Method D) 15.1 min, 99.38% area; 4-FBnCl 652 ppm by GC. ^{1}H NMR data matched that recorded

previously.

4 h sample: acid **74** (27.09 g, 81.0 mmol, 92%; total yield: 27.82 g, 83.2 mmol 94%). HPLC (Method D) 15.1 min, 99.29% area; 4-FBnCl 648 ppm by GC. ^{1}H NMR data matched that recorded previously.

General Procedure 3: Crystallisation Experimental Design Work

Crystallisations were carried out in Systag Flexylab equipment. The portions were charged to the vessels at 20 °C and the temperature was adjusted to the set point (A) over 15 min with stirring at 250 rpm. The reaction mixture was stirred at temperature for 15 min. Formic acid (B) was charged over the required time (C) to crystallise the product, and then the batch was stirred at the same temperature for 15 min. The temperature was adjusted to the isolation temperature (D) at 0.5 °C/min. The slurry was stirred for 1 h then an aliquot of the slurry (5 mL) was taken, which was filtered and washed with 4:1 water/IPA (2 x 5 mL) and then with IPA (5 mL). All washes were completed with room temperature solvent. After a further 23 h the main batch was isolated by filtration and washed with 4:1 water/IPA (2 x 40 mL) and then with IPA (40 mL). The solids were dried overnight *in vacuo* at 50 °C, 50 – 100 mbar, to yield acid **74** as a white solid (E).

Preparation of Reaction Mixture for Crystallisation Design

Thiouracil **95** (200.0 g, 884 mmol) was slurried in a mixture of water (1120 mL) and IPA (200 mL). Concentrated aqueous sodium hydroxide solution (132.5 g, 1.68 mol, 50.7% w/w aqueous solution) was charged, washed in with water (100 mL), and then followed by sodium carbonate (23.4 g, 221 mmol). The resulting solution was heated to 40 ± 3 °C and 4-FBnCl (134.8 g, 932 mmol) was charged, and washed in with IPA (120 mL). The reaction mixture was stirred for 2.5 h, cooled to room temperature, and then stored overnight at 6 °C. The batch was split into ten equal portions (175 mL) for use in the crystallisations, assuming 20 g input of thiouracil **95**.

Tables 23 & 25

Crystallisations were carried out using General Procedure 3. Runs 1-5 were completed by the author; runs 6-10 were carried out by Andrew Kennedy. Analytical results are reported in Table 38 (1 h samples) and Table 39 (24 h samples). The

inorganic content was determined as <0.1% w/w by sulfated ash analysis for all 24 h samples (1 h samples were not tested).

Run 1: A: 12.21 g, 265 mmol; B: 20 °C; C: 175 min; D: 0 °C; E: 1 h: 0.73 g, 2.18 mmol, 2%; 24 h: 27.2 g, 81.3 mmol, 92%; total yield: 27.93 g, 83.5 mmol, 94%.

Run 2: A: 12.21 g, 265 mmol; B: 20 °C; C: 5 min; D: 20 °C; E: 1 h: 0.54 g, 1.61 mmol, 2%; 24 h: 27.2 g, 81.3 mmol, 92%; total yield: 27.74 g, 83.0 mmol, 94%.

Run 3: A: 10.17 g, 221 mmol; B: 25 °C; C: 90 min; D: 10 °C; E: 1 h: 0.68 g, 2.03 mmol, 2%; 24 h: 27.4 g, 81.9 mmol, 93%, total yield: 28.08 g, 84.0 mmol, 95%.

Run 4: A: 8.14 g, 177 mmol; B: 30 °C; C: 175 min; D: 0 °C; E: 1 h: 0.71 g, 2.12 mmol, 2%; 24 h: 26.8 g, 80.2 mmol, 91%; total yield: 27.51 g, 82.3 mmol, 93%.

Run 5: A: 8.14 g, 177 mmol; B: 30 °C; C: 5 min; D: 20 °C; E: 1 h: 0.65 g, 1.94 mmol, 2%; 24 h: 26.7 g, 79.9 mmol, 90%; total yield : 27.35 g, 81.8 mmol, 93%.

Run 6: A: 8.14 g, 177 mmol; B: 20 °C; C: 5 min; D: 0 °C; E: 1 h: 0.72 g, 2.15 mmol, 2%; 24 h: 27.02 g, 80.8 mmol, 91%; total yield: 27.74 g, 83.0 mmol, 94%.

Run 7: A: 12.21 g, 265 mmol; B: 30 °C; C: 5 min; D: 0 °C; E: 1 h: 0.65 g, 1.94 mmol, 2%; 24 h: 27.35 g, 81.8 mmol, 93%; total yield: 28.00 g, 83.7 mmol, 95%.

Run 8: A: 8.14 g, 177 mmol; B: 20 °C; C: 175 min; D: 20 °C; E: 1 h: 0.84 g, 2.51 mmol, 3%; 24 h: 26.59 g, 79.5 mmol, 90%; total yield: 27.43 g, 82.0 mmol, 93%.

Run 9: A: 10.17 g, 221 mmol; B: 25 °C; C: 90 min; D: 10 °C; E: 1 h: 0.82 g, 2.45 mmol, 3%; 24 h: 26.83 g, 80.2 mmol, 91%; total yield: 27.65 g, 82.7 mmol, 94%.

Run 10: A: 12.21 g, 265 mmol; B: 30 °C; C: 175 min; D: 20 °C; E: 1 h: 0.78 g, 2.33 mmol, 3%; 24 h: 27.09 g, 81.0 mmol, 92%; total yield: 27.87 g, 83.4 mmol, 94%.

Run	4-FBnCl / ppm[a]	Mother liquors assay / mg/mL[b]	Uracil 97 / peak area[b]	Acid 74 / % area[c]	Benzyl ester 96 / % area[c]
1	719	1.0	7.573	99.17	0.42
2	1375	2.2	5.775	99.22	0.34
3	549	1.9	9.060	99.19	0.40
4	339	2.1	18.796	99.19	0.46
5	994	4.2	10.754	99.27	0.35
6	1276	1.1	6.576	99.24	0.35
7	1155	0.9	12.404	99.27	0.34
8	694	3.7	7.818	99.16	0.43
9	611	1.3	7.983	99.19	0.42
10	432	2.0	17.022	99.21	0.43

[a] Determined by GC.

[b] HPLC Method A, with assay of acid **74**.

[c] HPLC Method D.

Table 38: Data for 1 h samples.

Run	4-FBnCl / ppm[a]	Mother liquors assay / mg/mL[b]	Uracil 97 / peak area[b]	Acid 74 / % area[c]	Benzyl ester 96 / % area[c]
1	668	0.66	7.843	99.17	0.42
2	1198	2.27	16.525	99.24	0.34
3	512	1.59	10.507	99.20	0.40
4	330	1.36	18.790	99.20	0.46
5	914	4.10	19.656	99.26	0.35
6	1153	1.00	6.774	99.19	0.35
7	1126	0.64	12.676	99.24	0.34
8	661	3.52	12.969	99.16	0.43
9	558	1.23	8.677	99.18	0.42
10	402	1.99	23.080	99.20	0.43

[a] Determined by GC.

[b] HPLC Method A, with assay of acid **74**.

[c] HPLC Method D.

Table 39: Data for 24 h samples.

The 24 h 4-FBnCl data required a square root transformation when modelling in DX7 in order to remove an outlying data point. The presence of an outlier suggests either anomalous data, or an incorrect model. All models should be checked with various diagnostic tests.[12] As an example, Figure 48 shows run 7 to be an outlier compared to the other data. Once the transform is applied no outliers are present. An alternative strategy is to exclude the outlying point from the data and build a model in its absence. No other responses showed outlying data points when modelled, and no other transforms were required.

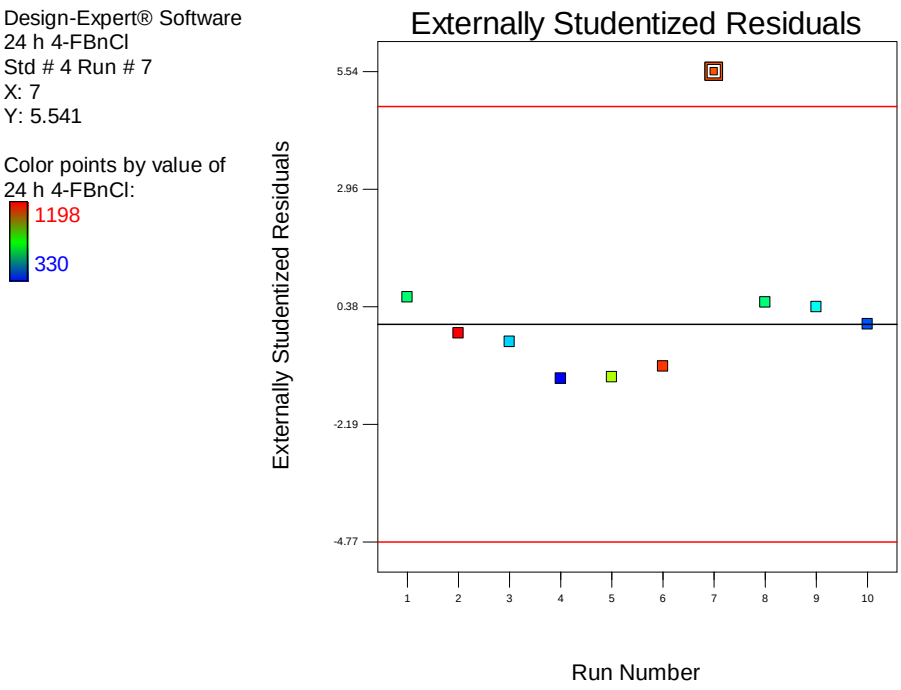

Figure 48: Diagnostic test (externally studentised residuals) applied to model from non-transformed 24 h 4-FBnCl data.

Aliasing Structure for Design

[Block]	=	Block - 0.8 * AB - 0.8 * CD
[A]	=	A + BCD
[B]	=	B + ACD
[C]	=	C + ABD
[D]	=	D + ABC
[AC]	=	AC + BD
[AD]	=	AD + BC

The aliasing structure shows that single factors can be determined with confidence, being only aliased with three-factor interactions, which are unlikely to be present. The two-factor interactions are aliased with one another. The block effect is aliased with AB and CD. If these interactions are identified as part of a model, the interaction will be indistinguishable from the block effect.

6.3.2 Experimental for Section 4.3.2

Preparation of darapladib intermediate grade *N*-(2-(diethylamino)ethyl)-2-(2-((4-fluorobenzyl)thio)-4-oxo-4,5,6,7-tetrahydro-1*H*-cyclopenta[d]pyrimidin-1-yl)-*N*-((4'-(trifluoromethyl)-[1,1'-biphenyl]-4-yl)methyl)acetamide (71-IG)

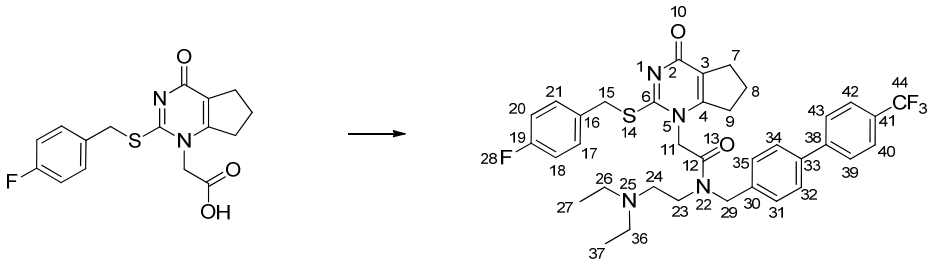

Darapladib **71** is rotameric about the amide bond, hence a number of the signals in the NMR spectra are observed to exist as two signals in an approximate ratio of 65:35.

For convenience amine **77** is typically stored and used as a toluene concentrate and charged by volume using HPLC assay, or by mass after correcting for toluene content as determined by quantitative ^{1}H NMR spectroscopy.

General Procedure 4: Preparation of Darapladib

CDI (A) was stirred in MIBK (B) and heated to 70 ± 3 °C. Carboxylic acid **74** (C) was charged in portions over about 10 min to control CO_2 evolution. 4-FBnCl (D) was then charged (if required) and the reaction mixture stirred for the requisite time (E). Crystallisation of the batch to give a thick slurry typically occurred. Reaction completion was checked using HPLC Method A at 254 nm. Samples were quenched into *n*-butyl amine to observe imidazolide **102** as the corresponding butyl amide. Amine **77** (F) was added and washed in with MIBK (G) then heated to 92 ± 3 °C and stirred for the designated time (H). Reaction completion was checked using HPLC Method A at 254 nm with *n*-butyl amine quench as above. The reaction mixture was cooled to 45 °C and concentrated by vacuum distillation to the appropriate volume (I). The batch was cooled to 40 ± 3 °C, then methanol (J) was charged over about 5 min, and the batch was cooled to 20 °C at 1 °C/min. The slurry was stirred for 30 to 40 min at 20 °C, heated to 50 °C at 1 °C/min, stirred at 50 °C for 30 min, cooled to

2 °C at 0.3 °C/min then stirred at 2 ± 3 °C for at least 30 min. The solid was collected by filtration, washed twice with chilled methanol (K) and dried *in vacuo* at 47 °C, 50 – 100 mbar, to yield **71-IG** as an off-white solid (L, yield corrected for methanol content [M]).

Experimental for Sections 4.3.2.1 & 4.3.2.2: Purging and Fate of 4-FBnCl During Preparation of Darapladib IG

Experiments to prepare darapladib IG were carried out using General Procedure 4. Minor differences in processing were used in each case; these are briefly summarised for each entry and were not anticipated to lead to significant differences between batches. Full characterisation was carried out for a single batch; the remainder were analysed by HPLC, GC and ^{1}H NMR only.

Table 27

Entry 1: A: 11.6 g, 71.5 mmol; B: 120 mL; C: 20.0 g, 59.8 mmol (contained 968 ppm 4-FBnCl); D: N/A; E: 80 min; F: 23.0 g, 65.6 mmol (26.3 mL of a solution of amine **77** in toluene, with concentration determined as 875.8 mg/mL by HPLC assay on Method A at 256 nm); G: 20 mL; H: 125 min; I: 90 mL; J: 50 mL; K: 80 mL; L: 30.75 g, 46.1 mmol, 77%; M: 2.9% w/w. HPLC (Method B) 13.1 min, 99.43% area; 4-FBnCl <1 ppm by GC. ^{1}H NMR data matched that recorded below.
Note: Batch left overnight at 2 °C prior to isolation.

Entry 2: A: 11.6 g, 71.5 mmol; B: 120 mL; C: 20.0 g, 59.8 mmol (contained 1276 ppm 4-FBnCl); D: N/A; E: 90 min; F: 23.0 g, 65.6 mmol (26.3 mL of a solution of amine **77** in toluene with concentration determined as 875.8 mg/mL by HPLC assay on Method A at 256 nm); G: 20 mL; H: 150 min; I: 90 mL; J: 50 mL; K: 80 mL; L: 30.07 g, 45.1 mmol, 75%; M: 2.9% w/w. HPLC (Method B) 13.1 min, 99.39% area; 4-FBnCl <1 ppm by GC. ^{1}H NMR data matched that recorded below.
Note: Batch left overnight at 20 °C after crystallisation, then cooled to 2 ± 3 °C and stirred for 1.5 h before isolation.

Table 28

Entry 1: A: 17.5 g, 108 mmol; B: 180 mL; C: 30.0 g, 89.7 mmol; D: 124 µL, 1.04 mmol; E: 140 min; F: 34.6 g, 98.7 mmol (39.5 mL of a solution of amine **77** in

toluene with concentration determined as 875.8 mg/mL by HPLC assay on Method A at 256 nm); G: 30 mL; H: 130 min; I: 135 mL; J: 75 mL; K: 120 mL; L: 49.09 g, 73.6 mmol, 82%; M: 2.7% w/w. HPLC (Method B) 13.1 min, 99.33% area; 4-FBnCl <1 ppm by GC. ^{1}H NMR data matched that recorded below.
Note: Batch stirred overnight at 2 ± 3 °C prior to isolation.

Entry 2: A: 17.46 g, 109 mmol; B: 180 mL; C: 30.0 g, 89.7 mmol; D: 1.74 mL, 14.5 mmol; E: 90 min; F: 34.6 g, 98.7 mmol (39.5 mL of a solution of amine **77** in toluene with concentration determined as 875.8 mg/mL by HPLC assay on Method A at 256 nm); G: 30 mL; H: 135 min; I: 135 mL; J: 75 mL; K: 120 mL; L: 47.21 g, 70.8 mmol, 79%; M: 1.8% w/w. Mp 98.5 – 101.5 °C; FTIR ν / cm^{-1} 1658 ($C{=}O_{amide}$), 1632 ($C{=}O_{pyrimidone}$), 1607 (C=C aromatic), 1485 (C=C aromatic), 1323 (C-F, CF_3), 1157 (C-F, CF_3), 1111 (C-F, CF_3); ^{1}H NMR (400 MHz, $CDCl_3$) δ 0.99 (6H, t, *J* = 6.9 Hz, H27, H37), 2.01-2.15 (2H, 2 x m, H8), 2.51 (4H, q, *J* = 7.1 Hz, H26, H36), 2.58 and 2.62 (2H, 2 x t, *J* = 5.4 Hz, H24), 2.71 and 2.84 (2H, 2 x t, *J* = 7.3 Hz, H9), 2.81 (2H, t, *J* = 7.1 Hz, H7), 3.29 and 3.56 (2H, 2 x t, *J* = 5.4 Hz, H23), 4.44 and 4.52 (2H, 2 x s, H15), 4.62 and 4.95 (2H, 2 x s, H11), 4.68 and 4.70 (2H, 2 x s, H29), 6.89-6.99 (2H, 2 x t, *J* = 8.1 Hz, H18, H20), 7.28-7.39 (4H, 2 x td, *J* = 7.6, 2.0 Hz, 1 x m, H17, H21, H31, H35), 7.46 and 7.52 (2H, 2 x d, *J* = 7.6 Hz, H32, H34), 7.60 and 7.63 (2H, 2 x d, *J* = 8.1 Hz, H39, H43), 7.68-7.72 (2H, m, H40, H42); ^{13}C NMR (100 MHz, $CDCl_3$) δ 11.8 and 12.2 (CH_3, C27, C37), 20.7 and 20.8 (CH_2, C8), 28.3 and 28.4 (CH_2, C7), 31.8 and 32.0 (CH_2, C9), 36.4 and 36.6 (CH_2, C15), 46.1 and 46.4 (CH_2, C23), 47.4 and 47.8 (CH_2, C26, C36), 49.0 and 50.9 (CH_2, C29), 49.8 and 50.0 (CH_2, C11), 51.4 and 51.6 (CH_2, C24), 115.5 and 115.6 (CH, d, $^{2}J_{C\text{-}F}$ = 21 Hz, C18, C20), 121.3 (C, C3), 124.3 (C, q, $^{1}J_{C\text{-}F}$ = 272 Hz, C44), 125.7-126.0 (CH, m, C40, C42), 126.8 and 128.7 (CH, C31, C35), 127.3 (CH, C39, C43), 127.6 and 128.0 (CH, C32, C34), 129.6 (C, q, $^{2}J_{C\text{-}F}$ = 33 Hz, C41), 131.1 (2 peaks, CH, d, $^{3}J_{C\text{-}F}$ = 8 Hz, C17, C21), 131.3 and 131.6 (C, d, $^{4}J_{C\text{-}F}$ = 3 Hz, C16), 135.8 and 136.8 (C, C30), 139.3 and 139.7 (C, C33), 143.6 and 144.0 (C, C38), 155.5 and 155.8 (C, C4), 160.8 (C, C6), 162.3 (C, d, $^{1}J_{C\text{-}F}$ = 247 Hz, C19), 164.9 and 165.5 (C, C12), 167.0 and 167.1 (C, C2); HRMS *m/z* calculated for $C_{36}H_{39}F_4N_4O_2S^+$ $[M+H]^+$ 667.2724, found 667.2733; HPLC (Method B) 13.1 min, 99.69% area; 4-FBnCl <1 ppm by GC.
Note: Batch stirred overnight at 40 °C after the distillation.

Samples taken for LCMS throughout this experiment were used to identify the species resulting from reaction with 4-FBnCl (section 4.3.2.2). LCMS showed the presence of imidazole derivative **104** $[M+H]^+$ *m/z* 177.14, 2.24 min, and either diamine **105** $[M+H]^+$ *m/z* 459.26, 5.36 min, or quaternary species **106** $[M]^+$ *m/z* 459.26, 5.36 min (identity later confirmed as **105**).
HPLC analysis (Method B) showed a peak at 19.2 min (0.03% area) which was confirmed as being **105** by re-running the sample in the presence of a spike of **105** at approximately 0.05% w/w.
The filtrate and cake washes were analysed by GC* relative to a standard prepared at 0.0012 µL/mL which showed no peak for 4-FBnCl. This equated to <0.6% of the initial 4-FBnCl charge being present in the filtrate and washes. No further quantitative analysis of the reaction liquors for 4-FBnCl was carried out at this stage.
The amounts of **104** and **105** in the filtrate and washes were quantified by addition of an internal standard (Appendix 2).

Entry 3: A: 11.64 g, 71.8 mmol; B: 120 mL; C: 20.0 g, 59.8 mmol; D: 1.16 mL, 9.68 mmol; E: 60 min; F: 28.1 g, 65.8 mmol (solution of amine **77** in toluene, 82.1%w/w, concentration determined by quantitative ^{1}H NMR spectroscopy); G: 20 mL; H: 120 min; I: 90 mL; J: 50 mL; K: 80 mL; L: 31.20 g, 46.8 mmol, 78%; M: 3.3% w/w. HPLC (Method B) 13.1 min, 99.81% area; 4-FBnCl <1 ppm by GC. ^{1}H NMR data matched that recorded above.
Note: Batch stirred for two nights at 2 ± 3 °C prior to isolation.
The reaction mixture was sampled at various time points (HPLC Methods A and B) and these data were used to prepare Figure 30 (see Table 41, page 162).
The amounts of **104** and **105** in the filtrate and washes were quantified by addition of an internal standard (see Appendix 2).

* Unpublished method. The sensitivity of this method was inferior to the documented method due to the use of a flame ionisation detector.

Experimental for Section 4.3.2.3: Preparation of 4-FBnCl Derived Impurities

Preparation of alkylated imidazoles 1-(4-fluorobenzyl)-1*H*-imidazole (104) and 1,3-bis(4-fluorobenzyl)-1*H*-imidazol-3-ium chloride* (111)

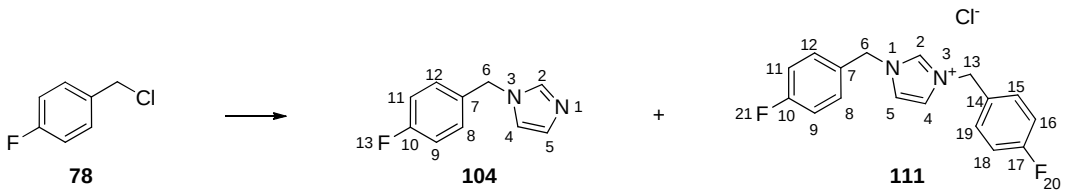

Imidazole (4.7 g, 69.0 mmol), potassium carbonate (2.4 g, 17.37 mmol) and THF (50 ml) were stirred together at room temperature for 10 min to give a suspension. 4-Fluorobenzyl chloride (4.14 ml, 34.6 mmol) was charged and the mixture heated at reflux for 24 h. The reaction mixture was filtered to remove solids, and then concentrated *in vacuo*. The residue was dissolved in DCM (50 mL) and extracted with water (50 mL). Compound **104** was isolated from the organic layer and species **111** was isolated from the aqueous layer.

The organic layer was extracted with water (50 mL), dried over magnesium sulfate then concentrated *in vacuo* to yield **104**[113] as a yellow oil, (3.89 g, 22.1 mmol, 64% yield). FTIR ν / cm^{-1} 1509 (aromatic C=C & C=N), 1222 (C-F); ^{1}H NMR (400 MHz, $CDCl_3$) δ 5.09 (2H, s, H6), 6.88 (1H, s, H4), 7.04 (2H, td, *J* = 8.6, 2.2 Hz, H9, H11), 7.09 (1H, s, H5), 7.13 (2H, td, *J* = 8.6, 3.2 Hz, H8, H12), 7.53 (1H, s, H2); ^{13}C NMR (100 MHz, $CDCl_3$) δ 50.1 (CH_2, C6), 116.0 (CH, d, $^{2}J_{C\text{-}F}$ = 21 Hz, C9, C11), 119.1 (CH, C4), 129.1 (CH, d, $^{3}J_{C\text{-}F}$ = 9 Hz, C8, C12), 130.1 (CH, C5), 132.0 (C, d, $^{4}J_{C\text{-}F}$ = 3 Hz, C7), 137.4 (CH, C2), 162.6 (C, d, $^{1}J_{C\text{-}F}$ = 246 Hz, C10); HRMS *m/z* calculated for $C_{10}H_{10}FN_2^+$ $[M+H]^+$ 177.0823, found 177.0820; HPLC (Method A) 2.1 min, 98.57% area.

The aqueous layer was extracted with DCM (50 mL) and the organic phase discarded. The aqueous phase was then extracted with DCM (4 x 50 mL). The four DCM layers were combined and dried over magnesium sulfate then concentrated *in*

* Assumes chloride salt was prepared. No analysis was carried out to determine actual counterion.

vacuo to yield a white oil (333.1 mg, 0.70 mmol, 2% yield), confirmed to be a mixture of **111**[114] and imidazole in approximately 2:1 ratio. FTIR ν / cm^{-1} 1512 (aromatic C=C), 1225 (C-F), 1062 (in plane aromatic C-H); ^{1}H NMR (400 MHz, $CDCl_3$) δ 5.45 (4H, s, H6, H13), 7.07 (4H, t, *J* = 8.6 Hz, H9, H11, H16, H18), 7.09 (s, imidazole C=CHN), 7.16 (2H, s, H4, H5), 7.43 (4H, td, *J* = 7.8, 2.2 Hz, H8, H12, H15, H19), 7.68 (s, imidazole NCH=N), 10.96 (1H, s, H2); ^{13}C NMR (100 MHz, $CDCl_3$) δ 52.9 (CH_2, C6, C13), 116.8 (CH, d, $^2J_{C\text{-}F}$ = 22 Hz, C9, C11, C16, C18), 121.7 (CH, C4, C5), 122.0 (CH, imidazole C=CHN), 128.4 (C, d, $^4J_{C\text{-}F}$ = 4 Hz, C7, C14), 131.0 (CH, d, $^3J_{C\text{-}F}$ = 8 Hz, C8, C12, C15, C19), 135.2 (CH, imidazole NCH=N), 137.7 (CH, C2), 163.4 (C, d, $^1J_{C\text{-}F}$ = 250 Hz, C10, C17); ^{1}H NMR (400 MHz, d_6-DMSO) δ 5.43 (4H, s, H6, H13), 7.01 (s, imidazole C=CHN), 7.27 (4H, t, *J* = 8.8 Hz, H9, H11, H16, H18), 7.52 (4H, td, *J* = 8.6, 3.2 Hz, H8, H12, H15, H19), 7.64 (s, imidazole NCH=N), 7.84 (2H, d, *J* = 1.5 Hz, H4, H5), 9.47 (1H, s, H2); HRMS *m/z* calculated for $C_{17}H_{15}F_2N_2^+$ $[M]^+$ 285.1198, found 285.1198; HPLC (Method A) 3.5 min, 95.58% area.

Preparation of *N*,*N*-diethyl-*N*'-(4-fluorobenzyl)-*N*'-((4'-(trifluoromethyl)-[1,1'-biphenyl]-4-yl)methyl)ethane-1,2-diamine (105)

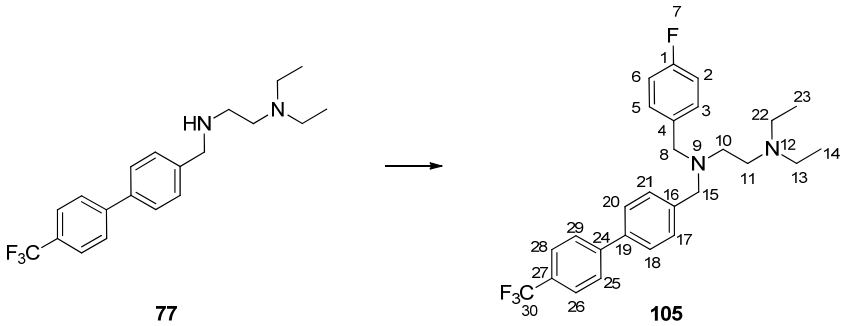

Amine **77** (6.4 g, 18.3 mmol), toluene (24 mL) and 4-fluorobenzyl chloride (2 mL, 16.7 mmol) were heated at 90 °C for 25 h. The reaction mixture was cooled to room temperature and toluene (10 mL) was added. Water (25 mL) then aqueous 2 M HCl (10 mL) were added and the layers were separated. The aqueous layer was extracted with toluene (20 mL) then charged with aqueous 2 M NaOH (35 mL). Ethyl acetate (50 mL) was added and the lower layer was removed. The remaining emulsion was passed through celite and the filtrate was heated to give separation. The aqueous layer was removed. The organic layer was dried over magnesium sulfate then

concentrated *in vacuo*. A portion of the residue (1.48 g) was purified by Biotage chromatography (110 g KP-NH column, 6% to 50% ethyl acetate in heptane, flow rate 40 mL/min) to yield **105** as a pale yellow oil, (0.917 g, 2.00 mmol, 12% yield). FTIR ν / cm^{-1} 1323 (C-F, CF_3), 1122 (C-F, CF_3), 1070 (C-F, CF_3); ^{1}H NMR (400 MHz, $CDCl_3$) δ 0.95 (6H, t, *J* = 7.1 Hz, H14, H23), 2.44 (4H, q, *J* = 7.1 Hz, H13, H22), 2.57 (4H, s, H11, H10), 3.59 (2H, s, H8), 3.64 (2H, s, H15), 6.99 (2H, t, *J* = 8.8 Hz, H2, H6), 7.33 (2H, td, *J* = 5.6, 2.7 Hz, H3, H5), 7.45 (2H, d, *J* = 8.1 Hz, H17, H21), 7.54 (2H, d, *J* = 8.1 Hz, H18, H20), 7.68 (4H, s, H25, H26, H28, H29); ^{13}C NMR (100 MHz, $CDCl_3$) δ 11.8 (CH_3, C14, C23), 47.5 (CH_2, C13, C22), 51.3 (CH_2, C11), 51.7 (CH_2, C10), 58.2 (CH_2, C8), 58.5 (CH_2, C15), 115.0 (CH, d, $^2J_{C\text{-}F}$ = 21 Hz, C2, C6), 124.3 (C, q, $^1J_{C\text{-}F}$ = 272 Hz, C30), 125.7 (CH, q, $^3J_{C\text{-}F}$ = 4 Hz, C26, C28), 127.1 (CH, C25, C29), 127.3 (CH, C18, C20), 129.2 (C, q, $^2J_{C\text{-}F}$ = 33 Hz, C27), 129.3 (CH, C17, C21), 130.1 (CH, d, $^3J_{C\text{-}F}$ = 8 Hz, C3, C5), 135.4 (C, d, $^4J_{C\text{-}F}$ = 3 Hz, C4), 138.4 (C, C19), 140.1 (C, C16), 144.6 (C, C24), 161.9 (C, d, $^1J_{C\text{-}F}$ = 243 Hz, C1); HRMS *m/z* calculated for $C_{27}H_{31}F_4N_2^+$ $[M+H]^+$ 459.2418, found 459.2415; HPLC (Method A) 5.3 min, 99.73% area.

HPLC analysis (Method A) of the reaction mixture suggested that two products had formed (71.52% area at 5.26 min and 3.52% area at 5.99 min). LCMS analysis suggested both were consistent with either **105** or **106**: $[M+H]^+$ *m/z* 459.15 at 5.34 min and $[M]^+$ *m/z* 459.15 at 5.95 min. Attempts to isolate a sample of the second product, presumed to be **106**, were unsuccessful, thus its structure was not proven.

Experimental for Section 4.3.2.4: Reaction Monitoring

Figure 29

Two experiments were carried out as detailed below, with reaction monitoring using ^{19}F NMR spectroscopy in d_6-DMSO to quantify the 4-FBnCl level relative to carboxylic acid **74** by integration of peaks for 4-FBnCl (-113.55 ppm, 1F) and carboxylic acid **74** (-114.83 ppm, 1F). At the sample concentration used, the limit of quantification of 4-FBnCl was determined as 1% w/w. The limit of detection was approximately 0.5% w/w.

Carboxylic acid **74** (10.0 g, 29.9 mmol) and MIBK (60 mL) were stirred together. 4-FBnCl (0.58 mL, 4.84 mmol) was added and the slurry was heated to the required temperature (70 or 90 ºC). CDI (5.82 g, 35.9 mmol) was added portion-wise over 7 to 10 min, and then the reaction mixture was sampled at various times and analysed by ^{19}F NMR spectroscopy (Table 40). No compounds were isolated from these experiments.

70 °C		90 °C	
Time / h	**4-FBnCl / % w/w relative to 74**	**Time / h**	**4-FBnCl / % w/w relative to 74**
0.5	6.5	0.5	3.9
1	5.7	1	1.8
2.5	3.6	2	0.5
18	0	6.5	0

*Table 40: ^{19}F NMR spectroscopic data during formation of imidazolide **102**.*

Compound **111** was detected in the reaction mixture using LCMS, $[M]^+$ *m/z* 285.12 at 3.57 min.

Figure 30

Data were obtained from the experiment in Table 28, entry 3, by completing analysis at various times using HPLC Methods A & B (Table 41). Data are not quantitative.

Time / min	Imidazole 104 / % area (Method A)	Diamine 105 / % area (Method B)
0	0.76	0.56
5	0.87	0.77
10	1.13	0.87
20	1.48	0.97
40	2.05	1.05
120	2.08	1.09

*Table 41: HPLC data for the formation of imidazole **104** and diamine **105**.*

Experimental for Section 4.3.2.5: Quantification of Impurities

Calculation of "*r*" values (Table 29)

Methyl *p*-tolyl sulfone **117** and biphenyl **118** were identified as appropriate internal standards for quantification of the impurities deriving from 4-FBnCl (Figure 49).

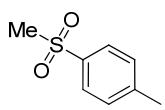

117

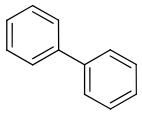

118

Figure 49: Internal standards used for quantification.

Table 42 shows the *r* values calculated for the various compounds under investigation during these studies.

Analyte	Internal standard	HPLC Method	*r* value
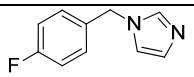 **104**	Methyl *p*-tolyl sulfone	Method A	3.204
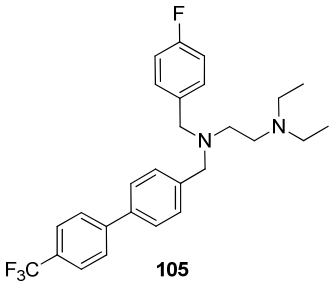 **105**	Biphenyl	Method B	1.844
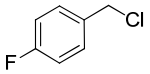 **78**	Methyl *p*-tolyl sulfone	Method A	1.484

Table 42: Calculated r values.

Calculation of *r* for each compound was achieved on the HPLC method stated using the equation:

$$r_x = \frac{(\%\ \text{area}_{IS} / \%\ \text{area}_x)}{(W_{IS} / W_x)}$$

Where: x = Analyte

IS = Internal Standard

W = Weight

Rearrangement of the above equation allows determination of the mass of the analyte in question in an analysed reaction mixture, containing an internal standard:

$$W_x = r_x \times W_{IS} \times \frac{\%\ area_x}{\%\ area_{IS}}$$

A sample of approximately 5 – 10 mg of the analyte in question, and 4 – 6 mg of the internal standard were accurately weighed, in triplicate, and dissolved in an appropriate solvent and run in triplicate on the relevant HPLC method. The value of *r* was calculated from each of the nine chromatographs obtained, and an average value for *r* was then calculated.

Table 30 (Data are shown in Appendix 2.)
The mother liquor and wash samples from entries 2 & 3 in Table 28 were reanalysed to quantify imidazole impurity **104** and diamine **105**. The relevant internal standard (approximately 5 mg, accurately weighed) was dissolved in each liquor or wash sample (1 mL). This solution (50 µL) was added to MeCN (1.5 mL, Method A) or MeCN/buffer solution (1.5 mL, Method B). Samples were analysed on the respective HPLC methods to calculate the mass of each impurity. The mass was converted to a yield based on the amount of 4-FBnCl charged in each experiment.

Figure 31 (Data are shown in Appendix 2.)
CDI (5.8 g, 35.8 mmol), MIBK (60 mL) and biphenyl (1.7727 g, 11.5 mmol) were heated to 70 ± 3 °C, then carboxylic acid **74** (10.0 g, 29.9 mmol) was added portion-wise over 8 min. 4-FBnCl (0.58 mL, 4.84 mmol) was added and the mixture was stirred for 50 min. Amine **77** (14.0 g, 32.8 mmol, 82.1% w/w solution in toluene) was added, and washed in with MIBK (10 mL). The reaction mixture was heated to 92 ± 3 °C then sampled at various times for analysis on HPLC Method B once a solution was obtained. After 120 min the reaction mixture was cooled to room temperature. Methyl *p*-tolyl sulfone (1.0596 g, 6.22 mmol) was added to the reaction mixture, which was resampled for analysis on HPLC Method A. No products were isolated from this experiment.

Figure 32 (Data are shown in Appendix 2.)
CDI (5.8 g, 35.8 mmol), MIBK (60 mL) and methyl *p*-tolyl sulfone (1.9886 g, 11.7 mmol) were heated to 70 ± 3 °C, then carboxylic acid **74** (10.0 g, 29.9 mmol) was added portion-wise over 6 min. 4-FBnCl (0.58 mL, 4.84 mmol) was added and the mixture was stirred, with sampling at various time points on HPLC Method A. After 64 min amine **77** (14.0 g, 32.8 mmol, 82.1% w/w solution in toluene) was added, and washed in with MIBK (10 mL). The batch was heated to 92 ± 3 °C. Samples were taken for HPLC analysis throughout the heat and stir. After 120 min at temperature the reaction mixture was cooled to room temperature. Biphenyl (1.2620 g, 8.18 mmol) was added to the reaction mixture, which was resampled for analysis on HPLC Method B. No products were isolated from this experiment.

Experimental for Section 4.3.2.6: Kinetics Investigations

General Procedure 5: Kinetics Experiments
Imidazole (A), methyl *p*-tolyl sulfone (B) and any additives (C) were dissolved in MIBK (D) and heated to the desired temperature (E). The temperature was allowed to stabilise then 4-FBnCl (F) was added. Samples were then taken at various time points, typically 1, 3, 7, 15, 30, 60, 120 min, and analysed on HPLC Method A. No products were isolated from these experiments.

Data obtained from the kinetics experiments are in Appendix 3.

Table 31 Carried out using General Procedure 5.
Entry 1: A: 7.1 g, 104 mmol; B: 1.0456 g, 6.14 mmol; C: N/A; D: 60 mL; E: 70 °C, F: 8.3 mL, 69.2 mmol.
A gummy solid was observed to form during the experiment. A sample was extracted, put on a filter and washed with MIBK, and then pulled dry under nitrogen (mass not recorded). ^{1}H NMR spectroscopy in d^{6}-DMSO showed the sample to consist predominantly of imidazole hydrochloride salt[123] and bis-alkylated compound **111**. Data for compound **111** were in agreement with that previously reported,[114] with minor differences consistent with changes in pH or sample concentration.

Entry 2: A: 1.39 g, 20.5 mmol; B: 0.2896 g, 1.70 mmol; C: N/A; D: 100 mL; E: 90 °C, F: 1.9722 g, 13.6 mmol.

Entry 3: A: 7.1 g, 104 mmol; B: 0.1484 g, 0.872 mmol; C: N/A; D: 100 mL; E: 90 °C, F: 0.9969 g, 6.90 mmol. Half life for 4-FBnCl calculated as 36.5 min using pseudo first order kinetics assumptions (Table 32).

Entry 4: A: 3.5 g, 51.4 mmol; B: 0.1325 g, 0.778 mmol; C: N/A; D: 100 mL; E: 90 °C, F: 0.9969 g, 6.90 mmol.

Entry 5: A: 0.7032 g, 10.3 mmol; B: 0.163 g, 0.958 mmol; C: N/A; D: 100 mL; E: 90 °C, F: 0.9885 g, 6.84 mmol.

Entry 6: A: 7.1 g, 104 mmol; B: 0.1466 g, 0.861 mmol; C: N/A; D: 100 mL; E: 80 °C, F: 0.9980 g, 6.90 mmol. Half life for 4-FBnCl calculated as 70.7 min using pseudo first order kinetics assumptions (Table 32).

Yield data were plotted for ease of comparison (Figures 33 to 36). The log plot was generated by taking natural logs of the calculated concentration (in $molL^{-1}$) for 4-FBnCl from each data set (Figure 37, see Appendix 3 for data). Data for estimation of the Arrhenius parameters for the reaction of 4-FBnCl with imidazole are provided in Appendix 3.

Figure 38

Data from the experiments in Figures 31 and 32 were used to compile this plot; see Appendix 3.

Table 34 Carried out using General Procedure 5.

Entry 1: A: 7.1 g, 104 mmol; B: 1.5269 g, 8.97 mmol; C: Amine **77** (19.84 g, 46.5 mmol, solution of amine **77** in toluene, 82.1% w/w, concentration determined by quantitative ^{1}H NMR spectroscopy); D: 100 mL; E: 90 °C, F: 0.9916 g, 6.86 mmol. Half life for 4-FBnCl calculated as 17.6 min using pseudo first order kinetics assumptions (Table 35).
Biphenyl (2.003 g, 13.0 mmol) was also added after the methyl *p*-tolyl sulfone for quantification of diamine **105**. HPLC data were also obtained on HPLC Method B.

Entry 2: A: 7.1 g, 104 mmol; B: 0.2111 g, 1.24 mmol; C: DIPEA (8.24 mL, 47.2 mmol); D: 100 mL; E: 90 °C, F:1.0043 g, 6.95 mmol. Half life for 4-FBnCl calculated as 26.7 min using pseudo first order kinetics assumptions (Table 35).

Entry 3: A: 7.1 g, 104 mmol; B: 0.1738 g, 1.02 mmol; C: TEEDA (8.15 g, 47.3 mmol); D: 100 mL; E: 90 °C, F: 1.0055 g, 6.95 mmol. Half life for 4-FBnCl calculated as 22.5 min using pseudo first order kinetics assumptions (Table 35).

Yield data were plotted as before (Figures 40 & 41). The log plot was generated by taking natural logs of the calculated concentration (in $molL^{-1}$) for 4-FBnCl from each data set (Figure 42, see Appendix 3 for data).

Experimental for Section 4.3.2.7: DynoChem® Modelling

Kinetics analysis of the data sets obtained was carried out in DynoChem® software from Performance Fluid Dynamics. The modelling used the "Consecutive side reactions" model template from the DynoChem® library as a starting point. The reaction was assumed to take place entirely within the liquid phase. The reactions defined within the model are shown on page 116. The data shown in Appendix 3 were used for modelling after conversion to molar data for each species.

The data from entry 3 in Table 31 were used to fit k_1. These data were used in conjunction with entry 6 in Table 31 to define E_{a1}. Table 34, entry 1 was used to fit k_3, and a further experiment was carried out at 80 °C (*vide infra*) in order to define E_{a3}. The remaining reaction parameters were assumed or taken from previously obtained data.[120] The parameters used within the model are summarised in Table 43.

Equation	Rate constant *k*	Equilibrium constant *K*	Activation energy E_a / $kJmol^{-1}$
1	3.70×10^{-4} $Lmol^{-1}s^{-1}$ at 90 °C	N/A	78.5
2	1 $m^3mol^{-1}s^{-1}$ at 90 °C	1.00	0
3	6.54×10^{-4} $Lmol^{-1}s^{-1}$ at 90 °C	N/A	49.6
4	1 $m^3mol^{-1}s^{-1}$ at 90 °C	1.00	0
5	1 $m^3mol^{-1}s^{-1}$ at 90 °C	1×10^{-3}	0
6	0.0047 s^{-1} at 92 °C	1.25×10^{-5} $molL^{-1}$	40.1
7	3.89×10^{-2} $Lmol^{-1}s^{-1}$ at 92 °C	N/A	0

Table 43: Reaction parameters used in modelling.

Supplementary Data for Kinetics Model

Carried out using General Procedure 5; data shown in Appendix 3.
A: 7.1 g, 104 mmol; B: 1.5449 g, 9.08 mmol; C: Amine **77*** (16.49 g, 47.0 mmol); D: 100 mL; E: 80 °C, F: 1.0087 g, 6.98 mmol. Biphenyl (1.9130 g, 12.4 mmol) was added after the methyl *p*-tolyl sulfone for quantification of diamine **105**. HPLC data were also obtained on HPLC Method B.
Following a check of the *r* values previously used a number of inaccuracies were noted, therefore *r* was recalculated for 4-FBnCl (1.351), imidazole derivative **104** (2.488) and diamine **105** (1.667) for use in this experiment. The change in *r* values is likely attributable to drift in the HPLC methods over time and a change in instrument for HPLC Method A.

Figure 44 was generated using the same data shown in Figure 38 (see Appendix 3).

Experimental for Section 4.3.2.8: Model Verification

Experiments were carried out using General Procedure 4. All reactants and reagents, including solvents, were charged by mass. Amine **77** was charged neat. Samples of the reaction mixture (30 μL) were taken during the reactive chemistry at various times (see Appendix 3). The mass of each sample was determined and samples were prepared for GC analysis by the extractive method documented above. The GC results were used to determine the mass of 4-FBnCl in each sample and, hence, the mass in the bulk reaction mixture. Samples were taken during both the formation of imidazolide **102** and the coupling reaction. Only the coupling data were used for kinetic model verification as this is the part of the reaction accounting for the majority of the 4-FBnCl reaction.

* Amine **77** was charged neat following concentration *in vacuo* and drying *in vacuo* (50-100 mbar, 50 °C) to remove toluene.

Figure 45

A: 6.92 g, 42.7 mmol; B: 56.39 g; C: 11.59 g, 34.7 mmol; D: 0.8617 g, 5.96 mmol; E: 62 min; F: 13.70 g, 39.0 mmol; G: 11.60 g; H: 115 min; I: 54 mL; J: 30 mL; K: 48 mL; L: 18.19 g, 27.3 mmol, 79%; M: 0.1% w/w. HPLC (Method B) 13.1 min, 99.49% area; 4-FBnCl <1 ppm by GC. ^{1}H NMR data matched that recorded previously.

Note: batch stirred overnight at 2 °C before isolating.

Figure 46

A: 8.78 g, 54.1 mmol; B: 71.07 g; C: 15.10 g, 45.2 mmol (contained 2104 ppm 4-FBnCl);* D: N/A; E: 75 min; F: 17.11 g, 48.7 mmol; G: 9.21 g; H: 103 min; I: 67.5 mL; J: 37.5 mL; K: 60 mL; L: 25.81 g, 38.3 mmol, 85%; M: 1.1% w/w. HPLC (Method B) 13.1 min, 99.74% area; 4-FBnCl <1 ppm by GC. ^{1}H NMR data matched that recorded previously.

Note: batch stirred overnight at 2 °C before isolating.

Figure 47

The log plots were generated using the data obtained from the two verification experiments documented above. See Appendix 3 for data.

* Acid **74** was charged as a single portion to ensure all the 4-FBnCl was charged to the reaction vessel in one go. Considerable frothing from CO_2 generation was observed as a result, which hampered sampling for the early time points.

7 References

1. Lee, S. A.; Robinson, G. E. *Process Development: Fine Chemicals from Grams to Kilograms;* 1st ed.; Oxford University Press Inc.: New York, 1995.
2. Yue, T. Y.; McLeod, D. D.; Albertson, K. B.; Beck, S. R.; Deerberg, J.; Fortunak, J. M.; Nugent, W. A.; Radesca, L. A.; Tang, L.; Xiang, C. D. *Org. Process Res. Dev.* **2006**, *10*, 262-271.
3. Curtius, T. *Ber.* **1890**, *23*, 3023-3033.
4. Scriven, E. F. V.; Turnbull, K. *Chem. Rev.* **1988**, *88*, 297-368.
5. Constable, D. J. C.; Jiminez-Gonzalez, C.; Henderson, R. K. *Org. Process Res. Dev.* **2007**, *11*, 133-137.
6. Alfonsi, K.; Colberg, J.; Dunn, P. J.; Fevig, T.; Jennings, S.; Johnson, T. A.; Kleine, H. P.; Knight, C.; Nagy, M. A.; Perry, D. A.; Stefaniak, M. *Green Chem.* **2008**, *10*, 31-36.
7. Brown Ripin, D. H.; Vetelino, M. *Synlett* **2003**, 2353.
8. Carey, J. S.; Laffan, D.; Thomson, C.; Williams, M. T. *Org. Biomol. Chem.* **2006**, *4*, 2337-2347.
9. Montalbetti, C. A. G. N.; Falque, V. *Tetrahedron* **2005**, *61*, 10827-10852.
10. Valeur, E.; Bradley, M. *Chem. Soc. Rev.* **2009**, *38*, 606-631.
11. Dunn, P. J.; Hoffmann, W.; Kang, Y.; Mitchell, J. C.; Snowden, M. J. *Org. Process Res. Dev.* **2005**, *9*, 956-961.
12. Carlson, R.; Carlson, J. E. *Design and Optimization in Organic Synthesis: Second revised and enlarged edition;* 1st ed.; Elsevier: Amsterdam, 2005.
13. Owen, M. R.; Luscombe, C.; Lai, L.-W.; Godbert, S.; Crookes, D. L.; Emiabata-Smith, D. *Org. Process Res. Dev.* **2001**, *5*, 308-323.
14. Barrios Sosa, A. C.; Williamson, R. T.; Conway, R.; Shankar, A.; Sumpter, R.; Cleary, T. *Org. Process Res. Dev.* **2011**, *15*, 449-454.
15. Hanrahan, G.; Lu, K. *Crit. Rev. Anal. Chem.* **2006**, *36*, 141-151.
16. Aggarwal, V. K.; Staubitz, A. C.; Owen, M. *Org. Process Res. Dev.* **2006**, *10*, 64-69.

17. *http://www.ich.org/products/guidelines/quality/article/quality-guidelines* ICHQ3A(R2): Impurities in New Drug Substances, **2006**. Date accessed: 28 June, 2012.
18. Wong, B. R.; Grossbard, E. B.; Payan, D. G.; Masuda, E. S. *Expert Opin. Invest. Drugs* **2004**, *13*, 743-762.
19. Taniguchi, T.; Kobayashi, T.; Kondo, J.; Takahashi, K.; Nakamura, H.; Suzuki, J.; Nagai, K.; Yamada, T.; Nakamura, S.; Yamamura, H. *J. Biol. Chem.* **1991**, *266*, 15790-15796.
20. Bajpai, M.; Chopra, P.; Dastidar, S. G.; Ray, A. *Expert Opin. Invest. Drugs* **2008**, *17*, 641-659.
21. Rhen, T.; Cidlowski, J. A. *N. Engl. J. Med.* **2005**, *353*, 1711-1723.
22. Ruzza, P.; Biondi, B.; Calderan, A. *Expert Opin. Ther. Pat.* **2009**, *19*, 1361-1376.
23. Malik, R.; Roy, I. *Expert Opin. Drug Discovery* **2008**, *3*, 1189-1207.
24. Singh, R.; Argade, A.; Payan, D. 2,4-Pyrimidinediamines compounds and their uses. PCT Int. Appl. WO 2003063794, 2003.
25. Masuda, E. S.; Schmitz, J. *Pulm. Pharmacol. Ther.* **2008**, *21*, 461-467.
26. Singh, R.; Bhamidipati, S.; Masuda, E. Prodrugs of 2,4-pyrimidinediamine compounds and their uses. PCT Int. Appl. WO 2006078846, 2006.
27. Rajinder, S.; Ankush, A.; Li, H.; Bhamidipati, S.; Carroll, D.; Sylvain, C.; Clough, J.; Keim, H. 2,4-Pyrimidinediamines for use in the treatment or prevention of autoimmune diseases. PCT Int. Appl. WO 2005012294, 2005.
28. Taylor, S. C. J. Salt form. PCT Int. Appl. WO 2009031011, 2009.
29. Lai, J. Y. Q.; Cox, P. J.; Patel, R.; Sadiq, S.; Aldous, D. J.; Thurairatnam, S.; Smith, K.; Wheeler, D.; Jagpal, S.; Parveen, S.; Fenton, G.; Harrison, T. K. P.; McCarthy, C.; Bamborough, P. *Bioorg. Med. Chem. Lett.* **2003**, *13*, 3111-3114.
30. Cywin, C. L.; Zhao, B. P.; McNeil, D. W.; Hrapchak, M.; Prokopowicz, A. S.; Goldberg, D. R.; Morwick, T. M.; Gao, A.; Jakes, S.; Kashem, M.; Magolda, R. L.; Soll, R. M.; Player, M. R.; Bobko, M. A.; Rinker, J.; DesJarlais, R. L.; Winters, M. P. *Bioorg. Med. Chem. Lett.* **2003**, *13*, 1415-1418.

31. Hirabayashi, A.; Mukaiyama, H.; Kobayashi, H.; Shiohara, H.; Nakayama, S.; Ozawa, M.; Miyazawa, K.; Misawa, K.; Ohnota, H.; Isaji, M. *Bioorg. Med. Chem.* **2008**, *16*, 7347-7357.
32. Atkinson, F. L.; Barker, M. D.; Campos, S. A.; Harrison, L. A.; Parr, N. J.; Patel, V. K. 6-Indolyl-4-yl-amino-5-halogeno-2-pyrimidinyl-amino derivatives. PCT Int. Appl. WO 2007028445, 2007.
33. Atkinson, F. L.; Barker, M. D.; Campos, S. A.; Parr, N. J.; Patel, V. K. Novel Compounds. PCT Int. Appl. WO 2006129100, 2006.
34. Atkinson, F. L.; Campos, S. A.; Harrison, L. A.; Parr, N. J.; Patel, V. K.; Vitulli, G. 1*H*-Indazoyl-4-yl-2,4-pyrimidinediamine derivatives. PCT Int. Appl. WO 2007085540, 2007.
35. Campos, S. A.; Harrison, L. A.; Parr, N. J.; Patel, V. K.; Vitulli, G. 1,1-Dioxido-2,3-dihydro-1,2-benzisothiazol-6-yl-1*H*-indazol-4-yl-2,4-pyrimidinediamine derivatives. PCT Int. Appl. WO 2007009681, 2007.
36. Ancliff, R. A.; Atkinson, F. L.; Barker, M. D.; Box, P. C.; Daniel, C.; Gore, P. M.; Guntrip, S. B.; Hasegawa, M.; Inglis, G. G. A.; Kano, K.; Miyazaki, Y.; Patel, V. K. Pyrrolopyrimidine derivatives as Syk inhibitors. PCT Int. Appl. WO 2007042299, 2007.
37. Gore, P. M.; Patel, V. K.; Walker, A. L.; Woodrow, M. Pyrrolopyrimidine derivatives as Syk inhibitors. PCT Int. Appl. WO 2007042298, 2007.
38. Atkinson, F. L.; Patel, V. K. Pyrimidinecarboxamide derivatives as inhibitors of Syk kinase. PCT Int. Appl. WO 2010097248, 2010.
39. Atkinson, F. L.; Barker, M. D.; Douault, C.; Garton, N. S.; Liddle, J.; Patel, V. K.; Preston, A. G. S.; Wilson, D. M. 7-(1*H*-Pyrazol-4-yl)-1,6-naphthyridine compounds as Syk inhibitors. PCT Int. Appl. WO 2011134971, 2011.
40. Suzuki, T.; Goto, T.; Hamashima, Y.; Sodeoka, M. *J. Org. Chem.* **2007**, *72*, 246-250.
41. Atkins, W. J. J.; Burkhardt, E. R.; Matos, K. *Org. Process Res. Dev.* **2006**, *10*, 1292-1295.
42. Hassner, A.; Stern, M. *Angew. Chem. Int. Ed. Engl.* **1986**, *25*, 478-479.
43. Kotha, S.; Lahiri, K.; Kashinath, D. *Tetrahedron* **2002**, *58*, 9633-9695.

44. Miyaura, N.; Yanagi, T.; Suzuki, A. *Synth. Commun.* **1981**, *11*, 513-519.
45. Leach, S. G. Unpublished Work, 2010.
46. Curtis, N. R.; Leach, S. G. Unpublished Work, 2010.
47. Curtis, N. R. Unpublished Work, 2010.
48. Corey, E. J.; Nicolaou, K. C.; Balanson, R. D.; Machida, Y. *Synthesis* **1975**, 590-591.
49. Boyer, J. H. *J. Am. Chem. Soc.* **1951**, *73*, 5865-5866.
50. Staudinger, H.; Hauser, E. *Helv. Chim. Acta* **1921**, *4*, 861-886.
51. Chen, C.; Frey, L. F.; Shultz, S.; Wallace, D. J.; Marcantonio, K.; Payack, J. F.; Vazquez, E.; Springfield, S. A.; Zhou, G.; Liu, P.; Kieczykowski, G. R.; Chen, A. M.; Phenix, B. D.; Singh, U.; Strine, J.; Izzo, B.; Krska, S. W. *Org. Process Res. Dev.* **2007**, *11*, 616-623.
52. Gartiser, T.; Selve, C.; Delpuech, J. J. *Tetrahedron Lett.* **1983**, *24*, 1609-1610.
53. Watson, R. Unpublished Work, 2010.
54. An, I. H.; Seong, H. R.; Ahn, K. H. *Bull. Korean Chem. Soc.* **2004**, *25*, 420-422.
55. Gomez, S.; Peters, J. A.; Maschmeyer, T. *Adv. Synth. Catal.* **2002**, *344*, 1037-1057.
56. Lange, M.; Pettersen, A. L.; Undheim, K. *Tetrahedron* **1998**, *54*, 5745-5752.
57. Hartung, W. H. *J. Am. Chem. Soc.* **1928**, *50*, 3370-3374.
58. Klenke, B.; Gilbert, I. H. *J. Org. Chem.* **2001**, *66*, 2480-2483.
59. Filira, F.; Biondi, L.; Gobbo, M.; Rocchi, R. *Tetrahedron Lett.* **1991**, *32*, 7463-7464.
60. Schwoegler, E. J.; Adkins, H. *J. Am. Chem. Soc.* **1939**, *61*, 3499-3502.
61. Keresszegi, C.; Buergi, T.; Mallat, T.; Baiker, A. *J. Catal.* **2002**, *211*, 244-251.
62. Curtis, N. R. Unpublished Work, 2011.
63. McKie, R. A. Unpublished Work, 2011.
64. Curtis, N. R.; Gray, M.; Vernon, L. E.; Walkington, A. J. Unpublished Work, 2011.

65. Roger, V. L.; Go, A. S.; Lloyd-Jones, D. M.; Benjamin, E. J.; Berry, J. D.; Borden, W. B.; Bravata, D. M.; Dai, S.; Ford, E. S.; Fox, C. S.; Fullerton, H. J.; Gillespie, C.; Hailpern, S. M.; Heit, J. A.; Howard, V. J.; Kissela, B. M.; Kittner, S. J.; Lackland, D. T.; Lichtman, J. H.; Lisabeth, L. D.; Makuc, D. M.; Marcus, G. M.; Marelli, A.; Matchar, D. B.; Moy, C. S.; Mozaffarian, D.; Mussolino, M. E.; Nichol, G.; Paynter, N. P.; Soliman, E. Z.; Sorlie, P. D.; Sotoodehnia, N.; Turan, T. N.; Virani, S. S.; Wong, N. D.; Woo, D.; Turner, M. B. *Circulation* **2012**, *125*, 188-197.
66. Macphee, C. H. *Curr. Opin. Pharmacol.* **2001**, *1*, 121-125.
67. Zalewski, A.; Macphee, C. *Arterioscler., Thromb., Vasc. Biol.* **2005**, *25*, 923-931.
68. Farnier, M.; Davignon, J. *Am. J. Cardiol.* **1998**, *82*, 3J-10J.
69. Nissen, S. E.; Nicholls, S. J.; Sipahi, I.; Libby, P.; Raichlen, J. S.; Ballantyne, C. M.; Davignon, J.; Erbel, R.; Fruchart, J. C.; Tardif, J. C.; Schoenhagen, P.; Crowe, T.; Cain, V.; Wolski, K.; Goormastic, M.; Tuzcu, E. M. *J. Am. Med. Assoc.* **2006**, *295*, 1556-1565.
70. *http://www.drugs.com/top200.html* Top 200 drugs, **2010**. Date accessed: 28 June, 2012.
71. Macphee, C. H.; Tew, D. G.; Southan, C. D.; Hickey, D. M. B.; Gloger, I. S.; Lawrence, G. M. P.; Rice, S. Q. J. Lipoprotein associated phospholipase A_2, inhibitors thereof and use of the same in diagnosis and therapy. PCT Int. Appl. WO 9500649, 1995.
72. Tew, D. G.; Southan, C.; Rice, S. Q. J.; Lawrence, G. M.; Li, H.; Boyd, H. F.; Moores, K.; Gloger, I. S.; Macphee, C. H. *Arterioscler., Thromb., Vasc. Biol.* **1996**, *16*, 591-599.
73. Zalewski, A.; Nelson, J. J.; Hegg, L.; Macphee, C. *Clin. Chem.* **2006**, *52*, 1645-1650.
74. Packard, C. J.; O'Reilly, D. S. J.; Caslake, M. J.; McMahon, A. D.; Ford, I.; Cooney, J.; Macphee, C. H.; Suckling, K. E.; Krishna, M.; Wilkinson, F. E.; Rumley, A.; Lowe, G. D. O.; Docherty, G.; Burczak, J. D. *N. Engl. J. Med.* **2000**, *343*, 1148-1155.

75. Tew, D. G.; Boyd, H. F.; Ashman, S.; Theobald, C.; Leach, C. A. *Biochemistry* **1998**, *37*, 10087-10093.
76. Macphee, C. H.; Moores, K. E.; Boyd, H. F.; Dhanak, D.; Ife, R. J.; Leach, C. A.; Leake, D. S.; Milliner, K. J.; Patterson, R. A.; Suckling, K. E.; Tew, D. G.; Hickey, D. M. B. *Biochem. J.* **1999**, *338*, 479-487.
77. Tew, D. G.; Hickey, D. M. B. Clavulanic acid derivatives for treating atherosclerosis. PCT Int. Appl. WO 9710247, 1997.
78. Pinto, I. L.; Boyd, H. F.; Hickey, D. M. B. *Bioorg. Med. Chem. Lett.* **2000**, *10*, 2015-2017.
79. Boyd, H. F.; Flynn, S. T.; Hickey, D. M. B.; Ife, R. J.; Jones, M.; Leach, C. A.; Macphee, C. H.; Milliner, K. J.; Rawlings, D. A.; Slingsby, B. P.; Smith, S. A.; Stansfield, I. G.; Tew, D. G.; Theobald, C. J. *Bioorg. Med. Chem. Lett.* **2000**, *10*, 395-398.
80. Hickey, D. M. B.; Ife, R. J.; Leach, C. A.; Pinto, I. L.; Porter, R. A.; Smith, S. A. Pyrimidone compounds and pharmaceutical compositions containing them. PCT Int. Appl. WO 9924420, 1999.
81. Boyd, H. F.; Fell, S. C. M.; Flynn, S. T.; Hickey, D. M. B.; Ife, R. J.; Leach, C. A.; Macphee, C. H.; Milliner, K. J.; Moores, K. E.; Pinto, I. L.; Porter, R. A.; Rawlings, D. A.; Smith, S. A.; Stansfield, I. G.; Tew, D. G.; Theobald, C. J.; Whittaker, C. M. *Bioorg. Med. Chem. Lett.* **2000**, *10*, 2557-2561.
82. Boyd, H. F.; Hammond, B.; Hickey, D. M. B.; Ife, R. J.; Leach, C. A.; Lewis, V. A.; Macphee, C. H.; Milliner, K. J.; Pinto, I. L.; Smith, S. A.; Stansfield, I. G.; Theobald, C. J.; Whittaker, C. M. *Bioorg. Med. Chem. Lett.* **2001**, *11*, 701-704.
83. Leach, C. A.; Smith, S. A. Pyrimidinone derivatives for the treatment of atherosclerosis. PCT Int. Appl. WO 2000010980, 2000.
84. Bloomer, J. C.; Boyd, H. F.; Hickey, D. M. B.; Ife, R. J.; Leach, C. A.; Macphee, C. H.; Milliner, K. J.; Pinto, I. L.; Rawlings, D. A.; Smith, S. A.; Stansfield, I. G.; Stanway, S. J.; Taylor, M. A.; Theobald, C. J.; Whittaker, C. M. *Bioorg. Med. Chem. Lett.* **2001**, *11*, 1925-1929.
85. Hickey, D. M. B.; Ife, R. J.; Leach, C. A.; Smith, S. A. Pyrimidine compounds. PCT Int. Appl. WO 2000066566, 2000.

86. Boyd, H. F.; Fell, S. C. M.; Hickey, D. M. B.; Ife, R. J.; Leach, C. A.; Macphee, C. H.; Milliner, K. J.; Pinto, I. L.; Rawlings, D. A.; Smith, S. A.; Stansfield, I. G.; Stanway, S. J.; Theobald, C. J.; Whittaker, C. M. *Bioorg. Med. Chem. Lett.* **2002**, *12*, 51-55.
87. Fenwick, A. E.; Hickey, D. M. B.; Ife, R. J.; Leach, C. A.; Pinto, I. L.; Smith, S. A. Pyrimidinone compounds. PCT Int. Appl. WO 2000066567, 2000.
88. Blackie, J. A.; Bloomer, J. C.; Brown, M. J. B.; Cheng, H. Y.; Elliott, R. L.; Hammond, B.; Hickey, D. M. B.; Ife, R. J.; Leach, C. A.; Lewis, V. A.; Macphee, C. H.; Milliner, K. J.; Moores, K. E.; Pinto, I. L.; Smith, S. A.; Stansfield, I. G.; Stanway, S. J.; Taylor, M. A.; Theobald, C. J.; Whittaker, C. M. *Bioorg. Med. Chem. Lett.* **2002**, *12*, 2603-2606.
89. Blackie, J. A.; Bloomer, J. C.; Brown, M. J. B.; Cheng, H. Y.; Hammond, B.; Hickey, D. M. B.; Ife, R. J.; Leach, C. A.; Lewis, V. A.; Macphee, C. H.; Milliner, K. J.; Moores, K. E.; Pinto, I. L.; Smith, S. A.; Stansfield, I. G.; Stanway, S. J.; Taylor, M. A.; Theobald, C. J. *Bioorg. Med. Chem. Lett.* **2003**, *13*, 1067-1070.
90. Hickey, D. M. B.; Ife, R. J.; Leach, C. A.; Pinto, I. L.; Smith, S. A.; Stanway, S. J. Pyrimidine-4-one derivatives as LDL-PLA_2 inhibitors. PCT Int. Appl. WO 2001060805, 2001.
91. Ross, L. O.; Goodman, L.; Baker, B. R. *J. Am. Chem. Soc.* **1959**, *81*, 3108-3114.
92. Oxford Asymmetry International plc, Unpublished Work, 2000.
93. Mulholland, K. R.; Ross, A. R.; Slater, G. R.; Smith, G. E. Novel processes. PCT Int. Appl. WO 2003016287, 2003.
94. Bruynes, C. A.; Jurriens, T. K. *J. Org. Chem.* **1982**, *47*, 3966-3969.
95. GSK Tonbridge Pilot Plant, Unpublished Work, 2002.
96. Mountain, C. E. Information from GSK internal memo, Unpublished Work, 2002.
97. Albinson, F. D.; Allworth, K. L.; Faruk, E.; Mountain, C. E.; Shapland, P.; Smith, D.; Tray, D. R.; Wooster, N. F. Unpublished Work, 2003.
98. Felpin, F. X.; Ayad, T.; Mitra, S. *Eur. J. Org. Chem.* **2006**, 2679-2690.
99. Albinson, F. D.; Davies, S. H. Unpublished Work, 2009.

100. Crawford, C. F.; Lloyd, S.; Ng, S.; Wade, C. E. Unpublished Work, 2009.
101. Cardwell, K. S.; Crawford, C. F.; Davies, S. H.; Wade, C. E. Novel Processes. PCT Int. Appl. WO 2011146494, 2011.
102. Therkelsen, F. D.; Hansen, A.-L. L.; Pedersen, E. B.; Nielsen, C. *Org. Biomol. Chem.* **2003**, *1*, 2908-2918.
103. Crawford, C. F.; McKie, R. A.; Mountain, C. E. Unpublished Work, 2010.
104. Harling, S. J. Unpublished Work, 2012.
105. GSK Cork Pilot Plant, Unpublished Work, 2010.
106. Davies, S. H. Unpublished Work, 2010.
107. Tray, D. R. Unpublished Work, 2010.
108. GSK Jurong Pilot Plant, Unpublished Work, 2010.
109. Davies, S. H. Unpublished Work, 2009.
110. Chow, S. S.; See Toh, Y. H. Unpublished Work, 2010.
111. See Toh, Y. H. Unpublished Work, 2010.
112. Owen, C. P.; Dhanani, S.; Patel, C. H.; Shahid, I.; Ahmed, S. *Bioorg. Med. Chem. Lett.* **2006**, *16*, 4011-4015.
113. Roumen, L.; Peeters, J. W.; Emmen, J. M. A.; Beugels, I. P. E.; Custers, E. M. G.; de Gooyer, M.; Plate, R.; Pieterse, K.; Hilbers, P. A. J.; Smits, J. F. M.; Vekemans, J. A. J.; Leysen, D.; Ottenheijm, H. C. J.; Janssen, H. M.; Hermans, J. J. R. *J. Med. Chem.* **2010**, *53*, 1712-1725.
114. Vlahakis, J. Z.; Lazar, C.; Crandall, I. E.; Szarek, W. A. *Bioorg. Med. Chem.* **2010**, *18*, 6184-6196.
115. Atkins, P. W. *The Elements of Physical Chemistry;* 2nd ed.; Oxford University Press: Oxford, UK, 1996.
116. Fujii, T.; Nishida, H.; Abiru, Y.; Yamamoto, M.; Kise, M. *Chem. Pharm. Bull.* **1995**, *43*, 1872-1877.
117. Gero, A. *J. Am. Chem. Soc.* **1954**, *76*, 5158-5159.
118. Sari, H.; Covington, A. K. *J. Chem. Eng. Data* **2005**, *50*, 1425-1429.
119. Frenna, V.; Vivona, N.; Consiglio, G.; Spinelli, D. *J. Chem. Soc., Perkin Trans. 2* **1985**, 1865-1868.
120. Davies, S. H.; Freiria, M.; Ng, L.-S.; Oliveira, T. Unpublished Work, 2006.
121. Taylor, E. C.; McKillop, A.; Hawks, G. H. *Org. Synth.* **1972**, *52*, 36.

122. Zhang, L.; Wang, X.; Wang, J.; Grinberg, N.; Krishnamurthy, D.; Senanayake, C. H. *Tetrahedron Lett.* **2009**, *50*, 2964-2966.

123. Laus, G.; Stadlwieser, J.; Klötzer, W. *Synthesis* **1989**, 773-775.

Appendices

Appendix 1: Preparation of Carboxylic Acid 74 at Scale

Cork Pilot Plant Campaign 1[105]

Thiouracil **95** (1.0 equiv.) was stirred in water (5.4 vol) and IPA (1 vol). Concentrated aqueous KOH (1.90 equiv.) was added followed by a water line wash (0.5 vol) and the solid dissolved. K_2CO_3 (0.15 equiv.) was charged and the mixture was then heated to 40 °C. 4-FBnCl (0.95 equiv.) was added followed by IPA (0.6 vol, line wash). After at least 2.5 h complete reaction was confirmed by HPLC (Method C). The level of 4-FBnCl was also checked by GC. The batch was cooled to 20 °C and formic acid (0.5 equiv.) was charged. After stirring for 30 min (during which time the batch crystallised) a second formic acid charge (1.7 equiv.) was added over 45-60 min. After at least 1 h the solid was isolated by filtration and washed twice with 4:1 water/IPA (2 x 2 vol), then with IPA (2 vol) and dried under reduced pressure at 50 °C. Four batches were prepared using 32 kg input of thiouracil **95** per batch. The average yield was 90.7%. The 4-FBnCl content in the isolated material was determined using GC as 209 ppm for batch 1, with the remaining three batches all <20 ppm.

Cork Pilot Plant Campaign 2a[105]

Procedure as for Campaign 1 with the following changes:
Concentrated aqueous NaOH (1.90 equiv.), Na_2CO_3 (0.25 equiv.), 4-FBnCl (0.98 equiv.) and first formic acid charge (0.6 equiv.). GC was not used for reaction monitoring. Four batches were prepared using 52.5 kg input of thiouracil **95** per batch. The average yield was 91.7%. The 4-FBnCl content in the isolated material was determined using GC as <15 ppm for all batches.

Cork Pilot Plant Campaign 2b[105]

Procedure as for Campaign 1 with the following changes:
Concentrated aqueous NaOH (1.99 equiv.), Na_2CO_3 (0.16 equiv.), 4-FBnCl (1.05 equiv.) and first formic acid charge (0.6 equiv.). GC was not used for reaction monitoring. Two batches were prepared using 52.5 kg input of thiouracil **95** per

batch. The average yield was 95.8%. The 4-FBnCl content in the isolated material was determined using GC as 226 ppm for batch 1 and 290 ppm for batch 2.

Appendix 2: Quantification of Impurities

Table 30: Entry 1 (Table 28, entry 2).

Sample	Methyl *p*-tolyl sulfone / % area[a]	104 / % area[a]	Mass 104 / g	104/ % yield	Biphenyl / % area[b]	105 / % area[b]	Mass 105 / g	105 / % yield
Liquors	9.316	7.426	1.778	69.5	9.893	3.291	0.464	10.4
Wash 1	26.087	5.334	0.425	16.6	24.281	2.372	0.094	2.1
Wash 2	71.648	0.951	0.017	0.7	77.05	0.314	0.004	0.1

[a] HPLC Method A.

[b] HPLC Method B.

Table 30: Entry 2 (Table 28, entry 3).

Sample	Methyl *p*-tolyl sulfone / % area[a]	104 / % area[a]	Mass 104 / g	104/ % yield	Biphenyl / % area[b]	105 / % area[b]	Mass 105 / g	105 / % yield
Liquors	8.562	9.135	1.266	74.2	11.571	5.309	0.402	9.0
Wash 1	22.245	3.071	0.263	15.4	27.083	1.629	0.085	1.9
Wash 2	71.877	1.588	0.026	1.5	69.662	0.84	0.007	0.2

[a] HPLC Method A.

[b] HPLC Method B.

Figure 31: Data taken from HPLC Method B.

Time / min	Temp / °C	Biphenyl / % area	Diamine 105 / % area	Diamine 105 / g	Diamine 105 / % yield
0	88	11.59	0.69	0.19	8.75
5	91	11.54	0.82	0.23	10.39
10	91	11.61	0.88	0.25	11.11
20	90.5	11.38	0.93	0.27	12.04
40	91	11.54	0.98	0.28	12.49
80	91.5	11.61	1.00	0.28	12.72
120	92	11.71	1.00	0.28	12.60

Quantification of imidazole derivative **104** showed 87.6% yield.

Total 4-FBnCl yield was 100.2% by reaction to imidazole **104** and amine **105**.

Figure 32: Data taken from HPLC Method A.

Time (total) / min	**Time (Coupling) / min**	**Methyl *p*-tolyl sulfone / % area**	**Imidazole derivative 104 / % area**	**4-FBnCl / % area**	**Imidazole derivative 104 / g**	**4-FBnCl / g**	**Imidazole derivative 104/ % yield**	**4-FBnCl / % yield**
2	-	22.52	0	5.21	0	0.68	0	97.56
5	-	22.65	0	5.26	0	0.69	0	97.90
10	-	28.52	0.26	6.18	0.06	0.64	6.83	91.37
20	-	27.21	0.39	5.71	0.09	0.62	10.60	88.56
30	-	26.72	0.51	5.56	0.12	0.61	14.31	87.78
63	-	29.44	1.01	5.17	0.22	0.52	25.65	74.10
74	-	17.16	0.68	-	0.25	-	29.60	-
80	0	14.42	0.72	-	0.32	-	37.33	-
85	5	14.03	0.84	-	0.38	-	44.77	-
90	10	13.98	0.97	-	0.44	-	51.66	-
101	21	13.83	1.19	-	0.55	-	64.15	-
120	40	13.66	1.38	-	0.64	-	75.49	-
160	80	13.48	1.54	-	0.73	-	85.16	-
200	120	13.62	1.61	-	0.75	-	88.04	-

At t = 64 min amine **77** was charged. Due to the formation of darapladib 4-FBnCl could no longer be quantified. At t = 80 min a solution was obtained, and this was defined as t = 0 for the coupling reaction.

Quantification of amine **105** showed 11.8% yield.

Total 4-FBnCl yield was 99.8% by reaction to imidazole **104** and amine **105**.

Appendix 3: Tabulated Kinetics Data

Masses of analytes were determined as described in the experimental section using the calculated *r* values.

Table 31: entry 1, HPLC Method A.

Time / min	Methyl *p*-tolyl sulfone / % area	4-FBnCl / % area	Imidazole derivative 104 / % area	4-FBnCl / g	Imidazole derivative 104 / g	4-FBnCl / % yield	Imidazole derivative 104 / % yield
0	100	0	0	0	0	0	0
1	13.20	86.17	0.63	10.13	0.16	101.34	1.32
3	13.54	84.68	1.79	9.71	0.44	97.10	3.64
7	13.61	82.39	4.00	9.40	0.98	93.96	8.07
15	14.35	76.85	8.36	8.31	1.95	83.11	16.02
30	14.90	69.65	14.27	7.26	3.21	72.58	26.34
60	16.00	59.87	22.18	5.81	4.65	58.09	38.12
120	19.87	47.96	30.10	3.75	5.07	37.46	41.64
240	24.95	30.41	40.48	1.89	5.44	18.92	44.60
420	32.99	16.66	47.07	0.78	4.78	7.84	39.22
1380	39.03	0.00	56.96	0	4.89	0	40.12

Table 31: entry 2, HPLC Method A.

Time / min	Methyl *p*-tolyl sulfone / % area	4-FBnCl / % area	Imidazole derivative 104 / % area	4-FBnCl / g	Imidazole derivative 104 / g	4-FBnCl / % yield	Imidazole derivative 104 / % yield
0	91.00	0	0	0	0	0	0
1	17.89	80.28	0.13	1.93	0.01	97.79	0.27
3	17.56	80.43	0.32	1.97	0.02	99.84	0.70
7	18.11	79.44	0.70	1.89	0.04	95.61	1.49
15	18.04	78.61	1.49	1.87	0.08	94.99	3.19
31	18.02	76.80	3.08	1.83	0.16	92.92	6.61
60	18.17	74.00	5.50	1.75	0.28	88.79	11.70
122	18.51	67.64	9.95	1.57	0.50	79.63	20.76
240	20.11	58.15	16.35	1.24	0.75	63.02	31.38
1140	27.55	29.64	35.21	0.46	1.19	23.45	49.33

Table 31: entry 3, HPLC Method A.

Time / min	Methyl *p*-tolyl sulfone / % area	4-FBnCl / % area	Imidazole derivative 104 / % area	4-FBnCl / g	Imidazole derivative 104 / g	4-FBnCl / % yield	Imidazole derivative 104 / % yield
0	80.345	0	0	0	0	0	0
1	17.89	76.41	1.27	0.94	0.03	94.37	2.79
3	18.19	74.30	3.13	0.90	0.08	90.25	6.73
7	18.81	69.49	7.08	0.81	0.18	81.61	14.72
15	19.43	61.41	14.25	0.70	0.35	69.85	28.71
30	21.00	47.84	25.85	0.50	0.59	50.34	48.16
60	23.10	28.43	42.27	0.27	0.87	27.20	71.62
120	25.24	9.67	57.88	0.08	1.09	8.46	89.74
240	26.18	1.20	64.83	0.01	1.18	1.01	96.92
390	26.03	0.00	66.15	0	1.21	0	99.48

Table 31: entry 3, data for log plot (Figure 37).

Time / min	4-FBnCl / mol	Concentration 4-FBnCl / mol L^{-1}	ln[4-FBnCl]
0	0	0	
1	0.006507	0.065067	-2.732334
3	0.006223	0.062228	-2.776949
7	0.005627	0.056269	-2.87761
15	0.004816	0.048160	-3.033224
30	0.003471	0.034710	-3.360717
60	0.001875	0.018753	-3.976394
120	0.000583	0.005834	-5.144014
240	6.99E-05	0.000699	-7.265808
390	0	0	

Half life calculated as 36.5 min.

Table 31: entry 4, HPLC Method A.

Time / min	Methyl *p*-tolyl sulfone / % area	4-FBnCl / % area	Imidazole derivative 104 / % area	4-FBnCl / g	Imidazole derivative 104 / g	4-FBnCl / % yield	Imidazole derivative 104 / % yield
0	93.17	0	0	0	0	0	0
1	17.41	80.83	0.50	0.91	0.01	91.53	1.00
3	17.30	80.11	1.27	0.91	0.03	91.27	2.56
7	17.51	78.36	2.78	0.88	0.07	88.23	5.55
15	17.67	75.16	5.80	0.84	0.14	83.85	11.46
30	18.62	68.20	11.52	0.72	0.26	72.22	21.61
60	19.72	56.59	21.66	0.56	0.47	56.58	38.36
120	21.79	37.78	37.69	0.34	0.73	34.18	60.37
240	24.60	16.45	55.27	0.13	0.95	13.18	78.44
390	26.05	5.73	64.02	0.04	1.04	4.34	85.80
1320	26.64	0	68.83	0	1.10	0	90.20

Table 31: entry 4, data for log plot (Figure 37).

Time / min	4-FBnCl / mol	Concentration 4-FBnCl / mol L^{-1}	ln[4-FBnCl]
0	0	0	
1	0.006316	0.063164	-2.762022
3	0.006298	0.062981	-2.764927
7	0.006088	0.060885	-2.798774
15	0.005786	0.057863	-2.849684
30	0.004984	0.049835	-2.999030
60	0.003905	0.039047	-3.242978
120	0.002358	0.023584	-3.747197
240	0.000910	0.009096	-4.699910
390	0.000299	0.002993	-5.811517
1320	0	0	

Table 31: entry 5, HPLC Method A.

Time / min	Methyl *p*-tolyl sulfone / % area	4-FBnCl / % area	Imidazole derivative 104 / % area	4-FBnCl / g	Imidazole derivative 104 / g	4-FBnCl / % yield	Imidazole derivative 104 / % yield
0	81.25	0	0	0	0	0	0
1	19.46	75.98	0	0.94	0	95.56	0.00
3	19.43	76.03	0.12	0.95	0	95.77	0.27
7	19.53	75.77	0.27	0.94	0.01	94.95	0.60
15	19.54	75.34	0.59	0.93	0.02	94.36	1.30
30	19.24	74.70	1.16	0.94	0.03	95.01	2.60
60	19.55	72.97	2.21	0.90	0.06	91.36	4.90
120	19.56	70.09	4.11	0.87	0.11	87.70	9.12
240	19.87	65.29	7.28	0.79	0.19	80.42	15.88
480	20.34	57.59	11.98	0.68	0.31	69.28	25.53
1380	22.96	38.80	22.78	0.41	0.52	41.36	43.01

Table 31: entry 5, data for log plot (Figure 37).

Time / min	4-FBnCl / mol	Concentration 4-FBnCl / mol L^{-1}	ln[4-FBnCl]
0	0	0	
1	0.006534	0.065336	-2.728210
3	0.006548	0.065480	-2.726009
7	0.006492	0.064915	-2.734670
15	0.006451	0.064515	-2.740860
30	0.006496	0.064959	-2.734000
60	0.006246	0.062465	-2.773156
120	0.005996	0.059960	-2.814081
240	0.005498	0.054982	-2.900749
480	0.004737	0.047370	-3.049770
1380	0.002828	0.028279	-3.565642

Table 31: entry 6, HPLC Method A.

Time / min	Methyl *p*-tolyl sulfone / % area	4-FBnCl / % area	Imidazole derivative 104 / % area	4-FBnCl / g	Imidazole derivative 104 / g	4-FBnCl / % yield	Imidazole derivative 104 / % yield
0	94.38	0	0	0	0	0	0
1	18.09	80.28	0.58	0.97	0.02	96.76	1.24
3	18.23	79.17	1.51	0.94	0.04	94.68	3.21
7	18.36	77.22	3.32	0.92	0.09	91.72	6.99
15	18.87	73.15	6.87	0.84	0.17	84.53	14.06
30	19.54	65.27	13.70	0.73	0.33	72.83	27.08
60	21.18	51.37	25.62	0.53	0.57	52.89	46.72
120	23.48	30.30	43.66	0.28	0.87	28.13	71.81
240	25.59	9.59	60.73	0.08	1.11	8.17	91.65
390	26.62	2.73	66.73	0.02	1.18	2.23	96.81
1290	27.00	0	69.02	0	1.20	0	98.71

Table 31: entry 6, data for log plot (Figure 37).

Time / min	4-FBnCl / mol	Concentration 4-FBnCl / mol L^{-1}	ln[4-FBnCl]
0	0	0	
1	0.006679	0.066790	-2.706205
3	0.006535	0.065354	-2.727942
7	0.006331	0.063309	-2.759730
15	0.005835	0.058347	-2.841345
30	0.005027	0.050274	-2.990270
60	0.003651	0.036506	-3.310268
120	0.001942	0.019421	-3.941410
240	0.000564	0.005641	-5.177661
390	0.000154	0.001542	-6.474821
1290	0	0	

Half life calculated as 70.7 min.

Table 32: Half lives and calculation of Arrhenius parameters.

Experiment	Temperature T / K	Pseudo first order rate constant *k*' / min^{-1}	$t_{½}$ / min	ln(*k*' / min^{-1})	1/ T / K^{-1}
Table 31, entry 3	363	0.019	36.5	-3.96332	0.002755
Table 31, entry 6	353	0.0098	70.7	-4.62537	0.002833

E_a estimated as 70.5 $kJmol^{-1}$, A estimated as 2.68×10^8 min^{-1}.

Figure 38: Combined data to estimate 4-FBnCl (from Figures 31 & 32, see Appendix 2).

Time / min	Imidazole derivative 104 / % yield	Diamine 105 / % yield	Total yield / %	4-FBnCl yield (assumed) / %	4-FBnCl remaining / g
0	37.3	8.7	46.0	54.0	0.38
5	44.8	10.4	55.0	44.8	0.31
10	51.7	11.1	62.8	37.2	0.26
20	64.1	12.0	76.1	23.9	0.17
40	75.5	12.5	88.0	12.0	0.08
80	85.2	12.7	97.9	2.1	0.01
120	88.0	12.6	100.6	0	0

Figure 38: Data for log plot.

Time / min	4-FBnCl / mol	Concentration 4-FBnCl / mol L^{-1}	ln[4-FBnCl]
0	0.002614	0.037350	-3.28743
5	0.002169	0.030986	-3.47421
10	0.001801	0.025730	-3.66011
20	0.001157	0.016531	-4.10254
40	0.000581	0.008300	-4.79151
80	0.000102	0.001452	-6.53448
120	0	0	

Half life calculated as 17.2 min.

The above data was also employed for generation of Figure 44.

Table 34: entry 1, HPLC Method A.

Time / min	Methyl *p*-tolyl sulfone / % area	4-FBnCl / % area	Imidazole derivative 104 / % area	4-FBnCl / g	Imidazole derivative 104 / g	4-FBnCl / % yield	Imidazole derivative 104 / % yield
0	20.55	0	0	0	0	0	0
1	18.96	8.33	0.00	1.00	0	100.48	0.00
3	19.07	7.62	0.37	0.91	0.09	91.32	7.77
7	19.43	6.35	0.77	0.74	0.19	74.67	16.11
16	19.44	3.93	1.44	0.46	0.36	46.21	29.92
30	19.44	2.56	2.14	0.30	0.54	30.04	44.62
60	19.55	0.82	2.71	0.09	0.68	9.56	56.21
120	19.50	0	2.90	0	0.73	0	60.20
240	18.98	0	2.83	0	0.73	0	60.36

Table 34: entry 1, data for log plot (Figure 42).

Time / min	4-FBnCl / mol	Concentration 4-FBnCl / mol L^{-1}	ln[4-FBnCl]
0	0	0	
1	0.006892	0.068915	-2.67488
3	0.006263	0.062629	-2.77053
7	0.005121	0.051210	-2.97182
16	0.003169	0.031694	-3.45163
30	0.002060	0.020601	-3.88242
60	0.000656	0.00656	-5.02675
120	0	0	
240	0	0	

Half life calculated as 17.6 min.

Table 34: entry 1, HPLC Method B.*

Time	Biphenyl / % area	Diamine 105 / % area	Diamine 105 / g	Diamine 105 / % yield
0	13.52	0	0	0
1	13.69	0.26	0.06	2.02
3	13.65	0.70	0.17	5.43
7	13.58	1.49	0.37	11.61
16	13.13	2.79	0.71	22.53
30	13.61	4.03	0.99	31.42
60	13.44	5.07	1.26	40.02
120	13.53	5.30	1.31	41.55
240	13.79	5.36	1.30	41.26

Table 34: entry 2, HPLC Method A.

Time / min	Methyl *p*-tolyl sulfone / % area	4-FBnCl / % area	Imidazole derivative 104 / % area	4-FBnCl / g	Imidazole derivative 104 / g	4-FBnCl / % yield	Imidazole derivative 104 / % yield
0	95.94	0	0	0	0	0	0
1	23.81	73.04	1.17	0.96	0.03	95.71	2.72
3	24.04	70.88	3.17	0.92	0.09	91.99	7.28
7	24.71	66.11	7.18	0.84	0.20	83.46	16.05
15	25.94	57.07	14.78	0.69	0.39	68.65	31.50
30	27.81	42.25	26.70	0.48	0.65	47.41	53.07
60	30.86	21.32	44.42	0.22	0.97	21.55	79.55
120	33.02	4.96	57.69	0.05	1.18	4.68	96.54
240	33.75	0.21	61.83	0	1.24	0.19	101.23

* *r* value used for diamine **105** was 1.667 as determined during later studies. This ensured an improved mass balance was obtained.

Table 34: entry 2, data for log plot (Figure 42).

Time / min	4-FBnCl / mol	Concentration 4-FBnCl / mol L^{-1}	ln[4-FBnCl]
0	0	0	
1	0.006648	0.066482	-2.71082
3	0.006390	0.063896	-2.75050
7	0.005798	0.057975	-2.84774
15	0.004769	0.047687	-3.04310
30	0.003293	0.032932	-3.41330
60	0.001497	0.014972	-4.20156
120	0.000325	0.003253	-5.72813
240	1.35E-05	0.000135	-8.91142

Half life calculated as 26.7 min.

Table 34: entry 3, HPLC Method A.

Time / min	Methyl *p*-tolyl sulfone / % area	4-FBnCl / % area	Imidazole derivative 104 / % area	4-FBnCl / g	Imidazole derivative 104/ g	4-FBnCl / % yield	Imidazole derivative 104 / % yield
0	93.56	0	0	0	0	0	0
1	20.66	76.96	1.12	0.96	0.03	95.57	2.46
3	20.98	73.74	3.40	0.91	0.09	90.18	7.36
7	21.64	67.97	7.71	0.81	0.20	80.59	16.19
15	22.82	57.10	15.94	0.65	0.39	64.20	31.74
30	24.89	39.56	29.18	0.41	0.65	40.78	53.27
60	27.61	16.80	46.19	0.16	0.93	15.61	76.02
120	29.30	2.85	56.15	0.03	1.07	2.50	87.08
240	29.75	0	58.45	0	1.09	0	89.28

Table 34: entry 3, data for log plot (Figure 42).

Time / min	4-FBnCl / mol	Concentration 4-FBnCl / mol L^{-1}	ln[4-FBnCl]
0	0	0	
1	0.006647	0.066468	-2.71104
3	0.006272	0.062715	-2.76915
7	0.005604	0.056045	-2.8816
15	0.004465	0.044647	-3.10896
30	0.002836	0.02836	-3.56277
60	0.001086	0.010857	-4.52292
120	0.000174	0.001736	-6.35639
240	0	0	

Half life calculated as 22.5 min.

Supplementary data for kinetics model, HPLC Method A (with recalculated *r* values).

Time / min	Methyl *p*-tolyl sulfone / % area	4-FBnCl / % area	Imidazole derivative 104 / % area	4-FBnCl / g	Imidazole derivative 104 / g	4-FBnCl / % yield	Imidazole derivative 104 / % yield
0	19.09	0	0	0	0	0	0
1	17.68	7.84	0	0.93	0.00	91.81	0
3	17.39	7.53	0.293	0.90	0.06	89.55	5.27
7	17.61	6.91	0.537	0.82	0.12	81.15	9.54
15	16.63	5.32	1.041	0.67	0.24	66.24	19.58
30	17.50	3.86	1.781	0.46	0.39	45.70	31.83
60	17.46	1.93	2.465	0.23	0.54	22.85	44.14
120	17.57	0.63	2.962	0.07	0.65	7.36	52.74
240	17.36	0	3.028	0	0.67	0	54.54

Supplementary data for kinetics model, HPLC Method B (with recalculated *r* values).

Time / min	Biphenyl / % area	Diamine 105 / % area	Diamine 105 / g	Diamine 105 / % yield
0	13.31	0	0	0
1	13.22	0.18	0.04	1.37
3	13.27	0.46	0.11	3.47
7	13.26	1.02	0.24	7.65
15	13.26	2.01	0.48	15.10
30	13.25	3.37	0.81	25.38
60	13.32	4.94	1.18	36.98
120	13.27	5.86	1.41	44.03
240	13.31	6.10	1.46	45.67

Figure 45:

Time (total) / min	Time (coupling) / min	Temp / °C	Sample mass / g	GC result / mg/mL	Mass 4-FBnCl in 2 mL sample / mg	Mass 4-FBnCl in reaction mixture / g	4-FBnCl / mol
1	-	-	0.0276	0.141763	0.2835	0.7783	0.005383
3	-	-	0.0262	0.133223	0.2664	0.7705	0.005329
7	-	-	0.0277	0.136339	0.2727	0.7458	0.005158
15	-	-	0.0277	0.139587	0.2792	0.7636	0.005281
30	-	-	0.0267	0.128477	0.2570	0.7291	0.005043
60	-	67.4	0.0260	0.110097	0.2202	0.6416	0.004438
67	5	73.7	0.0278	0.077086	0.1542	0.5472	0.003785
72	10	90.8	0.0297	0.076082	0.1522	0.5055	0.003497
82	20	91.1	0.0297	0.054264	0.1085	0.3606	0.002494
102	40	91.9	0.0300	0.028965	0.0579	0.1905	0.001318
142	80	91.8	0.0279	0.008017	0.0160	0.0567	0.000392
182	120	92.0	0.0267	0.002265	0.0045	0.0167	0.000116

4-FBnCl result at t_{total} = 60 min sample was used as $t_{coupling}$ = 0 for modelling purposes. Amine **77** added when t_{total} = 62 min.

Figure 46:

Time (total) / min	Time (coupling) / min	Temp / °C	Sample mass / g	GC result / mg/mL	Mass 4-FBnCl in 2 mL sample / mg	Mass 4-FBnCl in reaction mixture / g	4-FBnCl / mol
1	-	70	0.0121	0.001068	0.0021	0.0168	0.000116
3	-	69.9	0.006	0.000681	0.0014	0.0216	0.000149
8	-	70.4	0.0262	0.00316	0.0063	0.0229	0.000158
15	-	70.7	0.0361	0.004365	0.0087	0.0230	0.000159
30	-	70	0.0307	0.003468	0.0069	0.0214	0.000148
75	-	70	0.0329	0.003276	0.0066	0.0189	0.000131
80	4.5	80.3	0.0264	0.001526	0.0031	0.0143	9.89E-05
85	9.5	88	0.0287	0.0015	0.0030	0.0129	8.94E-05
95	19.5	91.2	0.0237	0.000955	0.0019	0.0100	6.89E-05
115	39.5	91.9	0.0311	0.000716	0.0014	0.0057	3.94E-05
155	79.5	92	0.0281	0.000171	0.0003	0.0015	1.04E-05
195	119.5	91.4	0.0307	5.06E-05	0.0001	0.0004	2.82E-06

4-FBnCl result at t_{total} = 75 min sample was used as $t_{coupling}$ = 0 for modelling purposes. Amine **77** added when t_{total} = 75.5 min.

Table 36: entry 1, data for log plot (Figure 47).

Time / min	4-FBnCl / mol	Concentration 4-FBnCl / mol L^{-1}	ln[4-FBnCl]
5	0.003785	0.045058	-3.0998
10	0.003497	0.041626	-3.17902
20	0.002494	0.029689	-3.51697
40	0.001318	0.015689	-4.15478
80	0.000392	0.004669	-5.36671
120	0.000116	0.001379	-6.58669

Half life calculated as 22.7 min.

Table 36: entry 2, data for log plot (Figure 47).

Time / min	4-FBnCl / mol	Concentration 4-FBnCl / mol L^{-1}	ln[4-FBnCl]
4.5	9.89E-05	9.42E-07	-13.8754
9.5	8.94E-05	8.52E-07	-13.976
19.5	6.89E-05	6.56E-07	-14.2368
39.5	3.94E-05	3.75E-07	-14.7967
79.5	1.04E-05	9.93E-08	-16.1251
119.5	2.82E-06	2.69E-08	-17.4321

Half life calculated as 22.2 min.